

Transformation af udskillelser på atomar skala

Danielsen, Hilmar Kjartansson

Publication date:
2013

Document Version
Også kaldet Forlagets PDF

[Link back to DTU Orbit](#)

Citation (APA):
Danielsen, H. K. (2013). Transformation af udskillelser på atomar skala Dansk Metallurgisk Selskab. [Lyd og/eller billed produktion (digital)], Kolding, Danmark, 16/01/2013

DTU Library
Technical Information Center of Denmark

General rights

Copyright and moral rights for the publications made accessible in the public portal are retained by the authors and/or other copyright owners and it is a condition of accessing publications that users recognise and abide by the legal requirements associated with these rights.

- Users may download and print one copy of any publication from the public portal for the purpose of private study or research.
- You may not further distribute the material or use it for any profit-making activity or commercial gain
- You may freely distribute the URL identifying the publication in the public portal

If you believe that this document breaches copyright please contact us providing details, and we will remove access to the work immediately and investigate your claim.

Karakterisering på alle længdeskalaer

DMS

DANSK METALLURGISK SELSKAB
Vintermødet
2013
Koldingfjord

Foredrag
præsenteret ved
Vintermødet 16. til 18. januar 2013
Hotel Koldingfjord
Kolding

Redaktion:
Trine Nybo Lomholt

Eftertryk kun tilladt med forfatternes tilladelse

FORORD

Dansk industri skal bl.a. overleve på kvalitet, og det er vigtigt, at virksomhederne kan dokumentere denne kvalitet overfor deres kunder. Vintermødet 2013 har derfor fokus på karakterisering af materialer, processer og komponenter, som spænder fra nanometer til meterskala og fra forskning & udvikling til monitorering af komponenter i drift.

Vintermødet sigter mod en bred dækning af emnet med foredrag, der bl.a. dækker mikroskopi, kemisk analyse, mekanisk prøvning, skadesanalyse, kvalitetskontrol mm.

Dette års virksomhedsbesøg foregik på Alfa Laval i Kolding. Alfa Laval Kolding er specialist i løsninger til håndtering af væsker af enhver viskositet, hurtig rengøring af lukket procesudstyr og intelligent, automatiseret kontrol. På fabrikken i Kolding produceres pumper og ventiler til fødevareindustrien, bryggerier, mejerier, farmaceutiske- og kosmetiske industrier. Alfa Laval Kolding beskæftiger i dag ca. 550 medarbejdere.

Trine Nybo Lomholt

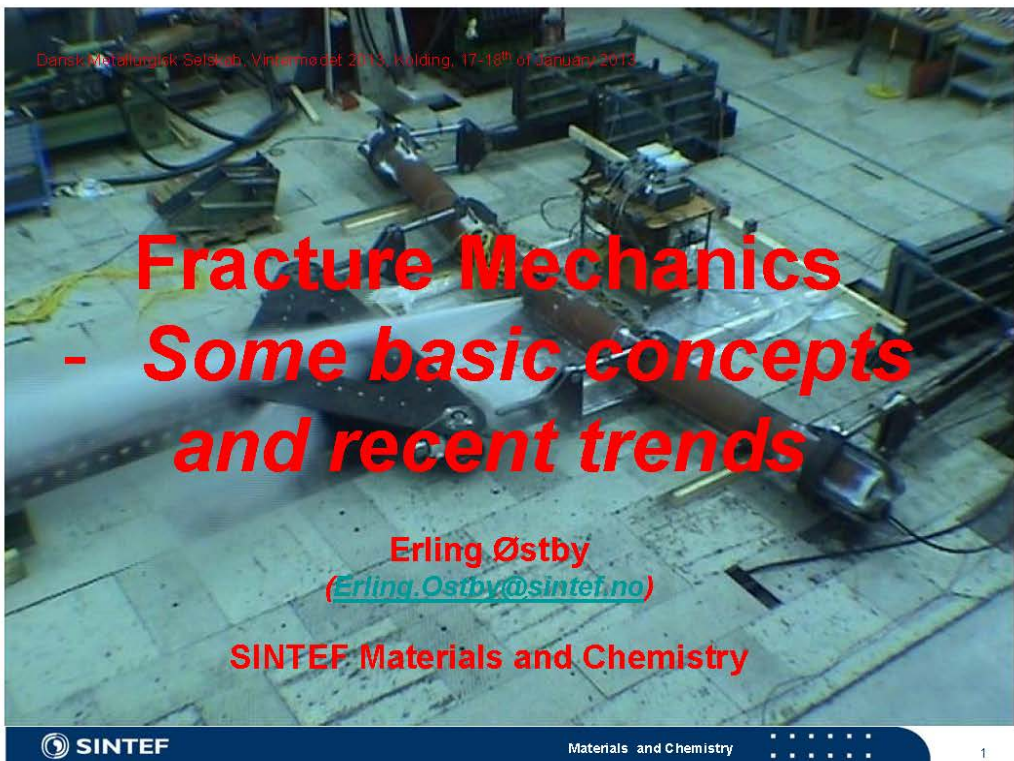
INDHOLDSFORTEGNELSE

Fracture mechanics - Some basic concepts and recent trends Erling Østby, SINTEF	1
Off-line testing af friktion og smøring i pladeformgivning Niels Bay, DTU Mekanik	24
Industriens udnyttelse af de store internationale røntgen og neutronfaciliteter Henning Friis Poulsen, DTU Fysik	48
Studier af rekrySTALLisation med 3DXRD Dorte Juul Jensen, DTU Vindenergi	60
Den nyeste generation af røntgen diffraktometre med tilhørende temperaturcelle Flemming Grumsen, DTU Mekanik	78
NDT – relevante teknikkers muligheder og begrænsninger Peter Villumsen, Force	89
Metrology and Quality Assurance Maria Holmberg, Teknologisk Institut	101
Determining geometrically necessary dislocation densities by EBSD Philip Littlewood, DTU Mekanik	111
Transformation af udskillelser på atomar skala Hilmar Danielsen, DTU Mekanik	121
Structural and chemical characterization by electron microscopy – spanning the micro and nano regime Jakob Birkedal Wagner, DTU CEN	133
Nanostruktur og styrke af stål deformert ved valsning og med shot peening Niels Hansen, DTU Vindenergi	144
Homogen og lokaliseret tøjningsudvikling af nanostruktureret aluminium Jacob Kidmose, DTU Vindenergi	164
Baggrund for Innovationskonsortiet REEgain om magnetiske materialer Jens Christiansen, Teknologisk Institut	175

Superleder tapes karakteriseret fra nanometer pinning til meter store spoler Asger Bech Abrahamsen, DTU Vindenergi	189
Mikrostruktur karakterisering af SG-støbejern Karl Martin Pedersen, Siemens Wind Power A/S	198
Kvalitetssikring af støbegods i MAN B&W motorer Knud Strand, MAN	212
Ny metode til kvantificering af grafitstørrelse og –morfologi i støbejern Steen Krogh Jensen, MAN	231
Materialevalg/Stålfremstilling Stig Rubæk, Metal-Consult	252
Varmebehandling og karakterisering af nye udskilningshærdbare superlegeringer Uffe Bihlet, MAN og DTU Mekanik	268
GD-OES applications Io Mizushima, IPU	286
Egenskaber for korrosion og rensbarhed af rustfrit stål overflader Rasmus Lage	295

Fracture mechanics - Some basic concepts and recent trends

Erling Østby, SINTEF



SINTEF

Materials and Chemistry

1

SINTEF Materials and Chemistry

- SINTEF Materials and Chemistry is a contract research division offering high competence within
 - materials technology,
 - applied chemistry,
 - and applied biology
- 400 employees
 - 100 Oslo, 300 Trondheim, approx. 25% non-Norwegian from 44 countries
- 8 departments + staff
- Core areas of R&D
 - Oil & Gas industry, approx. 150 man-years
 - along the whole value chain from increased oil production, drilling, flow assurance, pipelines, to refineries and petrochemical
 - the largest independent research institution in the world on oil spill
 - Land-based industries, approx. 120 man-years
 - aluminum, ferro alloys, mineral industry, manufacturing industry, pharmaceutical industry (biotech), and food industry.
 - Environmentally friendly energy, approx. 120 man-years
 - Silicon-based solar, CCS, bio-refinery, offshore wind, hydrogen technology.



Executive Vice President Torstein Haarberg together with former and present employees at SINTEF Materials and Chemistry

SINTEF

Materials and Chemistry

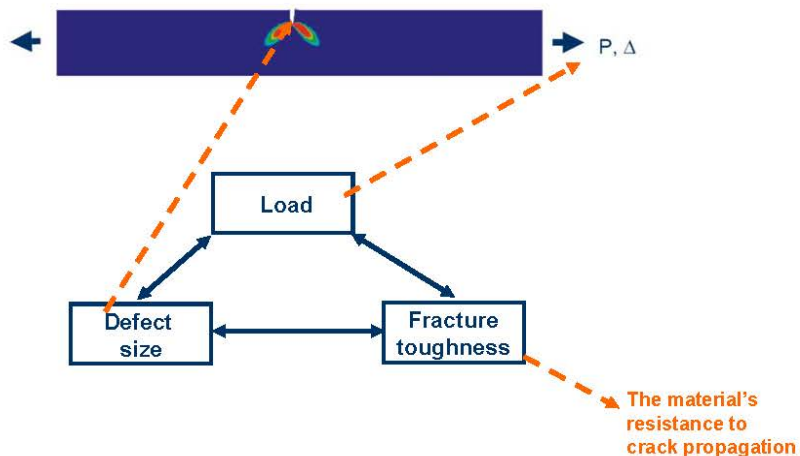
2

Outline

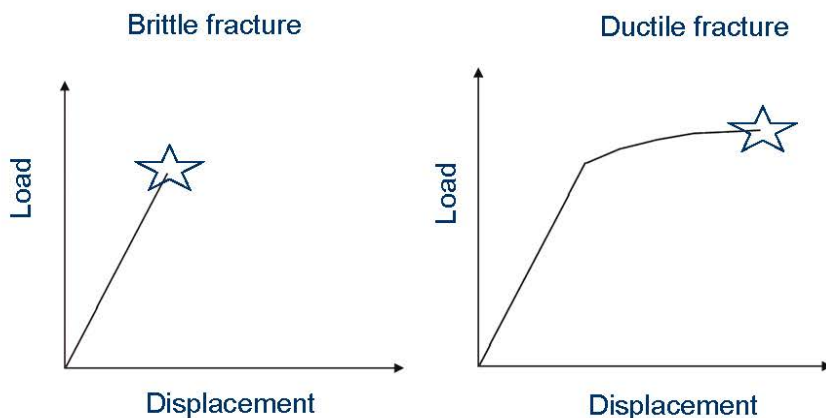
- Some basic fracture mechanics concepts
- Examples of emerging/new topics
 - Constraint effect – “new knowledge”
 - Fracture under large global deformations - “application under harsher conditions”
 - Use of numerical simulation tools – “taking the analysis further”
 - Testing techniques – “new information”
 - Probabilistic fracture assessments – “quantified safety level”
 - ... and a few words on multi-scale approaches – “tomorrow”
- Wrap-up

Some basic fracture mechanics

Basic fracture mechanics

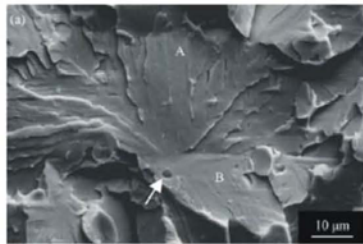


Types of fracture – global perspective



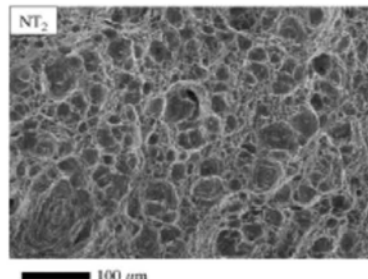
Types of fracture – materials perspective

Brittle fracture (cleavage fracture)



- Fracture propagates along given planes in the crystal
- Requires little energy for crack propagation

Ductile fracture



- Fracture propagates through formation and coalescence of voids in the material
- Requires more energy (and local deformation)

How to quantify the loading of the crack

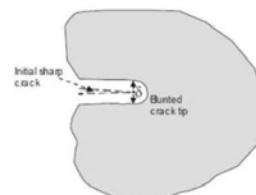
■ Elastic conditions – Stress intensity factor, K

$$\xleftarrow{\text{Diagram of a crack in a plate}} \sigma / (\varepsilon) \quad K = \sigma \sqrt{\pi a} f(a/t) \quad [\text{MPam}^{1/2}]$$

■ With significant plasticity – J-integral or CTOD (δ)

$$J = \int_{\Gamma} (w dy - T_i \frac{\partial u_i}{\partial x} ds)$$

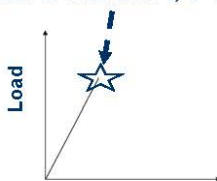
$$J=m\sigma_y\delta$$



When will the material fracture?

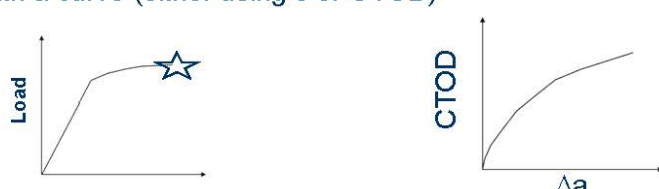
■ Brittle fracture:

- Fracture occurs when a critical K , J or CTOD value is reached

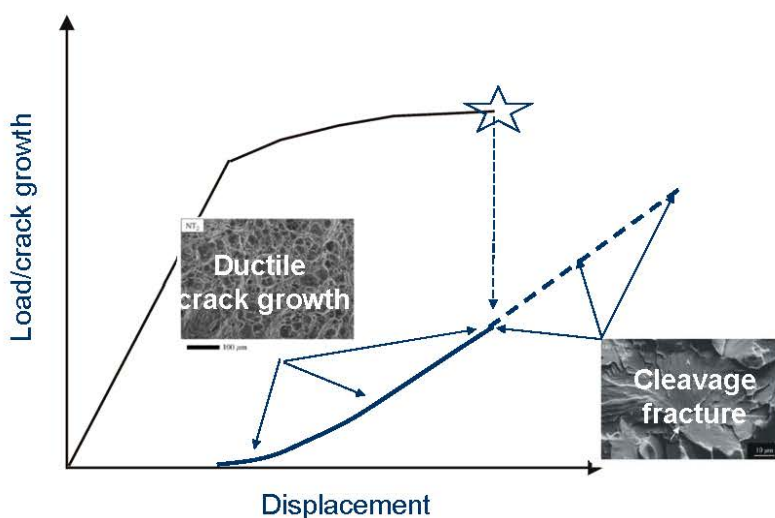


■ Ductile fracture:

- The fracture resistance is not represented with a single value, but with a curve (either using J or CTOD)

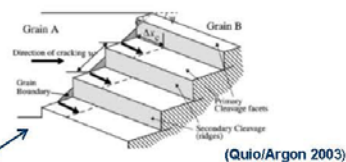
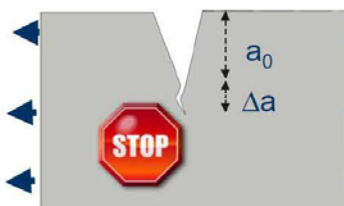


A transition in fracture mechanism may sometimes occur

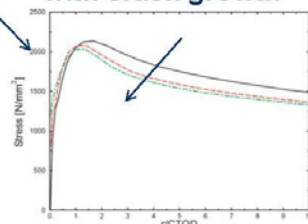


Crack arrest – when cracks stop growing

Materials barriers



Reduced loading with crack growth

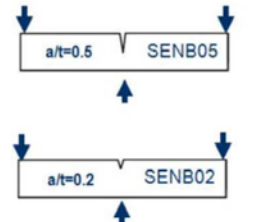


Emerging/new topics

Constraint effects in fracture

■ Key points:

- Fracture toughness no longer a material parameter!!!
- There is an influence from the geometry and mode of loading applied



■ Case:

- The effect of specimen geometry in brittle fracture toughness of a HAZ microstructure



Classical fracture mechanics parameters – Believed to fully describe the crack tip conditions....

■ Elastic conditions – Stress intensity factor, K

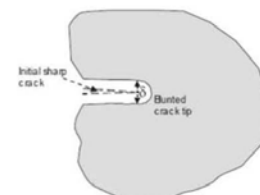
$$\leftarrow \boxed{\text{Diagram of a crack tip in a plate under tension}} \rightarrow \sigma / (\varepsilon) \quad K = \sigma \sqrt{\pi a} f(a/t) \quad [\text{MPam}^{1/2}]$$

■ With significant plasticity – J-integral or CTOD (δ)

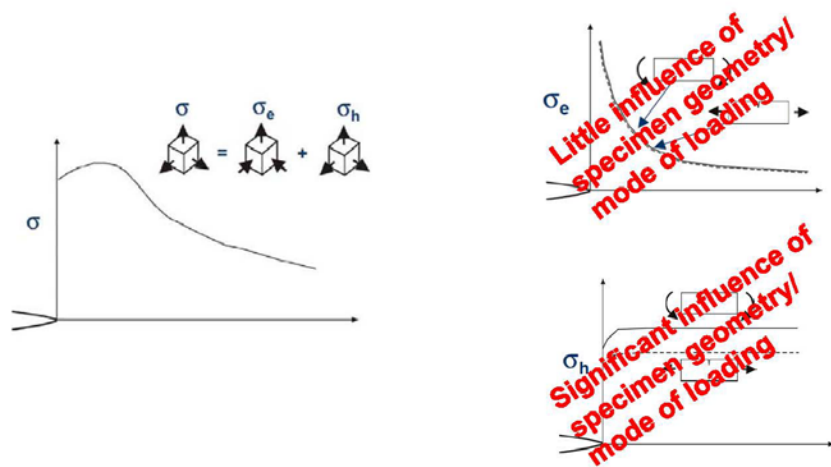
A schematic diagram of a crack tip in a circular plate under tension. A small element ds is shown at an angle θ from the crack tip. A coordinate system with x and y axes is indicated.

$$J = \int_{\Gamma} (w dy - T_i \frac{\partial u_i}{\partial x} ds)$$

$$J = m \sigma_y \delta$$

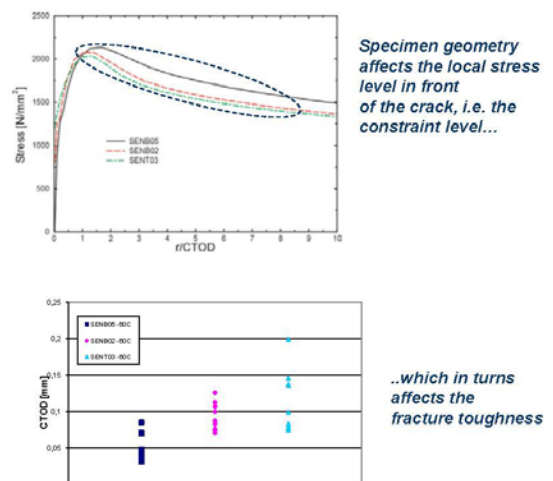
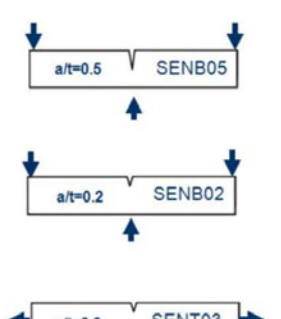


"... but there was more"



..and the so-called constraint effect was "born"

Example – effect of constraint on local crack-tip stress field/fracture toughness



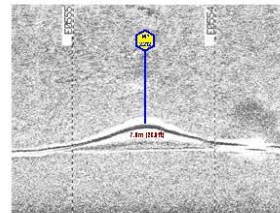
Fracture under large imposed deformations

■ Key points:

- Most fracture mechanics approaches developed for situations with macroscopic elastic behaviour
- Technological pull to allow for larger utilization of materials
- Need fracture assessment schemes that applies under large global deformations

■ Case:

- Fracture under large deformations in pipelines/strain-based design

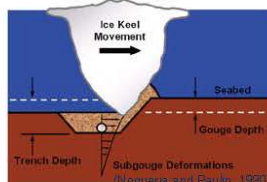


Large deformation scenarios for pipelines

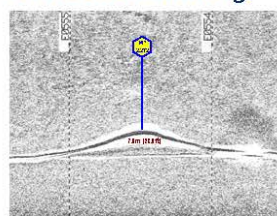
Pipeline installation



Ice loading



On-bottom snaking



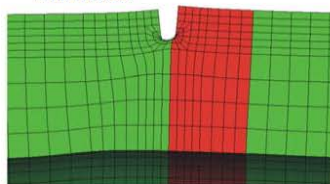
Earthquakes



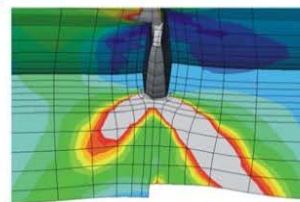
→ Pipelines must in many cases be designed to withstand a given deformation or strain level – i.e. strain-based design principles should be used

Some effects to consider

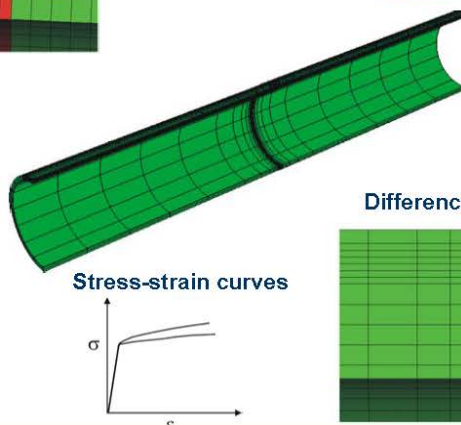
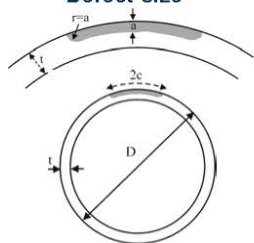
Mismatch



Misalignment



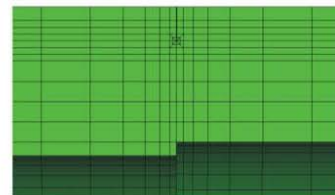
Defect size



Stress-strain curves

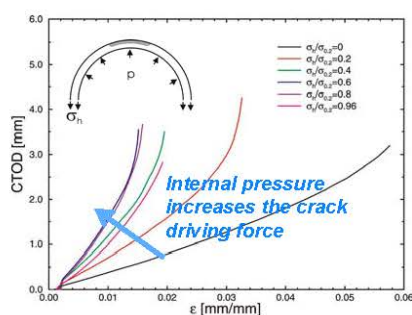


Difference in wall thickness

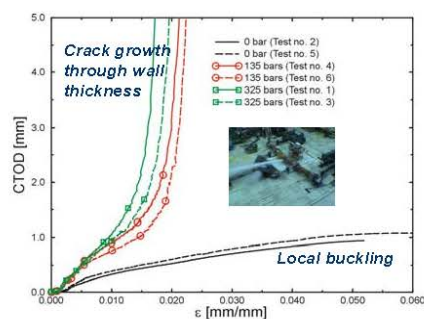


The effect of biaxial loading

Initial FE studies



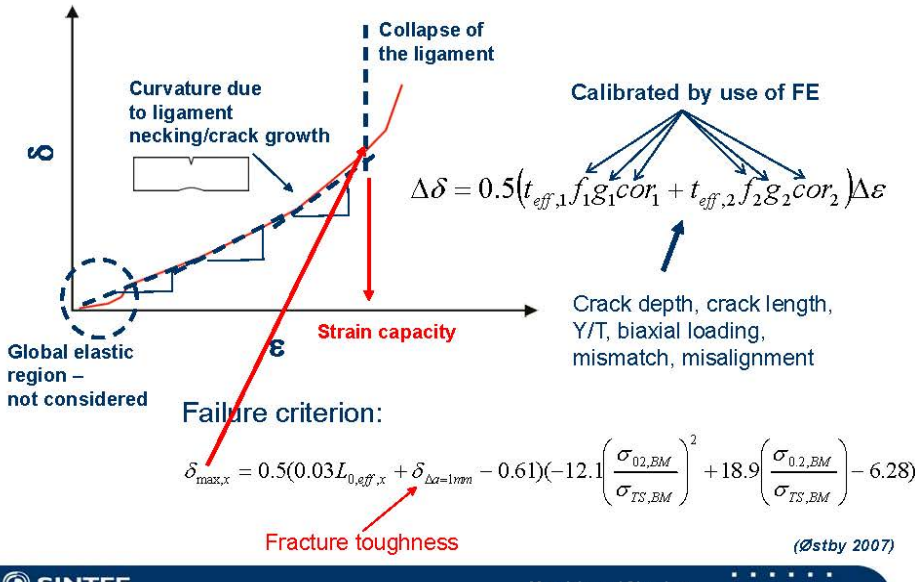
Large-scale experimental validation



(Jayadevan et al. 2004, Østby et al. 2005)

(Østby and Hellesvik 2007, 2008)

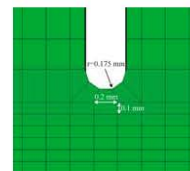
Simplified strain-based fracture assessment model



Numerical simulations

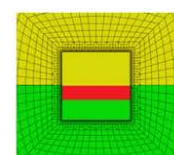
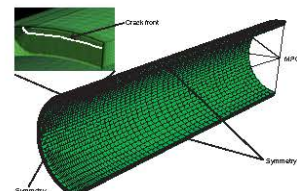
Key points:

- Analytical solutions often not accurate enough
- Numerical (FE) fracture mechanics simulations becoming more usual also in the industry
- Quicker implementation of new knowledge
- Coupling with more advanced material models and micromechanical-based fracture criteria becomes easier



Cases:

- Small and large-scale modelling of ductile fracture in pipelines
- The effect of local materials properties in ductile fracture
- Geometry and materials constraint effects in brittle fracture
- Including "microstructure"



The Gurson-Tvergaard-Needleman model and criterion for void coalescence

Yield function:

$$\phi(q, \bar{\sigma}, f, \sigma_m) = \frac{q^2}{\sigma^2} + 2q_1f \cosh\left(\frac{3q_2\sigma_m}{2\sigma}\right) - 1 - (q_1f)^2 = 0$$

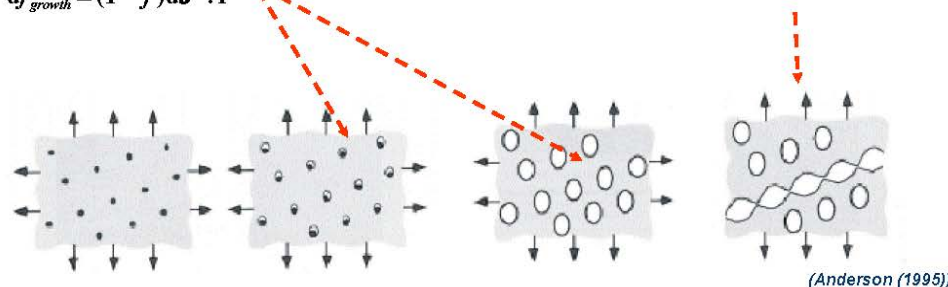
Thomason's limit load criterion

$$\frac{\sigma_1}{\bar{\sigma}} < \left(\alpha \left(\frac{1}{r} - 1 \right)^2 + \frac{\beta}{\sqrt{r}} \right) (1 - \pi r^2)$$

Void growth

$$df_{growth} = (1-f)d\epsilon^p : I$$

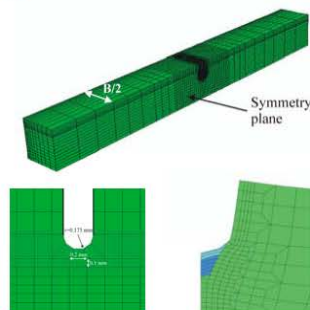
$$r = \sqrt[3]{(3f/4\pi)e^{(x_1+x_2)/2}} / \sqrt{e^{(x_1+x_2)/2}}$$



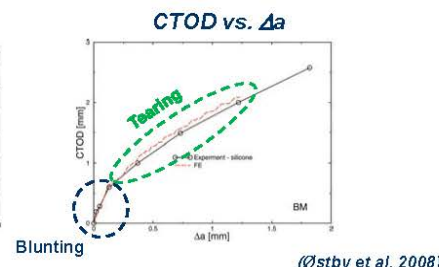
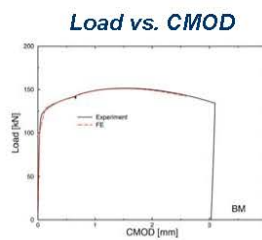
- An interesting approach for modelling of ductile crack growth

Crack growth modelling – SENT small-scale testing

Seamless X65 pipe



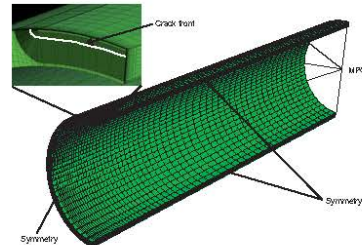
Comparisons between experiment and simulation



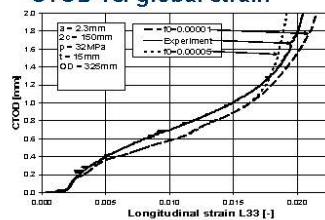
(Østby et al. 2008)

Crack growth modelling - Large-scale testing

325 bar internal pressure

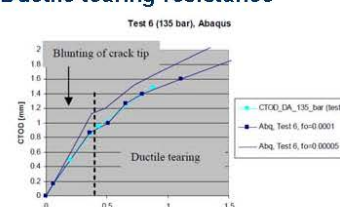


CTOD vs. global strain



(Sandvik et al. 2008)

Ductile tearing resistance



(Dybwid et al. 2009)

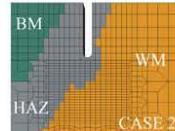
Invers modelling... to help understanding the influence of local features – Ex. HAZ X80 weld

FE configuration

Defect at fusion line



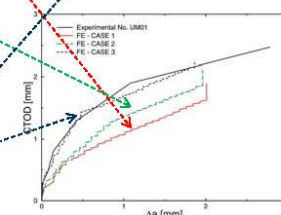
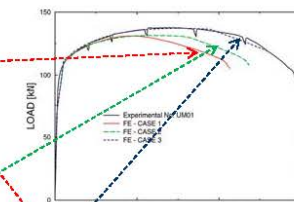
Defect shifted somewhat into HAZ
-The effect of defect position



Defect shifted somewhat into HAZ with local increase in strength
-The effect of defect position
-The effect of crack-tip shielding



Comparison with experiment



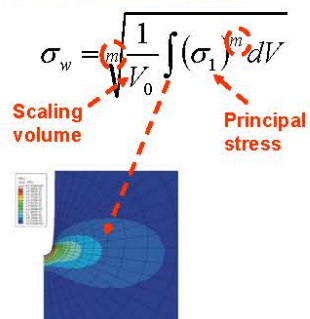
(Østby et al. 2009)

Micromechanical models for brittle fracture – The Weibull stress approach

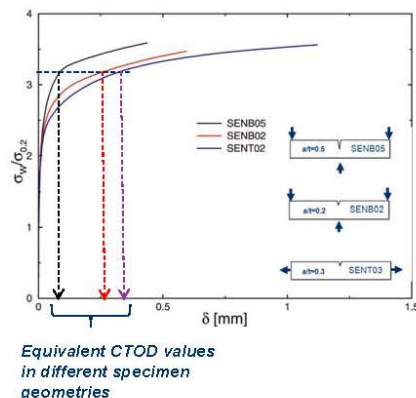
Failure probability, P_f :

$$P_f = 1 - \exp\left(-\left(\frac{\sigma_w}{\sigma_u}\right)^m\right)$$

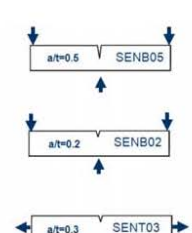
The Weibull stress:



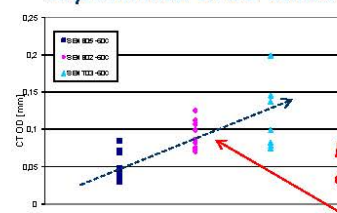
Toughness scaling principle



Constraint effect – Ex. HAZ microstructure

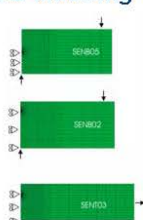


Experimental CTOD values

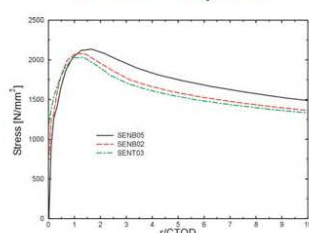


ICCGHAZ 420 MPa steel

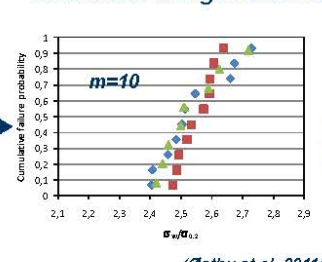
FE modeling



Local crack tip fields



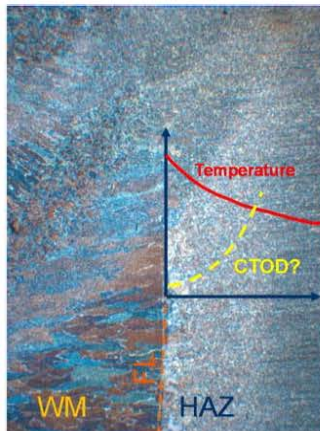
Calibration using Weibull stress



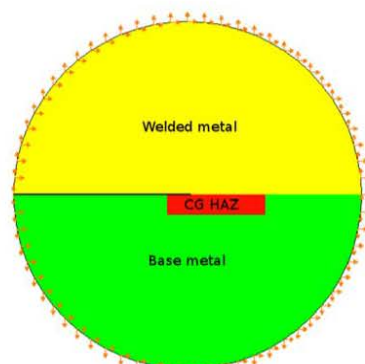
(Østby et al. 2011b)

FE modeling of inhomogeneous material systems - HAZ

Real HAZ

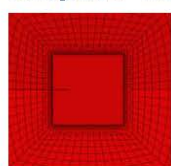


Idealized FE representation

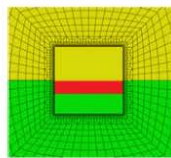


Transferability from weld thermal simulation to real HAZ toughness using the Weibull stress model

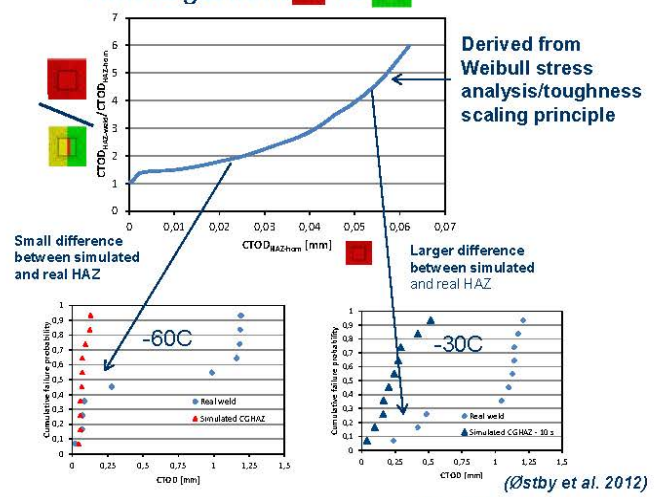
"Homogeneous" HAZ



"HAZ" in weld



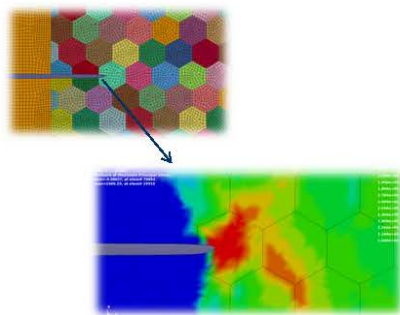
"How to get from to "



(Østby et al. 2012)

Including "microstructure"...

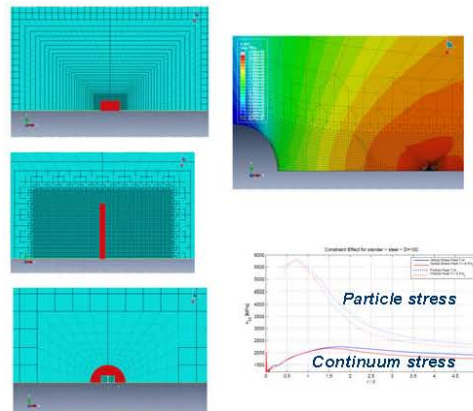
Grains



Crystal plasticity – accounting for grain orientation

(Kane et al. 2011)

Particles/inclusions



SINTEF

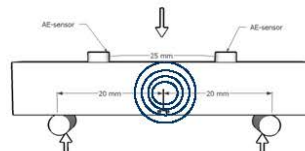
Materials and Chemistry

31

Testing techniques

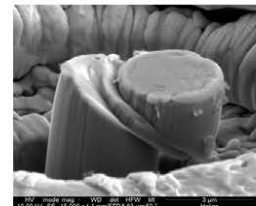
■ Key points:

- More knowledge about properties at lower levels ("Karakterisering på alle længdeskalaer")
- Helpful for improved understanding of fracture
- Modelling requires more input regarding material properties



■ Cases:

- Acoustic emission and local crack arrest
- FIB/Nano indentation
- FIB/TEM



SINTEF

Materials and Chemistry

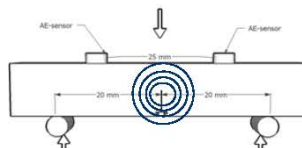
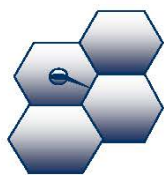
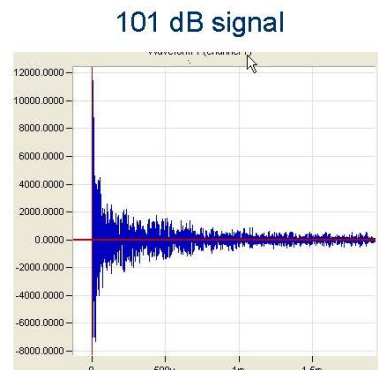
32

Interpretation of acoustic emission signals

■ AE signal:

$$A = 20 \log \left(\frac{V}{V_{ref}} \right) - A_{pre_amp} \text{ [dB]}$$

- A – amplitude in dB
- V – voltage signal transducer
- V_{ref} – reference voltage (1µV)
- A_{pre_amp} – pre-amplification used (in this case -20dB)



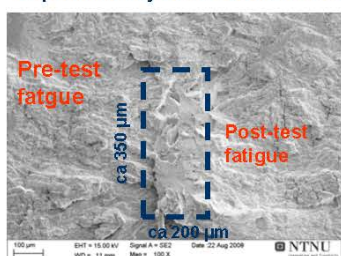
SINTEF

Materials and Chemistry

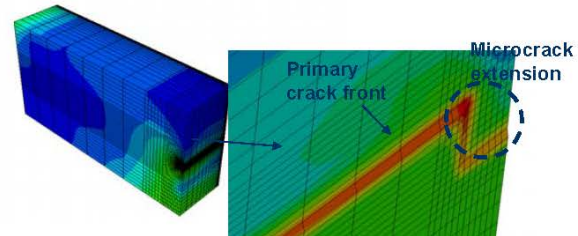
33

Correlation between AE signals and arrested microcracks

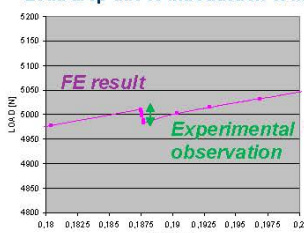
Experimentally observed microcrack



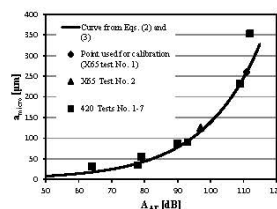
FE modelling of microcrack extension



Load drop due to introduction of microcrack



Assistance in validation
of correlation between
AE signal amplitude
and microcrack size



(Østby et al. 2012)

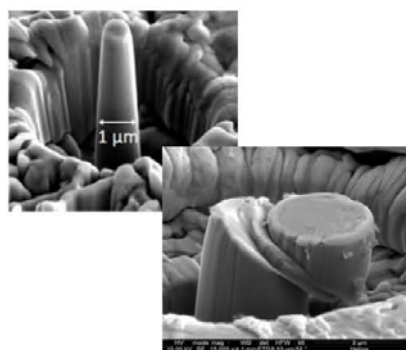
SINTEF

Materials and Chemistry

34

FIB/nano indentation/TEM

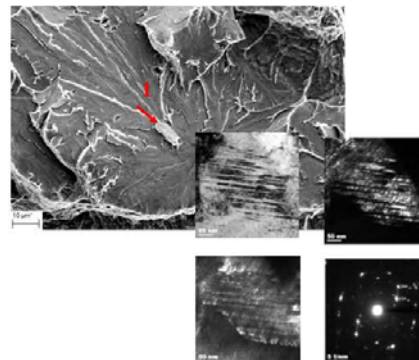
FIB/nanoindentation



Plastic properties at small-scales

(Haugen et al. 2012)

FIB/TEM



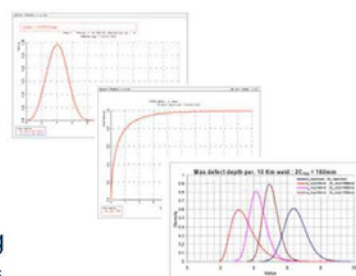
Investigation of nature of fracture initiating particles

(Mohseni et al. 2012)

Probabilistic fracture mechanics

■ Key points:

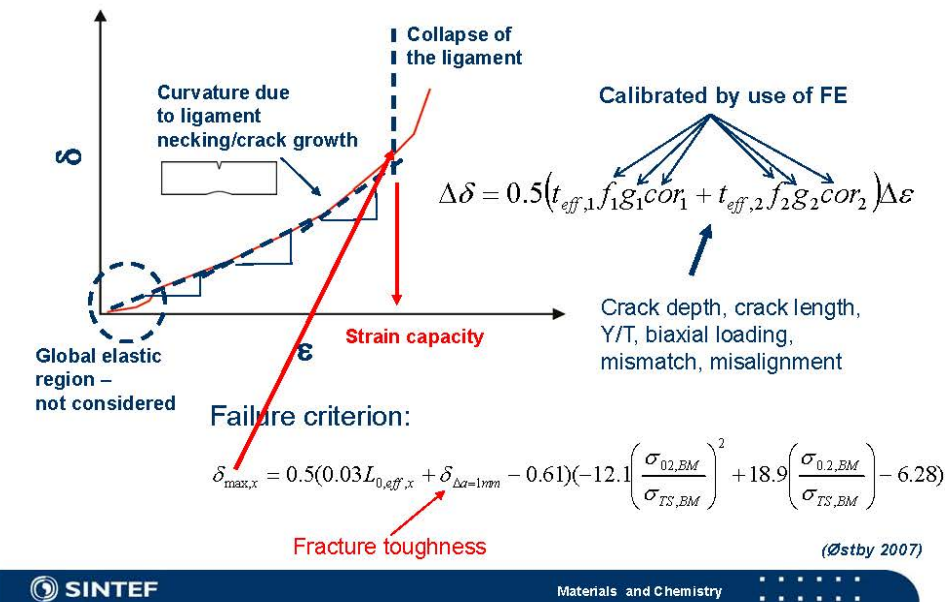
- Natural scatter and variability in parameters entering the problem
- Deterministic analysis in some cases of limited value
- Uncertainty around accuracy of models
- Probabilistic approaches open for linking to given failure probabilities/safety levels



■ Case:

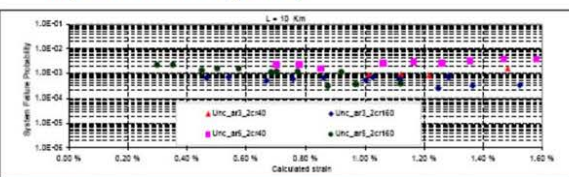
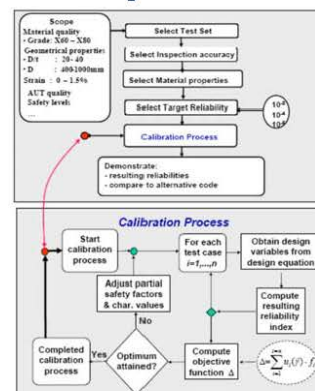
- Calibration of safety factors in fracture assessment of pipelines

Simplified fracture assessment model



Calibration of partial safety factors

- Scatter in input parameters
- Model uncertainty
- Variability in applied strains (basis from Hotpipe project)
- Statistical distributions of defects (valuable input from Hydro)



(G. Sigurdsson, DNV)

Proposed design format

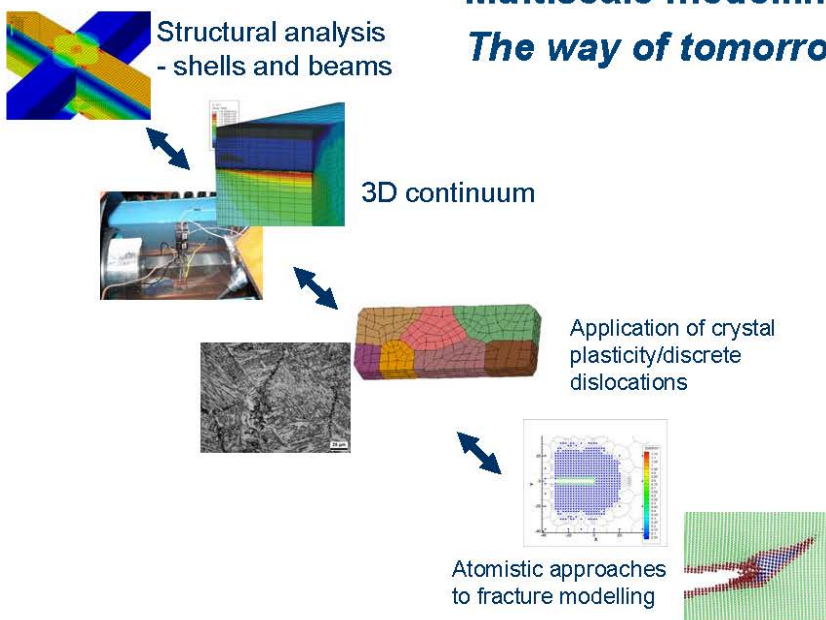
$$\varepsilon_{\max} \leq \min \left\{ \frac{\varepsilon_{cap}^c(t_c; \sigma_h; a_c \cdot \gamma_a; 2c_c; \alpha_c / \gamma_j; (a_{rep} \text{ or } Std(a_m)))}{\gamma_L}, \frac{0.015}{\gamma_L} \right\}$$

- ε_{\max} – best estimate applied strain
- ε_{cap} – deformation capacity
(calculated based on simplified model)
- γ_L – safety factor applied strain
- γ_a – safety factor defect depth
- γ_j – safety factor fracture toughness

- Safety factors depend on the safety class
- Different safety factors for installation (system effect) and operation
- Safety factor for applied strain under operation depends upon "CoV" of best estimate

Tomorrow....?

Multiscale modelling – The way of tomorrow?



Wrap-up...

- Fracture mechanics has been developed into a useful tool:
 - Materials developments
 - Design/structural integrity assessments
- New issues are being introduced and new application areas emerge
- The use of numerical simulation tools is becoming increasingly more important
- Important future development trends:
 - Further development of link to materials science
 - Development of multiscale schemes
- **Vision...**
 - ...predictions rather than calibration/"description"

Acknowledgments

- The financial support from the Norwegian Research Council and the industry to the Fracture Control Offshore Pipelines and Arctic Materials projects is greatly acknowledged
- The contributions from colleagues at SINTEF, NTNU, and DNV is also highly acknowledged

Off-line testing af friktion og smøring i pladeformgivning

Niels Bay, DTU Mekanik

Off-line testning af friktion og smøring i pladeformgivning

Niels Bay, Ermanno Ceron

DTU-Mekanik

Projektpartnere:

Grundfos, SSAB, Outokumpu Stainless, Uddeholm

**Dansk Metallurgisk Selskabs Vintermøde
Kolding
Januar 2013**

1 Niels Bay, Ermanno Ceron – Off-line testning af friktion og smøring i pladeformgivning
Dansk Metallurgisk Selskabs Vintermøde, Kolding, Januar 2013

Indhold

- Introduktion
- Faldgruber ved off-line testning
- Off-line plade-tribo-testning
- Eksempel på analyse af konkret produktion
- Off-line test resultater
- Produktionstest resultater, sammenligning med off-line test
- Konklusion

2

E. Ceron, N. Bay

Niels Bay, Ermanno Ceron – Off-line testning af friktion og smøring i pladeformgivning
Dansk Metallurgisk Selskabs Vintermøde, Kolding, Januar 2013

Introduction

Legislation

Since 2000 legislation in Europe and Japan has been increasingly restrictive as regards industrial application of hazardous lubricants

2006-2007 EU introduced new legislations, REACH, aiming at high level of protection of human health and the environment from risk posed by chemicals.

REACH makes industry responsible for assessing and managing the risks and providing appropriate safety information to their users.

The new legislations have forced metal forming industry to look for new environmentally benign tribo-systems.

This causes however great challenges.

3 N. Bay

Niels Bay, Ermanno Ceron – Off-line testning af friktion og smøring i pladeformgivning
Dansk Metallurgisk Selskabs Vintermede, Kolding, Januar 2013

Lubrication in tribologically difficult sheet metal forming

Tribologically difficult materials:

High strength steel, stainless steel, aluminium, titanium

Tribologically difficult processes:

Deep drawing with low radius of curvature

Ironing

Fine blanking

Chlorinated additives

Chloroparaffins suspected to have harmful effects on human health

- Risk of dioxin formation
- High recycle costs

4 N. Bay

Niels Bay, Ermanno Ceron – Off-line testning af friktion og smøring i pladeformgivning
Dansk Metallurgisk Selskabs Vintermede, Kolding, Januar 2013

Tribological problems in sheet metal forming

- High normal pressures
- Elevated tool/work piece interface temperatures

i.e. severe stressing of the lubricant with possible breakdown as a consequence.



Breakdown may cause:

- Local pick-up on tool surface
- Scoring of subsequently formed work piece surface



The sequence of events normally referred to as galling



5 N. Bay

Niels Bay, Ermanno Ceron – Off-line testning af friktion og smøring i pladeformgivning
Dansk Metallurgisk Selskabs Vintermøde, Kolding, Januar 2013

Challenges

- Introduction of new lubricants in manufacturing production is costly (production breaks, cleaning of tools)
- Industry is reluctant to carry out production tests due to bad experience (premature galling leading to unexpected production stops)
- Off-line testing of new tribo-systems
- It is vital to ensure testing conditions emulate production conditions
- Otherwise a tribo-system, which is approved in the simulative test, may turn out to be malfunctioning in the production tool, thus leading to the problems described above.

6 N. Bay

Niels Bay, Ermanno Ceron – Off-line testning af friktion og smøring i pladeformgivning
Dansk Metallurgisk Selskabs Vintermøde, Kolding, Januar 2013

Environmentally friendly sheet forming lubricants (except dry film)

Only a few lubricant manufacturers have focused on development of new, environmentally friendly lubricants

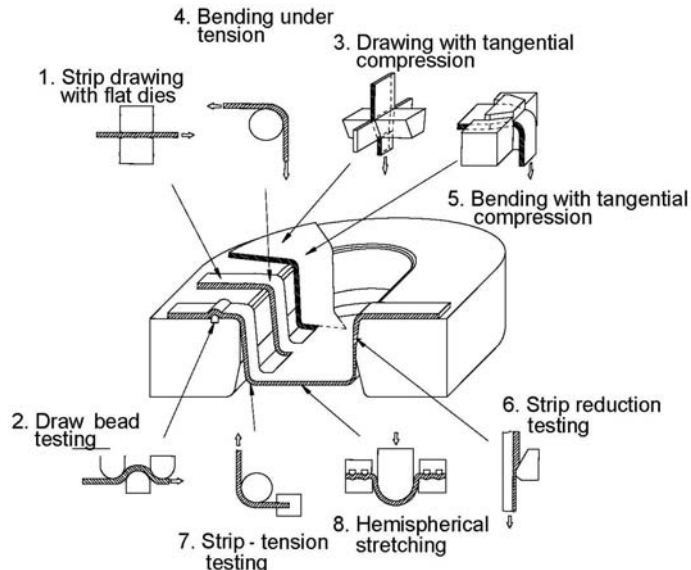
- **Masa Oil, Finland:** Biodegradable oils derived from tall oil extracted from fir tree. Fatty acid ester based.
- **Rhenus Lub, Germany:** Refined mineral oils with special additives of natural fatty components, synthetic esters, sulphur additives.
- **IRMCO Fluids, USA:** Oil free, low viscosity, water soluble lubricants made from vegetables and fruit.

7

E. Madsen, E. Ceron, N. Bay

Niels Bay, Ermanno Ceron – Off-line testning af friktion og smøring i pladeformgivning
Dansk Metallurgisk Selskabs Vintermede, Kolding, Januar 2013

Simulative sheet tribo-tests



8

N. Bay, K. Krebs Nielsen

Niels Bay, Ermanno Ceron – Off-line testning af friktion og smøring i pladeformgivning
Dansk Metallurgisk Selskabs Vintermede, Kolding, Januar 2013

Indhold

- Introduktion
- **Faldgruber ved off-line testning**
- Off-line plade-tribo-testning
- Eksempel på analyse af konkret produktion
- Off-line test resultater
- Produktionstest resultater, sammenligning med off-line test
- Konklusion

9

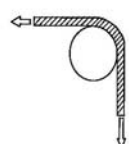
E. Ceron, N. Bay

Niels Bay, Ermanno Ceron – Off-line testning af friktion og smøring i pladeformgivning
Dansk Metallurgisk Selskabs Vintermøde, Kolding, Januar 2013

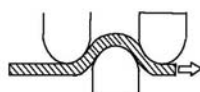
Selected off-line tests

Sheet forming tribology

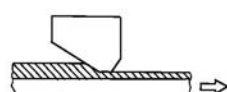
Bending-Under-Tension



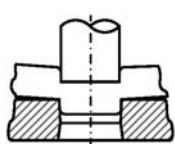
Draw Bead Test



Strip Reduction Test



Punching Test



Test	Normal pressure	Surface expans.	Temp.	Tribological severity
BUT	low	0	low	low
DBT	medium	0	medium	medium
SRT	high	medium	high	high
PUT	medium-high	infinite	very high	very high

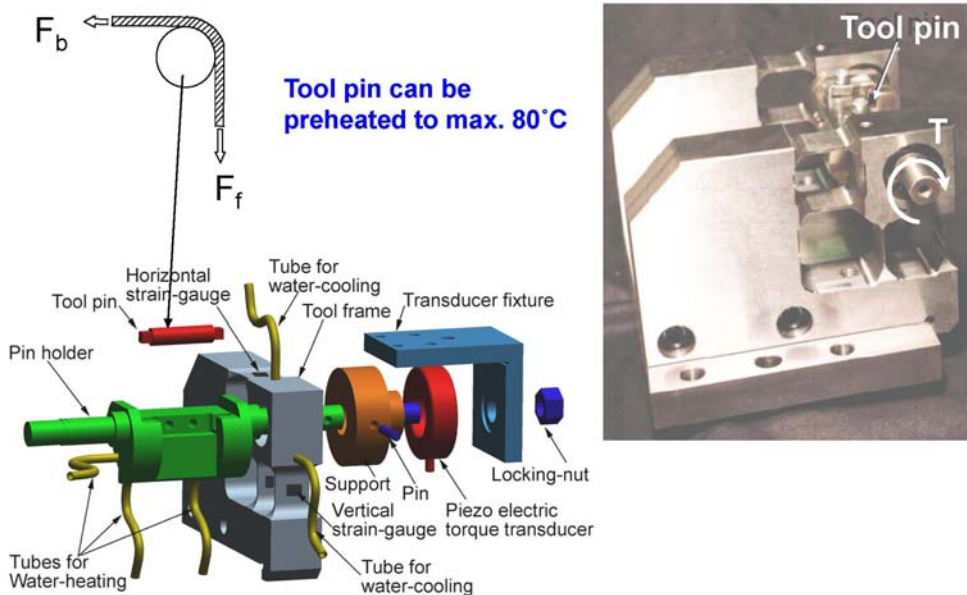
10

N. Bay

Niels Bay, Ermanno Ceron – Off-line testning af friktion og smøring i pladeformgivning
Dansk Metallurgisk Selskabs Vintermøde, Kolding, Januar 2013

Bending under tension - BUT

11



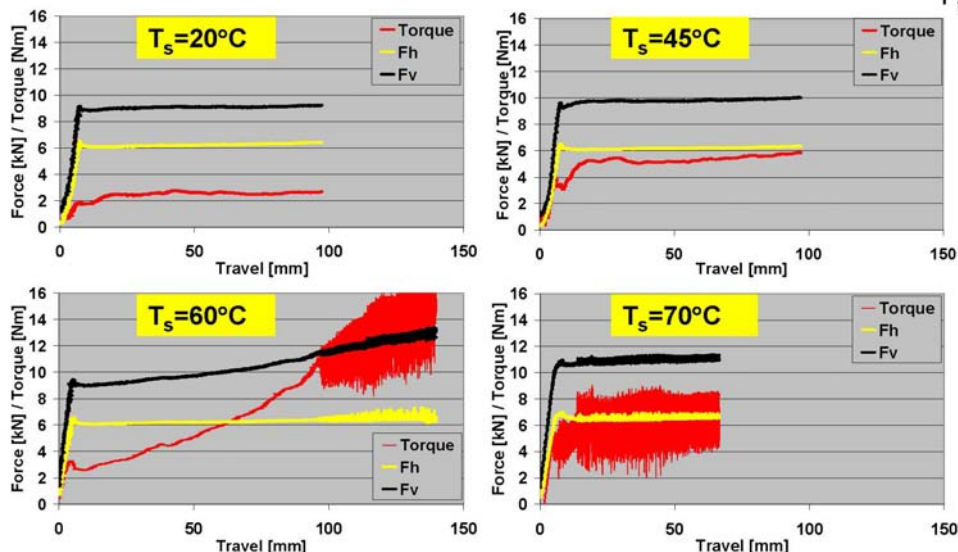
D.D. Olsson, K. Chodnikiewicz,

J.L. Andreasen, N. Bay
11 Niels Bay, Ermanno Ceron – Off-line testning af friktion og smøring i pladeformgivning
Dansk Metallurgisk Selskabs Vintermøde, Kolding, Januar 2013

Bending Under Tension - BUT

Stainless steel Wn.1.4401, Plain mineral oil without additives,
 $v=80\text{mm/s}$

12



J.L. Andreasen, D.D. Olsson, K.
Chodnikiewicz, N. Bay

12 Niels Bay, Ermanno Ceron – Off-line testning af friktion og smøring i pladeformgivning
Dansk Metallurgisk Selskabs Vintermøde, Kolding, Januar 2013

Faldgruber ved off-line testning -1

- For lav værktøjstemperatur
- For lav emnetemperatur (flertrinsoperationer)
- Ændrede procesparametre
 - Normaltryk
 - Glidelængde
 - Glidehastighed
 - Overfladeekspansion
 - Tid mellem tests
 - Kontakt/ikke kontakt mellem slag
- Ændrede smørebetingelser
 - Påføringsteknik
 - Emne- og værktøjsgeometri
- For få gentagelser

13

E. Ceron, N. Bay

Niels Bay, Ermanno Ceron – Off-line testning af friktion og smøring i pladeformgivning
Dansk Metallurgisk Selskabs Vintermøde, Kolding, Januar 2013

Faldgruber ved off-line testning - 2

- Ændrede egenskaber af emnemateriale
 - Flertrins operationer, f.eks. dybtrækning + krængetrækning/re-trækning
 - Dybtrækning + strækningsreduktion
- Ændret overfladetopografi
 - Emne (f.eks. ved flertrinsoperationer)
 - Værktøj (retning af hypper ved drejning, slibning, polering)

Production tool



Simulative tool (BUT)



14

E. Ceron, N. Bay

Niels Bay, Ermanno Ceron – Off-line testning af friktion og smøring i pladeformgivning
Dansk Metallurgisk Selskabs Vintermøde, Kolding, Januar 2013

Indhold

- Introduktion
- Faldgruber ved off-line testning
- **Off-line plade-tribo-testning**
- Eksempel på analyse af konkret produktion
- Off-line test resultater
- Produktionstest resultater, sammenligning med off-line test
- Konklusion

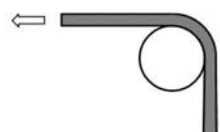
15

E. Ceron, N. Bay

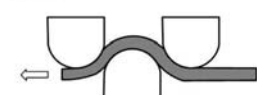
Niels Bay, Ermanno Ceron – Off-line testning af friktion og smøring i pladeformgivning
Dansk Metallurgisk Selskabs Vintermøde, Kolding, Januar 2013

New, universal sheet tribotester

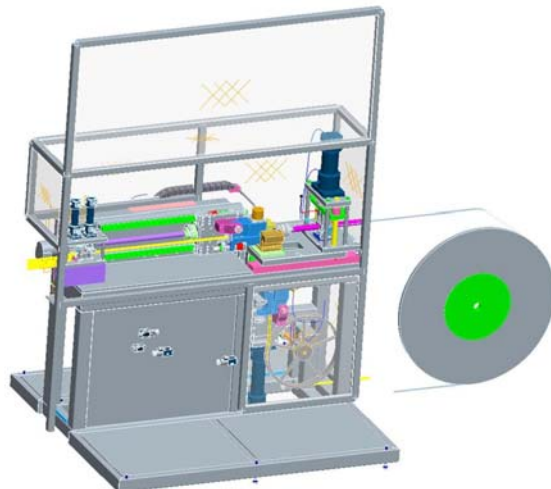
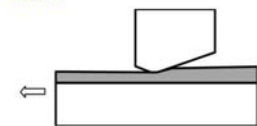
BUT



DBT



SRT



16 E. Ceron, N. Paldan,
 J. Gregersen, N. Bay

Niels Bay, Ermanno Ceron – Off-line testning af friktion og smøring i pladeformgivning
Dansk Metallurgisk Selskabs Vintermøde, Kolding, Januar 2013

Universal sheet tribo-tester

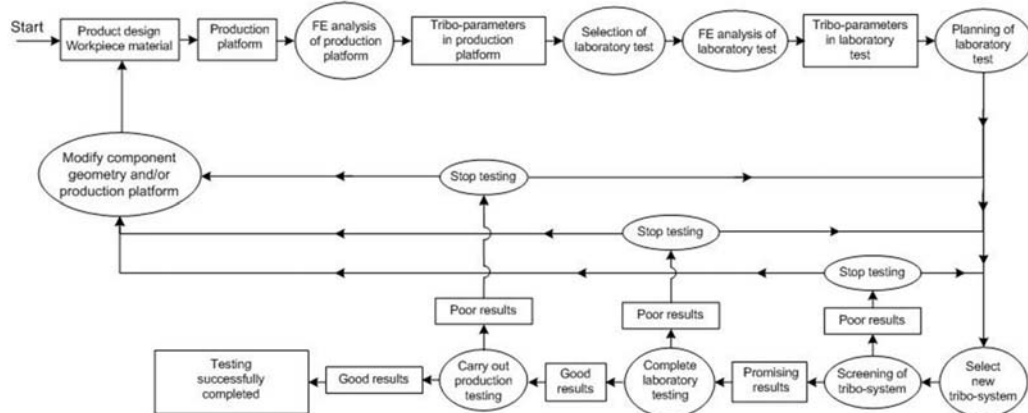
- Automatic PLC controlled running of repeated tests
 - Material feed from coil of more than 1000m
 - Adjustable sliding lengths, speed, cycle time and total number of strokes
 - Ensuring appropriate emulation of production conditions with heating and cooling cycle
 - Easy programming by Labview



17

J. Gregersen, N. Bay

Methodology for predicting lubrication performance in production



E. Ceron, N. Bay

Niels Bay, Ermanno Ceron – Off-line testning af friktion og smøring i pladeformgivning
Dansk Metallurgisk Selskabs Vintermøde, Kolding, Januar 2013

Indhold

- Introduktion
- Faldgruber ved off-line testning
- Off-line plade-tribo-tester
- **Ekssempel på analyse af konkret produktion**
- Off-line test resultater
- Produktionstest resultater, sammenligning med off-line test
- Konklusion

19

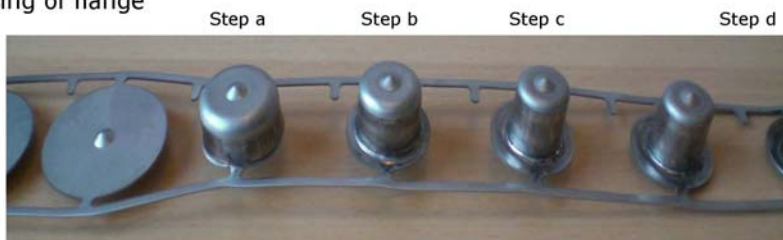
E. Ceron, N. Bay

Niels Bay, Ermanno Ceron – Off-line testning af friktion og smøring i pladeformgivning
Dansk Metallurgisk Selskabs Vintermøde, Kolding, Januar 2013

Production test example

Deep drawing in progressive tool - Grundfos

- a. Deep drawing
- b. 1st redrawing
- c. 2nd redrawing **Tribologically the most severe operation**
- d. Sharp pressing of flange



Workpiece material: EN 1.4301

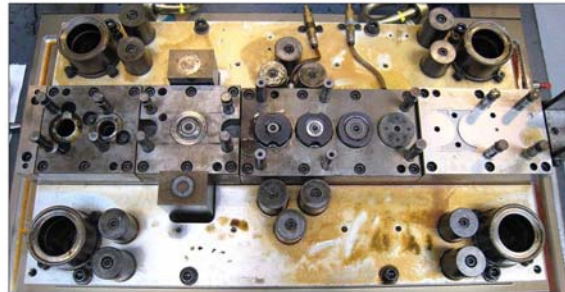
Production rate: 40 spm

Step c

E. Ceron, E. Madsen, N. Bay

Niels Bay, Ermanno Ceron – Off-line testning af friktion og smøring i pladeformgivning
Dansk Metallurgisk Selskabs Vintermøde, Kolding, Januar 2013

Deep drawing in progressive tool Grundfos

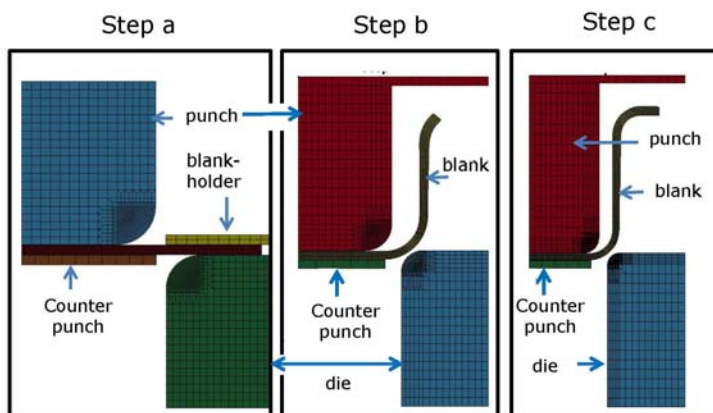


E. Ceron, E. Madsen, N. Bay

Ermanno Ceron – Off-line testning af friktion og smøring i pladeformgivning
Dansk Metallurgisk Selskabs Vintermøde, Kolding, Januar 2013

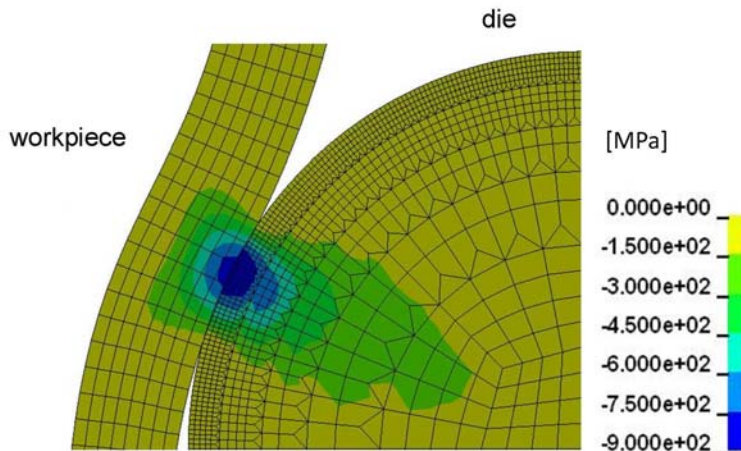
Simulation of deep drawing and 2 redrawings

- LS-DYNA 2D implicit model
- The blank is transferred from one process to the following updating flow stress and equivalent strain



Distribution of radial stress in step c

Maximum contact pressure $p_{\max} = 900 \text{ MPa}$



23 E. Ceron, N. Bay

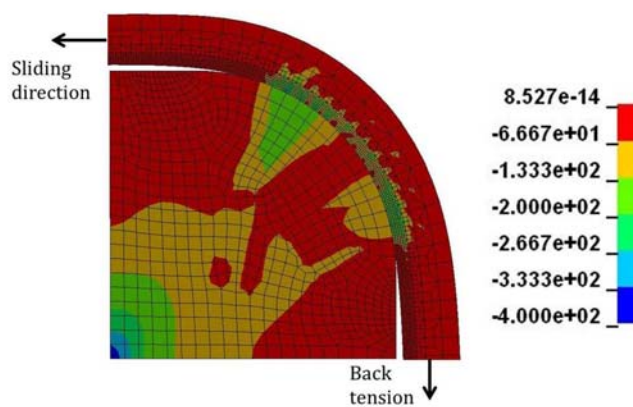
Niels Bay, Ermanno Ceron – Off-line testning af friktion og smøring i pladeformgivning
Dansk Metallurgisk Selskabs Vintermøde, Kolding, Januar 2013

Simulation of BUT test

Round pin with radius $R = 3,5$

Maximum contact pressure 360 MPa
with maximum back tension 300 MPa

(i.e. only 40% of maximum pressure in production tool)



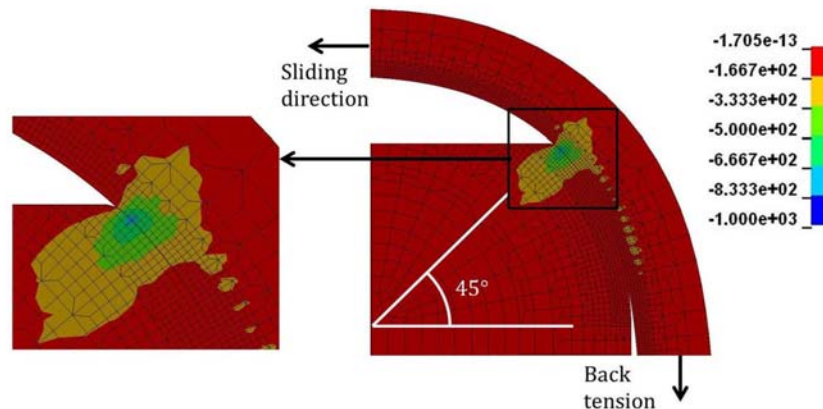
24 E. Ceron, N. Bay

Niels Bay, Ermanno Ceron – Off-line testning af friktion og smøring i pladeformgivning
Dansk Metallurgisk Selskabs Vintermøde, Kolding, Januar 2013

Distribution of radial stresses in BUT test

By modifying the BUT test tool to a 45° contact instead, sufficient contact pressure can be reached

Maximum contact pressure $p_{max} = 1000 \text{ MPa}$ with back tension 300 MPa

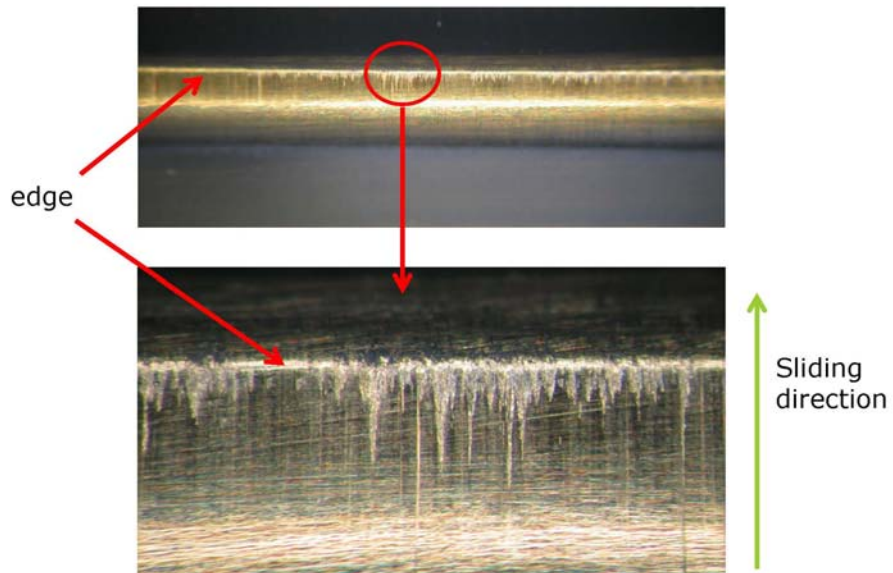


25

E. Ceron, N. Bay

Niels Bay, Ermanno Ceron – Off-line testning af friktion og smøring i pladeformgivning
Dansk Metallurgisk Selskabs Vintermøde, Kolding, Januar 2013

Lubricant film breakdown in BUT test Severe pick and galling



26

E. Ceron, N. Bay

Niels Bay, Ermanno Ceron – Off-line testning af friktion og smøring i pladeformgivning
Dansk Metallurgisk Selskabs Vintermøde, Kolding, Januar 2013

Tribo-systems investigated

Tribo-system	Workpiece material	Tool material	Lubricant
1	EN 1.4301	Vancron 40	rhenus SU 166 A
2	DP 800	Vancron 40	ANTICORIT PLS 100T
3	EN 1.4162 LDX 2101®	Vancron 40	rhenus SU 166 A

rhenus SU 166 A: mineral oil with EP additives, 160 mm²/s at 40°C

ANTICORIT PLKS 100T: mineral oil, 100 mm²/s at 40°C

27

E. Ceron, N. Bay

Niels Bay, Ermanno Ceron – Off-line testning af friktion og smøring i pladeformgivning
Dansk Metallurgisk Selskabs Vintermøde, Kolding, Januar 2013

Indhold

- Introduktion
- Faldgruber ved off-line testning
- Off-line plade-tribo-tester
- Eksempel på analyse af konkret produktion
- **Off-line test resultater**
- Produktionstest resultater, sammenligning med off-line test
- Konklusion

28

E. Ceron, N. Bay

Niels Bay, Ermanno Ceron – Off-line testning af friktion og smøring i pladeformgivning
Dansk Metallurgisk Selskabs Vintermøde, Kolding, Januar 2013

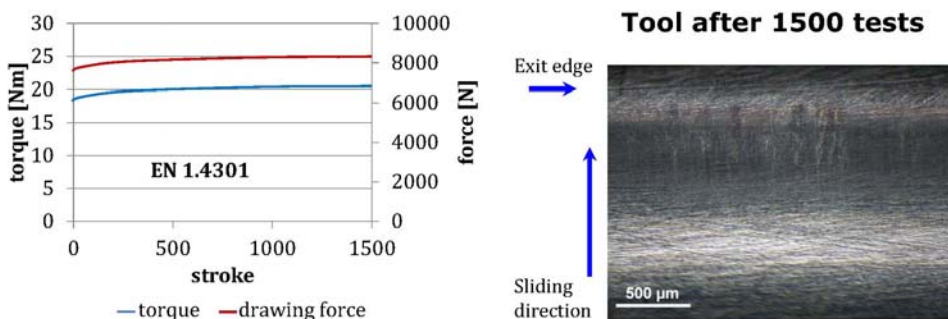
BUT test

Tribo-system 1:

Material: EN 1.4301

Lubricant: rhenus SU 166 A

Test rate: 40 and 95 spm



29

E. Ceron, N. Bay

Niels Bay, Ermanno Ceron – Off-line testning af friktion og smøring i pladeformgivning
Dansk Metallurgisk Selskabs Vintermøde, Kolding, Januar 2013

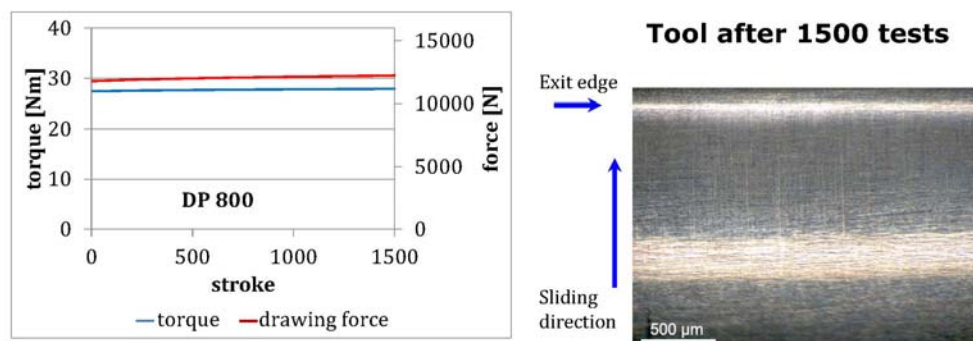
BUT test

Tribo-system 2:

Material: DP 800

Lubricant: ANTICORIT PLS 100T

Test rate: 40 and 95 spm



30

E. Ceron, N. Bay

Niels Bay, Ermanno Ceron – Off-line testning af friktion og smøring i pladeformgivning
Dansk Metallurgisk Selskabs Vintermøde, Kolding, Januar 2013

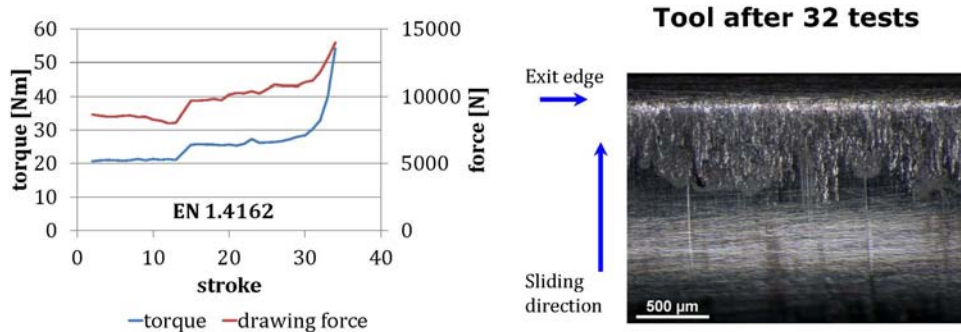
BUT test

Tribo-system 3

Material: EN 1.4162, LDX 2101®

Lubricant: rhenus SU 166 A

Test rate: 40 spm



31

E. Ceron, N. Bay

Niels Bay, Ermanno Ceron – Off-line testning af friktion og smøring i pladeformgivning
Dansk Metallurgisk Selskabs Vintermøde, Kolding, Januar 2013

Indhold

- Introduktion
- Faldgruber ved off-line testning
- Off-line plade-tribo-tester
- Eksempel på analyse af konkret produktion
- Off-line test resultater
- **Produktionstest resultater, sammenligning med off-line test**
- Konklusion

32

E. Ceron, N. Bay

Niels Bay, Ermanno Ceron – Off-line testning af friktion og smøring i pladeformgivning
Dansk Metallurgisk Selskabs Vintermøde, Kolding, Januar 2013

Production tests

Tribo-system 1

Cup No. 1500



Tribo-system 2

Cup No. 1500



Tribo-system 3

Cup No. 40



Tribo system 1 and 2: no galling even at 95 spm

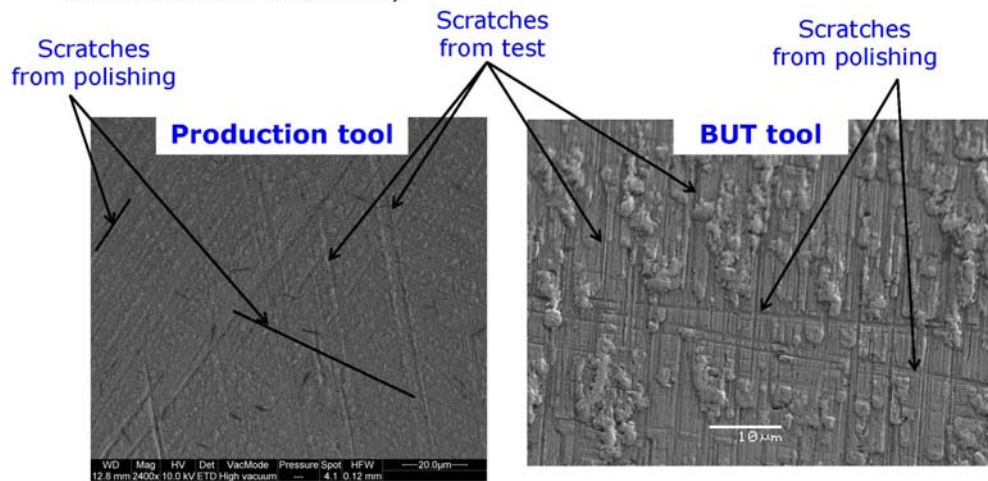
Tribo system 3: heavy galling after drawing 10 cups

E. Ceron, N. Bay

Niels Bay, Ermanno Ceron – Off-line testning af friktion og smøring i pladeformgivning
Dansk Metallurgisk Selskabs Vintermøde, Kolding, Januar 2013

SEM pictures of tools - EN 1.4301

- Few scratches on the surface
 - Slight amount of pick up can be seen like on BUT tool
 - (part in EL RØR has less chromium oxide due to previous redrawing, may cause fewer scratches on tool surface?)

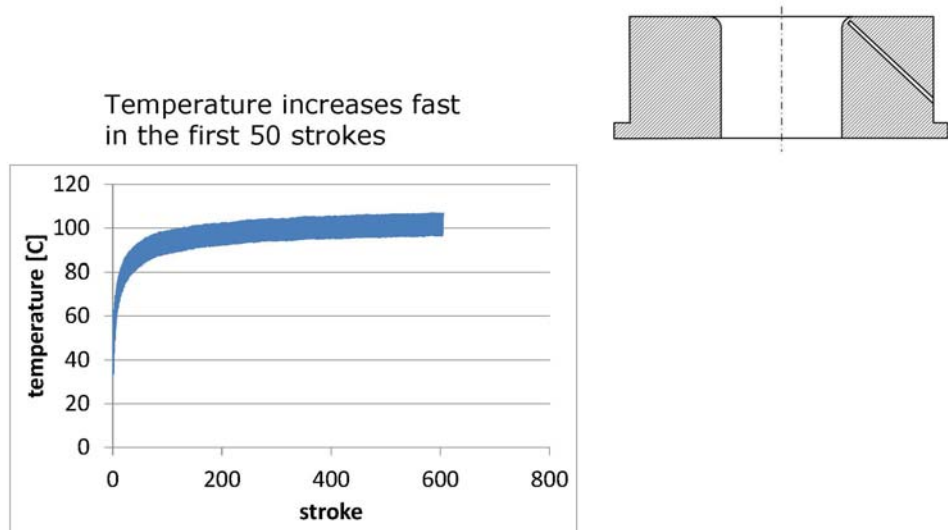


34

E. Ceron, N. Bay

Niels Bay, Ermanno Ceron – Off-line testning af friktion og smøring i pladeformgivning
Dansk Metallurgisk Selskabs Vintermøde, Kolding, Januar 2013

Tool temperature development – EN 1.4301



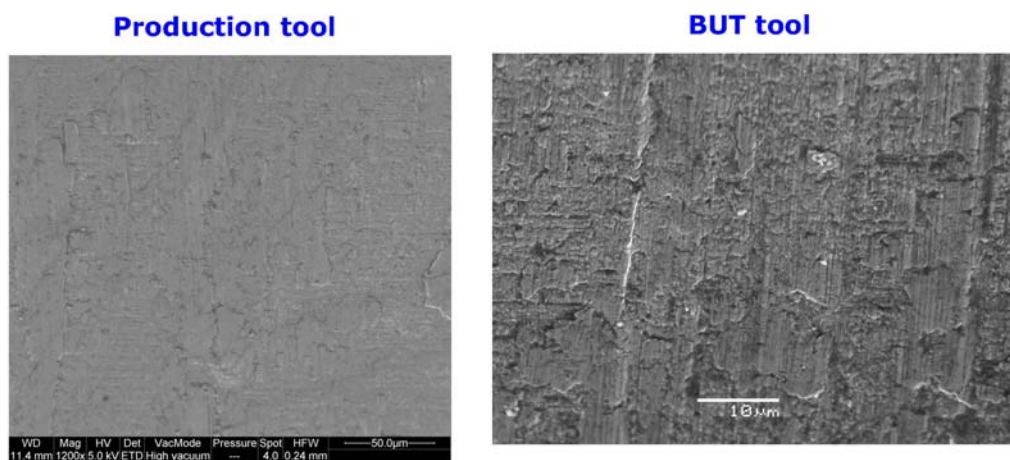
E. Ceron, N. Bay

Niels Bay, Ermanno Ceron – Off-line testning af friktion og smøring i pladeformgivning
Dansk Metallurgisk Selskabs Vintermøde, Kolding, Januar 2013

35

SEM pictures of tools – DP 800

- SEM picture of the tool surface
- Similar micro pick-up in production tool as in the BUT tool



36

E. Ceron, N. Bay

Niels Bay, Ermanno Ceron – Off-line testning af friktion og smøring i pladeformgivning
Dansk Metallurgisk Selskabs Vintermøde, Kolding, Januar 2013

Production tool 2 – LDX 2101

- Parts are not acceptable. Severe galling along rolling direction
- Pick-up occurs already in operation 2.



37

E. Ceron, N. Bay

Niels Bay, Ermanno Ceron – Off-line testning af friktion og smøring i pladeformgivning
Dansk Metallurgisk Selskabs Vintermøde, Kolding, Januar 2013

Production tool 3 – LDX 2101

- Pick-up occurs also in operation 3



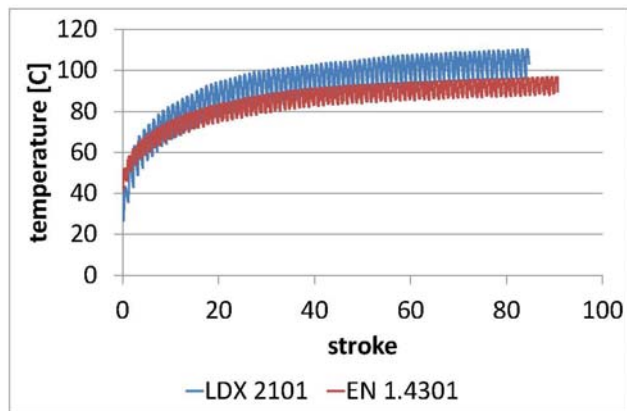
38

E. Ceron, N. Bay

Niels Bay, Ermanno Ceron – Off-line testning af friktion og smøring i pladeformgivning
Dansk Metallurgisk Selskabs Vintermøde, Kolding, Januar 2013

Tool temperature development

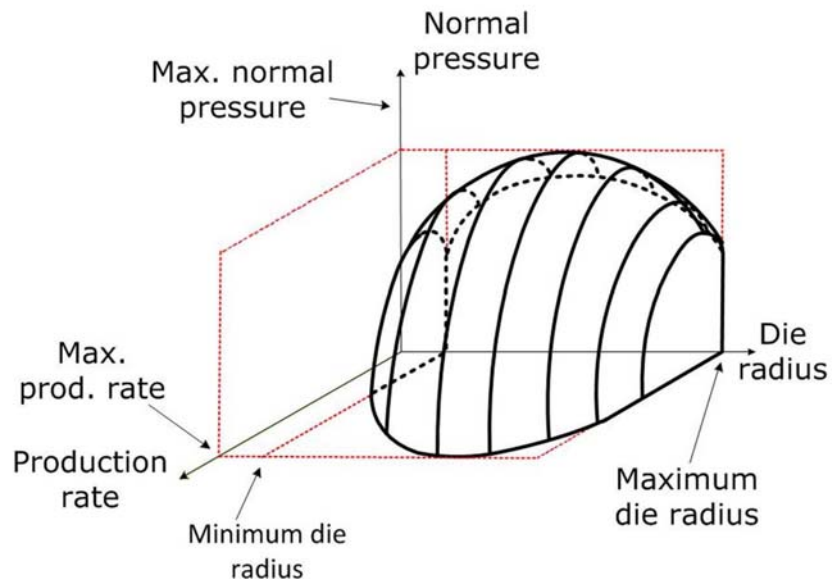
Comparison between LDX and EN 1.4301



39 E. Ceron, N. Bay

Niels Bay, Ermanno Ceron – Off-line testning af friktion og smøring i pladeformgivning
Dansk Metallurgisk Selskabs Vintermøde, Kolding, Januar 2013

Evaluation of a tribo-system for deep drawing production

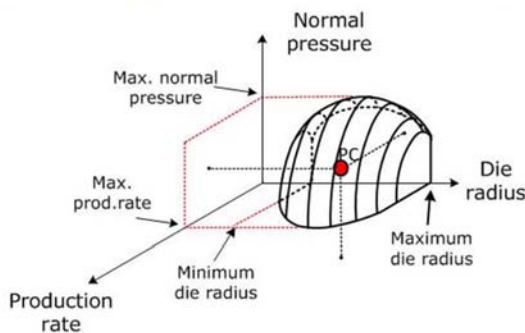


40 E. Ceron, N. Bay

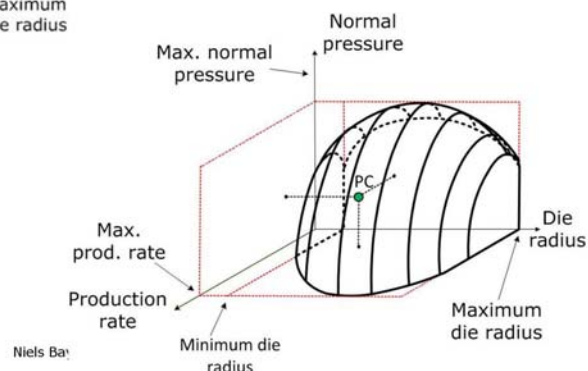
Niels Bay, Ermanno Ceron – Off-line testning af friktion og smøring i pladeformgivning
Dansk Metallurgisk Selskabs Vintermøde, Kolding, Januar 2013

Evaluation of a tribo-system for deep drawing production

Poor tribo-system production point above threshold surface



Promising tribo-system Production point below threshold surface



E. Ceron, N. Bay

41

Niels Bay

Conclusion – differences between production and laboratory

	Production	Laboratory
Work hardening	High (max strain = 2)	Low (max strain = 0,2)
Surface topography	Completely different from original	Original
Normal pressure	≈ 1000 MPa	≈ 1000 MPa but smaller contact area
Initial specimen temperature	$\approx 110^\circ\text{C}$	25°C
Temperature developed in the specimen	$\approx 200^\circ\text{C}$	$\approx 90-100^\circ\text{C}$
Temperature developed in the tool	$\approx 110^\circ\text{C}$ (EN1.4301)	$\approx 45^\circ\text{C}$ (EN1.4301)
Sliding speed	100-150mm/s	50mm/s
Thermal exchange	No workpiece/tool contact during idle time	workpiece/tool contact during idle time

42

E. Ceron, N. Bay

Niels Bay, Ermanno Ceron – Off-line testning af friktion og smøring i pladeformgivning
Dansk Metallurgisk Selskabs Vintermede, Kolding, Januar 2013

Indhold

- Introduktion
- Faldgruber ved off-line testning
- Off-line plade-tribo-tester
- Eksempel på analyse af konkret produktion
- Off-line test resultater
- Produktionstest resultater, sammenligning med off-line test
- **Konklusion**

43

E. Ceron, N. Bay

Niels Bay, Ermanno Ceron – Off-line testning af friktion og smøring i pladeformgivning
Dansk Metallurgisk Selskabs Vintermøde, Kolding, Januar 2013

Konklusion

Metodik til forudsigelse af smøremiddel performance i produktion

- Numerisk modellering af produktionsbetingelser
- Valg af simulativ test
- Numerisk modellering af simulativ test
- Off-line testning
- Produktions testning

Miljøvenlige alternativer til kloreret paraffinolie

- rhenus SU 166 A

44

E. Ceron, N. Bay

Niels Bay, Ermanno Ceron – Off-line testning af friktion og smøring i pladeformgivning
Dansk Metallurgisk Selskabs Vintermøde, Kolding, Januar 2013

END

Niels Bay, Ermanno Ceron – Off-line testning af friktion og smøring i pladeformgivning
Dansk Metallurgisk Selskabs Vintermøde, Kolding, Januar 2013

45

Industriens udnyttelse af de store internationale røntgen neutronfaciliteter

Henning Friis Poulsen, DTU Fysik

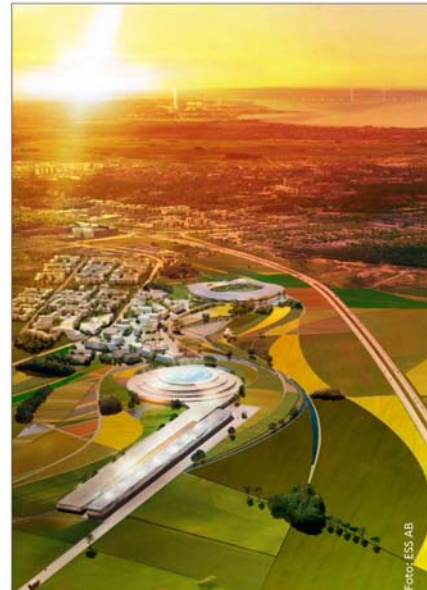
Industriens udnyttelse af de store internationale Røntgen og neutron faciliteter

Hening Friis Poulsen, DTU Fysik
hfp@fysik.dtu.dk

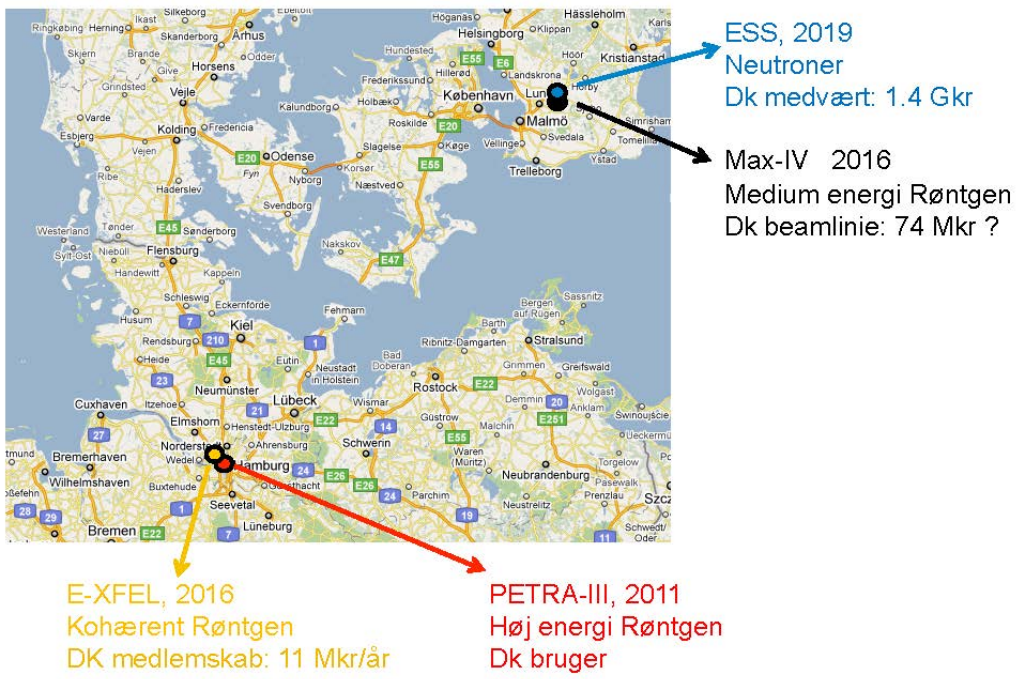


ESS & MAX-IV

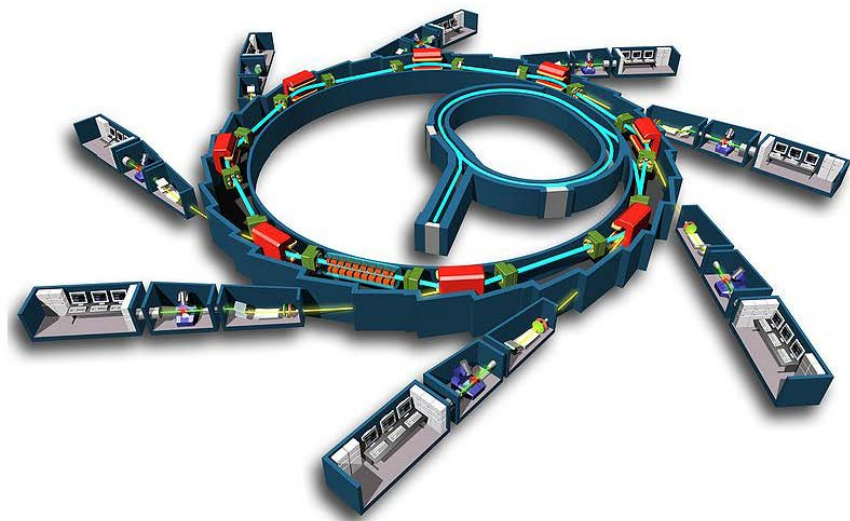
- ESS og MAX IV i Lund
 - ESS (2019), verdens bedste neutronkilde, finansieret af 17 europæiske lande (ca. 1,5 mia. euro)
 - MAX IV (2015), synkrotron, svensk finansieret (500 mio. euro)
- Det danske bidrag
 - ESS: 1.4 Mia kroner + 12.5% drift
 - Data Management Center i Kbh (62 ansatte)
 - MAX-IV: Dansk beamlinie (74 Mkr) ?
- Science parks omkring Lund og Københavnsområdet



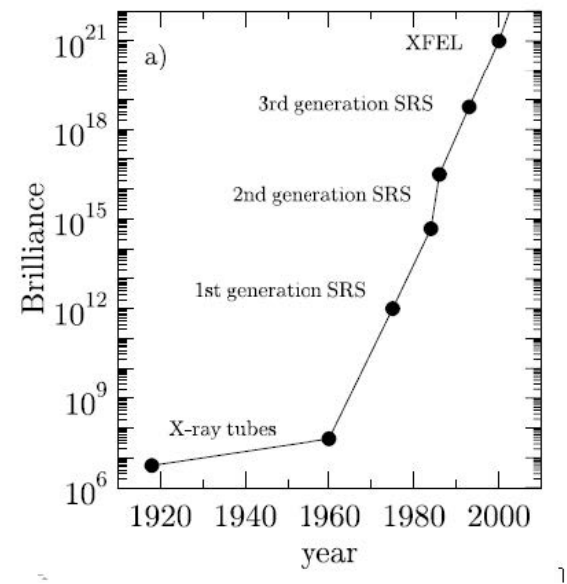
Verdens største mikroskop



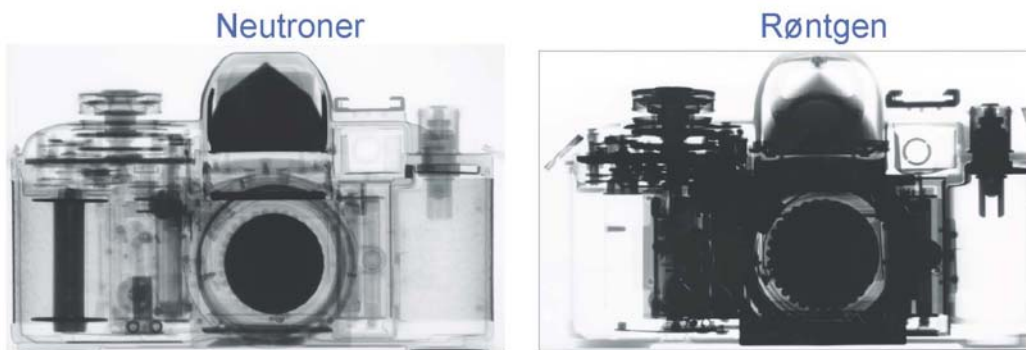
Hvad er en synktron?



Hvorfor bruge en synkrotron?



Forskel i tværsnit



Ser: H, C, O,

Ser: høje Z-numre

Virksomheder som brugere af store faciliteter

Udfordringer:

- Manglende kendskab og ekspertise
- Ventetid og usikkerhed omkring måletid
- "Data analysen koster en halv PhD"

Haldor Topsøe, Astra Zeneca, Novo Nordisk, Carlsberg .. er stærkt involveret

Mulige danske løsninger:

- Strategiske partnerskaber
- Portaler/science hubs

Individuelle løsninger:

- Opsøg akademiske partnere
- Ansæt erhvervs-PhD studerende
- Science Link



SCIENCE LINK
Part-financed by the European Union (European Regional Development Fund)

A banner for SCIENCE LINK. It features the text "SCIENCE LINK" in large white letters, followed by "Part-financed by the European Union (European Regional Development Fund)". To the right of the text is a small photograph of a scientific facility, likely a particle accelerator or similar equipment.

SCIENCE LINK opens up research facilities for commercial R&D purposes

Partners:

MAX-lab, Lund
Desy, Hamburg
HZG & HZB, Berlin

DTU is Danish representative

Offers:

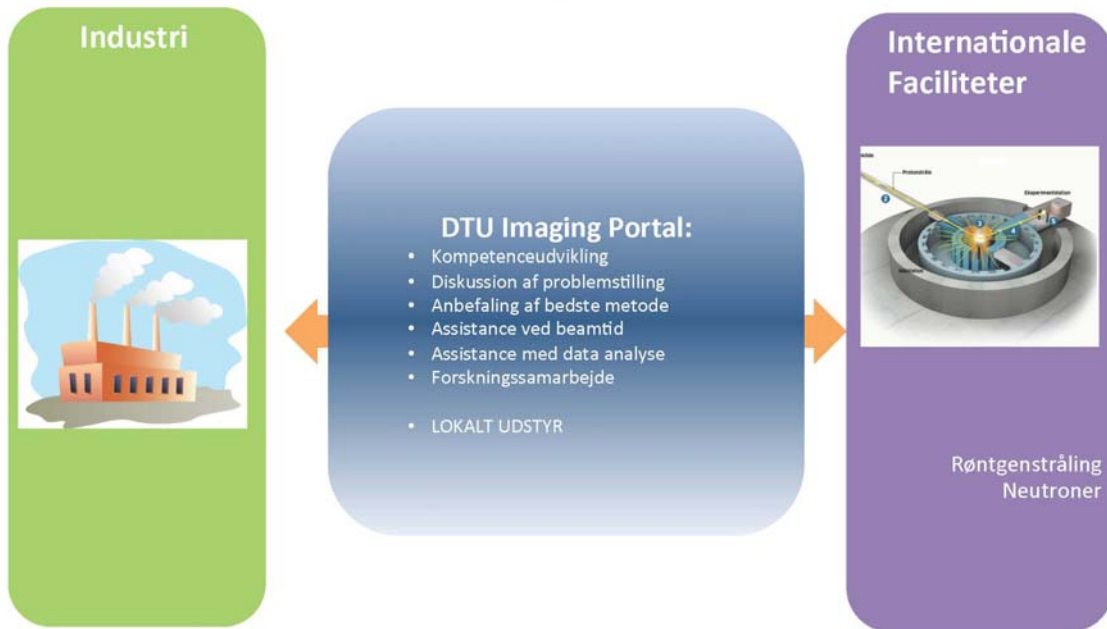
- Access to beamtime for industry
- Consultant for preparing, and executing beamtime
- Help with analyzing data

Contact: Martin Meedom Nielsen

DTU Physics
Phone: 51801561
mmee@fysik.dtu.dk



DTU som science hub/ portal for 3D imaging af materialer



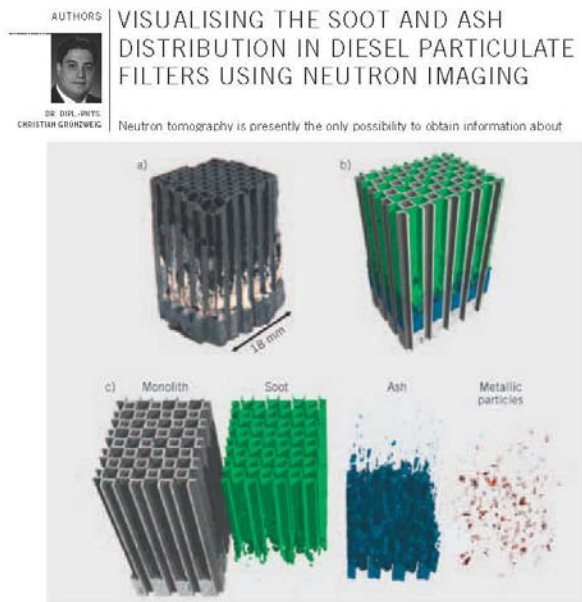
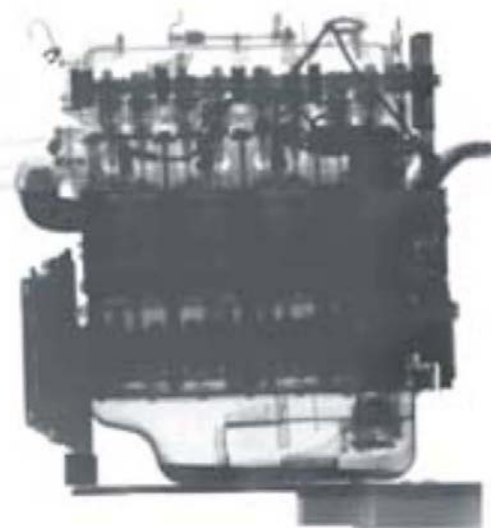
3D Imaging center



Best practice: University of Manchester

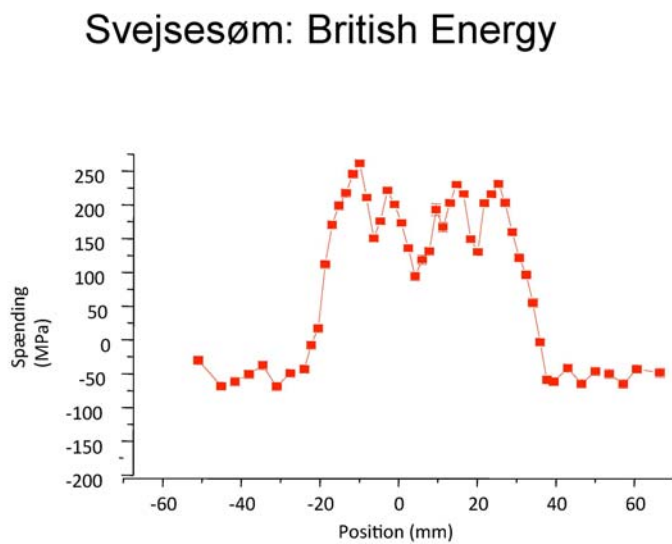
Strukturfondsprojekt (2013-2014): ESS og MAX-IV som vækstmotorer i regionen

Neutron Imaging



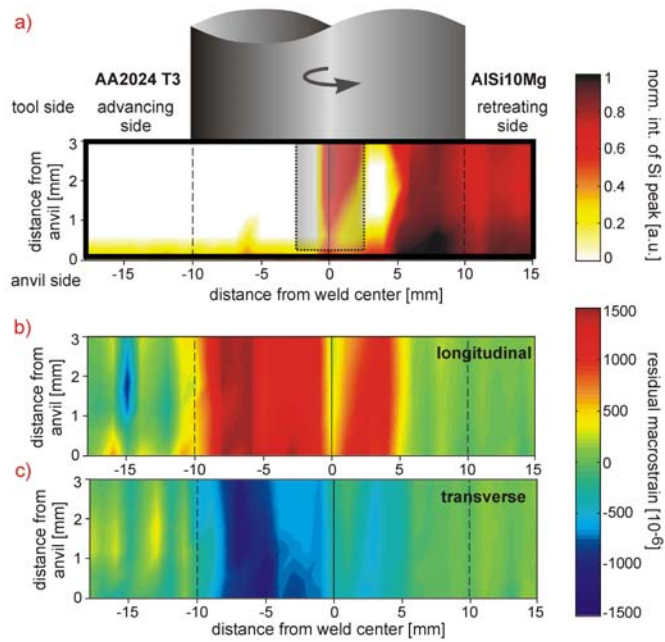
Courtesy: PSI, HMI/HZB, FRM2

Residual Spændinger

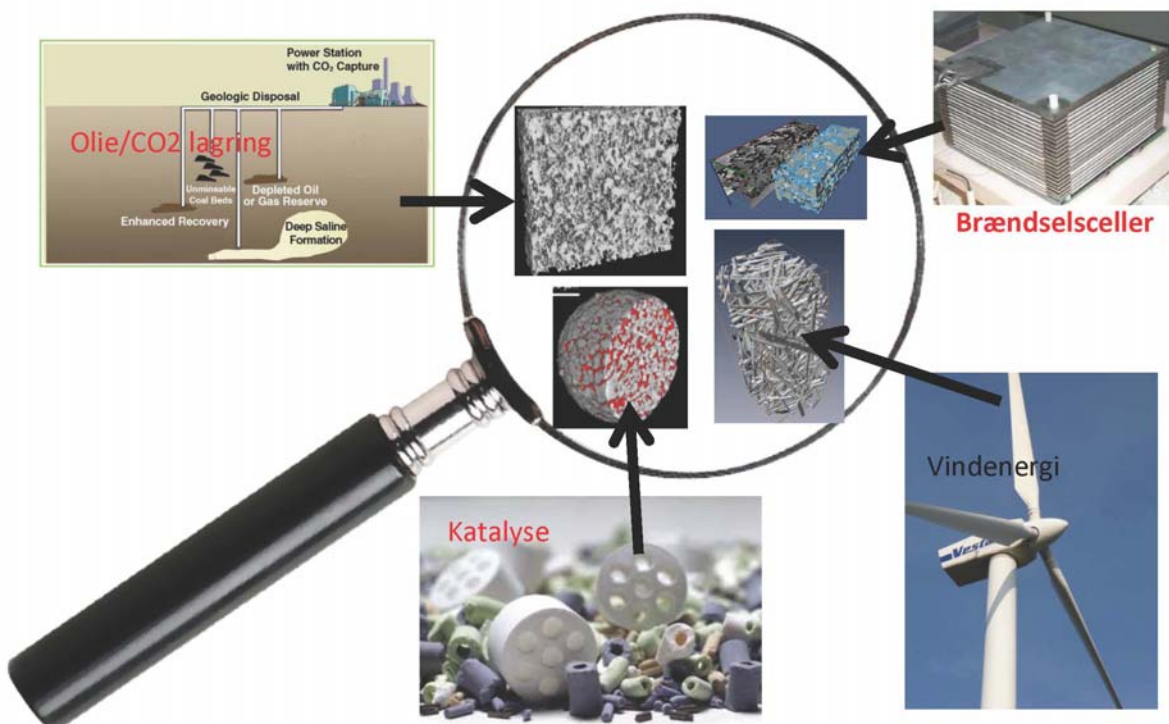


Courtesy: Open University, UK

3D strain map of friction stir weld



3D imaging af energimaterialer



Fase kontrast tomografi af Al folie

Materiale: Alcan Al folie

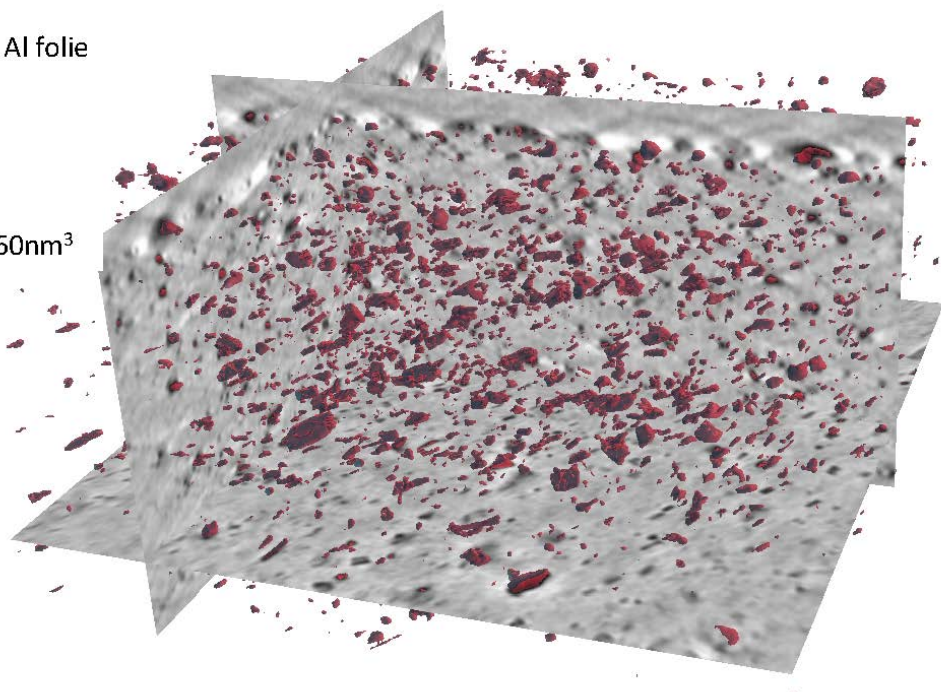
Type: Al8079

Energi: 17.5 keV

Volumen:

90x90x48 μm^3

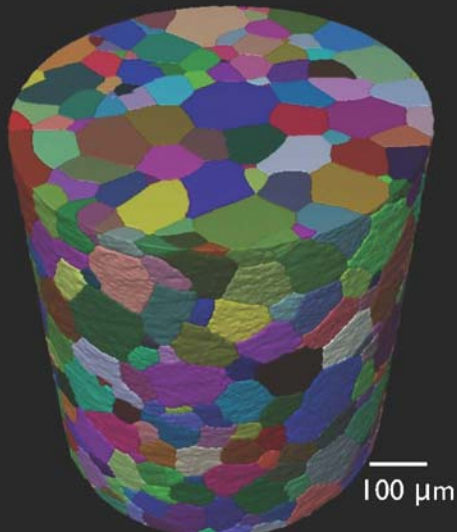
Voxel størrelse: 60nm 3



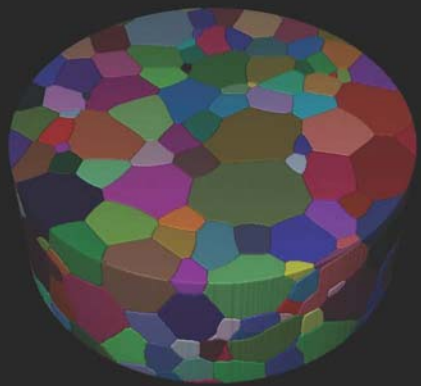
Slide fra P. Cloetens, ESRF

Kornvækst i Titanium

Eksperimentelt



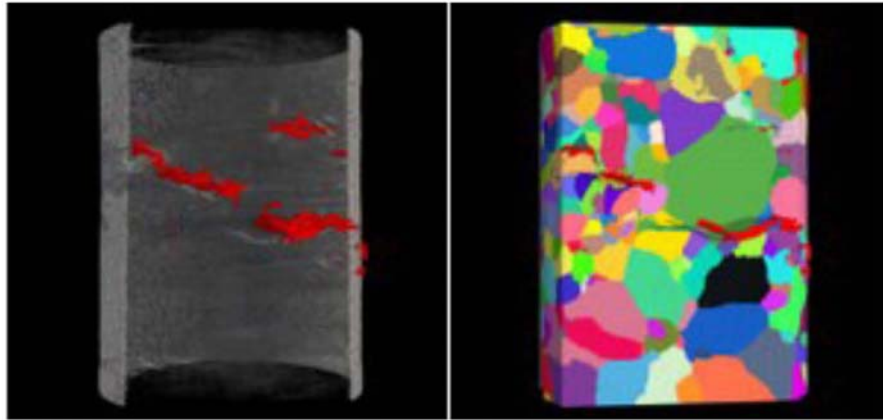
Phase field simuleringer



Risø: E.M. Lauridsen, S. Poulsen, A. Lyckegaard.
Northwestern: P. Voorhees, I. McKenna

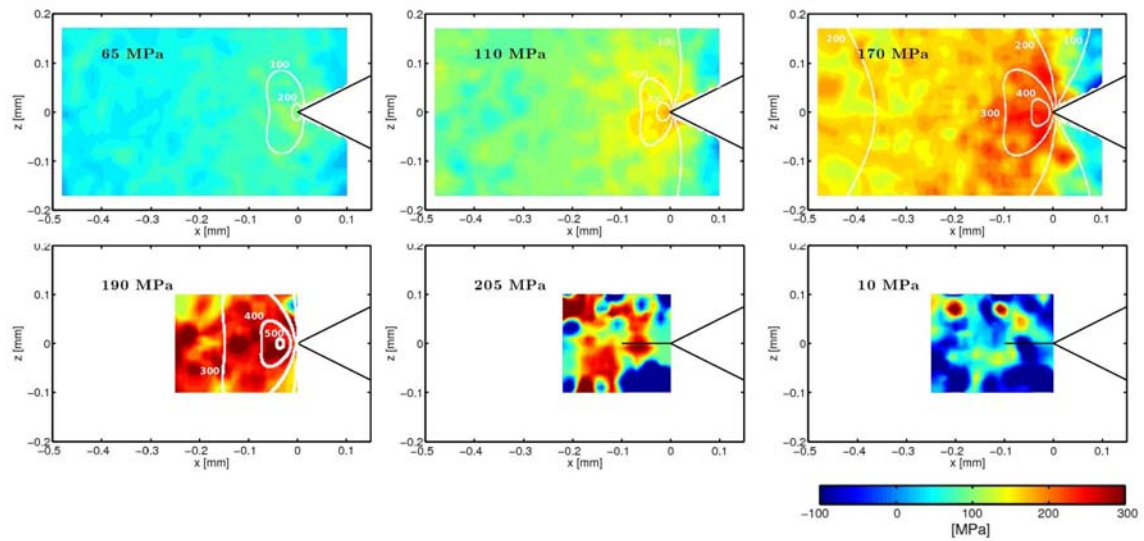
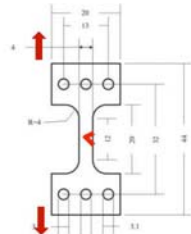
Navy Research Lab: R. Fonda
ESRF: W. Ludwig, A. King, S. Rolland

Stress corrosion revnedannelse i stål



A. King, G. Johnson, D. Engelberg, W. Ludwig, and J. Marrow, *Science* (2008) 321, 382 - 385

Spændinger omkring revnespids i Mg



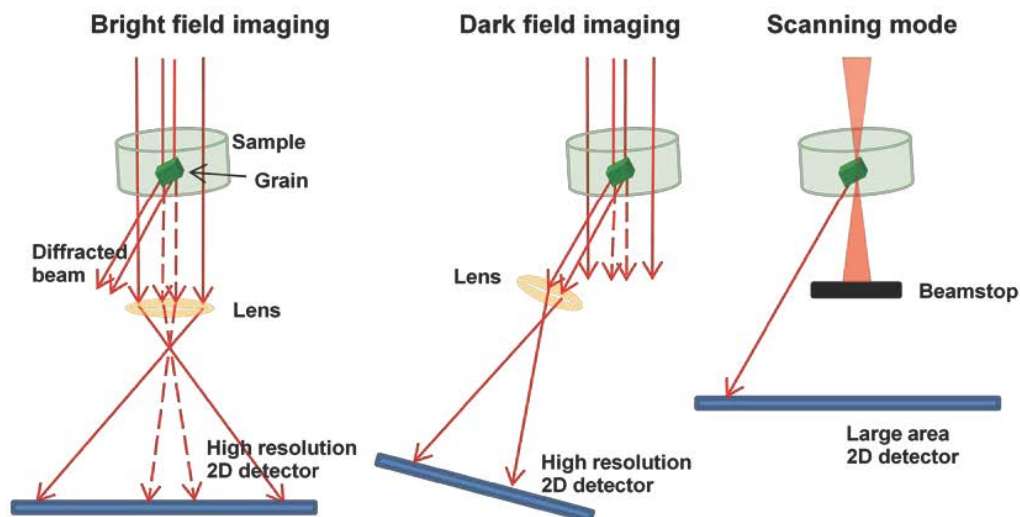
J. Oddershede, B. Camin, S. Schmidt, L.P. Mikkelsen, H.O. Sørensen, U. Lienert, H.F. Poulsen, W. Reimers. *Acta Mater.* **60**, 3570-3580 (2012).

diffraktions baseret
TEM TXM



Opløsning:	1 Å	20-30 nm
Tykkelse:	1 korn in 2D	1000 korn in 4D
Orienteringer:	0.01-0.1 grad	0.001 – 0.1 grad
Spændinger:	(indirekte)	direkte

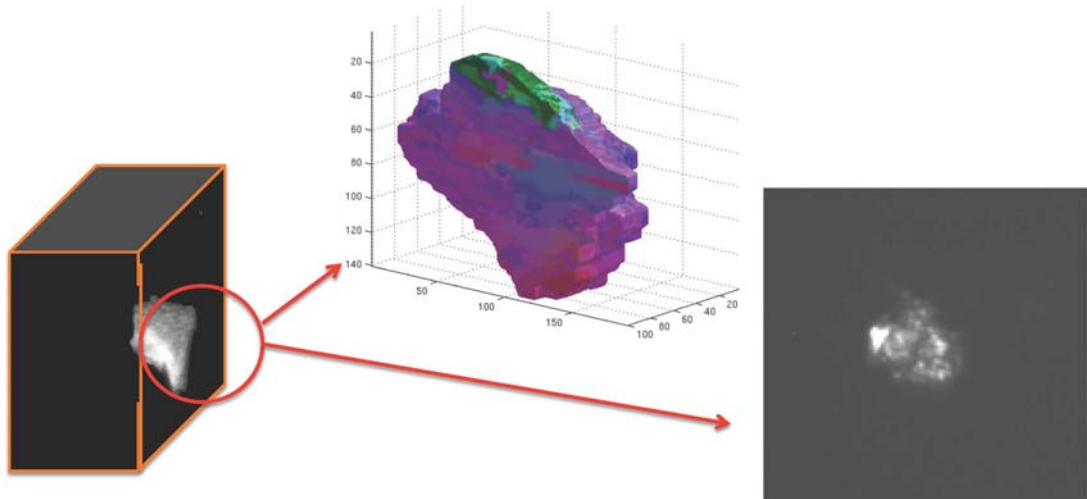
Diffraktions baseret Transmission Røntgen Mikroskopi



Arbejdsgruppe:

DTU: H.F. Poulsen, E.M. Lauridsen, S. Schmidt, W. Pantleon, J. Oddershede, Y. Zhang, H. Simons, J. Hübner, F. Jense
ESRF: A. Snigirev, I. Snigireva, W. Ludwig, A. King, C. Detlefs.

Mikroskopi



2 μm
0.5 deg

200 nm
0.15 deg

200 nm
0.01 deg

Arbejdsgruppe:

DTU: H.F. Poulsen, E.M. Lauridsen, S. Schmidt, W. Pantleon, J. Oddershede, Y. Zhang, H. Simons, J. Hübner, F. Jense
ESRF: A. Snigirev, I. Snigireva, W. Ludwig, A. King, C. Detlefs.

Studier af rekrySTALLisation med 3DXRD

Dorte Juul Jensen

Studier af rekrystallization med 3DXRD

D. Juul Jensen



Risø campus

$$f(x+\Delta x) = \sum_{i=0}^{\infty} \frac{(\Delta x)^i}{i!} f^{(i)}(x)$$
$$\int_a^b \Theta + \Omega \int \delta e^{i\pi} = \{2.7182818284\}$$
$$\Sigma!$$

DTU Wind Energy
Department of Wind Energy

Staff

MAC

KOM

**Senior scientists
(incl emerit.)**

7

8

Scientists

3

0

Engineers

0

6

Postdocs

3

3

PhD students

3

5

Technicians

3

7

Secretary

1

1

Guest scientists

3

1

DTU Wind Energy, Technical University of Denmark

Aim for Materials Science and Advanced Characterization (MAC) section



To perform materials science and development on a high international level with focus in particular on materials and components for wind energy applications

To advance existing techniques and to implement new characterization techniques and data analysis tools to match the needs of the scientific and engineering projects

Covering the whole range from basic science to applications

Work on length scales from nanometer to meter

DTU Wind Energy, Technical University of Denmark

DTU Wind Energy



Sections



Composites and Materials Mechanics
Materials Science and Advanced Characterization
Fluid Mechanics
Test and Measurement
Wind Turbines
Aeroelastic Design
Meteorologic Section
Wind Energy Systems

DTU Wind Energy, Technical University of Denmark

DTU Wind Energy



WIND ENERGY SYSTEMS

Wind resources and siting
Wind power integration and control
Offshore wind energy
Wind energy and society

WIND TURBINE TECHNOLOGY

Aeroelastic design
Structural design and safety
Mechanical components
Electro-technical components

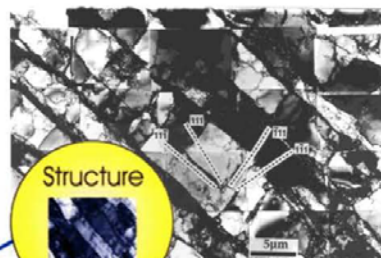
BASICS FOR WIND ENERGY

Aero and hydrodynamics
Boundary-layer meteorology and turbulence
Light, strong materials
Remote sensing and measurement technology

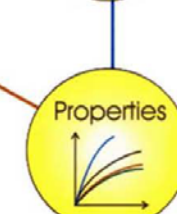
DTU Wind Energy, Technical University of Denmark



Processing



Structure



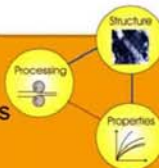
Properties



DTU Wind Energy, Technical University of Denmark



Materials:
Light and strong metals and alloys
Steels
Nanostructured materials



- Processing

Rolling, extrusion, etc.
Very high strain: ARB, DPD HPT
Annealing



- Structure

Advanced electron microscopy
Advanced x-ray characterization
Serial sectioning



- Properties

Mechanical testing (KOM)
Calometry
Hardness
Physical properties

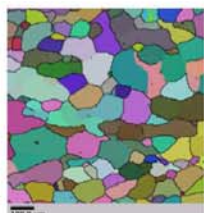


DTU Wind Energy, Technical University of Denmark

Electron microscopes @ DTU Wind Energy



3 SEM & 3 TEM



ZEISS SUPRA 35

JEOL JMS-840

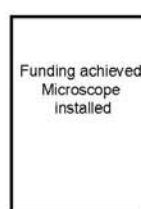
ZEISS EVO 60



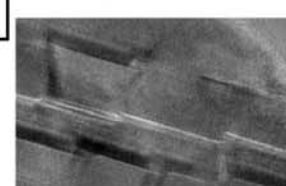
JEOL JEM-3000F



JEOL JEM-2000FX

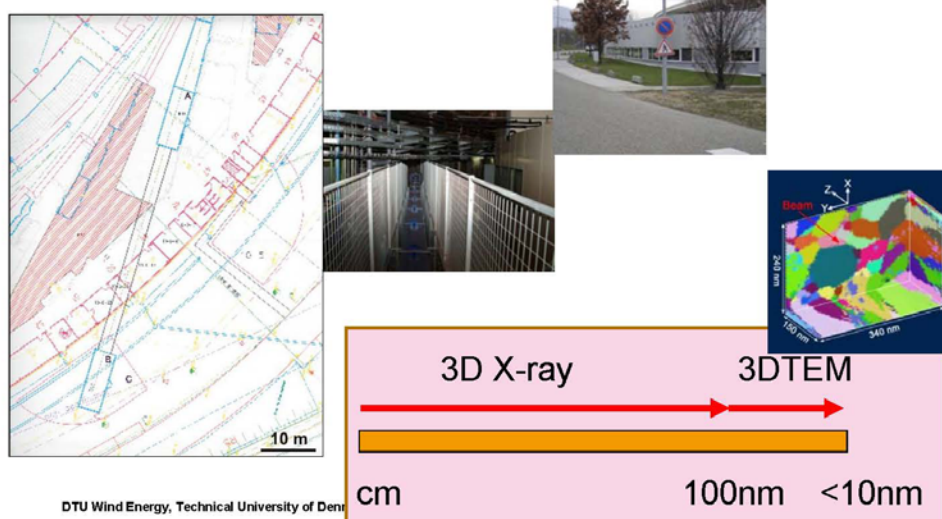


200 kV



DTU Wind Energy, Technical University of Denmark

3D X-ray microscopes at ESRF in France, APS in USA and Hasylab in Germany



Hard and wear resistant steel components

- Characterize structure to determine stress and strain gradients as input for numerical modelling of e.g. friction and wear
- Develop reliable testing techniques (e.g. microsamples) to analyse structure and properties of components damaged by impact, wear or fatigue

Light and strong metals and alloys

- Optimize strength and formability by thermomechanical processing – bulk samples and multilayers
- Advance analytical and numerical modelling of recovery and recrystallization through 2D and 3D characterization

Technique development

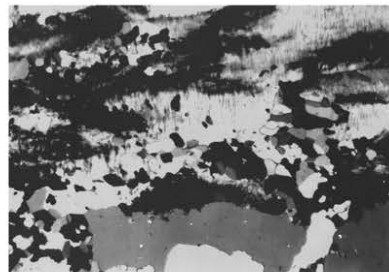
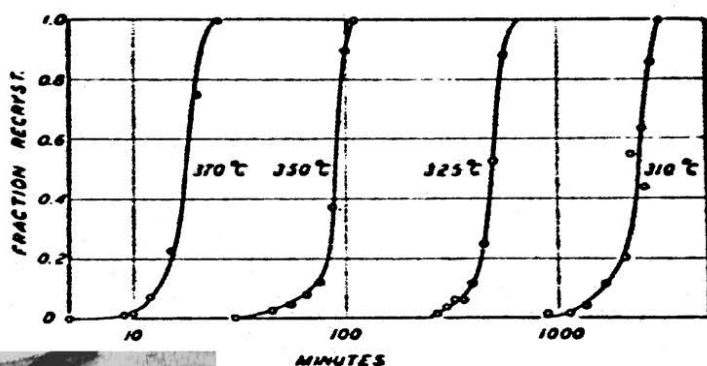
- Implement and develop techniques for characterization of damaged samples (incl lab residual stress measurements)
- Develop techniques for optimizing metals including surface hardening
- Superusers of all relevant 3D/4D techniques with focus on research results

DTU Wind Energy, Technical University of Denmark

Recrystallization Kinetics

DTU Wind Energy, Technical University of Denmark

Recrystallization kinetics - standard measurements



W.A. Anderson and R.F. Mehl: Trans. AIME, 1945, 161, 140-172.

Recrystallization Kinetics – Standard model

Assuming:

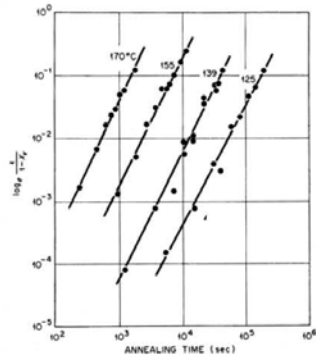
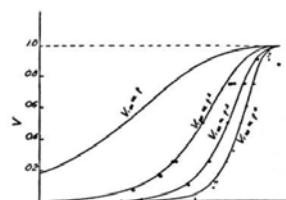
- Random distribution of nucleation sites
- All grains grow with the same time-independent growth rate
- All nuclei develop at $t = 0$ or as a linear function of t

$$V_v = 1 - \exp(-Bt^k)$$

t
B, k

Time

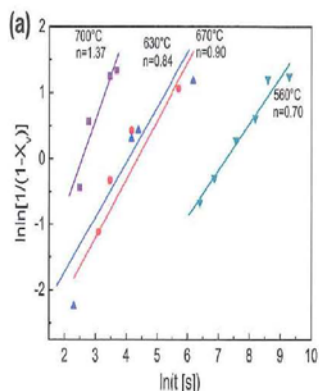
Constants related to nucleation rate,
growth rate and dimensionality of growth



DTU Wind Energy, Technical University of Denmark

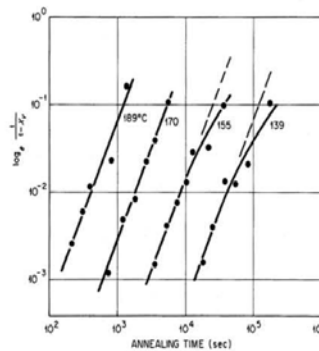
Experimental results - examples

Problems



Yaping Lü, Dmitri A. Molodov, Günter Gottstein, Acta Mat. 59 (2011) 3229-3243

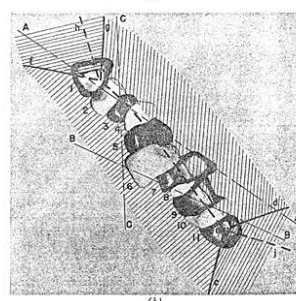
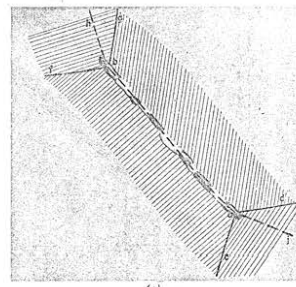
DTU Wind Energy, Technical University of Denmark



R.A. Vandermeer and P. Gorden: in 'Recovery and recrystallization of metals', (ed. L. Himmel), Interscience New York, 1963, 211-240

Clustered nucleation

Optical microscopy combined with serial sectioning



R.A. Vandermeer and P. Gorden: Trans. TMS-AIME, 1959, **215**, 577-588.

DTU Wind Energy, Technical University of Denmark

JMAK model

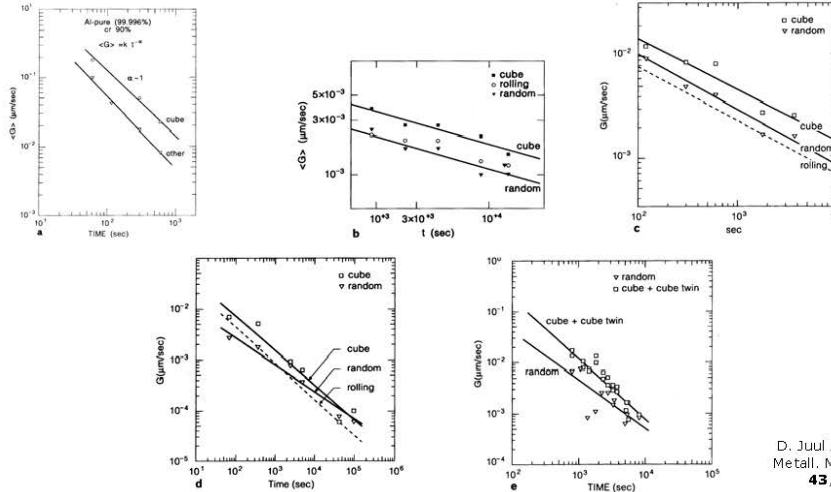
Assuming:

- Random distribution of nucleation sites
- All grains grow with the same time-independent growth rate
- All nuclei develop at $t = 0$ or as a linear function of t

DTU Wind Energy, Technical University of Denmark

Experimental methods and results

Average growth rates – time and orientation dependencies



D. Juul Jensen: Acta Metall. Mater., 1995,
43, 4117-4129.

DTU Wind Energy, Technical University of Denmark

Growth rates

- All grains grow with the same time-independent growth rate
- On average grains grow as $\langle G \rangle = k \cdot t^{-\alpha}$ or they have a fast decreasing growth rate followed by a period of constant growth and on average, cube grains often grow faster than other grains
- What do individual grains do?

DTU Wind Energy, Technical University of Denmark

3D X-ray Diffraction (3DXRD)

3D Microscope for in-situ characterization of recrystallization kinetics

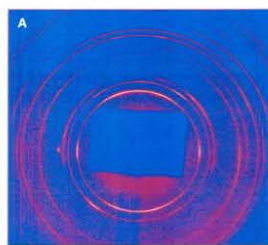
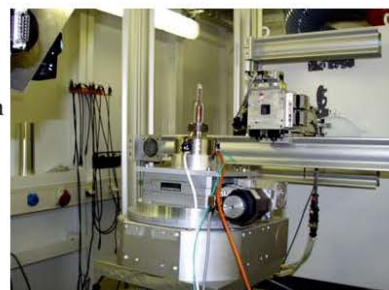
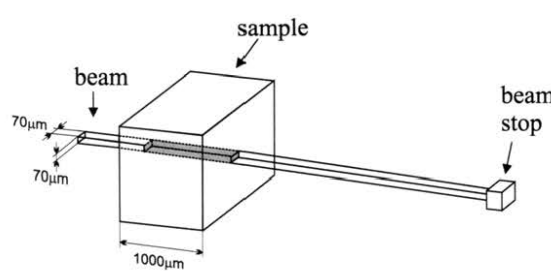


- Sub- μm spatial resolution
- Bulk penetration (0.1 mm – 1 cm)
- Non-destructive
- Fast measurements (seconds – minutes)

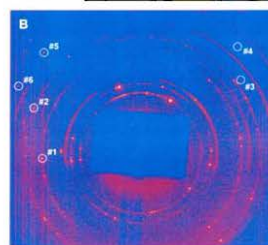


DTU Wind Energy, Technical University of Denmark

Recrystallization kinetic measurements



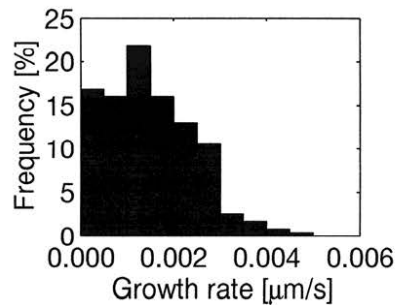
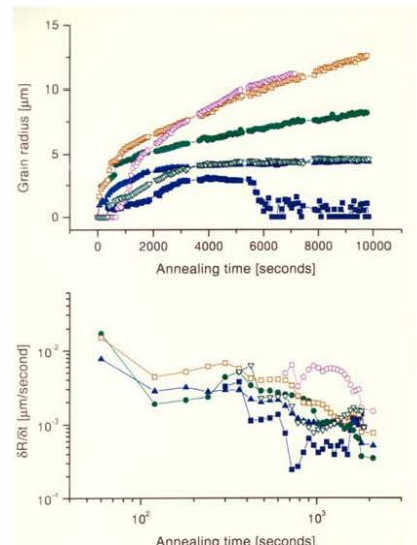
T = 0 min



T = 162 min

DTU Wind Energy, Technical University of Denmark

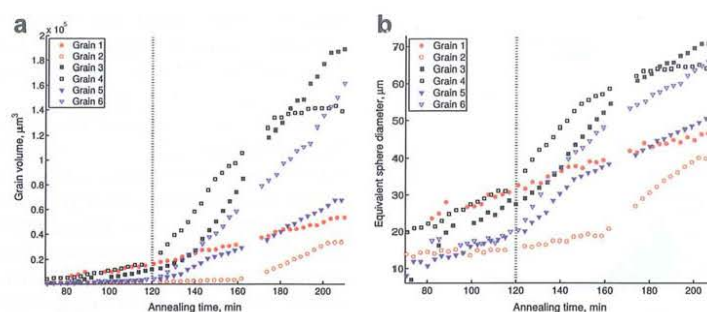
Al (AA 1050) cr 90%



E.M. Lauridsen, H.F. Poulsen, S.F. Nielsen and D. Juul Jensen: Acta Mater., 2003, **51**, 4423-4435
E.M. Lauridsen, D. Juul Jensen, H.F. Poulsen and U. Lienert: Scripta Mater., 2000, **43**, 561-566

DTU Wind Energy, Technical University of Denmark

Al (AA 1050) cr 50%



S.O. Poulsen et al. (2011)
Scripta Mater. **64**, 1003-1006.

DTU Wind Energy, Technical University of Denmark

Grain averaged activation energy for individual grains determined by 3DXRD



$$v = M \cdot F$$

$$v = M_0 \exp\left(-\frac{Q}{RT}\right) F$$

$$Q = R \left(\frac{1}{T_1} - \frac{1}{T_2} \right) \ln \frac{v_2}{v_1}$$

v	Growth rate
M	Mobility
F	Driving force
R	Gas constant
T	Absolute temperature
Q	Activation energy

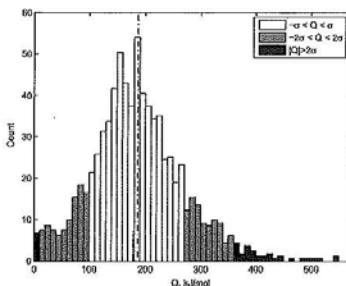
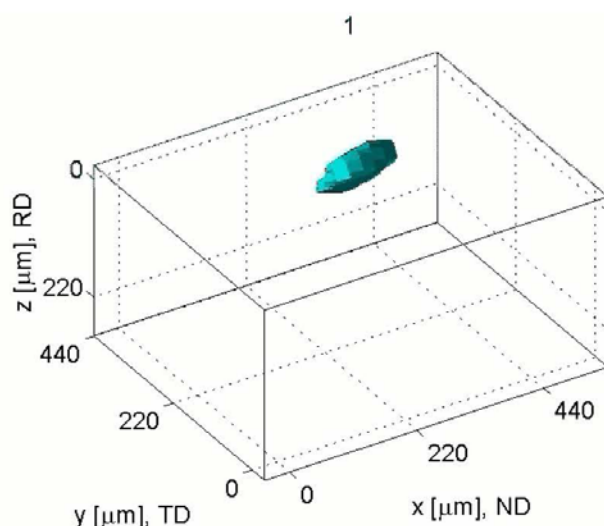


Figure 2. Distribution of grain-averaged activation energies. The mean of the distribution, $\langle Q \rangle = 187 \text{ kJ mol}^{-1}$, is indicated by the vertical line. The standard deviation is $\sigma = 82.9 \text{ kJ mol}^{-1}$, and the 1σ and 2σ confidence intervals are indicated by the colour of the bars.

S.O. Poulsen et al. (2011)
Scripta Mater. **64**, 1003-1006

DTU Wind Energy, Technical University of Denmark

Grain growth during recrystallization in weakly rolled aluminum single crystal



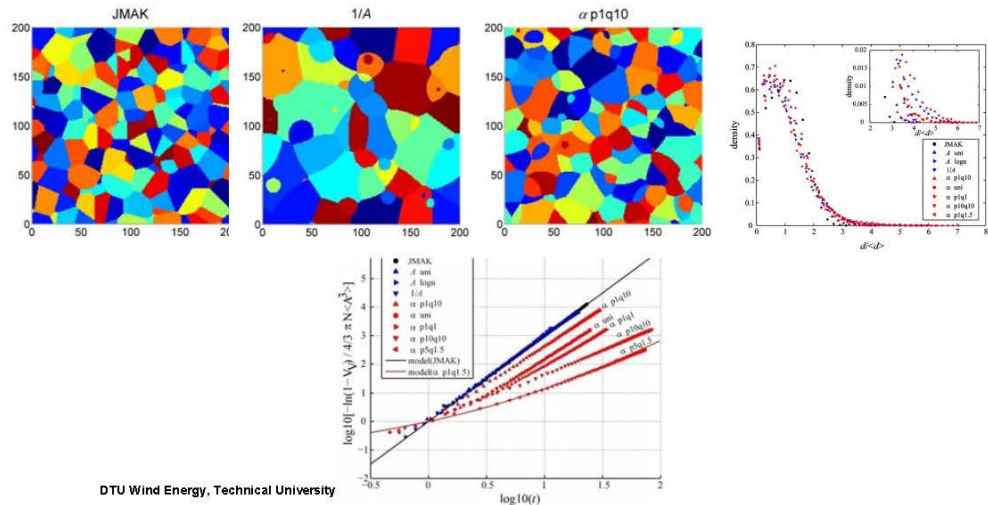
Schmidt, S., Nielsen, S.F., Gundlach, G., Margulies, L., Huang, X., Juul Jensen, D., Science, 2004, 229-232.

DTU Wind Energy, Technical University of Denmark

Simulations of effects of distribution of growth rates



$$r = A \cdot t^{1-\alpha}$$



DTU Wind Energy, Technical University



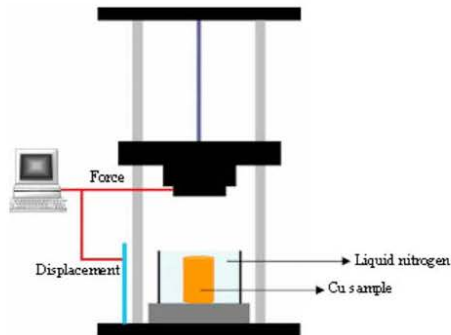
Nanometals

DTU Wind Energy, Technical University of Denmark

Kinetics in nanostructured copper

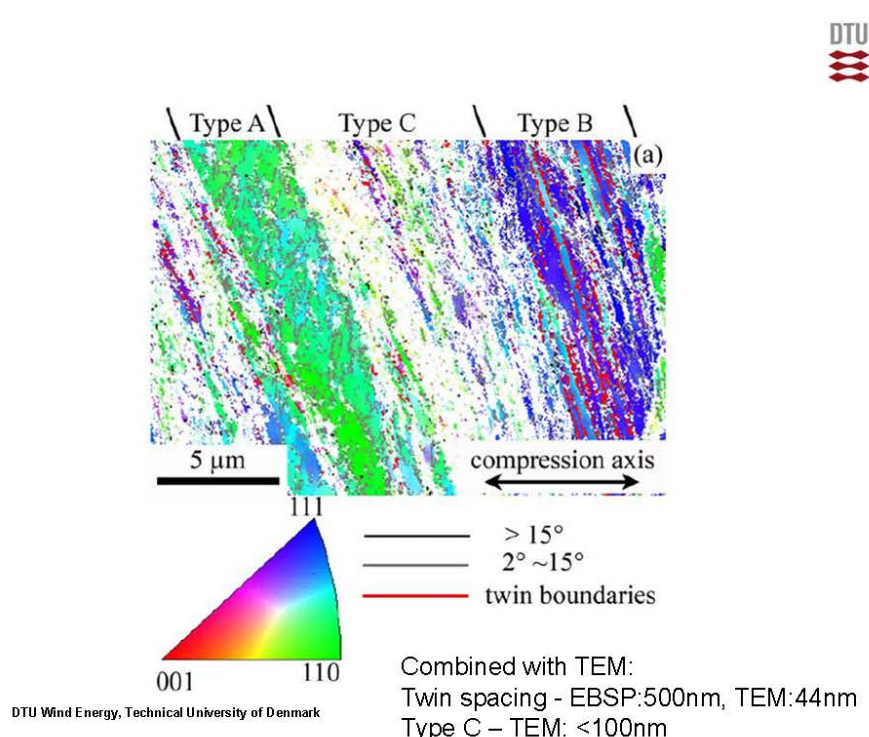


Copper DPD to $\varepsilon = 2.0$

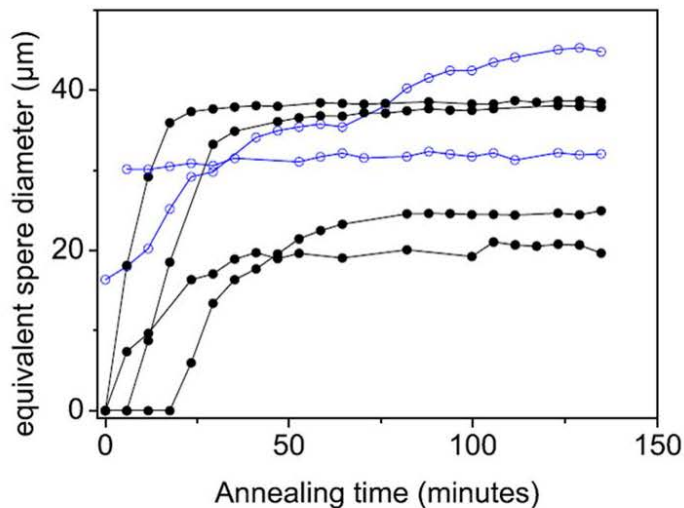


Lin et al., Risø 2012

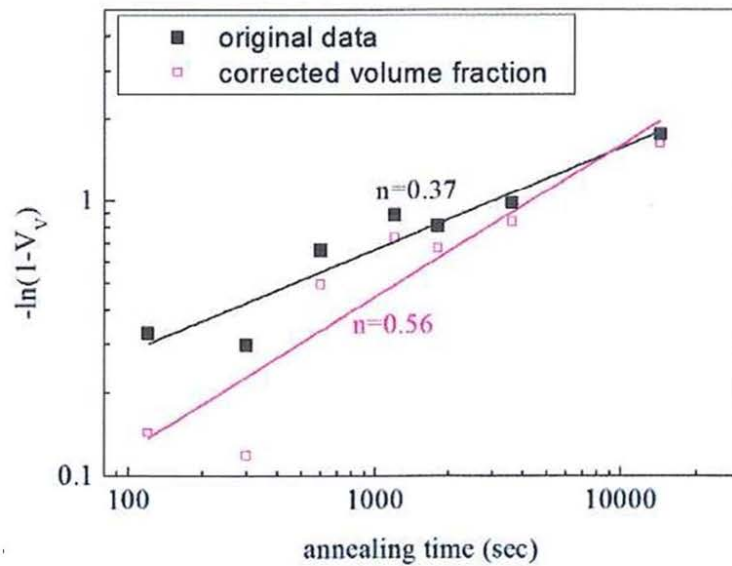
DTU Wind Energy, Technical University of Denmark



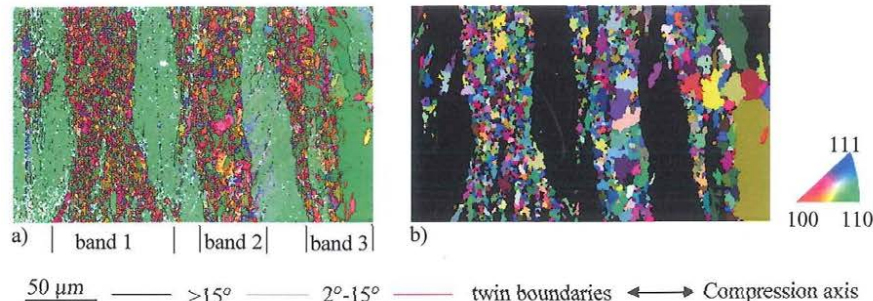
3DXRD measurements anneal at 120C



DTU Wind Energy, Technical University of Denmark



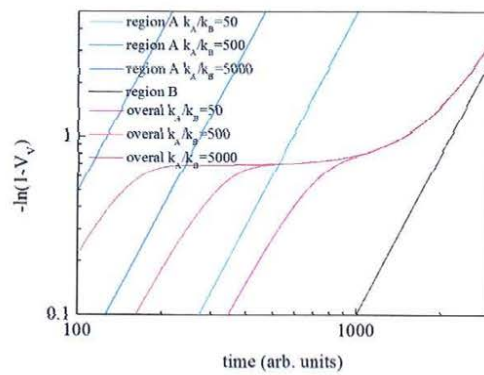
Kinetics in inhomogeneous deformed microstructures



Lin et al., Risø 2012

DTU Wind Energy, Technical University of Denmark

Kinetics in inhomogeneous deformed microstructures



Lin et al., Risø 2012

See also Doherty et al., Risø 1986

DTU Wind Energy, Technical University of Denmark

Conclusions

Recrystallization kinetics is strongly affected by:

- Spatial distribution of nucleation sites
- Time dependent and texture dependent growth rates
- Each recrystallizing grain has its own kinetics
- Wide distribution of activation energies
- Inhomogeneous deformation microstructures

3DXRD combined with electron microscopy are efficient tools to study recrystallization kinetics

Den nyeste generation af røntgen diffraktometre med
tilhørende temperaturcelle

Flemming Grumsen, DTU Mekanik

Den nyeste generation af XRD med tilhørende temperatur celle

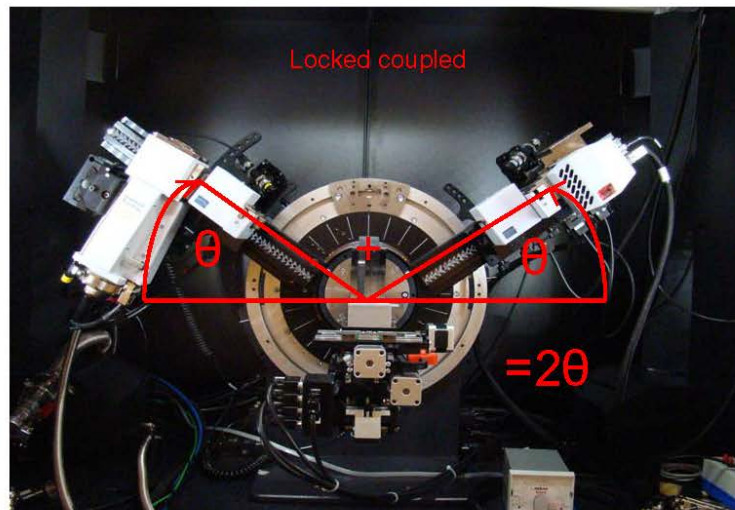
Flemming Bjerg Grumsen

Outline

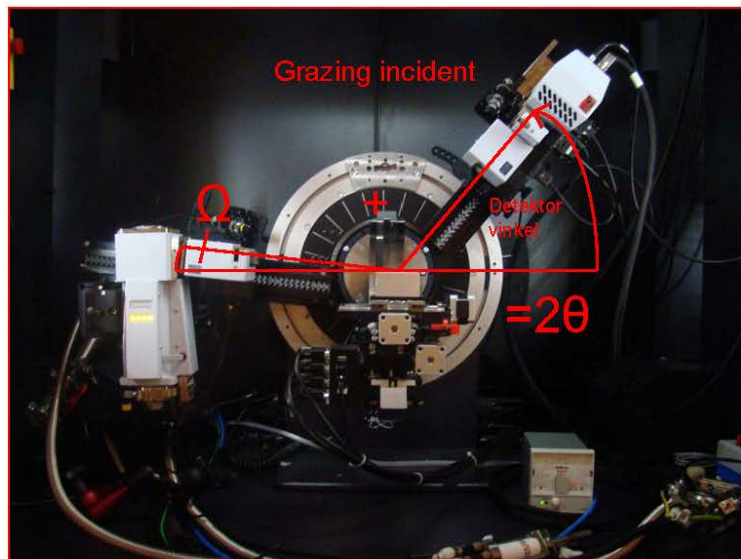
- Hvad er XRD?
- Hvad er nyt?
- Strip detektoren. Hvad kan den?
- Mikrodiffraktion med et eksempel
- Temperatur cellen
- Expanderet austenit
- Varmebehandling af expanderet austenit

Hvad er XRD?

- Braggs lov: $n \lambda = 2 d \sin\theta$

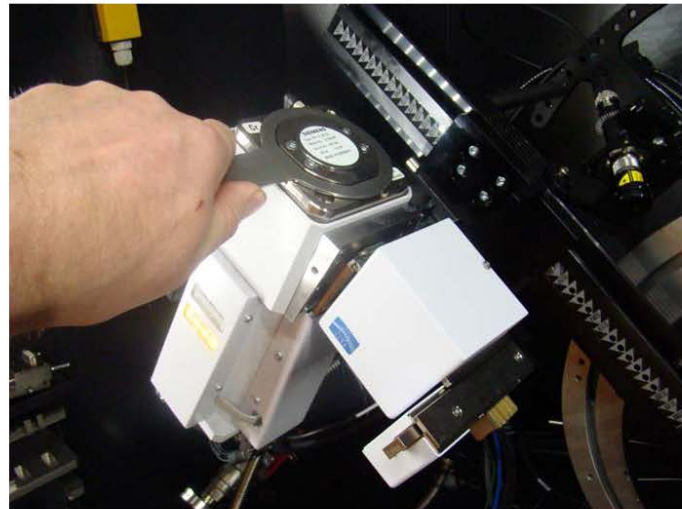


Hvad er XRD?



Hvad er nyt?

- Twist tube: linie- og punktfocus



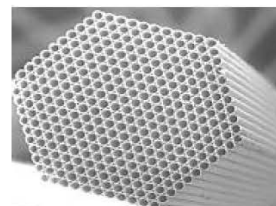
Hvad er nyt?

- Snap lock til skift mellem polycap, göbelspejl og divergence assembly

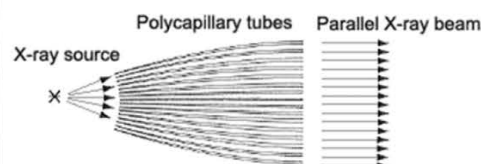


Hvad er nyt?

- Polycap til punkt fokus

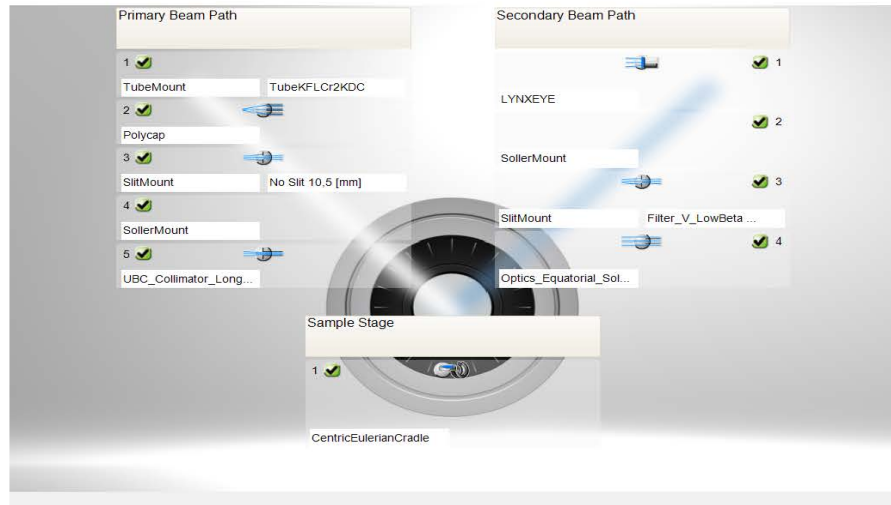


Mikrofibre til guided
Røntgen beam



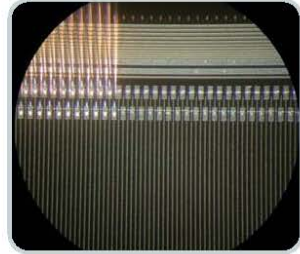
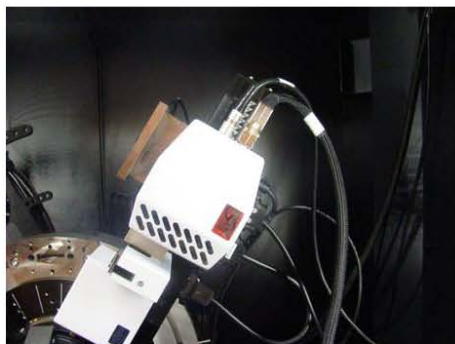
Fra kilde til næsten parallel beam

- ## Hvad er nyt?
- Automatisk registrering af optik (Da Vinci)



Hvad er nyt?

- Silicon strip 1d detektor (lynxeye)

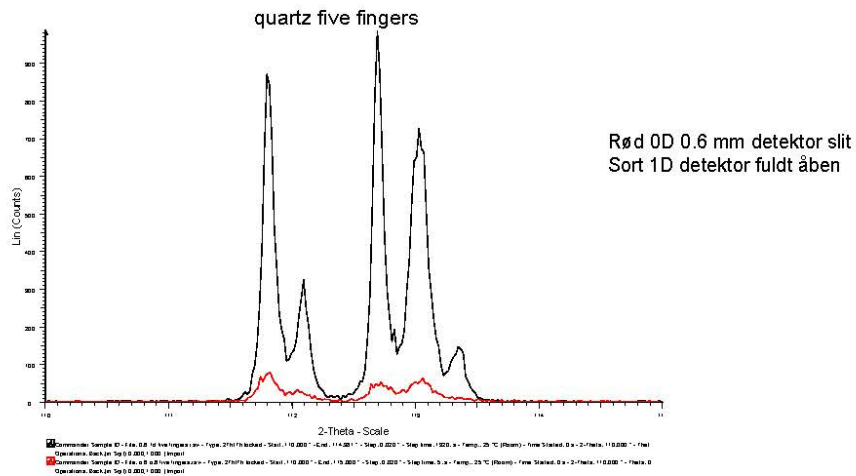


192 strips af 75 µm tykkelse
og 16 mm lange

Billede venligst udlånt af Bruker AXS

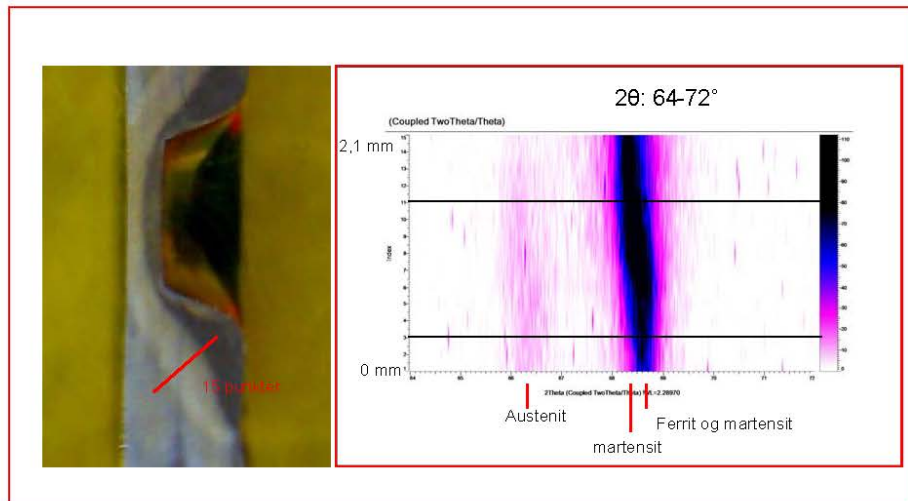
Stripdetektoren

- 0D: sammenlægger alle strips til en detektor
- 1D: hver strip fungerer separat og kompenserer for positionen

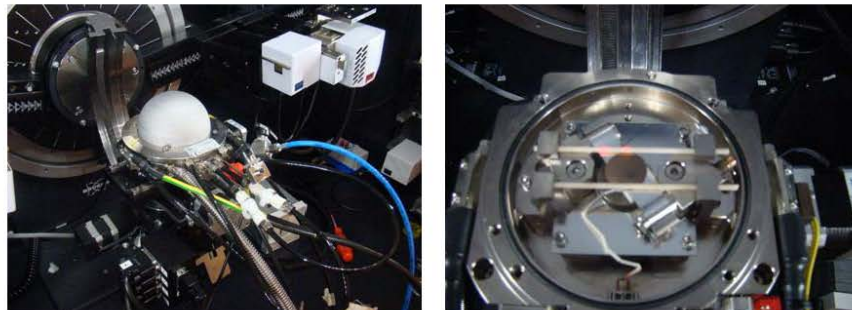


Mikrodiffraktion på Friction stir welding

Polycap med 0.3 mm collimator



Temperatur cellen

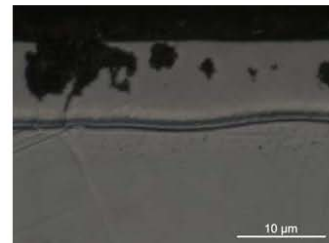
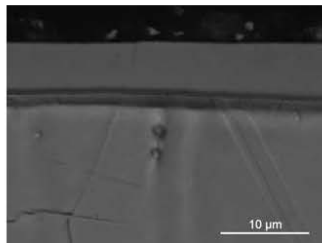


Temperatur spænd: 25-1100 °C eller -180 til 450 °C

Vacuum eller gas flow

Ramping 0,1 – 1 grad pr. sekund

nedbrydning og (Oxidation \odot) af ekspareret austenit

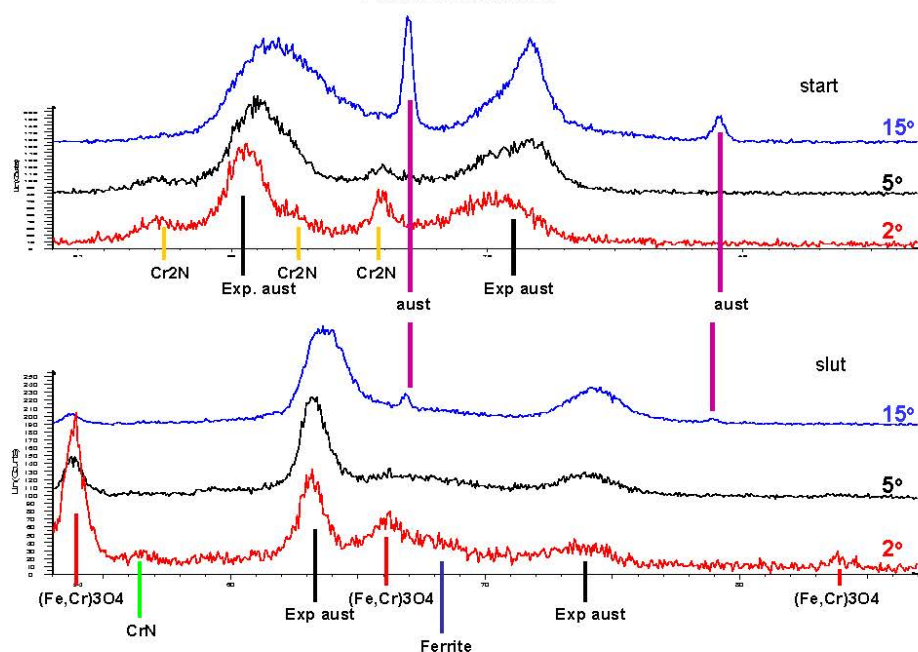


- Expanded austenit is metastabilt
- Ved temperaturer over 450 °C ned brydes den til
 - CrN
 - Ferrit

Forsøgsparametre

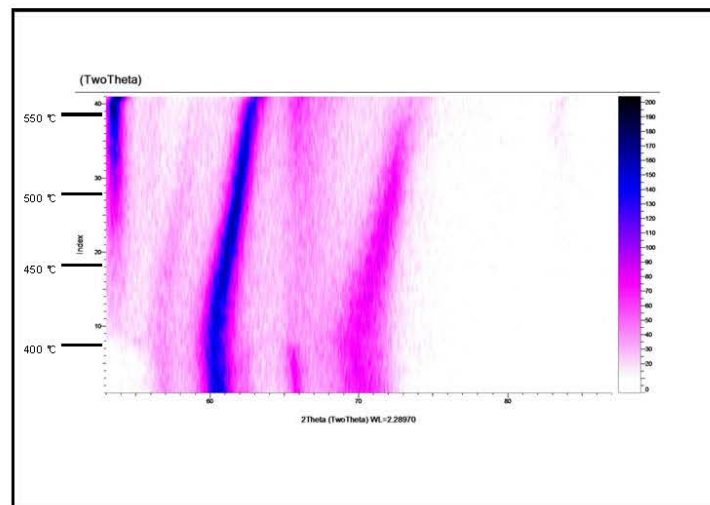
- Grazing incident 2, 5 og 15 grader, 2θ : 53° til 87°
30 min for hvert scan
- 30°C, 100 - 400 °C med 50 °C interval.
Ramping: 1 °C pr s.
- 400 °C til 560 °C med 5 °C interval. Ramping:
0,1 °C pr s.
- Afkøling til 30 °C. ramping: 1 °C pr s.

Resultater



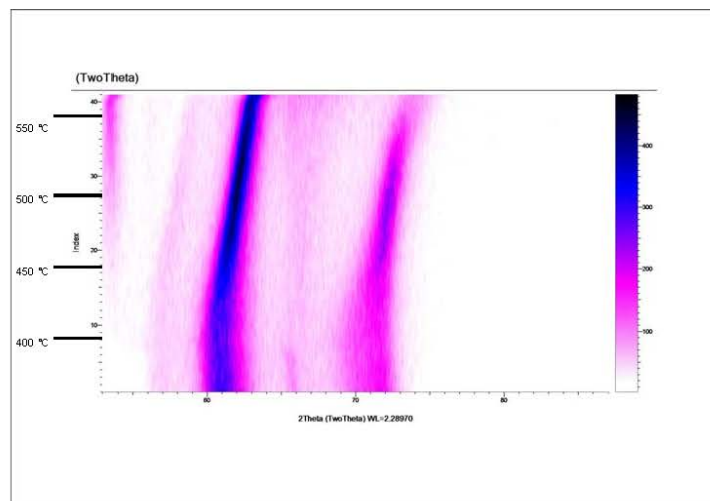
Resultater

2 ° grazing incident



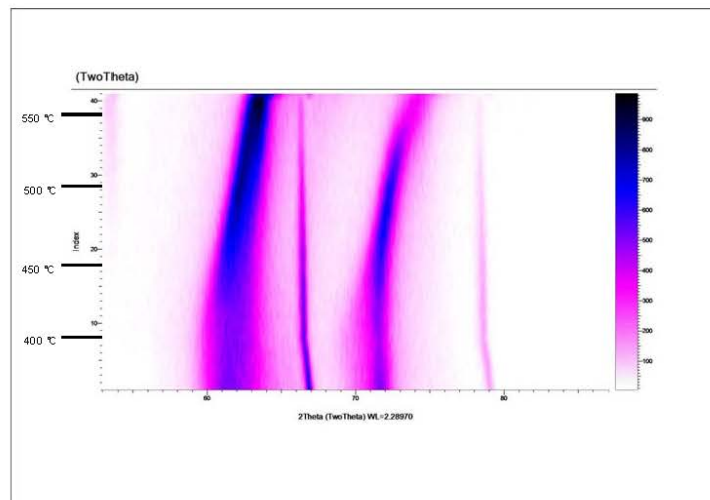
resultater

5 ° grazing incident



Resultater

15 ° grazing incident



Hvad kan man gøre for at undgå oxidation?

- Au eller Pt coating?
 - Ar/H₂ gas?
 - Metal med større affinitet til O₂ end prøven i kammeret?
-
- Og til sidst tak til Christian Hansson fra Bruker for support og til Trine Nybo Lomholt for nye ideer, når problemerne syntes uoverskuelige

NDT – relevant teknikkers muligheder og begrænsninger

Peter Willumsen, Force

NDT af svejsninger



Af Peter Villumsen
DS/EN 473 niveau 3



Metoder:

- Røntgen
- Ultralyd
- Magnetpulverprøvning
- Penetrantprøvning
- Tæthedsprøvning
- Hvirvelstrømsprøvning



Radiografi

Røntgen op til 300 kv.

Isotop (Gamma)

- Selen 75
- Ir 192
- Cobolt 60



Radiografi

Følsomhed 1-2% af godstykke



Radiografi bruges på alle emner/svejsninger i alle former for industri både i forbindelse med ny produktion og vedligehold.

Radiografi bruges til at finde fejl i volumen
Radiografi er 2 dimensional.

Fordele:

God til runde fejl eks. Pore
God til tynde godstykkelser

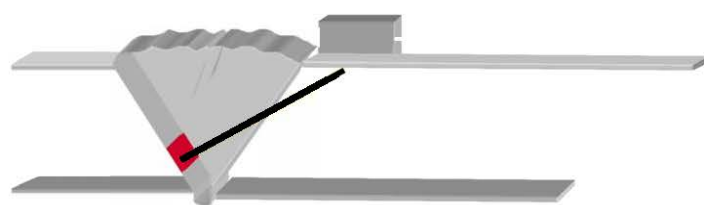


Ulemper:

Stråling
Begrænset godstykkelser

Ultralyd

Manuel eller automatisk



Manuel ultralyd bruges til:

- Tykkelse måling
- Lagdelings kontrol
- Materialefejl
- Svejsekontrol



0.37 mm i mindst 2 retninger

Luftspalte min.
1/10.000 mm

Manuel Ultralyd

Fordele:

God til plane fejl

God til tykke godstykkelser



Ulemper:

Kræver plads

Ingen dokumentation



Højt ydende automatiseret ultralyd inspektion

- Hurtig automatiseret inspektion
- Optimeret inspektion
- Dokumenteret
- Gentagen inspektion
- Stål, rustfrit stål, etc.



Magnetpulverprøvning

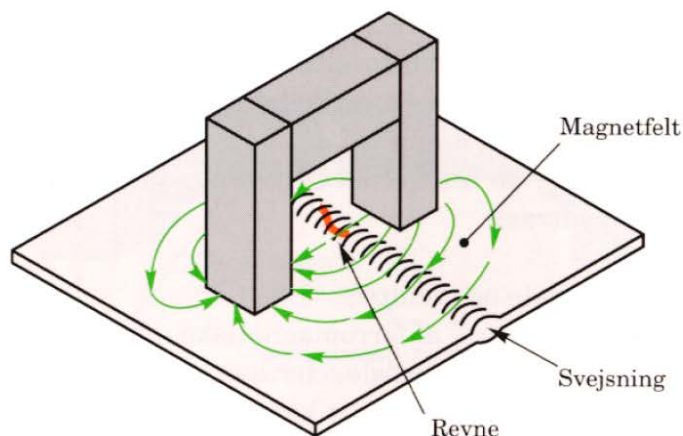
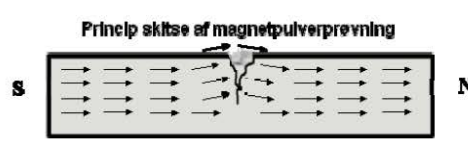
For indikationer åben til overfladen og kun på
magnetiske materialer.

Følsomhed
Ca. 0,1 – 1m μ

Magnetpulverprøvning

Kan udføres som prøvning med kontrast farve under alm. belysning.

Eller som fluorescerende prøvning i mørke med ultraviolet belysning



Fordele:

God til plane fejl åben til overfladen
Hurtig

Ulemper:

Kun overflade fejl
Ingen dokumentation

Penetrantprøvning (Kapillarprøvning)

Kan udføres som prøvning med kontrast farve under alm.
belysning.

Eller som fluorescerende prøvning i mørke med ultraviolet
belysning
Den mest følsomme metode

NDT af svejsninger



Penetrant bruges på ikke porøse materialer

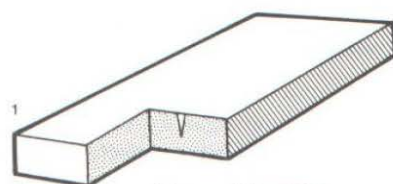
Primært på umagnetiske som eks, rustfrit stål,
aluminium, magnesium osv.

For indikationer åben til overfladen

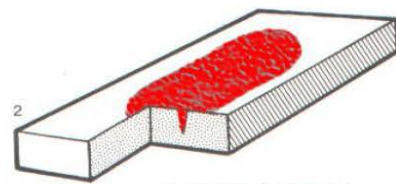
Følsomhed
Ca. 0,1 – 1μ



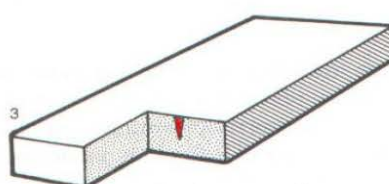
NDT af svejsninger



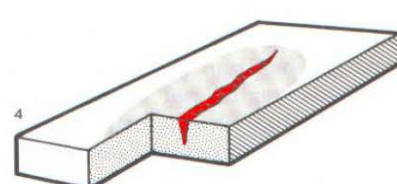
Revnen ikke synlig
på overfladen



Kapillarvæske trænger
ind i evt. revner og
porositeter



Hverken revne eller
kapillarvæske er syn-
lig på overfladen



Revnen „synlig“. Frem-
kalderen har suget
væsken ud af revnen
og dannet en bred in-
dikation oven på revnen

NDT af svejsninger



Fordele:

- God til fejl åben til overfladen
- Kan bruges som tæthedsprøvning
- Let at udføre

Ulemper:

- Kun overflade fejl
- Ingen dokumentation
- Kræver meget rengøring

NDT af svejsninger



Tæthedsprøvning

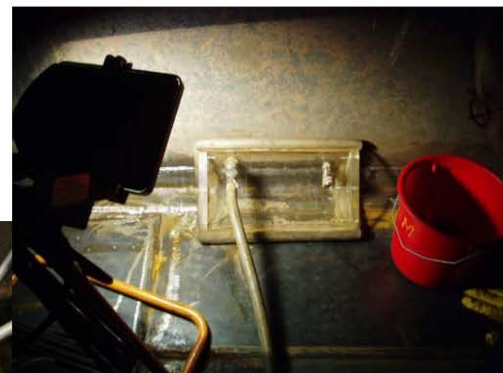
(Lækageprøvning)

Lækageprøvning er ikke bare en, men
mange metoder

De følgende er nogle af de mest
anvendte

Visuelle - Akustiske – Trykforandring –
Sporstoffer - Radioaktive sporstoffer -
Termografi – Hvirvelstrøm -
Farveforandring – Røggasser –
Krydkorrelator – kabilarprøvning

Vakuum box



Hvirvelstrømsprøvning

Undersøgelse af elektrisk ledende materialer,
primært metaller.

Metoden anvendes bl.a. til revne- og
korrosionsdetektion samt tykkelsesmålinger,
fx til undersøgelse af varmevekslerrør og i
flyindustrien til kontrol af fx turbineblade og
understel.

Slut...

Metrology and Quality Assurance

Maria Holmberg, Teknologisk Institut



Danish Technological Institute

Maria Holmberg
Metrology and Quality Assurance

THE DANISH TECHNOLOGICAL INSTITUTE

Founded 1906 by Gunnar Gregersen



"To support Danish industry, mainly small enterprises, by providing technical assistance in the form of teaching, advice, testing and technological research"

"Technological research - developed with the necessary scientific approach, but without the means of making science. The purpose is to develop new field for manufacturing "

Gunnar Gregersen

DTI - DIVISIONS AND CENTRES

BUILDING TECHNOLOGY

- Concrete
- Building Processes
- Indoor Climate and Humidity
- Masonry and Building Components
- New Industrialization
- Swimming Pool Technology
- Timber and Textiles

LIFE SCIENCE

- Food Technology
- IT Development
- Chemistry and Water Technology

ENERGY AND CLIMATE

- Energy Efficiency and Ventilation
- FEM-Secretariat
- Installation and Calibration
- Refrigeration and Heat Pump Technology
- Pipe Centre
- Renewable Energy and Transport
- Automobile Technology

PRODUCTION

- Micro technology and Surface Analysis
- Metrology and Quality Assurance**
- Robot Technology

BUSINESS DEVELOPMENT

- Policy and Business Development
- Human Resources Development
- Creativity and Growth
- Technology Partnership

TRAINING

- IT Training
- Conferences
- Leadership and Management Training

INTERNATIONAL CENTRE

METROLOGY & QUALITY ASSURANCE

Geometrical measurements – shape and dimensions of physical objects

Commercial activities

- Pilot production
- Product development
- Subcontractors/customers
- Training and courses



R&D activities

- Trouble shooting
- Product development
- Metrology
- Production and productivity



METROLOGY & QUALITY ASSURANCE



Metrology – DPLL (Danish Primary Laboratory for Length)

Designated institute within length – mechanical calibration of gauge block

Accreditation within geometrical measurements

EURAMET, TC-L (Technical Committee for Length)

CMC (Calibration and Measurement Capabilities)

EMRP projects

Multi-sensor metrology for microparts in innovative industrial projects



Fra programmet:



Dansk industri skal bl.a. overleve på kvalitet, og det er vigtig, at virksomhederne kan dokumentere denne kvalitet overfor deres kunder. Vintermødet 2013 har derfor fokus på **karakterisering af materialer, processer og komponenter**, spændende fra nanometer til meterskala og fra **forskning & udvikling** til **monitorering af komponenter i drift**.

Dokumentere kvalitet overfor deres kunder

*Geometrisk opmåling kan kvantificere dette – tolerancer, dimensioner, data
Reproducerbarhed*

Karakterisering af materialer, processer og komponenter

*Kombinere opmåling (dimension, form) med materiale karakterisering (densitet,
homogenitet, struktur)
Hvilke parametre repræsenterer hvad?*

Forskning & Udvikling

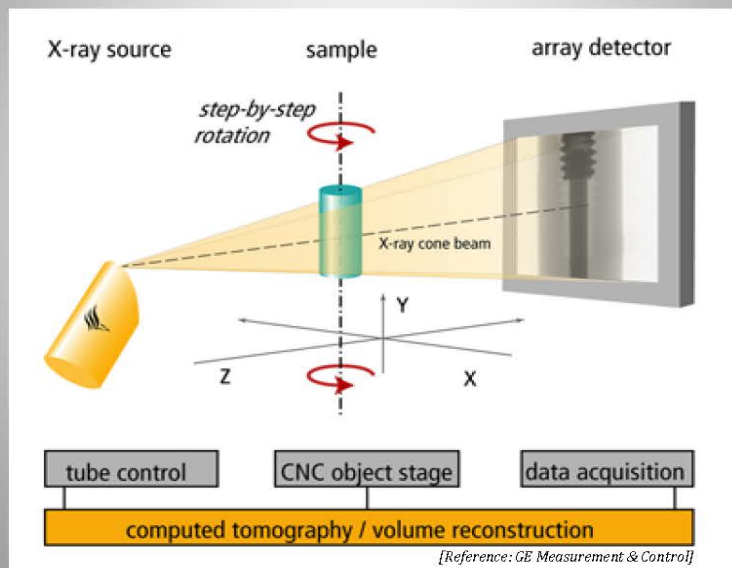
*Trouble shooting – vi ved ikke helt hvad vi kigger efter...
Metrologi & måleteknik i fremtiden – inklusive CT Scanning*

Monitorering af komponenter i drift

CT Scanning som ikke-destruktiv analyse med mulighed for 3D karakterisering

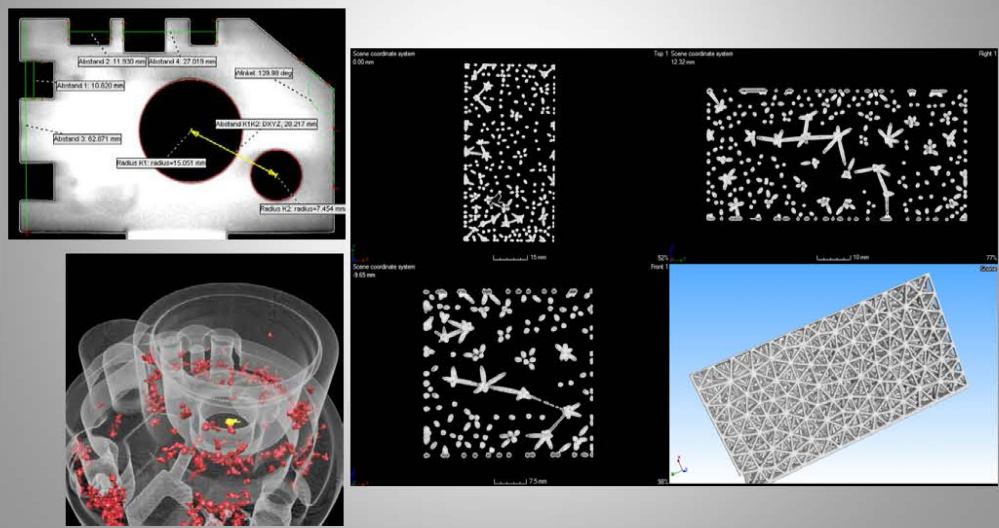
CT SCANNING

CT – Computed Tomography – Scanning



CT SCANNING

- Measuring size, form and position of geometrical features
- Non-destructive analysis of inner structures



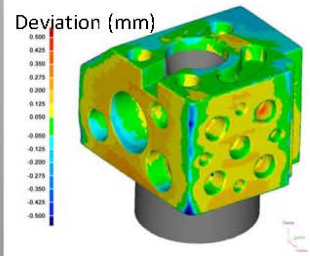
CT SCANNING



Zeiss METROTOM 1500

X-Ray tube: 225 kV
Detector: 1024 x 1024 pixels
Sample size: 30 x 30 x 30 cm
'Detectability': < 10 µm

Industrial CT Scanner
Manufacturing, Production,
In-line Scanning etc.



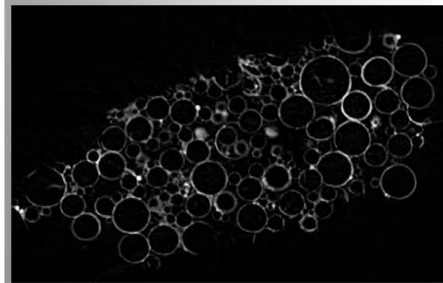
CT SCANNING



Bruker microCT, Skyscan 1172

X-Ray tube: 100 kV
Detector: 4000 x 2300 pixels
Sample size: 2 x 2 cm (possibility to combine scans)
'Detectability': < 1 µm

µCT Scanner
Material characterisation, R&D,
high resolution etc.



Document quality in regards to customers

Documentation in regards to customers and subcontractors in a supply chain

Often a combination of different technologies, for example CMM and CT Scanning

Manufacturing

'Quantification of quality' using geometrical measurements

Example - release of moulds for injection moulding into production



Characterisation of materials, processes and components

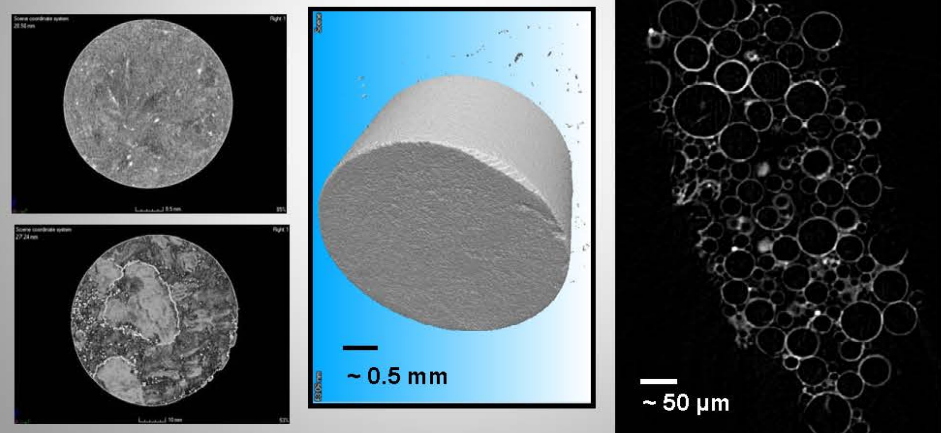
Combining geometrical measurements with material characterisation

How are used processes related to characteristics of resulting component?

Combining data on micro- and macro-scale

Material for use as a matrix aluminium syntactic metal foam

Hollow glass spheres ($\varnothing 20\text{-}80 \mu\text{m}$) that are bonded chemically to each other by water-based silane coating.



[Innovation consortium F•Mat, Søren Skov Bording, ssb@teknologisk.dk]

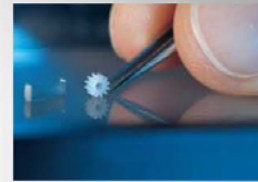
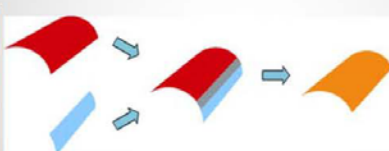
Research and Development



Metrology and geometrical measurements

EMRP project: Multi-sensor metrology for microparts in innovative industrial projects
Transferring new methods, systems, protocols from laboratory to production facilities.

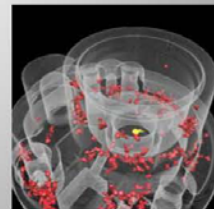
- Influence on uncertainty from parameter X
- Optimization of protocols (tolerances, time etc.)
- Data handling and data fusion



Development together with industry

Product development and trouble shooting
Designed/optimized solution for specific applications

- Automation and multiplying
- Sample holders for CT scan of several items simultaneously
- Software systems (macros) for automatic handling of data



Monitoring components 'in-line'



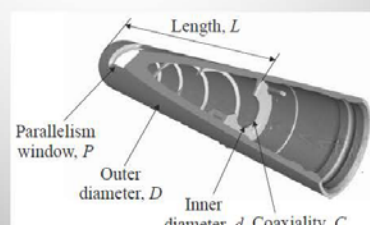
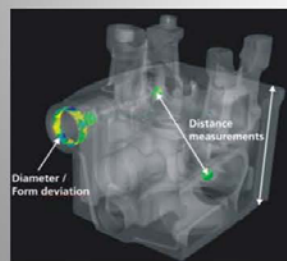
CT Scanning – Possibility to perform non-destructive testing in 3D

'In-line' CT Scanning system

Expensive and time consuming
Necessary to have 3D?
Need to be combined with software solutions



High-end products
Complex technology
Assembled items – components made of different materials etc.

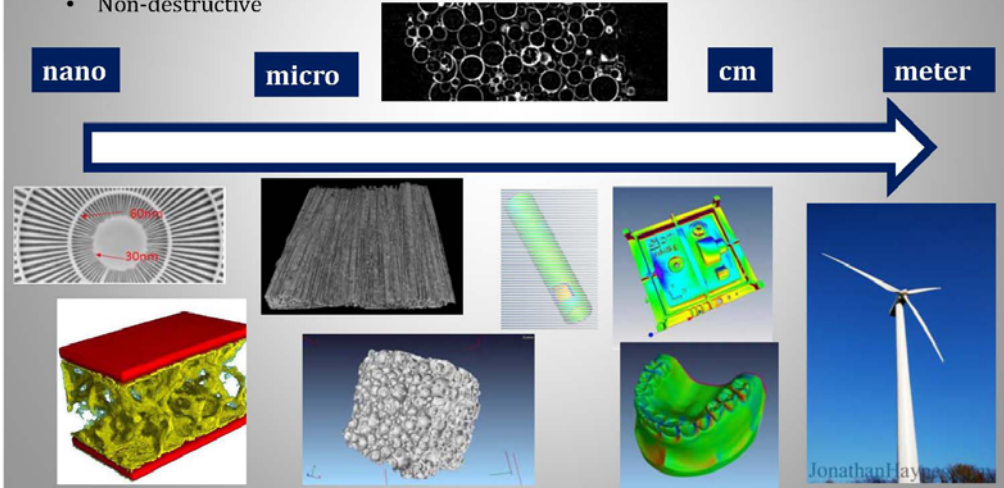


Characterization on all length scales - CT Scanning



Industrial CT Scanning in combination with µCT

- From micro to cm range
- Low density material
- Complex geometry
- Non-destructive



METROLOGY & QUALITY ASSURANCE



Maria Holmberg

PhD, Senior Consultant

Metrology and Quality Assurance
Production
Danish Technological Institute
Gregersensvej 8B
DK-2630 Taastrup
Denmark

+45 72 20 30 06

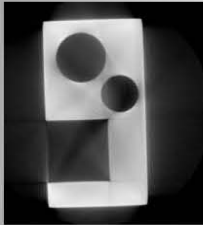
mahg@teknologisk.dk
www.teknologisk.dk

CT SCANNING



DANISH
TECHNOLOGICAL
INSTITUTE

Image artifacts



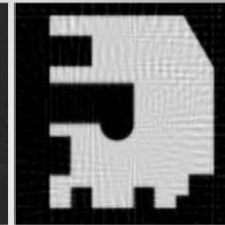
Beam-hardening



Cone-Beam



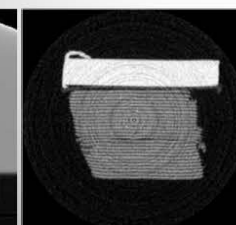
Misalignment



Undersampling



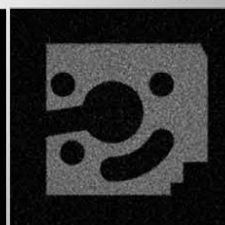
Truncation



Ring artifacts



Metal artifacts



Noise artifacts

Determining geometrically necessary dislocation densities by EBSD

Philip Littlewood, DTU Mekanik

Determining geometrically necessary dislocation densities by EBSD

Philip Littlewood

DTU Mechanical Engineering
Department of Mechanical Engineering

$$(EIv'')'' = q - \rho A \ddot{v} \int_a^b \Theta + \Omega \int \delta e^{i\pi} \sum!$$

Overview

- Theoretical basis for determining dislocation density by EBSD
- Cross-correlation method for EBSD patterns
- Application to deformed Ti alloys

DETERMINING DISLOCATION DENSITIES BY EBSD

3 DTU Mechanical Engineering, Technical University of Denmark Determining geometrically necessary dislocation densities by EBSD 17/01/2013

Dislocation and Curvature Tensors

- Dislocation Tensor [1]:

$$\alpha_{ij} = \sum nb_i r_j$$

- Relationship between Dislocation and Curvature Tensors (with/without elastic strain) [1,2]

$$\alpha_{ij} = \kappa_{ji} - \delta_{ij}\kappa_{kk}$$

$$\kappa_{pi} = -\alpha_{ip} + \frac{1}{2}\delta_{pi}\alpha_{kk} + e_{pj}\epsilon_{ik,j}^{el}$$

[1] J. F. Nye. *Acta Metallurgica*, 1:153-162, 1953.

[2] E. Kröner. *Continuum Theory of Dislocations and Self Stresses*. Springer, Berlin, 1958.

Limitations on Determining Dislocation Densities with EBSD

- Only dislocations contributing to lattice curvature (GNDs) can be detected
 - Dipoles, other multipoles are “invisible” (SSD)
- Dislocation tensor gives only nine equations
 - Systems other than simple cubic have too many dislocation types – no unique solution
 - Linear programming can be used to generate lower-bound solutions [1]
- Surface nature of EBSD makes information unavailable
 - Z-components of curvature cannot be measured
 - 5 components of dislocation tensor & difference of two others can be derived [2]
 - Can be overcome by 3D FIB-EBSD [3]

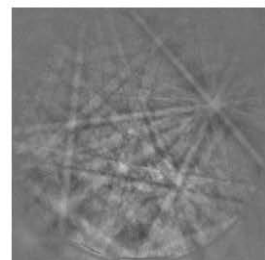
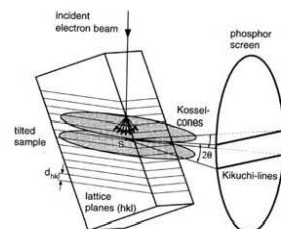
[1] S. Sun, B.L. Adams, C. Shet, S. Saigal, W. King. Scripta Materialia, 39:501-508, 1998.

[2] W. Pantleon. Scripta Materialia 58:994-997, 2008.

[3] E. Demir, D. Raabe, N. Zaafarani, S. Zaefferer. Acta Materialia, 57:559-569, 2009.

Cross-Correlation-Based GND Measurement

- Standard EBSD error is $\sim 1^\circ$
 - Magnified in calculations of misorientation
 - Cross-correlation method [1] was developed to improve resolution
- Distortion of crystal lattice causes shifts in EBSD patterns
 - Crystal distortion can be measured by measuring the shifts
 - Hydrostatic strains do not realign crystal planes and cannot be detected

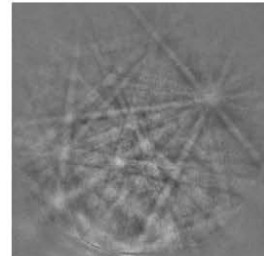
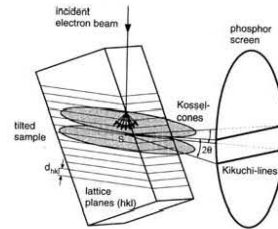


[1] A. J. Wilkinson, G. Meaden, D. Dingley. Ultramicroscopy 106:307-313, 2006.

Cross-Correlation-Based GND Measurement

- Standard EBSD error is $\sim 1^\circ$
 - Magnified in calculations of misorientation
 - Cross-correlation method [1] was developed to improve resolution
- Distortion of crystal lattice causes shifts in EBSD patterns
 - Crystal distortion can be measured by measuring the shifts
 - Hydrostatic strains do not realign crystal planes and cannot be detected

[1] A. J. Wilkinson, G. Meaden, D. Dingley.
Ultramicroscopy 106:307-313, 2006.



7

DTU Mechanical Engineering, Technical University of Denmark

Determining geometrically necessary dislocation densities by EBSD

17/01/2013

Calculating GND densities from pattern shifts

- A reference pattern is divided into regions
- Shifts of each region are measured at each point
- One region gives two equations:

$$r_1 r_3 \left[\frac{\partial u_1}{\partial x_1} - \frac{\partial u_3}{\partial x_3} \right] + r_2 r_3 \frac{\partial u_1}{\partial x_2} + r_3^2 \frac{\partial u_1}{\partial x_3} - r_1^2 \frac{\partial u_3}{\partial x_1} - r_1 r_2 \frac{\partial u_3}{\partial x_2} = Q_1 r_3$$

$$r_2 r_3 \left[\frac{\partial u_2}{\partial x_2} - \frac{\partial u_3}{\partial x_3} \right] + r_1 r_3 \frac{\partial u_2}{\partial x_1} + r_3^2 \frac{\partial u_2}{\partial x_3} - r_2^2 \frac{\partial u_3}{\partial x_2} - r_1 r_2 \frac{\partial u_3}{\partial x_1} = Q_2 r_3$$

- Measuring 4 regions allows 8 elements of distortion tensor to be derived
 - 9th element must be derived from boundary conditions
 - More than 4 regions allows least-squares fitting to improve accuracy

8

DTU Mechanical Engineering, Technical University of Denmark

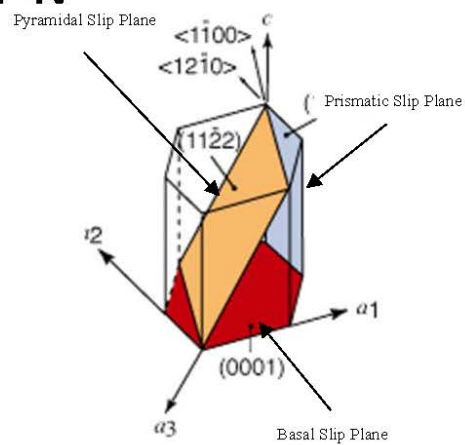
Determining geometrically necessary dislocation densities by EBSD

17/01/2013

APPLICATION: FATIGUE IN TITANIUM ALLOYS

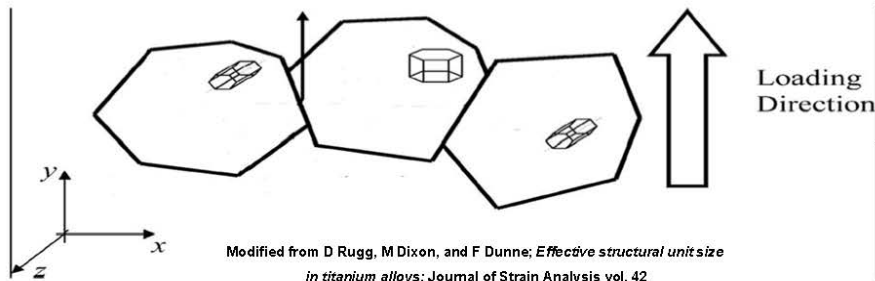
Crystallography of Ti-6Al-4V

- Two phases: HCP α and BCC β
 - Ti-6Al-4V as received is mostly α
- Three main slip planes in α
 - Slip along \underline{a} $<11\bar{2}0>$ and $\underline{c+a}$ $<11\bar{2}3>$ directions
 - $\underline{c+a}$ requires higher stress to activate ($\sim 3\text{-}4x$)



<http://web.earthsci.unimelb.edu.au/wilson/icel/introduction.html>

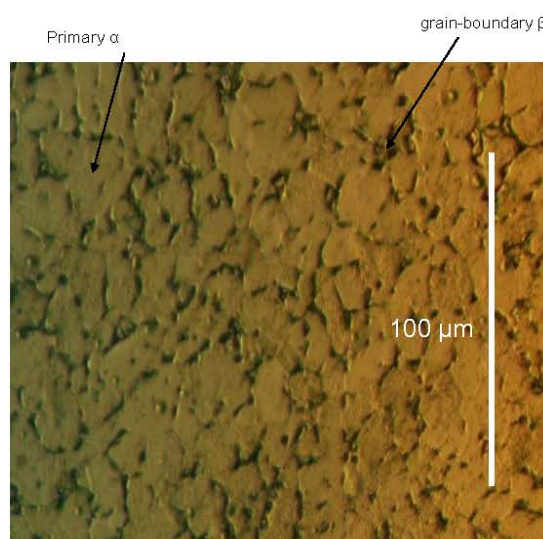
Crystal Anisotropy



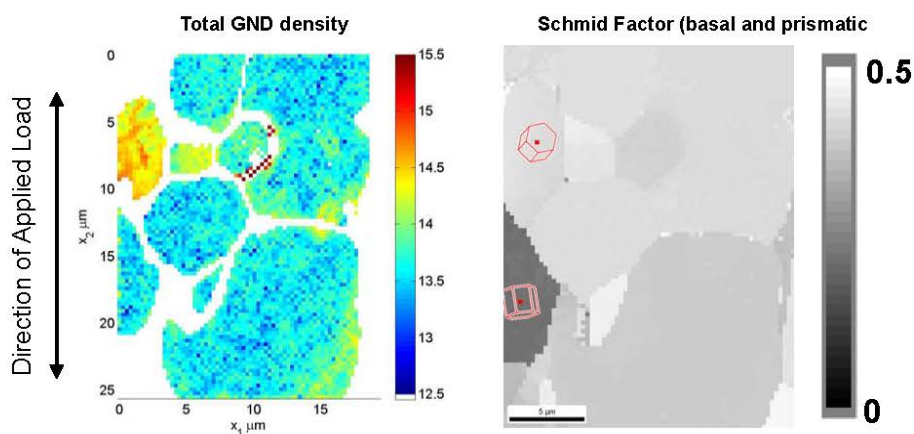
- No resolved shear stress on basal/prismatic planes in center grain
- Grain becomes resistant to plastic deformation relative to others

Fatigue Testing

- Material: Ti-6Al-4V rolled bar stock provided by Rolls-Royce
 - Globular primary α -phase grains, small amount of grain-boundary β phase
 - Average grain size $\sim 12 \mu\text{m}$
- Deformed in fatigue to failure
 - Peak stress 900 MPa, stress ratio 0.1
- Cross-correlation EBSD used to measure GND distributions



Relating GND Densities to Microstructure

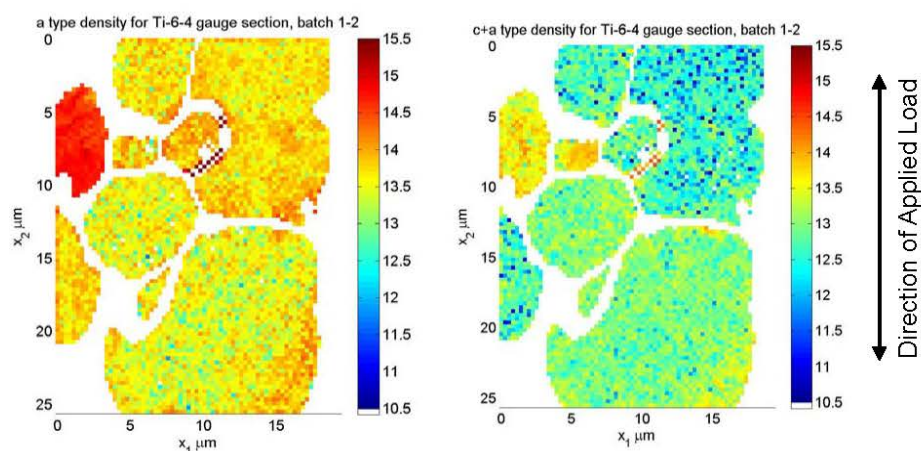


13 DTU Mechanical Engineering, Technical University of Denmark

Determining geometrically necessary dislocation densities by EBSD

17/01/2013

a vs c+a GND densities



14 DTU Mechanical Engineering, Technical University of Denmark

Determining geometrically necessary dislocation densities by EBSD

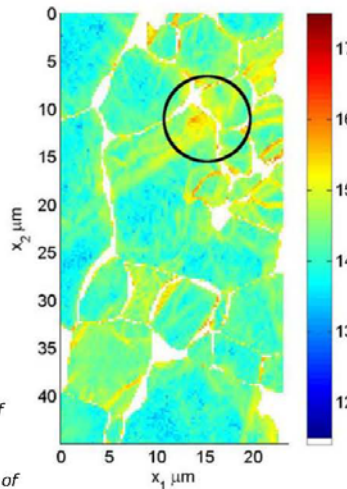
17/01/2013

GND Pile-Up

- First proposed as a crack initiation method by Stroh [1]
- Suggested by Bache and Evans as a mechanism in cold-dwell sensitivity [2]

[1] A. N. Stroh. *Proceedings of the Royal Society of London. Series A, Mathematical and Physical Sciences*, 223:404-414, 1954.

[2] W. J. Evans, M. R. Bache. *International Journal of Fatigue*, 16:443-452, 1994.

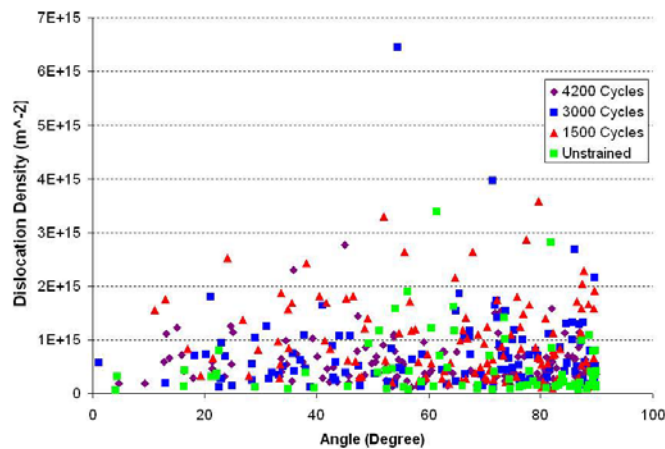


15 DTU Mechanical Engineering, Technical University of Denmark

Determining geometrically necessary dislocation densities by EBSD

17/01/2013

GND Statistics

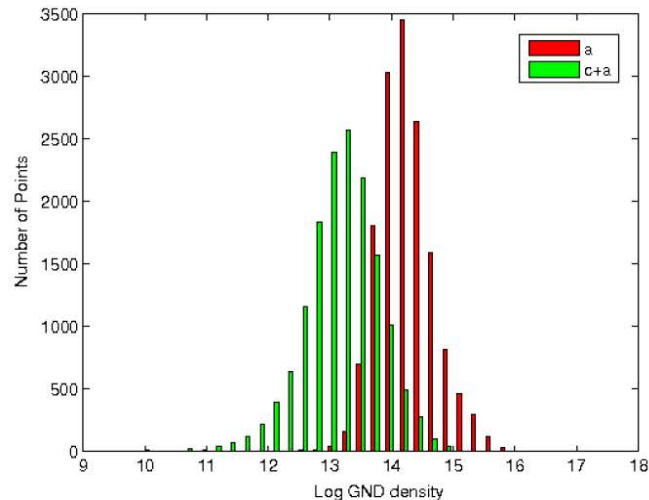


16 DTU Mechanical Engineering, Technical University of Denmark

Determining geometrically necessary dislocation densities by EBSD

17/01/2013

GND Statistics



Conclusions

- Cross-correlation based EBSD can be used to study storage of geometrically necessary dislocations on a microstructural level
- Grain-grain interactions play a significant role in inhomogeneous deformation in Ti-6Al-4V
 - No direct link between crystal orientation and GND density
- Dislocation pile-up along a slip band, and slip penetration into a neighbouring grain, have been observed.

Transformation af udskillelser på atomar skala

Hilmar Danielsen, DTU Mekanik

Transformation af udskillelser på atomar skala

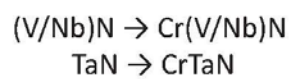
Hilmar K. Danielsen

DTU Mekanik



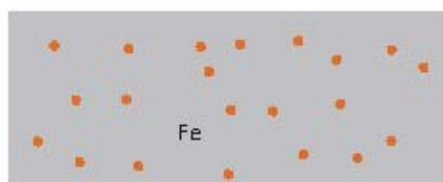
M = V, Nb or Ta

Two different 12%Cr martensitic steels investigated:

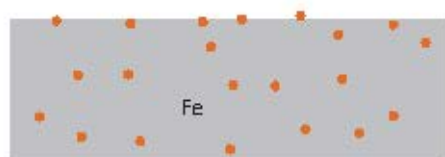


Fremstilling af prøver til TEM (carbon extraction replica)

Udgangspunkt



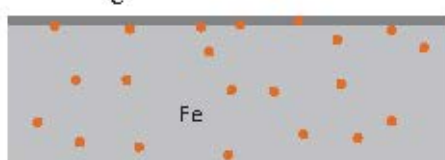
Ætsning



Ætsning



Kulpådampning

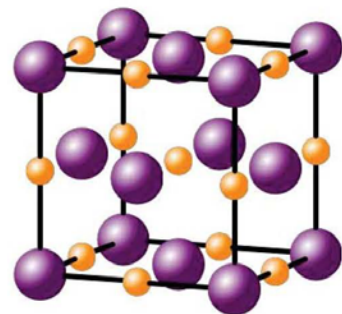


Investigations performed using FEI TITAN 300KV analytical TEM
with High Angle Annular Dark Field (HAADF)

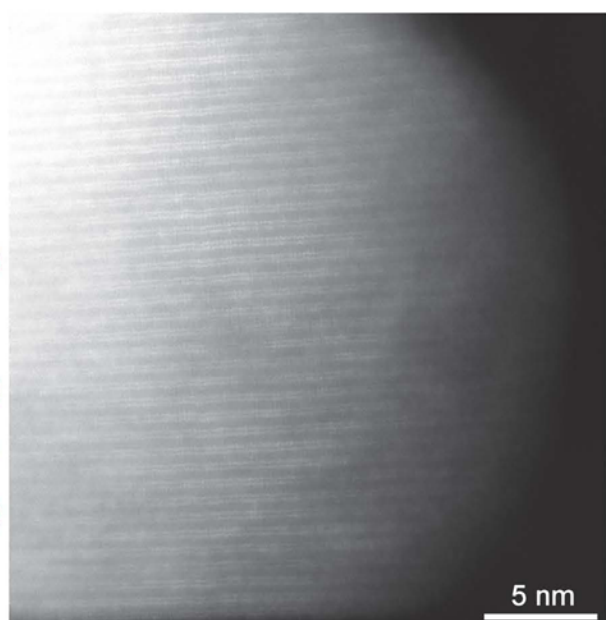
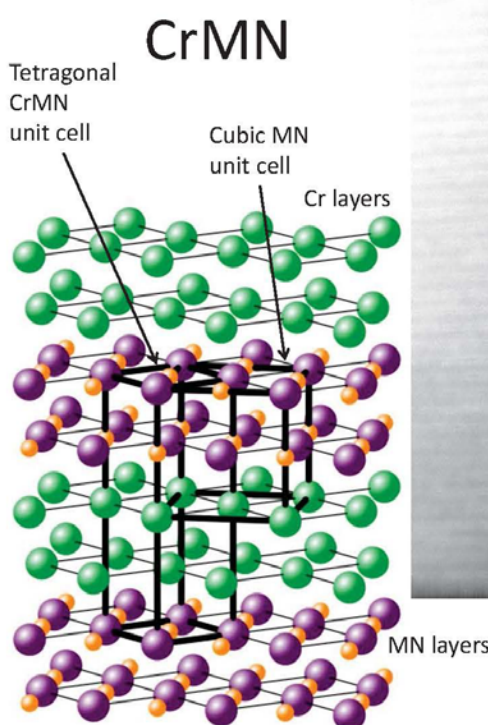
MN
(VN, NbN, TaN)



HAADF billede af (V,Nb)N



NaCl type enhedscelle



High resolution image of Cr(V,Nb)N
showing double layered structure.

$(V,Nb)N$

The cubic MN and tetragonal CrMN are bound together as one particle, it is possible to follow the atomic layers through the "interface".

$Cr(V,Nb)N$

5 nm

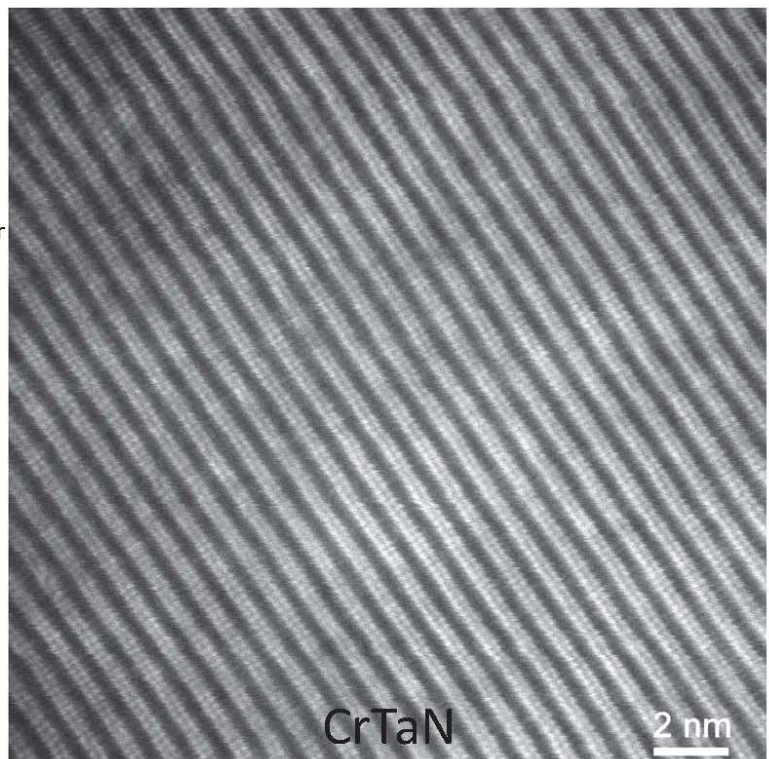
$Cr(V,Nb)N$

The $Cr(V,Nb)N$ does not have a perfect lattice, there are triple layers, layers changing from Cr to $(V,Nb)N$ etc.

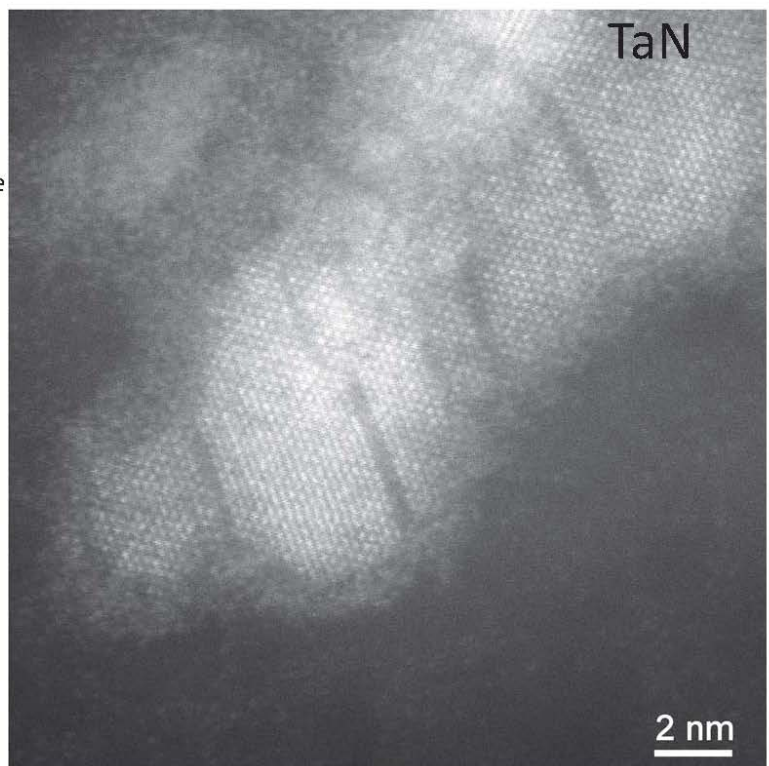


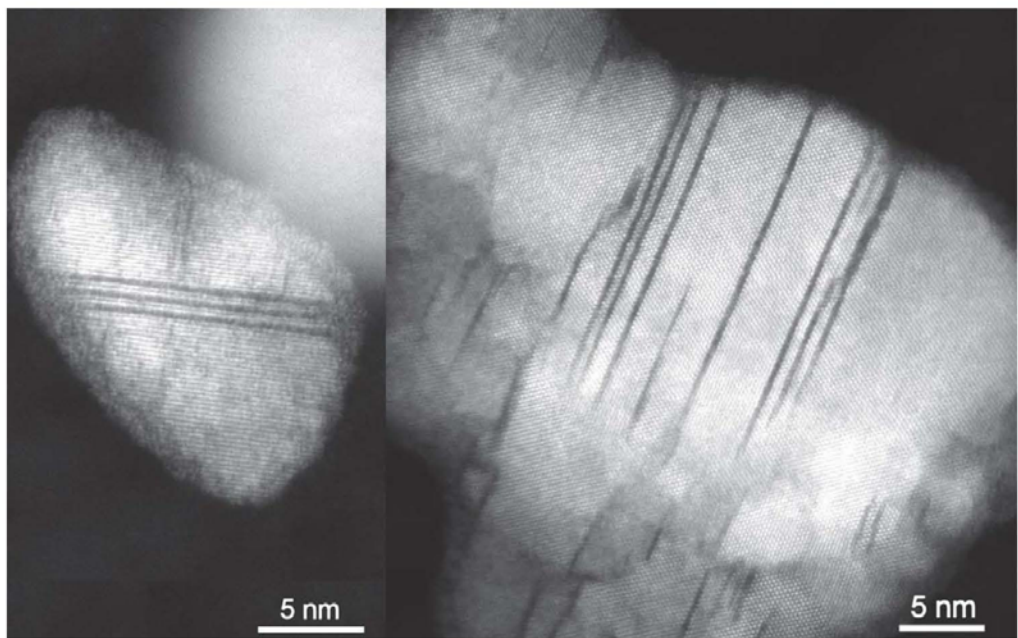
2 nm

CrTaN has much clearer contrast as Ta atoms are very heavy compared to Cr atoms. Ta atoms are clearly visible while the Cr atoms are very dark.

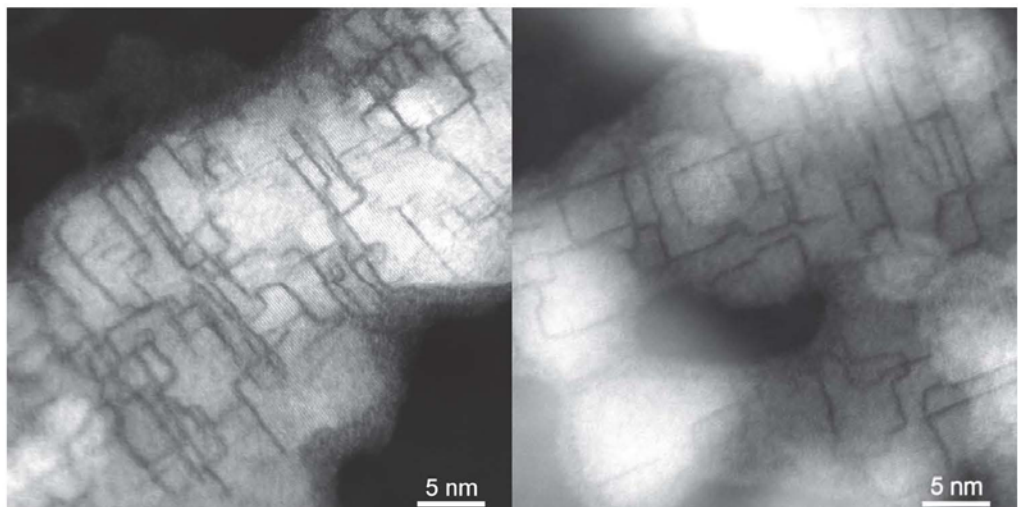


Cr atoms arrange themselves as double layers (dark lines)



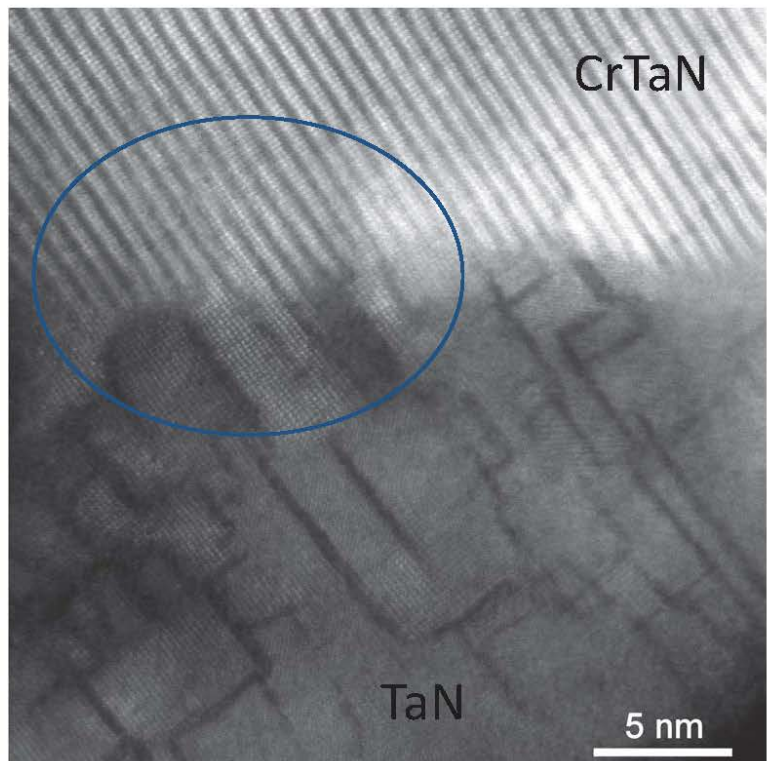


Transformation with a clear orientation relationship
Cr double layers appear as straight parallel lines through the TaN crystal structure

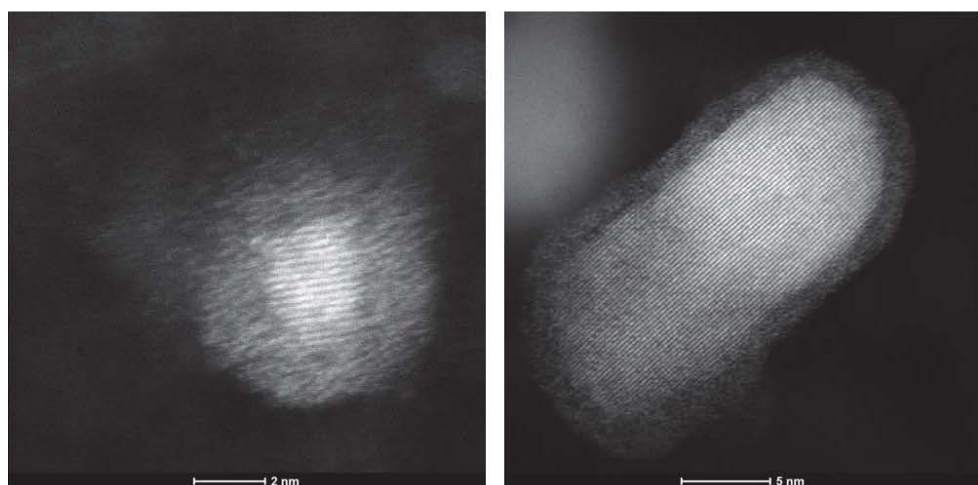


Transformation with a chaotic orientation relationship
Cr double layers have not decided upon the orientation of the future tetragonal crystal

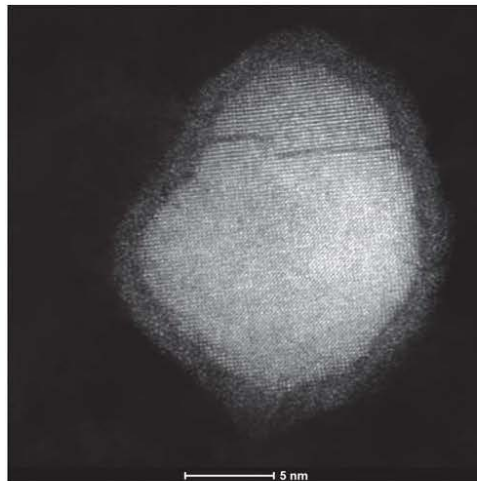
Interface between CrMN and MN. The crystal structure can be followed from one region to the other.



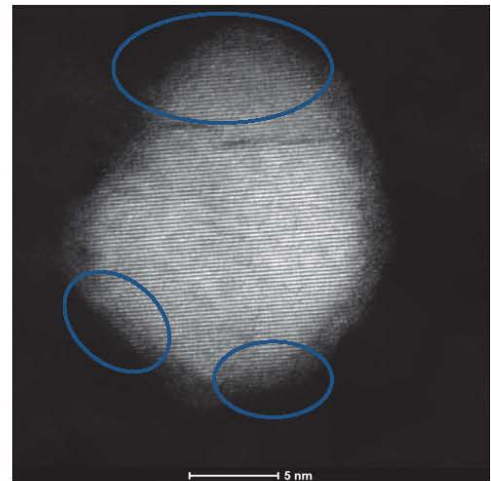
TaN particles with amorphous layer



Areas where the electron beam has been concentrated crystallize

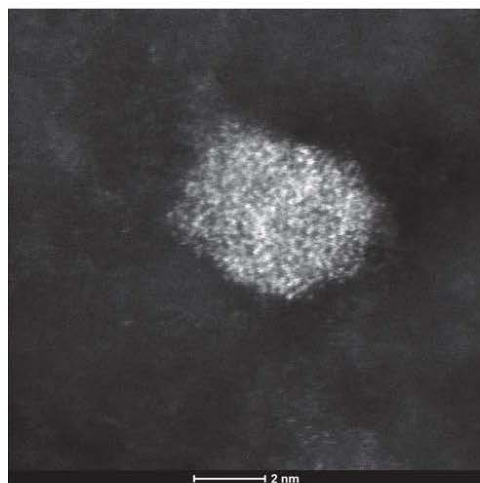


Before

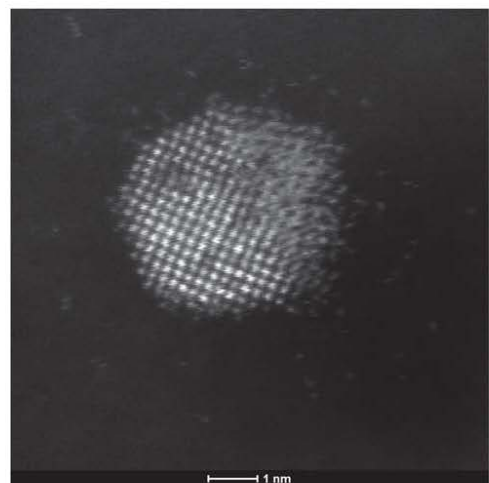


After

Entire interface crystallising after electron beam exposure

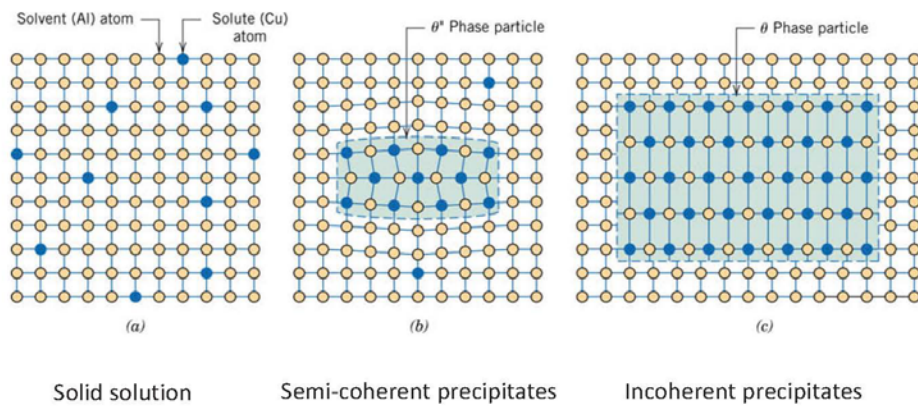


Before

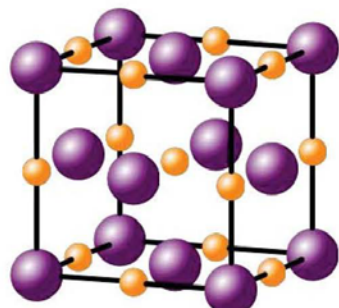


After

Precipitate interfaces



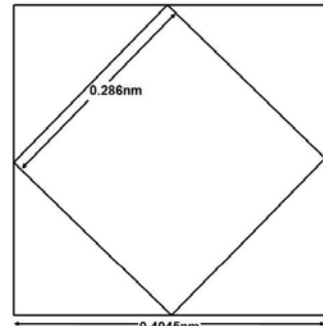
Semi and incoherent MN



Lattice parameters

VN: 0.413 nm
NbN: 0.439nm
Ta_N: 0.440nm

Baker-nutting relationship

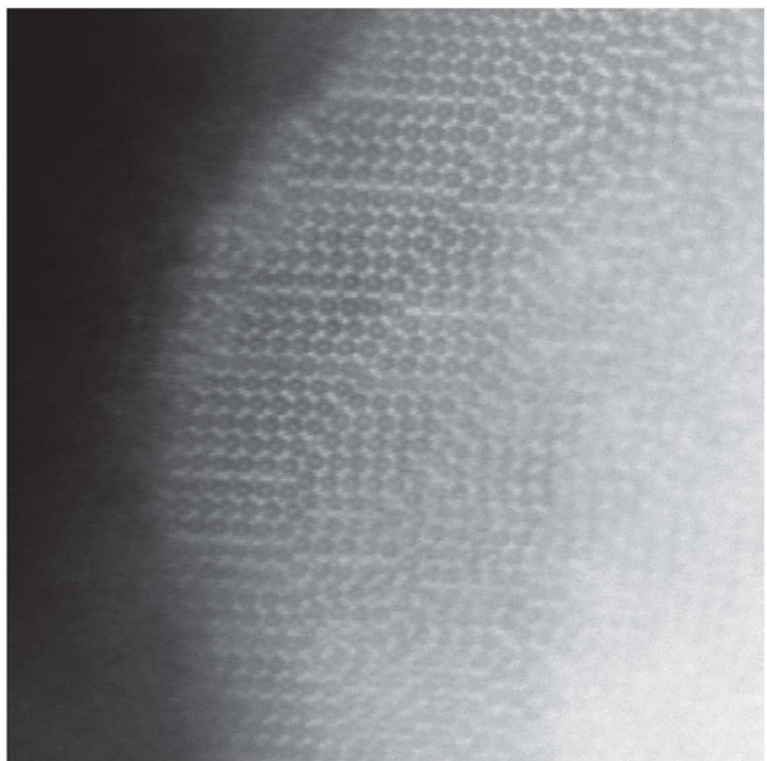
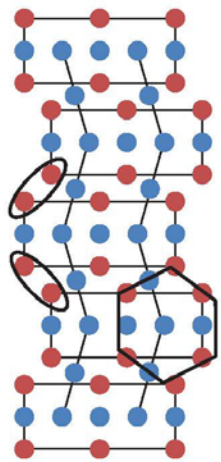


misfit: 2%
misfit: 9%
misfit: 9%

no amorphous layer
amorphous layer
amorphous layer

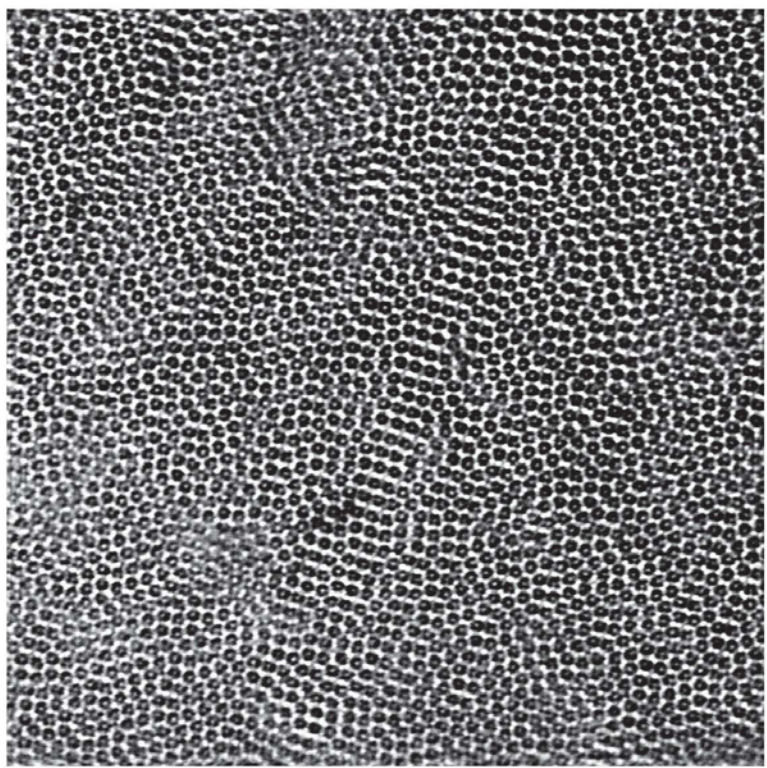
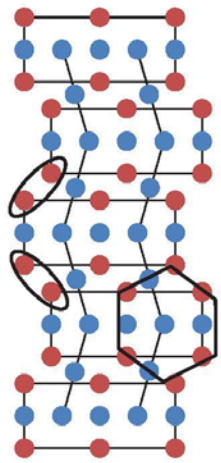
Edge of a large
 Fe_2W particle

● W
● Fe



Small Fe_2W
particle (thin)

● W
● Fe



Konklusion

- TaN kan transformere deres sammensætning og krystalstruktur til en anden type partikler
- Partikler kan have en meget uordnet krystalstruktur
- På atomar skala er vores prøver lette at påvirke (elektron stråle, ætsning osv)

Structure and Chemical Characterization by Electron Microscopy – Spanning the micro and nano regime

Jakob Birkedal Wagner, DTU CEN

Structural and Chemical Characterization by Electron Microscopy – Spanning the micro and nano regime

Jakob B. Wagner

Acknowledgements:

DTU Cen, Technical University of Denmark:
Hossein Alimadadi, Christian D. Damsgaard, Thomas W. Hansen

EPFL:
Quentin Jeangros

FEI:
Jörg Jinschek

DTU Cen
Center for Electron Nanoscopy

1

DTU Cen, Technical University of Denmark

DTU Center for Electron Nanoscopy

- Realized by a generous donation from the A.P. Møller og Hustru Chastine McKinney Møller's Fond til Almene Formaal
 - DKK 100,000,000 ~ €14,000,000
 - Grant announced In January 2006
 - "Establish a World Class Facility with a unique suite of advanced electron microscopes, in a purpose-built building"
 - Inaugurated In December 2007
-
- Hosting 7 electron microscopes
 - 2 high-end TEM (1 ETEM)
 - 1 work horse TEM
 - 2 dual beam SEM/FIB
 - 2 SEM



2

DTU Cen, Technical University of Denmark

FEI Microscopes at DTU Cen

- SEMs
 - Inspect 'S'
 - Workhorse
 - EDX/WDS
 - Quanta 3D FIB/SEM
 - Sample prep
 - Quanta 200 FEG
 - High res
 - Cryo
 - EDX
 - Helios Nanolab FIB/SEM
 - EBSD
 - EDX
- TEMs
 - Tecnai T20 G2
 - Workhorse
 - EDX/GIF
 - Titan 80-300 probe corrected
 - Holography
 - EDX/GIF
 - Titan 80-300 image corrected
 - ETEM
 - EDX/GIF

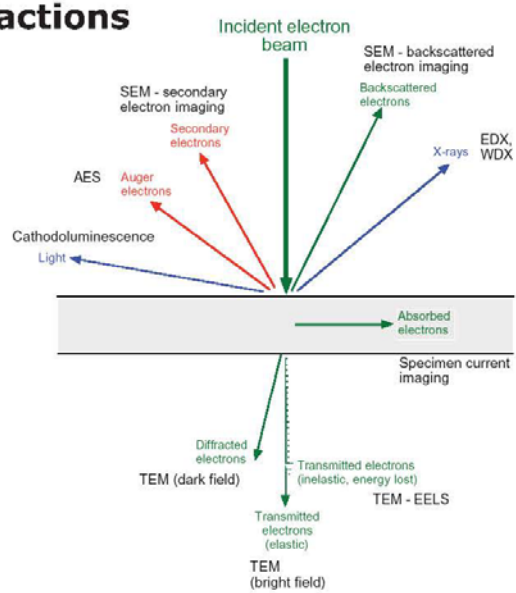
More info on the web: www.cen.dtu.dk

3

DTU Cen, Technical University of Denmark

Image Formation (at all scales) -Beam-specimen interactions

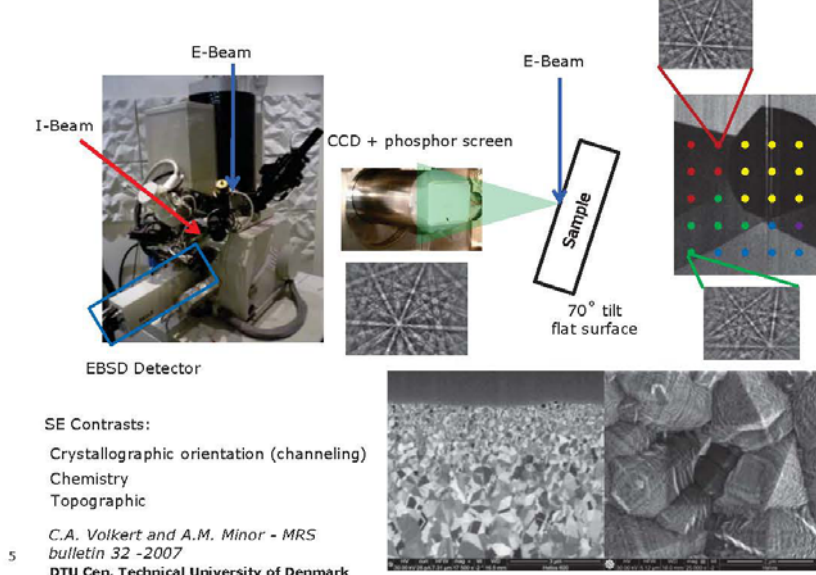
- The fast electrons is focused and controlled easily by electro-magnetic lenses
- Interaction between fast electrons and matter creates a variety of signals



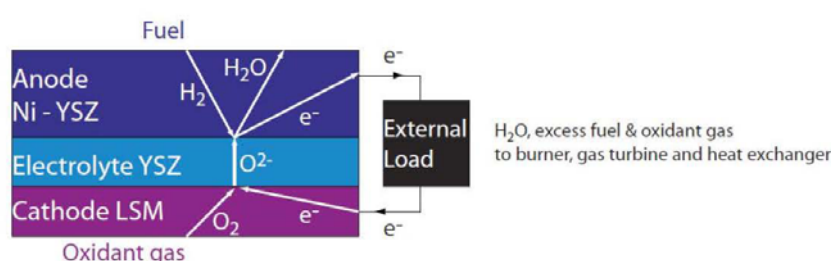
4

DTU Cen, Technical University of Denmark

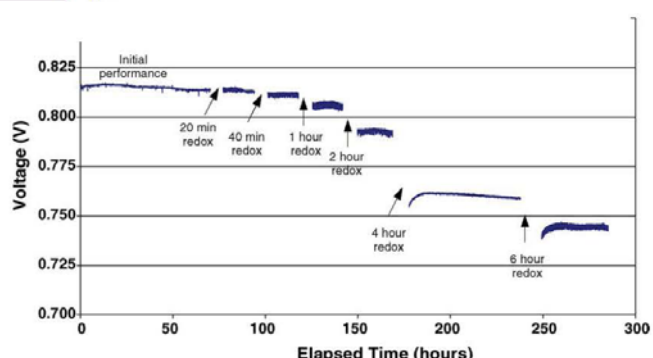
Dual Beam: EBSD, ion channeling imaging



Failure of Solid Oxide Fuel Cells



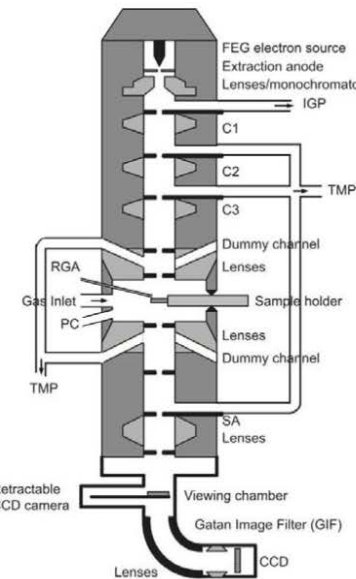
- Fuel Cell Anode Failure
 - Redox stability of NiO/YSZ based anode



12 DTU Cen, Technical University of Denmark

Environmental TEM

- C_S Image Corrector & Monochromator. E-cell
- Installed gas lines: N₂, He, Ar, O₂, H₂, CO, CO₂, CH₄ & H₂O
- Possible to attach other (premixed) gases
- Full control of composition using mass flow controllers
- Total pressure in E-Cell: up to 2000Pa
- Temperature depends on heating holder, gas pressure and gas composition (Example: approx. 700° C @ 100Pa H₂)
- Dynamic acquisition (at the moment 5 frames/s)
- EELS of gases possible



T. W. Hansen, J. B. Wagner and R. E. Dunin-Borkowski, *Mater. Sci. Technol.*, 26, 1338 (2010)

13

DTU Cen, Technical University of Denmark

Imaging at Different Length Scales

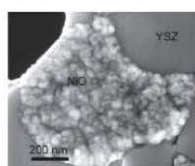
-2D to 3D and irreversible changes

ETEM sample

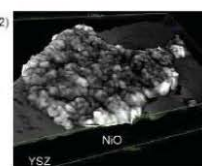
FIB slice of NiOx/YSZ based SOFC

Complementary and dynamic information from multiple facilities on the same sample is needed

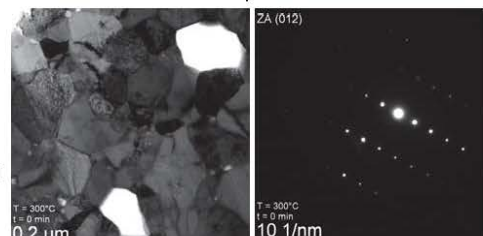
SEM sample



3D



Reduction
150Pa H₂

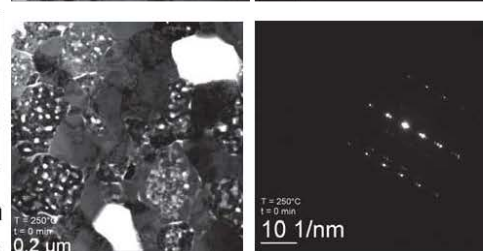


Q. Jeangros et al., *Acta Materialia* 58 (2010) 4578–4589

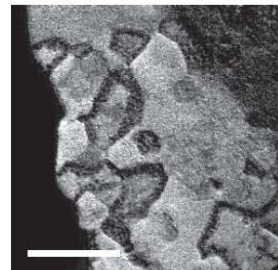
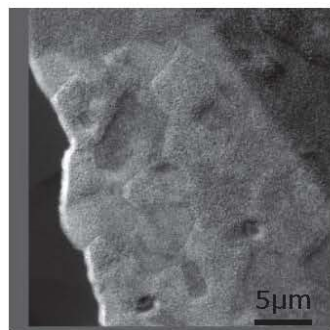
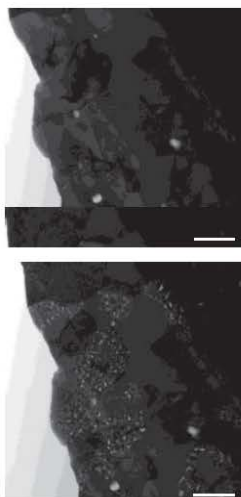
14

DTU Cen, Technical University of Denmark

Oxidation
320Pa O₂



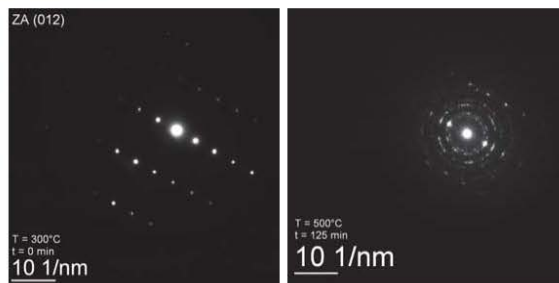
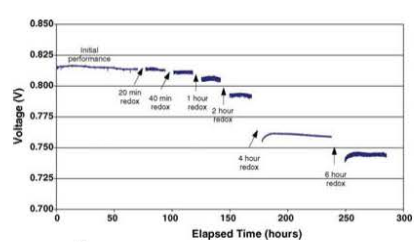
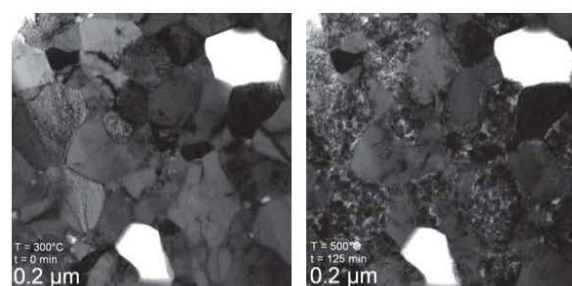
Elemental mapping (oxygen)



15 DTU Cen, Technical University of Denmark

From Structure to Application

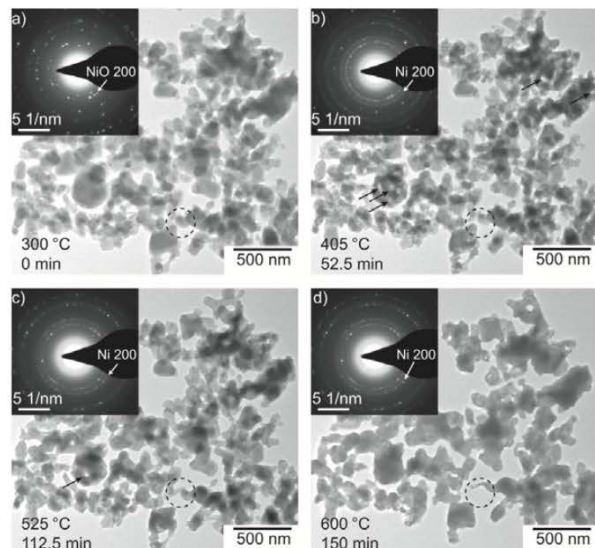
Q. Jeangros et al., Acta Materialia 58 (2010) 4578–4589



16 DTU Cen, Technical University of Denmark

Deeper insight in Nickel reduction using model system

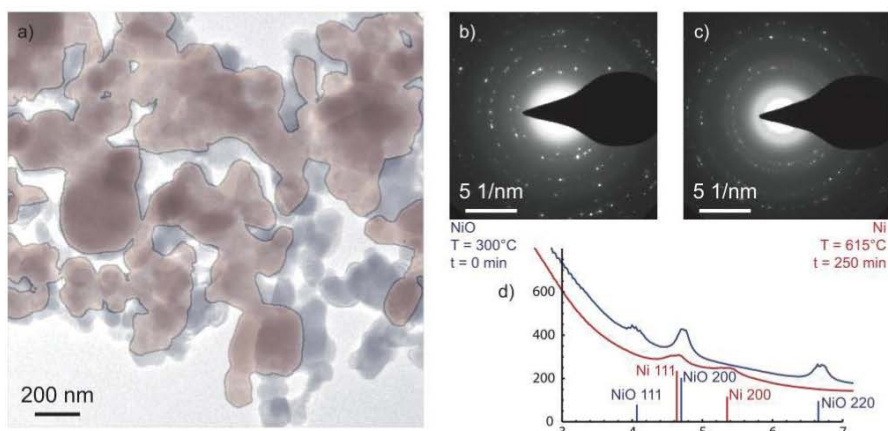
- NiO crystals
- 130Pa H₂



17

DTU Cen, Technical University of Denmark

Evolution during reduction



- In situ reduction in 130Pa H₂

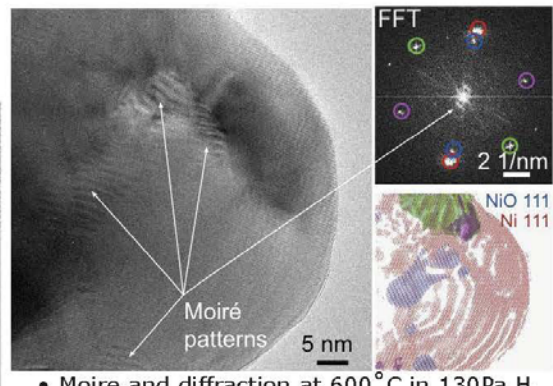
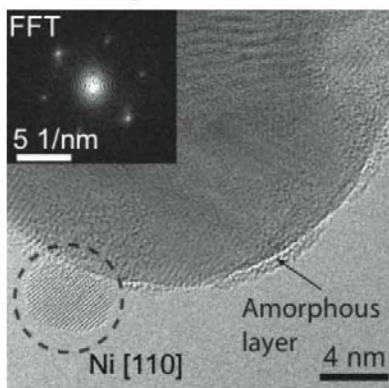
Q. Jeangros et al., J. Mat. Sci. DOI 10.1007/s10853-012-7001-2

18

DTU Cen, Technical University of Denmark

High Resolution ETEM

- Atomic arrangement visualized at 500 °C in 130Pa H₂

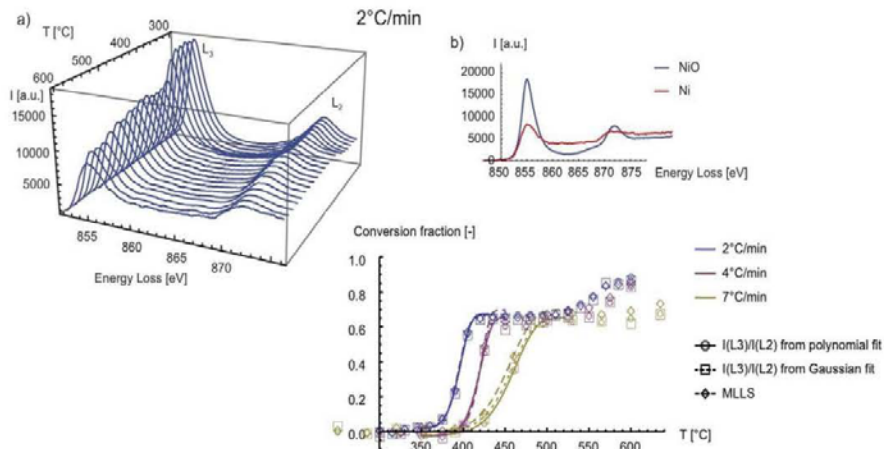


- Moire and diffraction at 600 °C in 130Pa H₂

Q. Jeangros et al., J. Mat. Sci. DOI 10.1007/s10853-012-7001-2

19 DTU Cen, Technical University of Denmark

Determination of Activation Energies - Spectroscopic Analysis



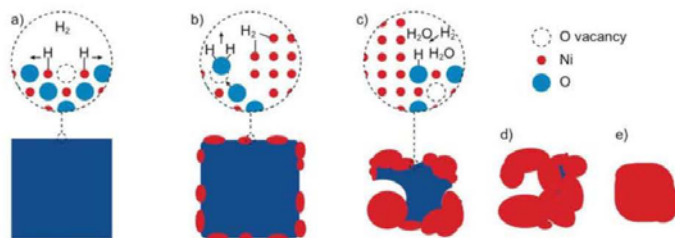
$$E_a (\text{NiO to Ni}) = 70 \pm 5 \text{ kJ/mol}$$

Similar results obtained from diffraction analysis

20 Q. Jeangros et al., J. Mat. Sci. DOI 10.1007/s10853-012-7001-2
DTU Cen, Technical University of Denmark

Methodology

- A complete dataset using different tools and techniques can be acquired
 - Different length scales
 - Different types of information (crystallographic, morphology, chemical, etc.)
- From analysis of such a dataset a coherent understanding of the process can be obtained

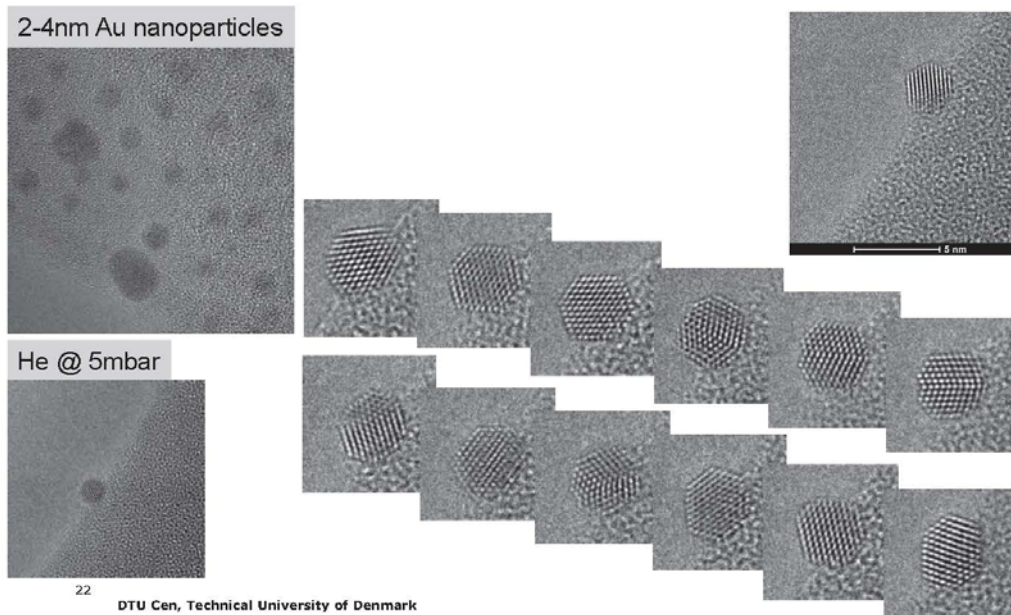


Q. Jeangros et al., J. Mat. Sci. DOI 10.1007/s10853-012-7001-2

21

DTU Cen, Technical University of Denmark

Nanoparticle mobility

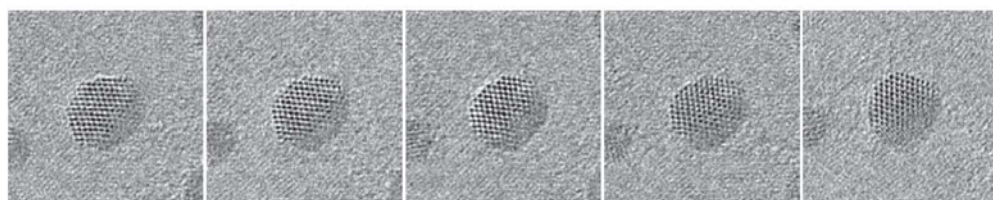
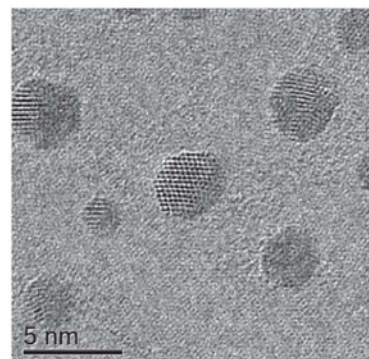


22

DTU Cen, Technical University of Denmark

Au/Graphene

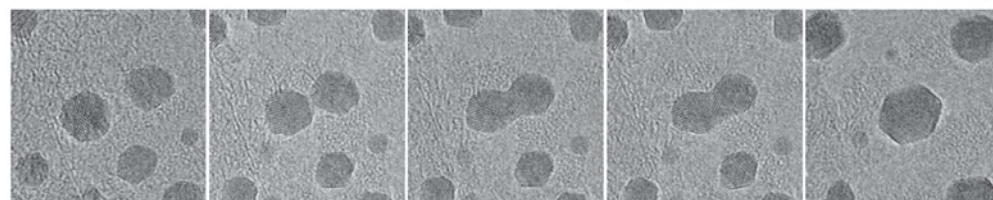
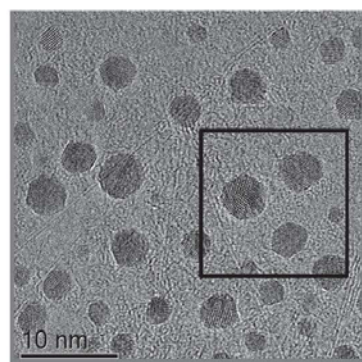
- Ca. 4x real time
- RT, Vacuum: Particles are mainly immobile
- Slight rotations are observed
- Coalescence events occur, but equilibrium shapes are only slowly obtained
- Surface reconstruction occurs
- All movies recorded at same beam current density (ca. 1A/cm²)



23 DTU Cen, Technical University of Denmark

Au/Graphene

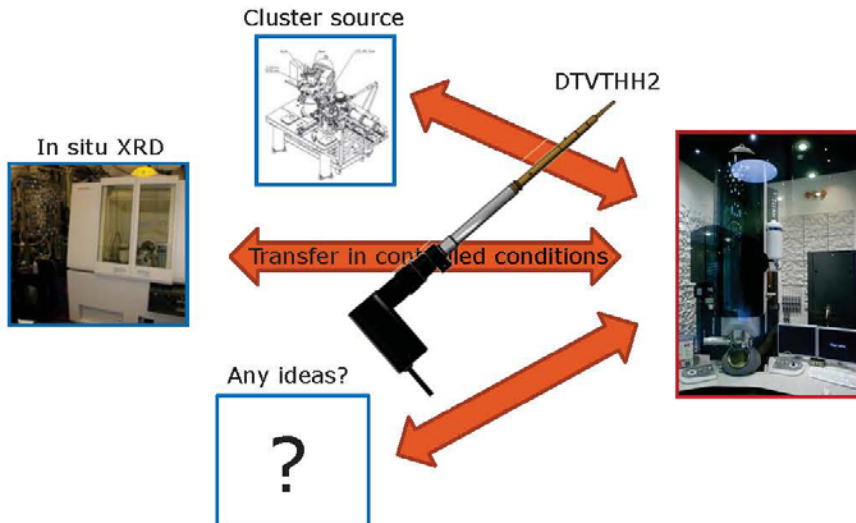
- Ca. 8x real time
- 104 °C, 200Pa H₂
- Cross correlation used for image alignment
- At low temperatures, particles wobble around equilibrium positions, but do not tend to migrate long distances
- Particles in close proximity can coalesce into single particles, but do not readily form single crystalline structures



24 DTU Cen, Technical University of Denmark

Outlook – longer term

Combining complimentary characterization and sample prep. techniques with TEM



25

DTU Cen, Technical University of Denmark

Interested in collaboration?

- Please contact us at cen.dtu.dk



The screenshot shows the homepage of the DTU Cen website. The header includes the DTU logo and navigation links for Location, Gen Home, DTU DK, Stemcy, Contact, Handbook, and Internet. The main content area features sections for "About DTU Cen", "Instrumentation", and "Access". The "About DTU Cen" section has a sub-section for "Microscopy". The "Instrumentation" section features a large image of an electron microscope. The "Access" section includes a "Microscope booking" button. At the bottom, there are links for "Show all news", "Calendar", and "Other calendar". The footer contains copyright information for DTU Cen, Lyngby, and the URL cen.dtu.dk.

26

DTU Cen, Technical University of Denmark

Nanostruktur og styrke af stål deformert ved valsning og med shot peening

Niels Hansen, DTU Vindenergi

Dansk Metallurgisk Selskabs Vintermøde 2013

Nanostruktur og styrke af stål deformeret ved valsning og ved shot peening

N. Hansen¹, X.D. Zhang¹, Y. Gao², X. Huang¹

¹Danish-Chinese Center for Nanometals, Wind Energy Department, Technical University of Denmark, Campus Risø, DK-4000 Roskilde, Denmark

²Beijing Institute of Aeronautical Materials, AVIC, Beijing 100095, P.R. China

$$\int_a^b \Theta + \Omega \delta e^{i\pi} = \sum_{i=0}^{\infty} \frac{(\Delta x)^i}{i!} f^{(i)}(x)$$

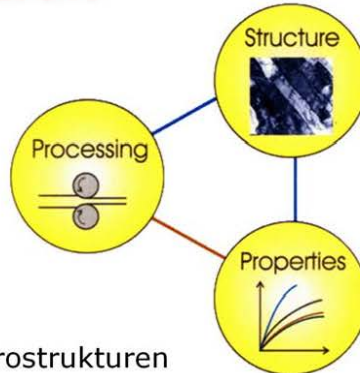
! ,

DTU Wind Energy
Department of Wind Energy

Plastisk deformation

Generelle principper

- Plastisk deformation forfiner mikrostrukturen
- En finere mikrostruktur følges af højere styrke
- Høj styrke kan opnås gennem kraftig plastisk deformation

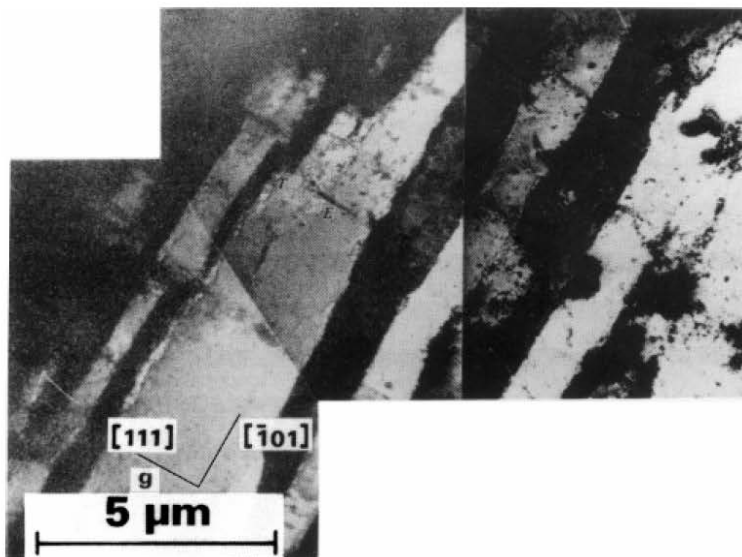


Evolution of deformation microstructures

Subdivision of grains/crystals by dislocation boundaries in characteristic 2D and 3D configurations.

3 DTU Wind Energy, Technical University of Denmark

Carpet structure in Cu



4 DTU Wind Energy, Technical University of Denmark

Cell structure in Fe

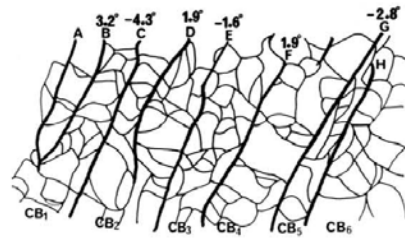
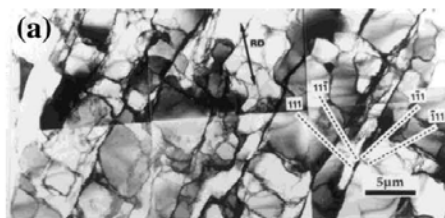


5 DTU Wind Energy, Technical University of Denmark

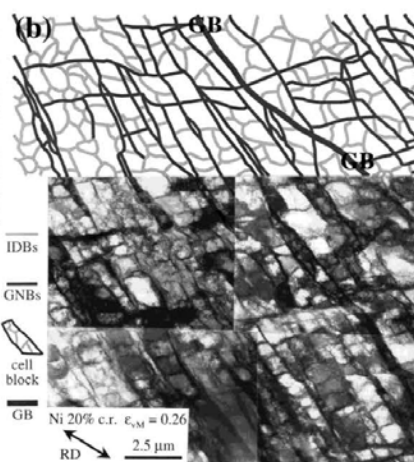
Cold deformed structures subdivided by extended almost planar boundaries (carpets) and short cell boundaries forming cell blocks



99.96% Al $\varepsilon_{VM} = 0.12$



99.99% Ni $\varepsilon_{VM} = 0.26$



6

DTU Wind Energy, Technical University of Denmark

Structural evolution during plastic deformation



Grains/crystals subdivide by formation of dislocation and high angle boundaries, creating hierarchical structures in a finer and finer scale down to the nanometer dimension as the strain and stress increased to a high level.

7 DTU Wind Energy, Technical University of Denmark

Large strain deformation



Structural length scale > 100 – 300 nm

Process examples are:

Rolling

Torsion

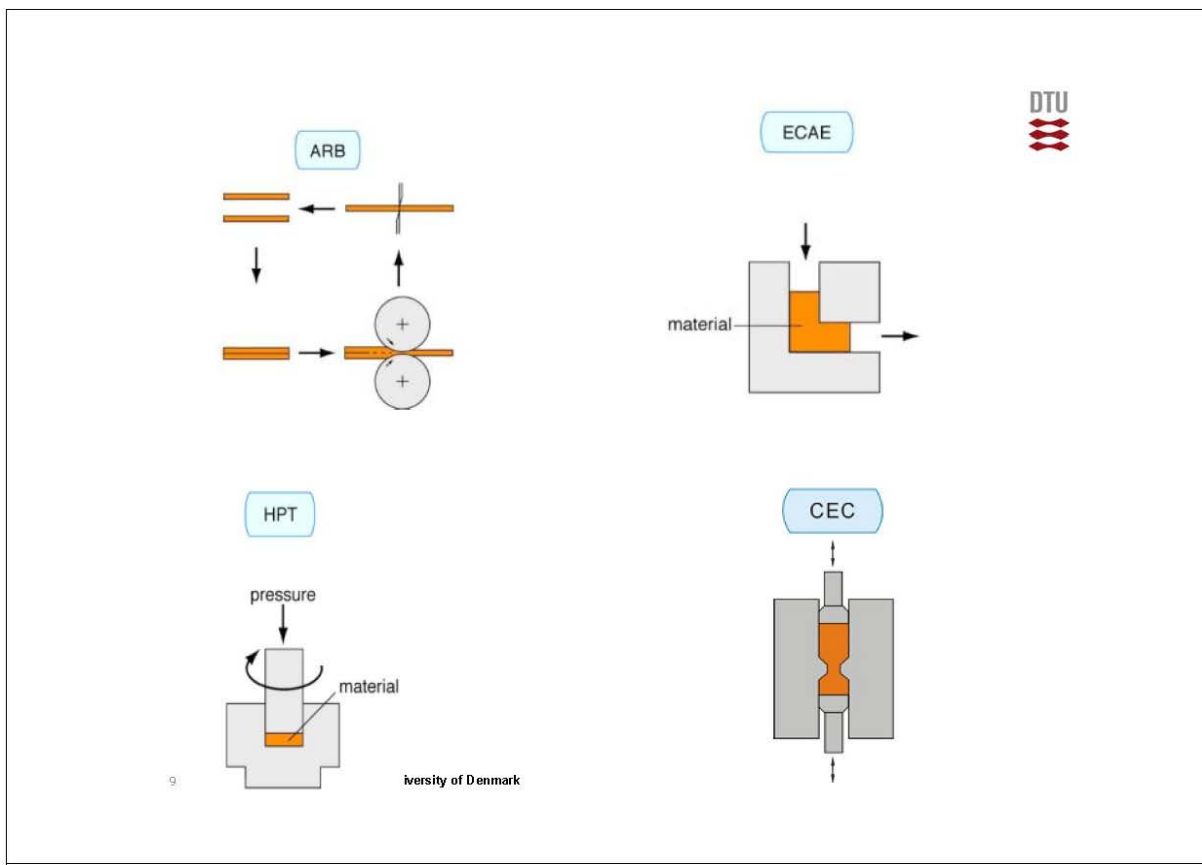
Drawing

Accumulative roll bonding

Equal channel angular extrusion

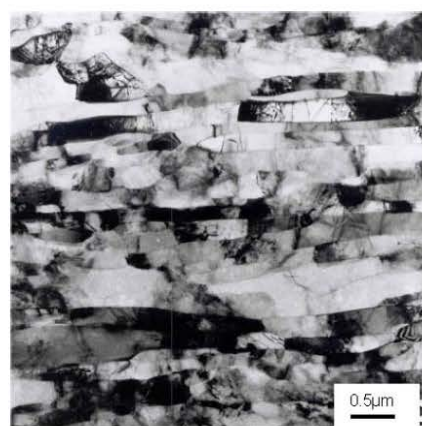
Multidirectional deformation

8 DTU Wind Energy, Technical University of Denmark

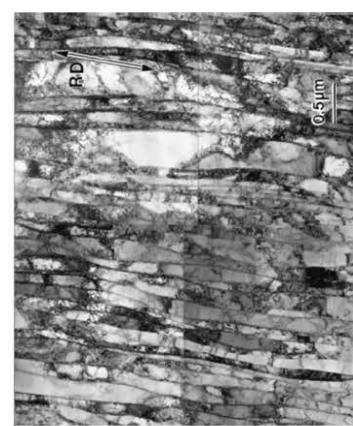


Al and Ni cold rolled to large strain

Al, $\varepsilon_{VM}=6$



Ni, $\varepsilon_{VM}=3.5$



Large strain deformation

Structural length scale $> 50 \text{ nm}$

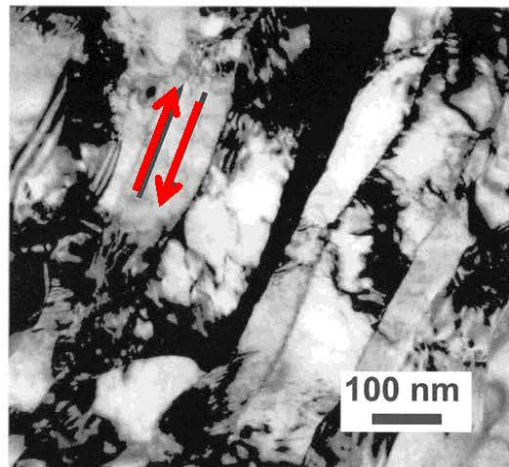
Process examples are:
High pressure torsion
Dynamic plastic deformation

Structural length scale $> 5 \text{ nm}$

Process examples are:
Ball milling
Surface mechanical attrition
Friction

11 DTU Wind Energy, Technical University of Denmark

TEM of 99.99% Ni cold-deformed by high pressure torsion to $\varepsilon_{VM} 12$. The shear direction is marked.

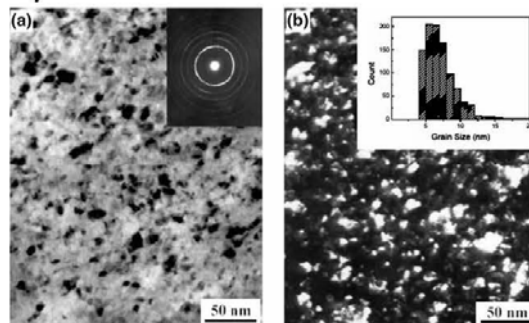


12 DTU Wind Energy, Technical University of Denmark

Surface mechanical attrition treatment (SMAT) of iron



- The surface layer is nanostructured with a boundary spacing about 10 nm.
- The subsurface layer is graded and extend to about 50 µm below the surface.



Bright field image (a) and dark field image (b) of 99.95% pure iron –
surface layer

13 DTU Wind Energy, Technical University of Denmark

Analysis of structure and strength
of low carbon steel deformed by
shot peening and by cold rolling



Applications

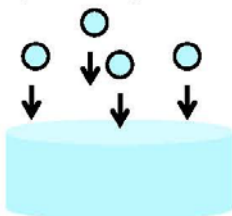


15 DTU Wind Energy, Technical University of Denmark

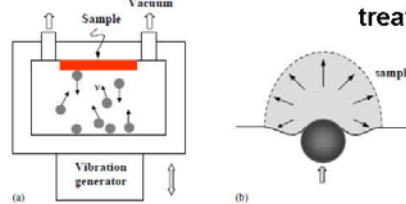
Particle Impact



Shot-peening



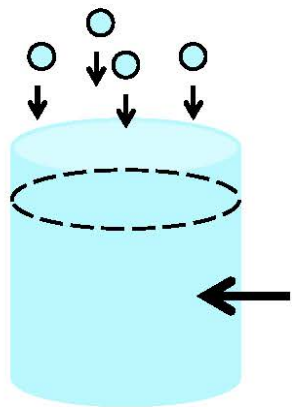
SMAT (surface mechanical attrition treatment)



	Shot-peening	SMAT
Shot size	0.05 ~ 1 mm	1 ~ 10 mm
Shot velocity	~ 100 m/s	1 ~ 20 m/s
Shot direction	Single direction (~ 90°)	Multi-direction (vibration frequency: 20 ~ 50 HZ)
Temperature increase	50-100 °C	50-100 °C
Thickness of graded nanostructures	~ 20 µm	~ 40 µm

15 DTU Wind Energy, Technical University of Denmark

Shot Peening (1)



0.8 mm high-carbon steel balls
High shot velocity: 260-300 m/s

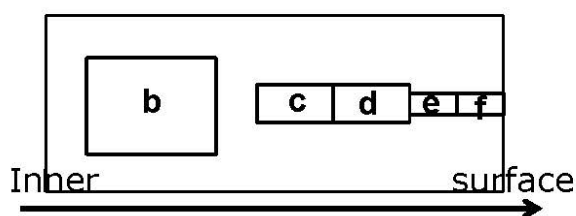
Cold rolling: low to high strain
Strain rate: about 0.3 s^{-1}

Material

Pure industrial iron: Fe-0.004C-0.44Al-0.017Ni-0.13Mn-0.0066P

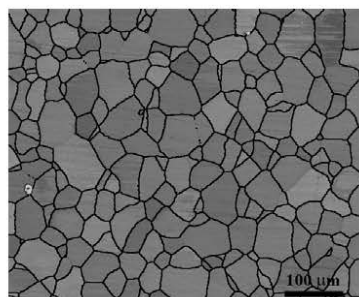
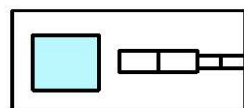
17 DTU Wind Energy, Technical University of Denmark

Shot-peening (2)



- b) 1200 - 600 μm from surface
- c) 460 - 260 μm from surface
- d) 260 - 60 μm from surface
- e) 60 - 30 μm from surface
- f) 30 - 0 μm from surface

b: 1200 - 600 μm from surface



Inner

surface

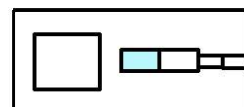
Black line: high angle boundary (Misorientation angle $> 15^\circ$)

18 DTU Wind Energy, Technical University of Denmark

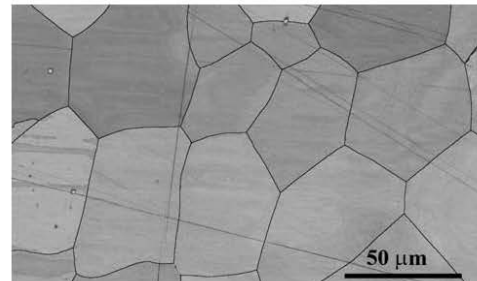
Shot-peening (3)



c: 460 - 260 μm from surface



d: 260 - 60 µm from surface



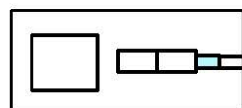
50 μm

Inner surface

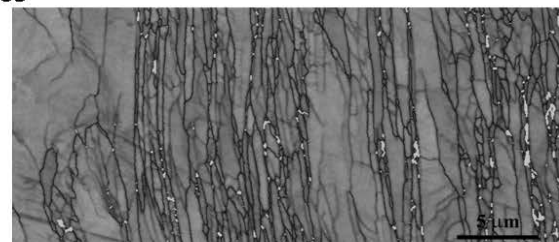
Shot-peening (4)



e: 60 - 30 μm from surface



f: 30 - 0 μm from surface



5

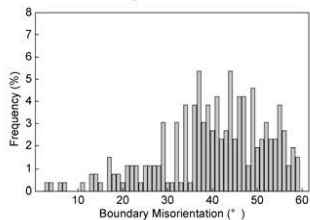
DTU Wind Energy, Technical University of Denmark Black line: high angle boundary (Misorientation angle > 15°)

Shot-peening (5)

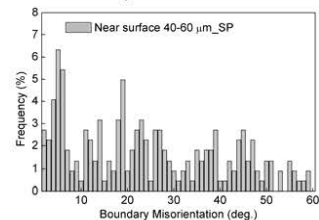


Lamellar boundary misorientation angle (EBSD)

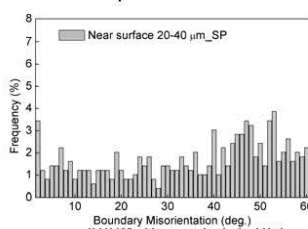
1200 - 600 μm from surface



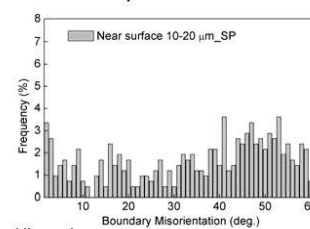
60 - 40 μm from surface



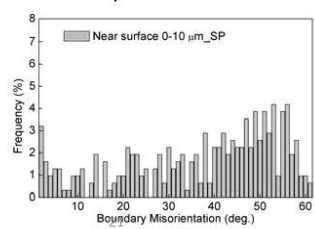
40 - 20 μm from surface



20 - 10 μm from surface



10 - 0 μm from surface



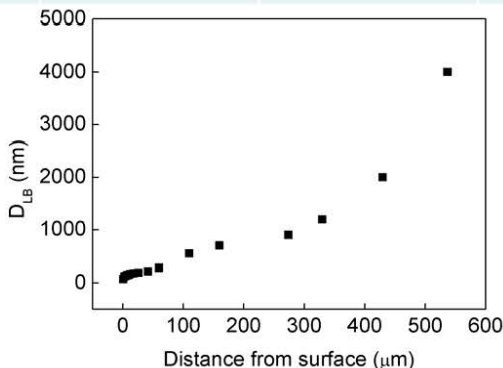
DTU Wind Energy, Technical University of Denmark

Shot-peening (6)



Structural parameters in a lamellar surface

	$\theta_{LB}(\text{deg.})$	$D_{LB}(\text{nm})$	Fraction of HABs (%), F_{HAB}
Near surface 0-20 μm SP	35.4	223	80.6
Near surface 20-40 μm SP	34.9	301	80.7
Near surface 40-60 μm SP	24.6	515	65.2

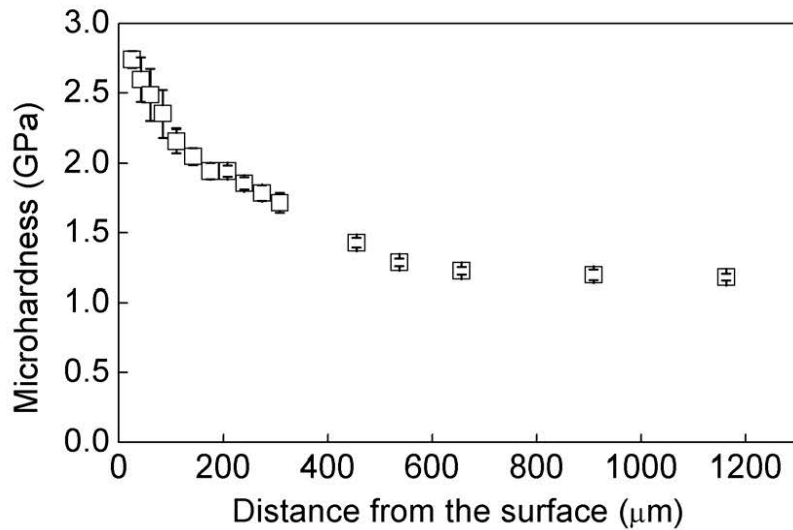


22 DTU Wind Energy, Te

Shot-peening (7)



Hardness vs distance from surface

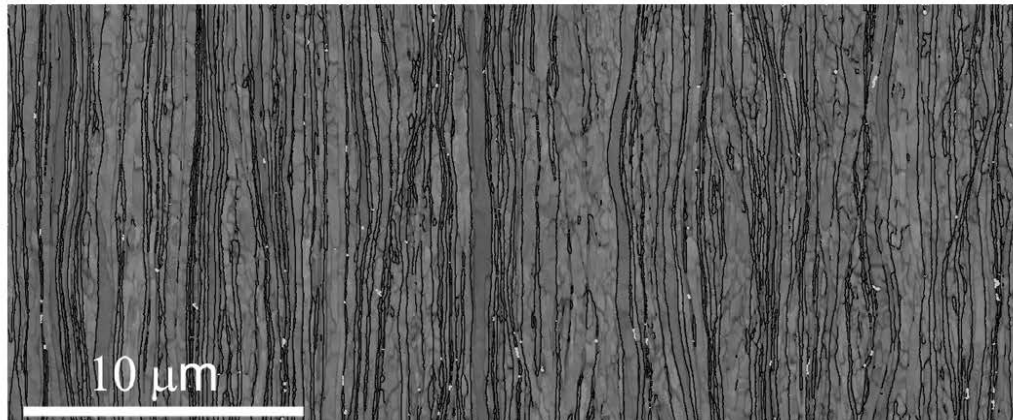


23 DTU Wind Energy, Technical University of Denmark



The microstructure in a shot-peened surface and subsurface is a graded lamellar structure, also observed in a friction and wear sample. The lamellar morphology also characterizes samples cold rolled to high strain.

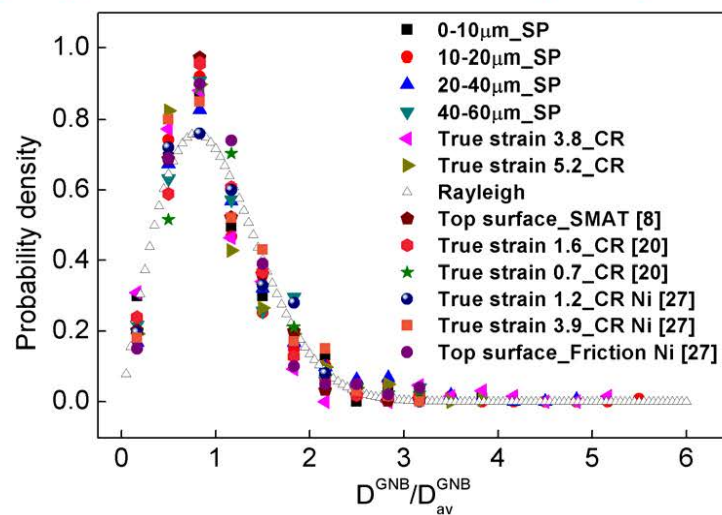
24 DTU Wind Energy, Technical University of Denmark



Microstructure of cold-rolled pure iron_Strain 4.26

25 DTU Wind Energy, Technical University of Denmark

Scaling of D^{GNB}
In samples deformed by shot peening (SP), cold rolling (CR), surface mechanical attrition (SMAT) and friction



26 DTU Wind Energy, Technical University of Denmark

Relationships between microstructural parameters and the stress and strain state in a graded surface layer as a basis for constitutive equations

- Stress estimate: microhardness, nanoindentation, miniature test samples.
- Strain estimate: displacement of structural markers as grain boundaries, twin boundaries and embedded pins.

Structure property relationships are difficult to obtain as surface layers are thin ($< 50 \sim 100 \mu\text{m}$) and the microstructure is graded at a nanostructural scale.

27 DTU Wind Energy, Technical University of Denmark

Indirect estimate of structure-property relationships in a graded structure

The deformed structures in shot-peened, friction and cold-rolled samples have similar characteristics, and is suggested to use the structure-property relationships for rolled (bulk) samples as a baseline for the analysis of graded surface structures.

28 DTU Wind Energy, Technical University of Denmark

Structure property relationships for cold-rolled samples

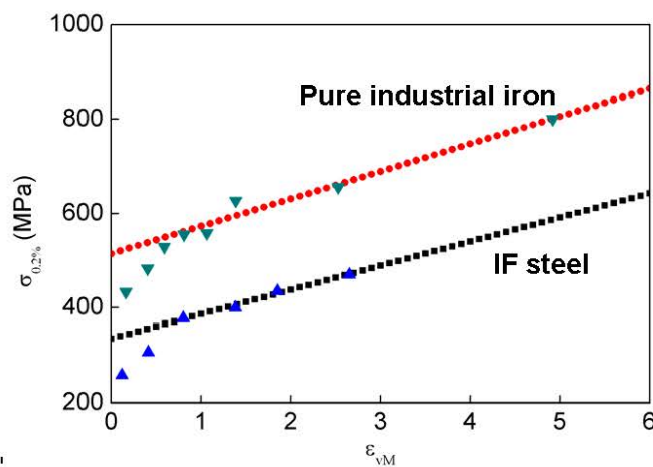
Establish master curves for the relationships:

- Stress (σ) and strain (ε)
- Stress (σ) and boundary spacing (D_{av})
- Strain (ε) and boundary spacing (D_{av})

29 DTU Wind Energy, Technical University of Denmark

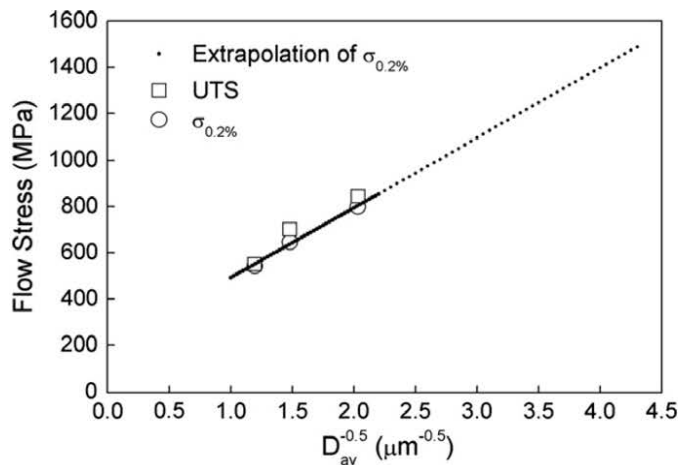
Flow stress (σ) as a function of the rolling strain (ε)

Parabolic hardening (Stage III)
Linear hardening (Stage IV)



30 DTU Wind E1

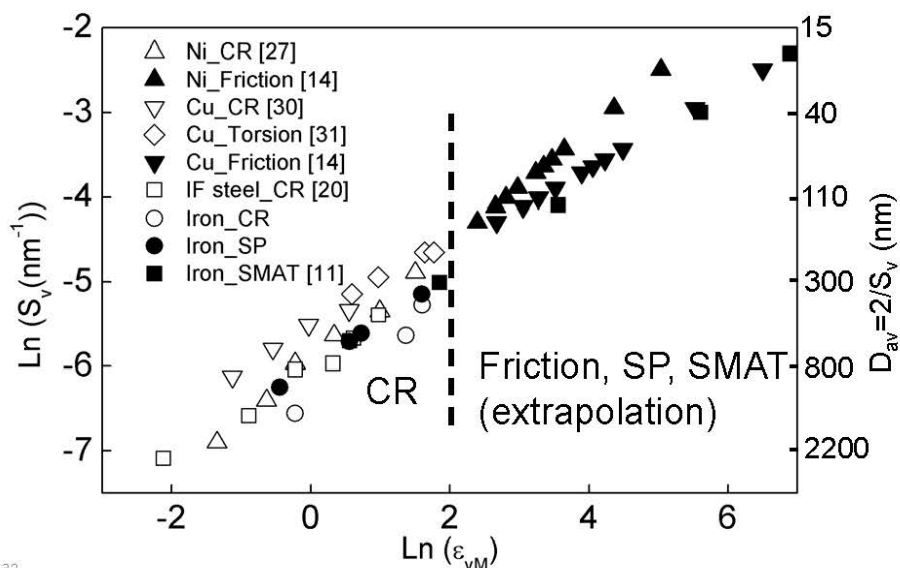
Flow stress (σ) as a function of boundary spacing (D_{av})



$$\sigma = 190.74 + 301.36 \times D_{av}^{-0.5}$$

31 DTU Wind Energy, Technical University of Denmark

Relationship between boundary spacing D_{av} ($=2/S_v$) and strain (ε)



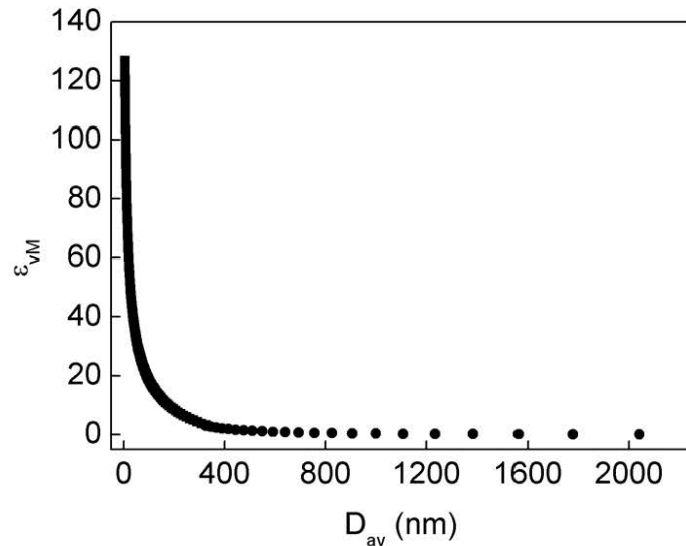
32

Stress and strain state in graded structures

Based on master curves for rolled samples the local stress and strain state in a graded surface strcture can be estimated by a measurement of D_{av} as a function of the distance from the surface.

33 DTU Wind Energy, Technical University of Denmark

Strain (ε) as a function of boundary spacing (D_{av})

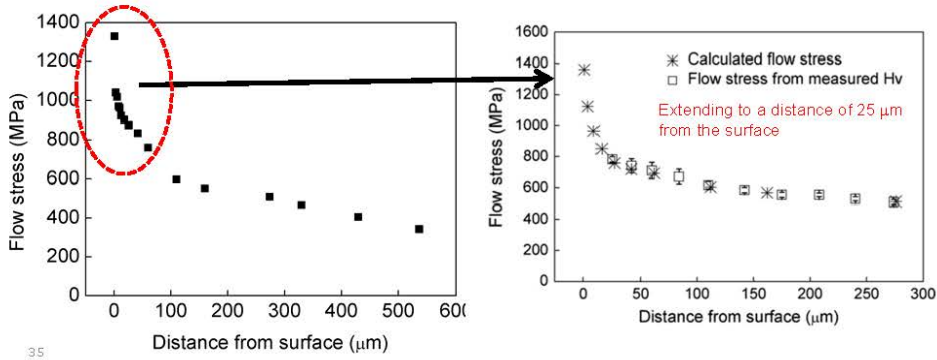


34

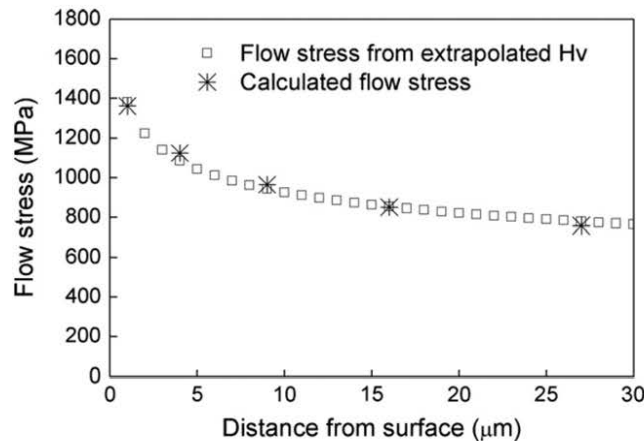
Stress distribution in a graded surface / subsurface layer



- Determined by microhardness, approx. 1/3 the flow stress
 - Determined indirectly based on a master curve for the relationship between σ and D_{av}



Stress distribution in the top surface layer (0-25 μm) of a SP sample



Konklusion

- Et hårdt overfladelag dannet ved plastisk deformation som f.eks. shot peening har en gradueret nanostruktur, der strækker sig 50-100 µm ind i materialet.
- Spændings- og tøjningstilstanden i overfladelaget kan analyseres ved lokalt at bestemme afstanden mellem dislokationsgrænser og korngrænser, D_{av} , der relaterer til styrken, σ , gennem ligningen

$$\sigma = K \cdot D_{av}^{-0.5}$$

K er en konstant for hårdt deformert materiale, der kan bestemmes ved at måle sammenhørende værdier for D_{av} og σ for grundmaterialet deformert f.eks. ved valsning til en høj deformationsgrad.

- Den foreslæede mikroskopiske metode til analyse af en lokal spændings- og tøjningstilstand i et deformert materiale kan anvendes generelt ved analyse af deformationszoner, f.eks. nær revner, partikler og korngrænser.

Homogen og lokaliseret tøjningsudvikling af nanostruktureret aluminium

Jacob Kidmose, DTU Vindenergi

Homogen og lokaliseret tøjningsudvikling af nanostruktureret aluminium

Fordele ved brugen af ARAMIS

Jacob Kidmose

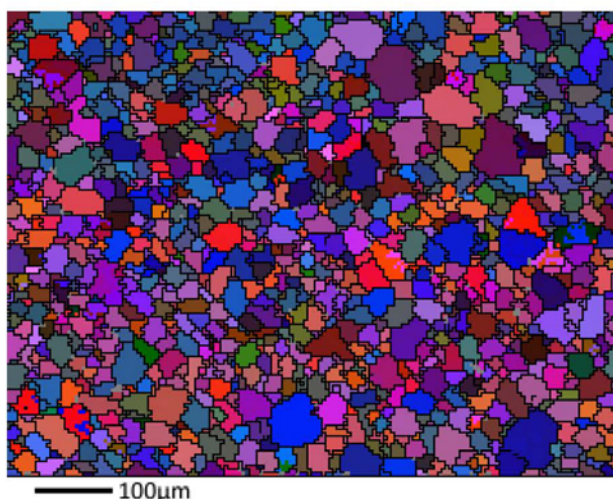
vejledere:
N. Hansen, G. Winther and X. Huang

$$f(x+\Delta x) = \sum_{i=0}^{\infty} \frac{(\Delta x)^i}{i!} f^{(i)}(x)$$
$$\int_a^b \Theta^{\sqrt{17}} + \Omega \int \delta e^{i\pi} = \{2.7182818284\}$$
$$\infty = \sum x^2 > , !$$

DTU Wind Energy
Department of Wind Energy

1

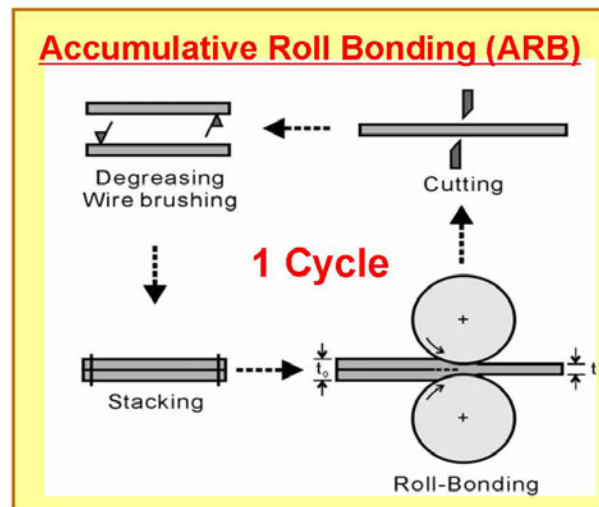
Start materiale



- Al1050
- 99.5%
- Kornstørrelse
30 μm.

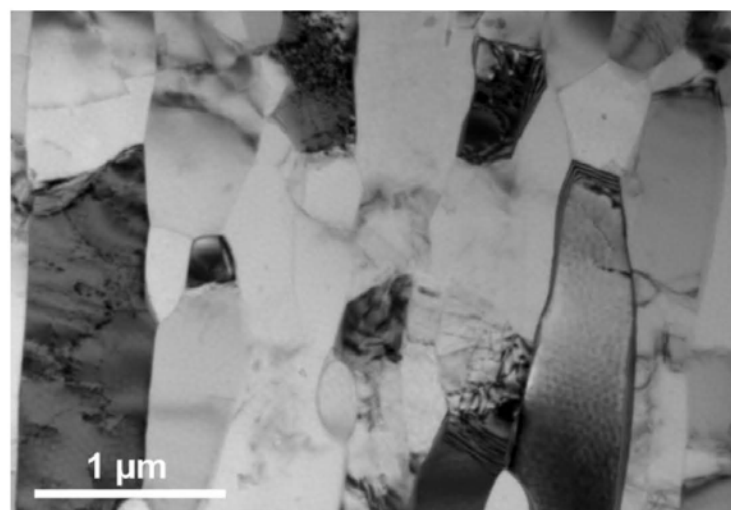
2 DTU Wind Energy, Technical University of Denmark

Accumulative Roll Bonding

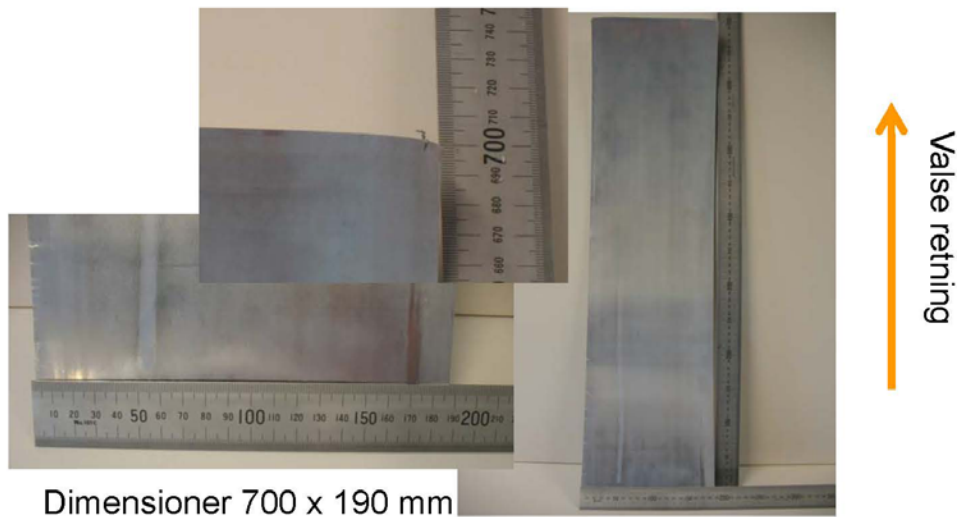


3 DTU Wind Energy, Technical University of Denmark

6C-ARB Microstruktur



4 DTU Wind Energy, Technical University of Denmark

6C-ARB1050Al plade

5 DTU Wind Energy, Technical University of Denmark

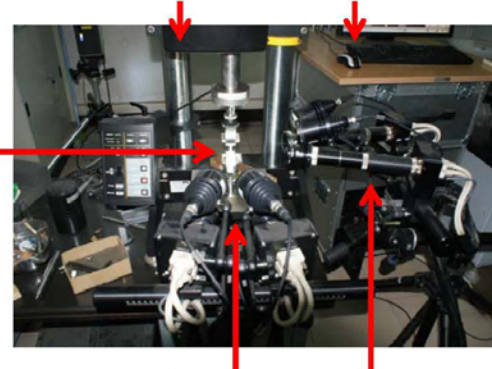
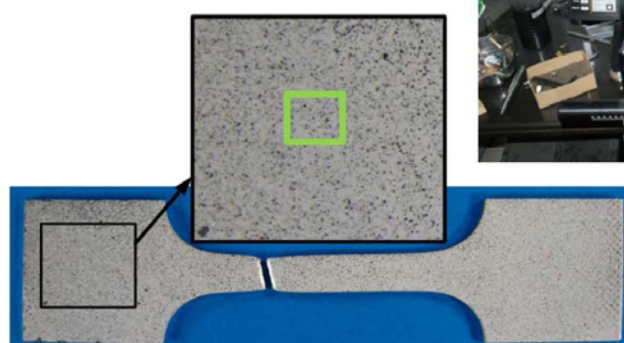
ARAMIS

- Dot pattern
- Facet size 0,75 mm

Sample

Tensile machine

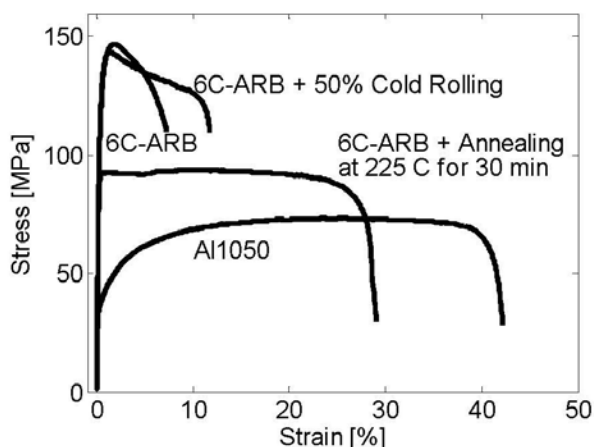
ARAMIS software

Side camera
system
(not used)Front camera
system

DTU Wind Energy, Technical University of Denmark

Mechanical properties

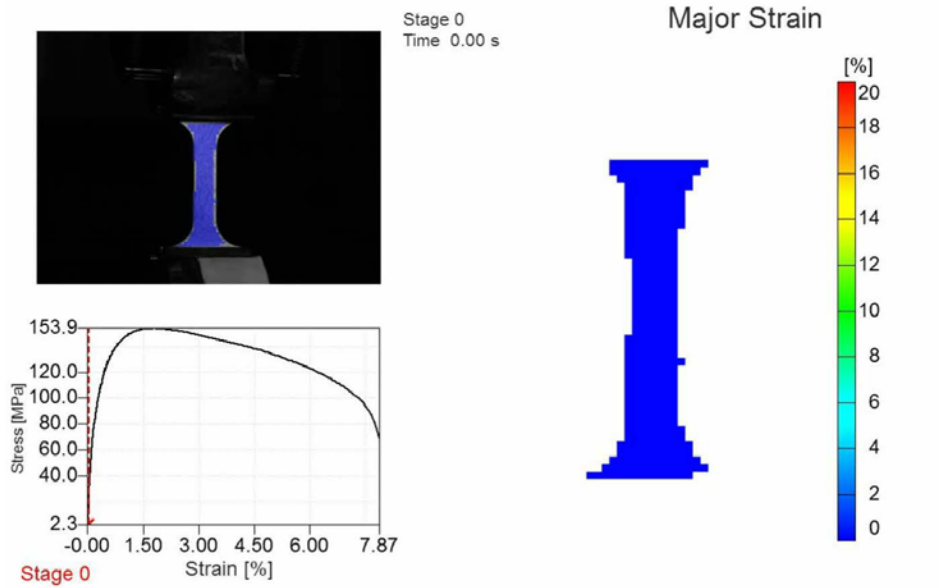
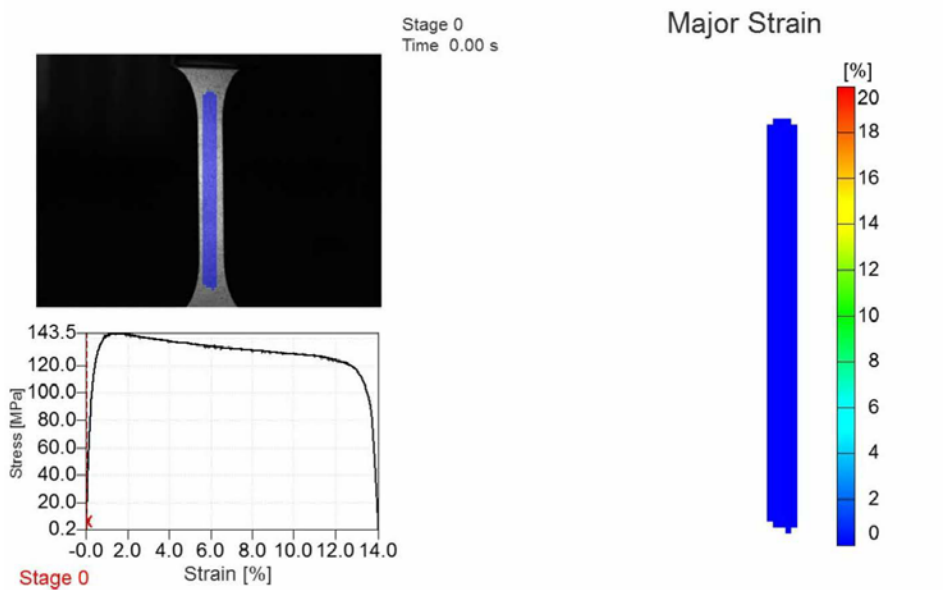
- AA1050
- 6C-ARB
- Varmbehandling
- 6C-ARB-225
- Valsning
- 6C-ARB-CR50



7 DTU Wind Energy, Technical University of Denmark

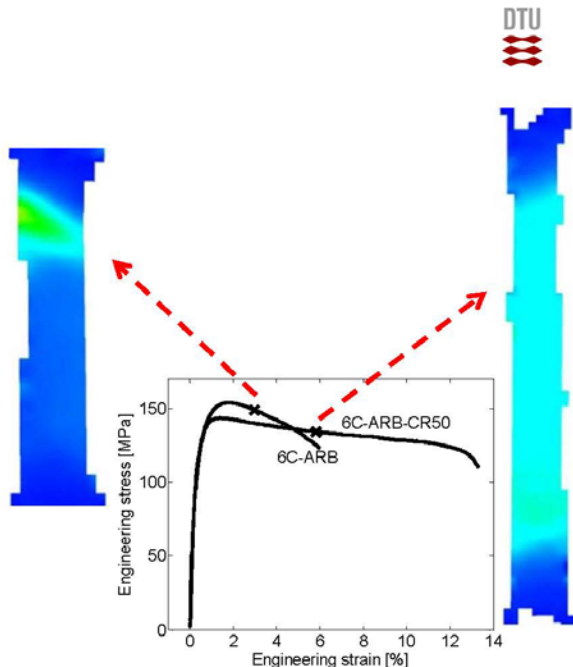
Homogen deformation

$$\begin{aligned}
 & \int_a^b \Theta^{17} + \Omega \int \delta e^{i\pi} = \\
 & f(x+\Delta x) = \sum_{i=0}^{\infty} \frac{(\Delta x)^i}{i!} f^{(i)}(x) \\
 & \infty = \{2.7182818284 \\
 & x^2 \sum! ,
 \end{aligned}$$

6C-ARB**6C-ARB-CR50**

Results

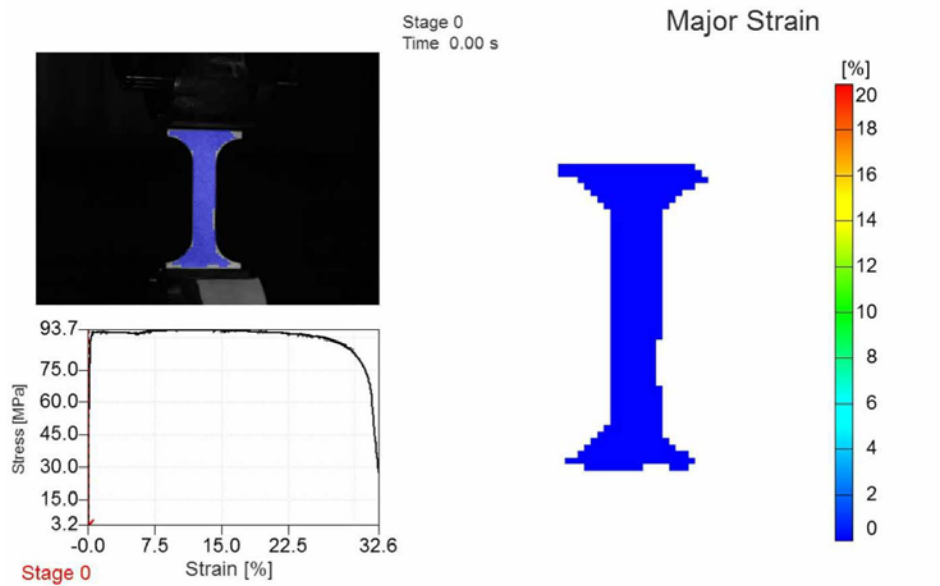
- 6C-ARB udvikler shear band lige efter brud styrken
- 6C-ARB-CR50 har homogene deformation flere procent efter brud styrke



DTU Wind Energy, Technical University of Denmark

Varmbehandling

$$\begin{aligned}
 f(x+\Delta x) = & \sum_{l=0}^{\infty} \frac{(\Delta x)^l}{l!} f^{(l)}(x) \\
 & \int_a^b \Theta + \Omega \int \delta e^{i\pi} = \\
 & \sqrt{17} \int \infty = \{2.7182818284 \\
 & \Sigma!
 \end{aligned}$$

6C-ARB-225**ARAMIS**

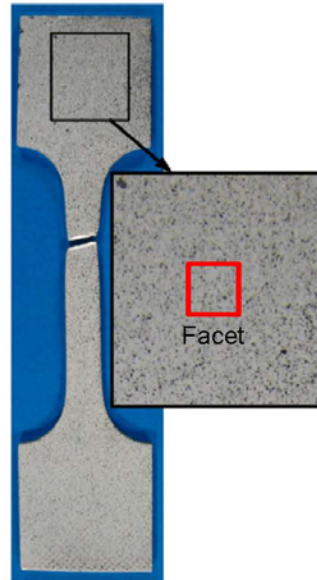
- En-akset træk prøve
 - tøjnings-spændings kurve
 - Sand tøjnings-spændings kurve (også gældende efter UTS)
 - Anisotropi

Sand tøjnings-spændings kurve

Volume konstant=> $\varepsilon_{\text{Tykkelse}} = -\varepsilon_{\text{bredde}} - \varepsilon_{\text{træk}}$

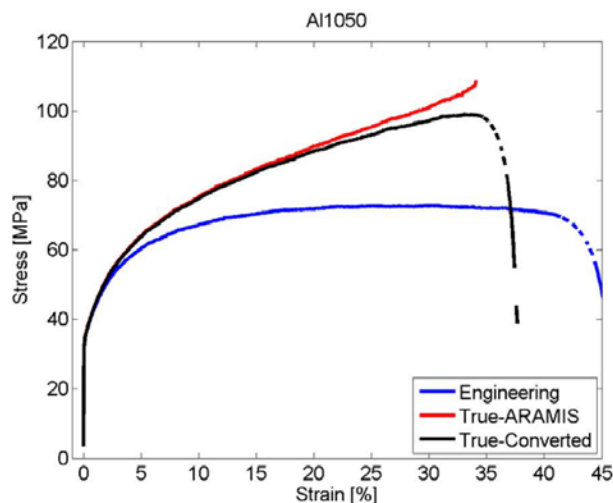
Udregning af tykkelses tøjningen over bredden af indsnævringens zonen

Derved fås det aktuelle tværsnits areal af indsnævringens zonen



DTU Wind Energy, Technical University of Denmark

Sand tøjnings-spændings kurve

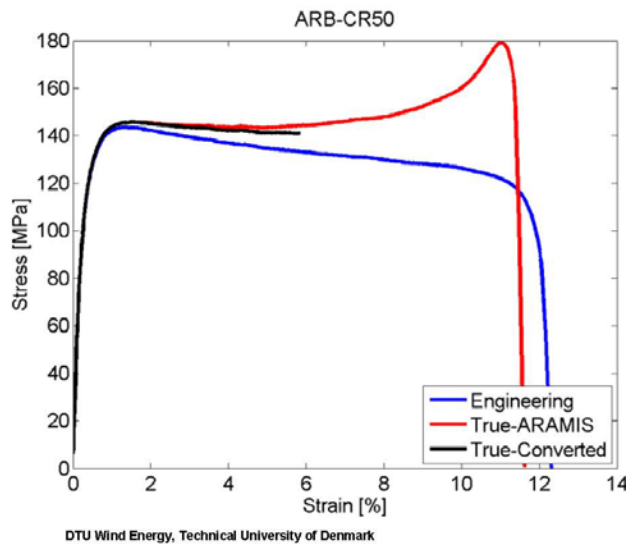


$$\sigma_t = \sigma_E(1 + \varepsilon_E)$$

$$\varepsilon_t = \ln(1 + \varepsilon_E)$$

DTU Wind Energy, Technical University of Denmark

Sand tøjnings-spændings kurve



ARAMIS

- En-akset træk prøve
 - tøjnings-spændings kurve
 - Sand tøjnings-spændings kurve (også gældende efter UTS)
 - Anisotropi

Spørgsmål?

Tak for jeres opmærksomhed.

$$f(x+\Delta x) = \sum_{i=0}^{\infty} \frac{(\Delta x)^i}{i!} f^{(i)}(x)$$

$\int_a^b \Theta + \Omega \int \delta e^{i\pi} =$
 $\infty = \{2.7182818284$
 $\chi^2 > \Sigma !,$

DTU Wind Energy
Department of Wind Energy

Baggrund for Innovationskonsortiet REEgain om magnetiske materialer

Jens Christiansen, Teknologisk Institut

Baggrund for Innovationskonsortiet REEGain om magnetiske materialer

Jens Christiansen og Martin Brorholt Sørensen

Indhold

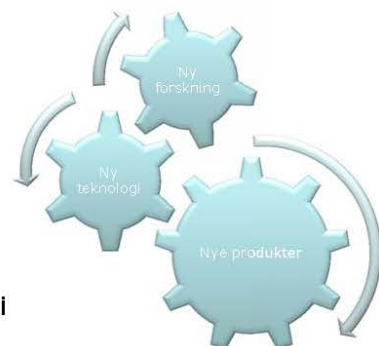
- Hvad er innovationskonsortier?
- Baggrunden for REEGain
- Virksomhedernes interesser
- Aktiviteterne REEGain

Hvad er et innovationskonsortium?

- Konkrete samarbejdsprojekter mellem virksomheder, forskningsinstitutioner og teknologiske serviceinstitutter
- Formålet er, at parterne i fællesskab udvikler viden eller teknologi, som ikke blot gavner enkelte virksomheder, men hele brancher indenfor dansk erhvervsliv
- Mindst 2 virksomheder, en forskningsinstitution og et teknologisk serviceinstitut
- Varighed på mellem 2 og 4 år

Hvad er et innovationskonsortium også?

- 'Kortslutning' mellem forskning, teknologiudvikling og produktudvikling
- Støtten til universiteterne og Teknologisk Institut balanceres med virksomhedernes indsats
- Ingen temaer, men vurderes ud fra virksomhedernes og samfundets behov
- Meget lidt bureaukrati, når projektet er i gang

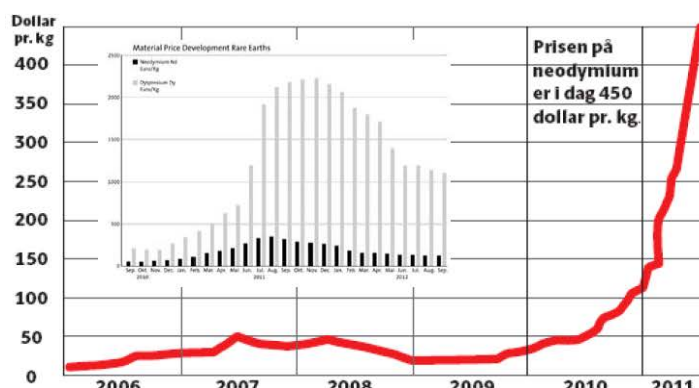


Artikler om magneter og sjældne jordarter



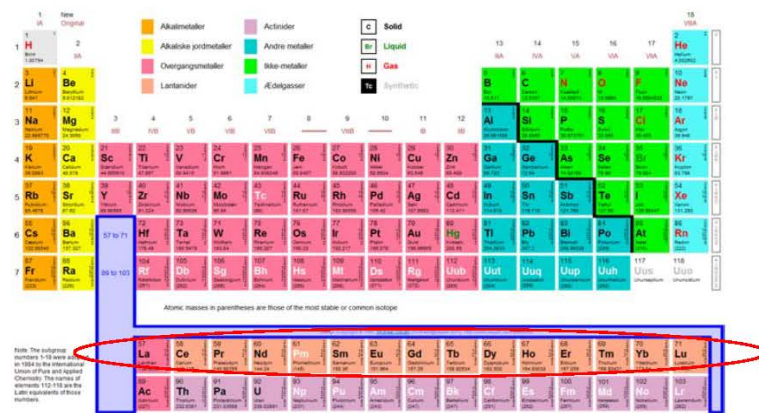
Skyhøje priser på vigtige råvarer

Priserne på **neodymium** er i denne måned roget helt op på en pris på **450 dollar eller knap 2.400 kr. pr. kilo**, der er den vigtigste af disse eftertragtede, strategisk vigtige råvarer. Det er en tidobling i forhold til prisen i slutningen af 2010. Samtidig svinger priserne meget, så de gør det svært og uforudsigeligt at indkøbe råvarer fra Kina. I dag betaler europæiske magnetproducenter over 30 procent mere for neodymium end de kinesiske konkurrenter.



Berlingske Business, august 2011

De Sjældne jordarter



Sjældne jordarters anvendelser



Kilde: mineralsUK

Sjældne jordarter i Toyota Prius



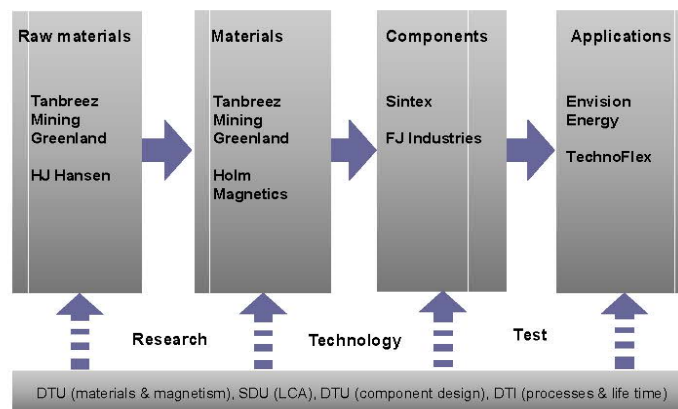
Kilde: mineralsUK

REEGain konsortiet

- DTU
- Syddansk universitet
- Teknologisk Institut
- Envision Energy APS
- FJ Industries A/S
- HJ Hansen A/S
- Holm Magnetics APS
- Sintex A/S
- Tanbreez Mining Greenland A/S
- Technoflex APS



Konsortium med fødekæde



TANBREEZ Mining Greenland A/S



Ta-Nb-REE-Z(r) - malm

Tre fraktioner:

1. Eudialyt (20%)

- REE
- Zirkonium
- Niob
- Tantal



2. Feldspat – nepheline (40%)

- Kan sælges som byggemateriale

3. Arfvedsonit (40%)

- Uudnyttet

Eudialyt	
Zirkonium oxide	1.8%
Niobium oxide	0.2%
Lette REE	0.5%
Tunge REE	0.15%

Arfvedsonit - uudnyttet fraktion (40%)

Udnyttelse

- Indeholder stor forekomst af lithium
- Magnetisk
- Udvikle metode til at udvinde lithium fra arfvedsonit



Mulige anvendelser af arfvedsonit

- "Sort sand"
- Sorte mursten?
- Salget skal kun dække omkostninger ved transporten - deponeringsomkostninger udgås

Lithium-anvendelser:

- Li-ion-batterier
- Produktion af glas (Li_2CO_3)
- Smøremidler (LiOH)
- Medicin
- Organisk kemi (LiAlH_4)

Genvinding af permanente magneter fra affald – *urban mining*



Magnetseparation fra kompressorer hos HJ Hansen





DANISH
TECHNOLOGICAL
INSTITUTE



H.J. HANSEN

Udvikling gennem generatører



DANISH
TECHNOLOGICAL
INSTITUTE

Shredder: 100 biler i timen



Formgivning af NdFeB magneter med *Metal Injection Moulding*

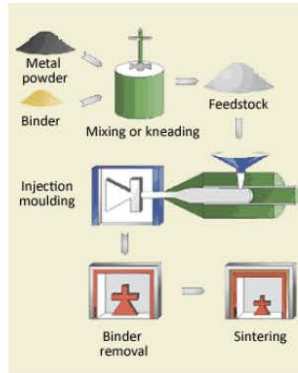


Styrker

- Kan automatiseres
- Mulighed for kompleks form
- Lavt spild
- snævre tolerancer i forhold til støbeprocesser

Svagheder

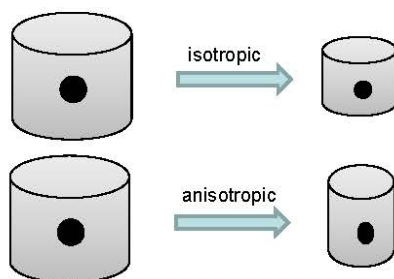
- Begrænsning på dimensioner
- Kræver stort styktal – eller høj stykpri



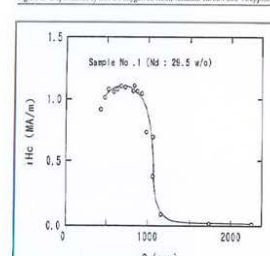
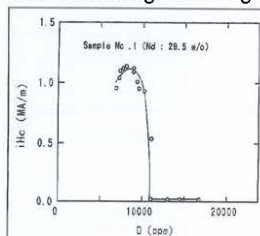
Udfordringer for MIM fremstillet NdFeB magneter



- Forhindring af oxidation
- Kontrol af karbon - legering reagerer med bindemidler ved forhøjet temperatur
- Kontrol med kornstruktur
- Anisotropisk krympning af aligned NdFeB
- Ingen komprimeringstryk



Magnetens evne til at modstå afmagnetisering



Osamu Yamashita, 1998

Magneter til vindmøller

- Kan magnetene designes, så de blot skal remagnetiseres?
- Kan mængden af magnetisk materiale reduceres?
- Hvor store magneter kan vi lave?
- Har vi sjældne jordarter nok?
- Kan simple blandinger af sjældne jordarter benyttes?



Foto: ing.dk

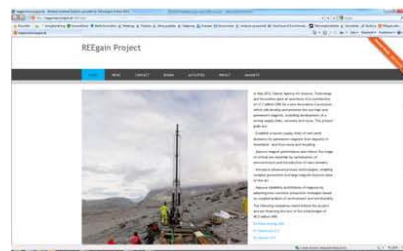
Pilotudstyr og analyselaboratorier Teknologisk Institut



Delprojekter i REEgain

- Mixed Rare-Earth-Fe-B sintered magnets – DTU Energy Conversion (manager), Holm Magnetics (exploitation manager)
- Minimizing Magnetic Materials by design and recycling - DTU Elektro (manager), SDU, Envision Energy (Exploitation manager), HJ Hansen, Sintex
- Minerals chemistry, separation and recycling - Tanbreez (manager), DTI, HJ Hansen
- Materials investigation and processing - Sintex (manager), DTI, FJ Industries
- Operational magnetic systems - reliability and surface protection - Technoflex (manager), DTI, Envision Energy, Sintex

Følg med i projektet på www.reegain.dk



Tak for opmærksomheden

Jens Christiansen, sektionsleder –
Materialedivisionen, jec@teknologisk.dk

Superleder tapes karakteriseret fra nanometer pinning
til meter store spoler

Asger Bech Abrahamsen, DTU Vindenergi

Superconductors characterized from nanometer pinning sites to meter size coils for direct drive wind generators

Asger B. Abrahamsen¹ and Bogi Bech Jensen²

¹Department of Wind Energy

²Department of Electrical Engineering

Technical University of Denmark

A collage of mathematical symbols and equations, including $f(x+\Delta x) = \sum_{i=0}^{\infty} \frac{(\Delta x)^i}{i!} f^{(i)}(x)$, $\int_a^b \Theta + \Omega \delta e^{ix} = \{2.7182818284$, $\sum!$, and ∞ .

Dansk Metallurgisk Selskab, Vintermøde 2013

January 16-18, Kolding, Denmark

DTU Wind Energy
Department of Wind Energy

Outline

- Motivation
- Scaling laws of turbines
- Superconductors
- Generators
- Conclusion

Cost Of Energy (COE)

$$COE = \frac{CAPEX + OPEX}{Energy\ production}$$

CAPEX: Capital Expenditure

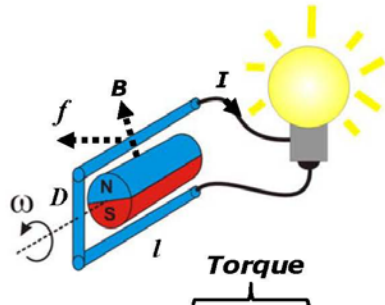
1.5 MEuro/MW* →

7.5 MEuro for 5 MW

OPEX: Operational Expenditure

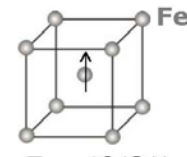
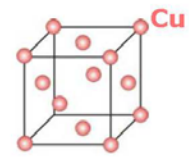
*EU 2030 target for offshore wind

Motivation for superconducting generator

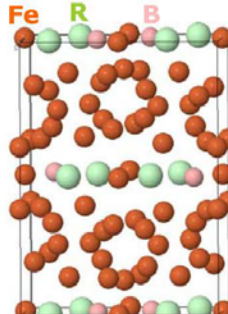


- 1G : Copper + Iron
- 2G : $R_2Fe_{14}B$ magnets+Fe
10 MW ~ 6 tons PM
- 3G : $RBa_2Cu_3O_{6+x}$ HTS + Fe
10 MW ~ 10 kg RBCO

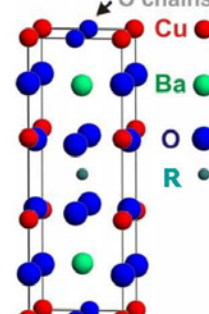
DTU Wind Energy, Technical University of Denmark



$T_c = 1043$ K
 $B_r \sim 0$ Tesla



$T_c = 583$ K
 $B_r \sim 1.4$ Tesla

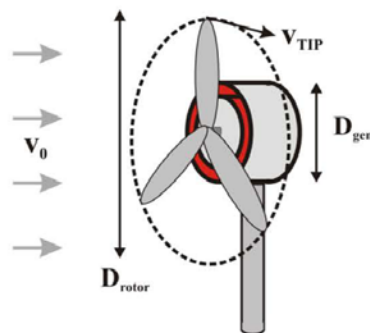


$T_c = 93$ K
 $B_{c2} \sim 100$ Tesla

Motivation: Up-scaling the turbine power

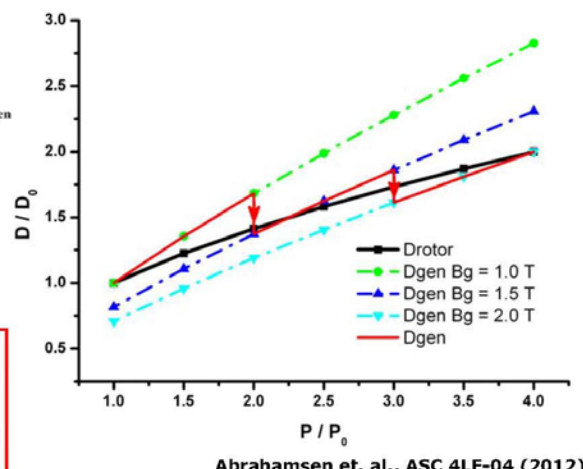


Constant tip speed \rightarrow	Rotor diameter	$D_{rotor} \sim P^{1/2}$
Torque	$T \sim P^{3/2}$	
Generator diameter	$D_{gen} \sim (BI)^{-1/2} P^{3/4}$	

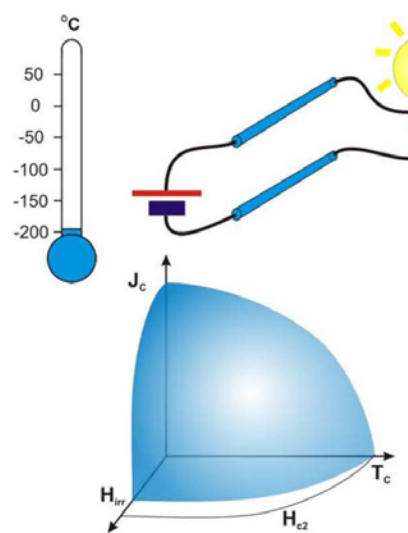


$$P = T\omega = \frac{1}{2}\rho D_{rotor}^2 v_0^3 C_p$$

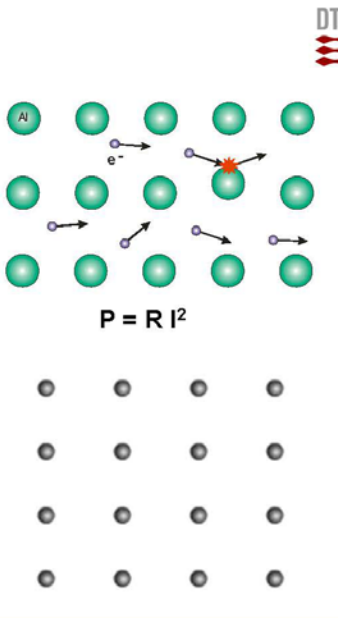
$$= B_g ID_{gen}^2 L_{gen} \omega$$



Superconductivity

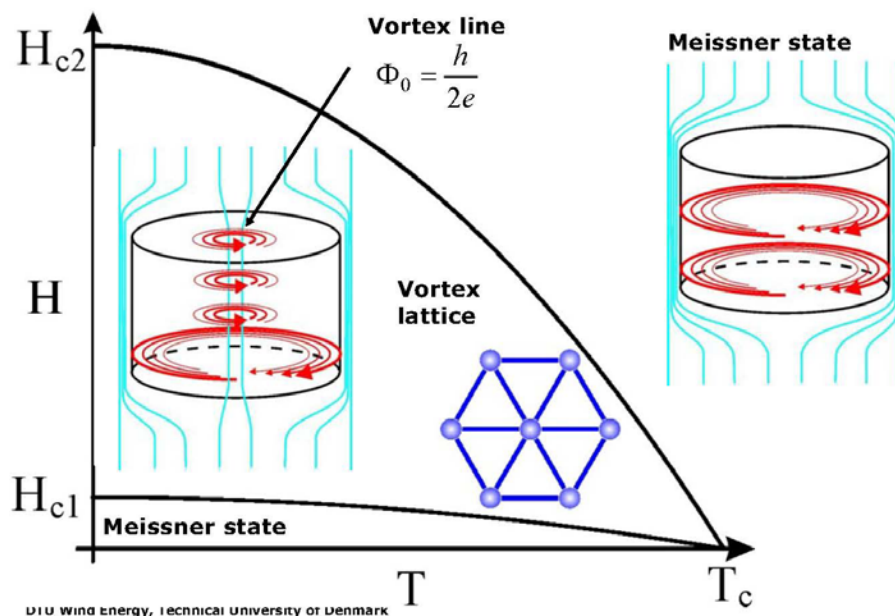


DTU Wind Energy, Technical University of Denmark



DTU

Critical fields



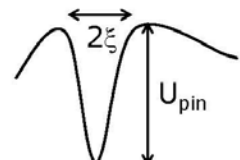
DTU Wind Energy, Technical University of Denmark

Critical current density

- Lorentz force on vortex line

- Pinning force

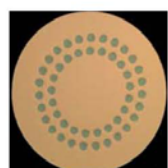
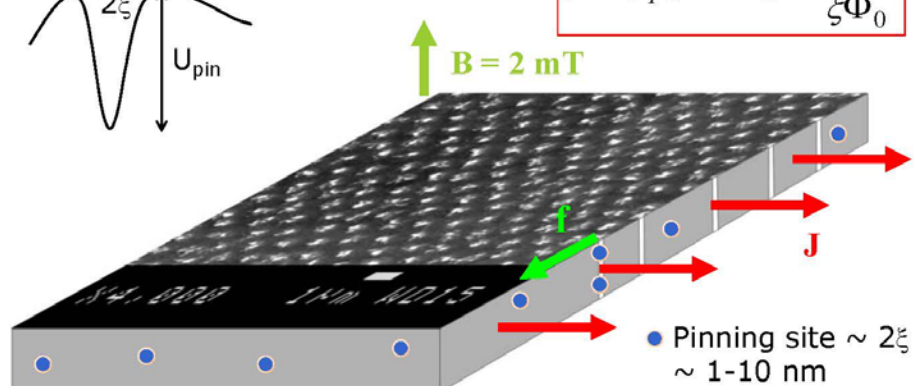
- Vortex movement when:



$$\vec{f} = \vec{J} \times \Phi_0 \vec{z}$$

$$f_{pin} = \frac{dU}{dx} \sim \frac{U_{pin}}{\xi}$$

$$f > f_{pin} \Rightarrow J_C \sim \frac{U_{pin}}{\xi \Phi_0}$$



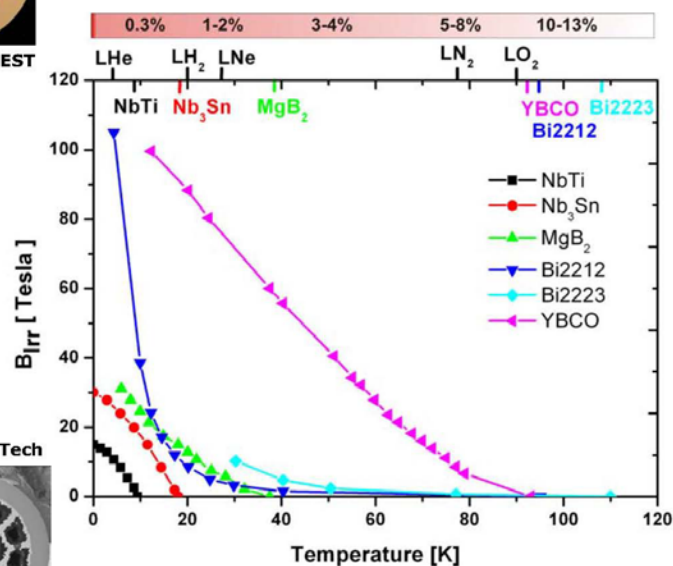
NbTi Bruker EST
0.4 €/m



1-4 €/m

MgB₂ HyperTech

Choice of superconductor



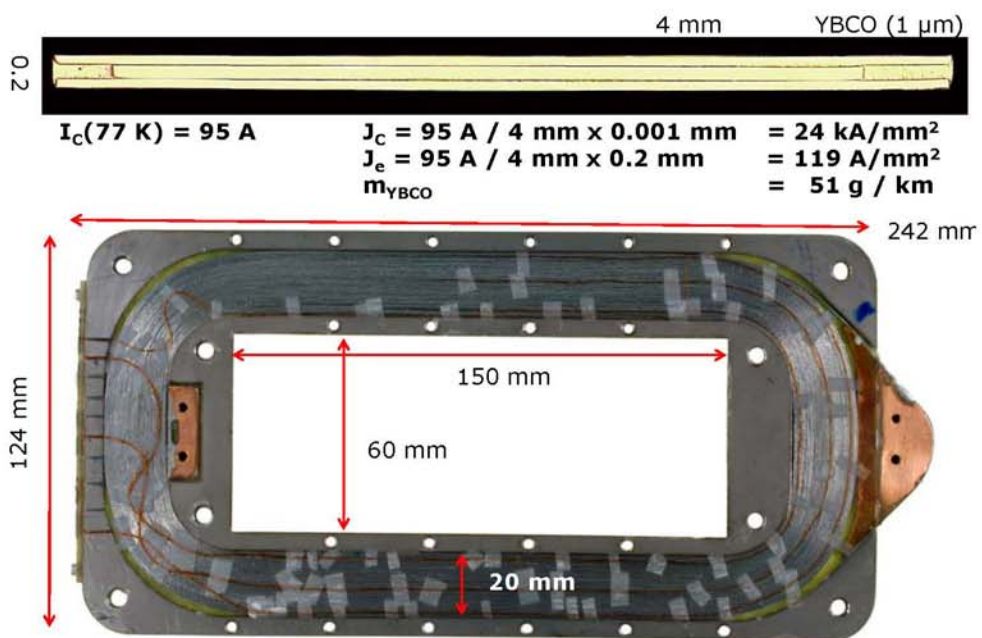
30 €/m 20 €/m



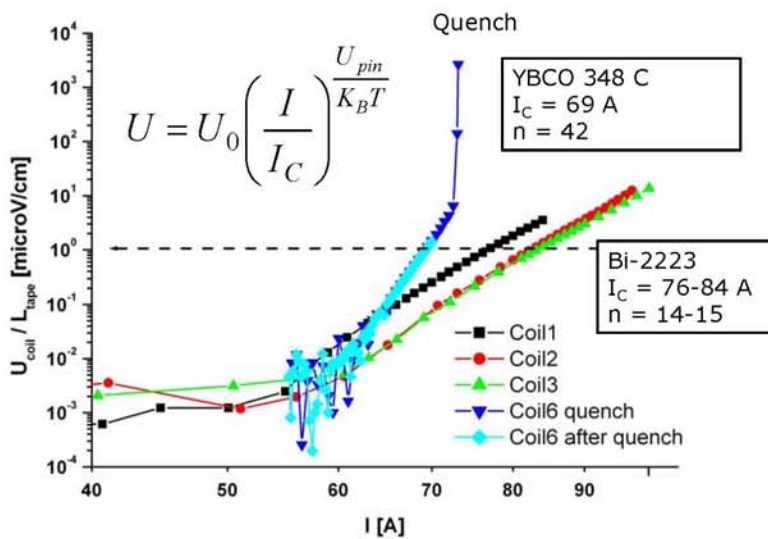
Jensen, Mijatovic & Abrahamsen, EWEA 2012

HTC tapes and coils

Superwind.dk DTU

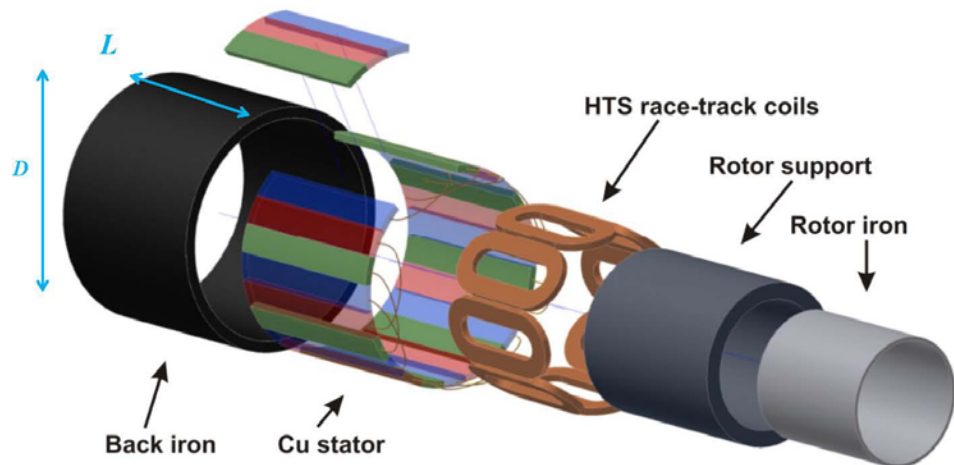


IV curves of coils @ 77 K in liquid nitrogen



DTU Wind Energy, Technical University of Denmark Abrahamsen et. al., "Feasibility of 5 MW superconducting wind turbine generator", Physica C471, 1464 (2011)

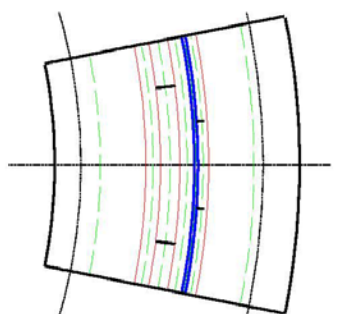
Radial flux machine



DTU Wind Energy, Technical University of Denmark

Abrahamsen et. al., SUST23,034019 (2010)

Superconducting generator and Je



$$D = 4.2 \text{ m}$$

$$L = 1.4 \text{ m}$$

$$t_r = 0.25 \text{ m}$$

$$t_{ic} = 0.04$$

$$t_s = 0.053$$

$$t_{oc} = 0.04$$

$$t_g = 0.01$$

$$t_{cu} = 0.029$$

$$t_{os} = 0.25$$

$$T = 4.2 \text{ MNm}$$

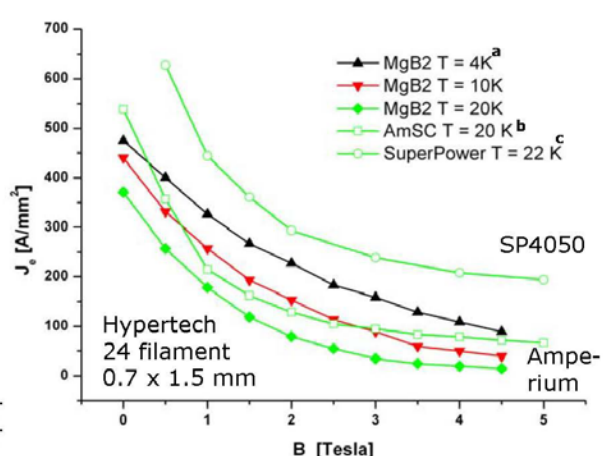
$$B_{Fe} = 2.5 \text{ T}$$

$$B_{airgap} = 2.4 \text{ T}$$

$$\text{Cu loss} = 5 \text{ \%}$$

$$B_{sup} \sim 3.3 \text{ T (FE)}$$

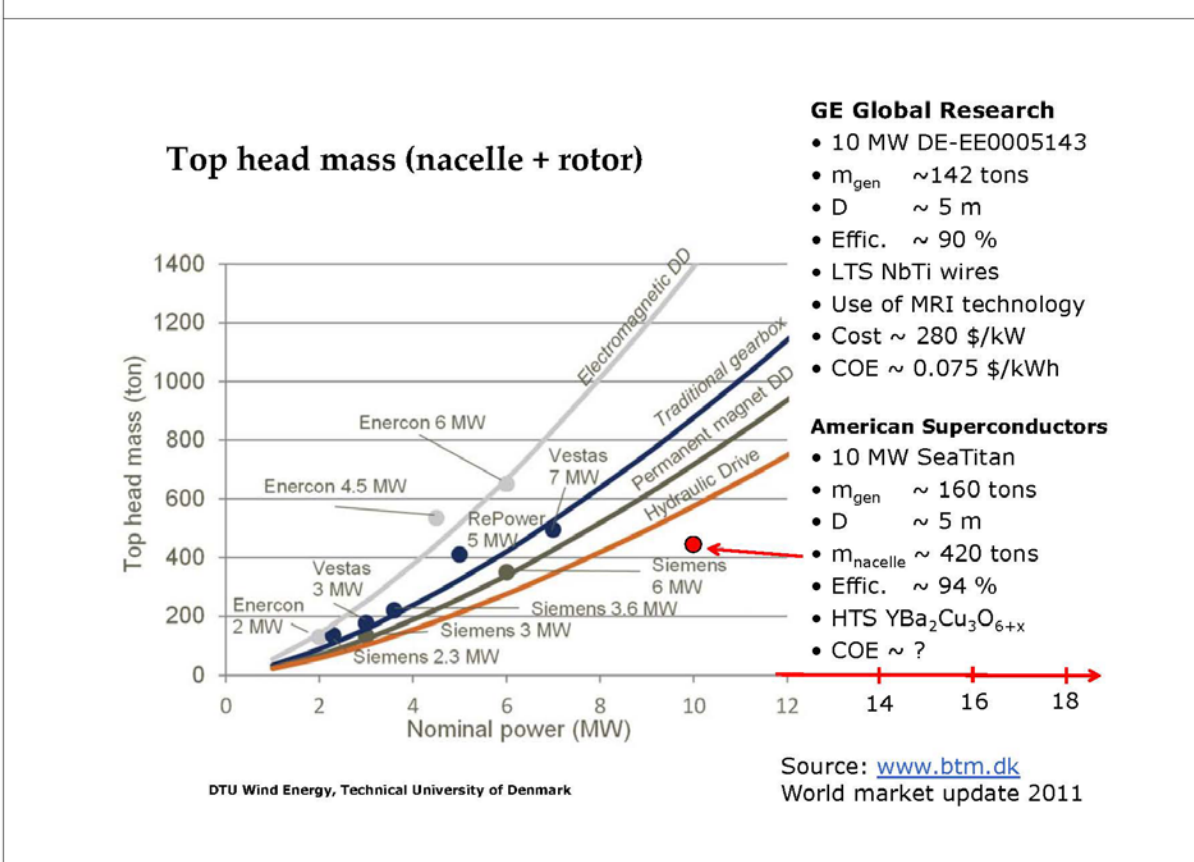
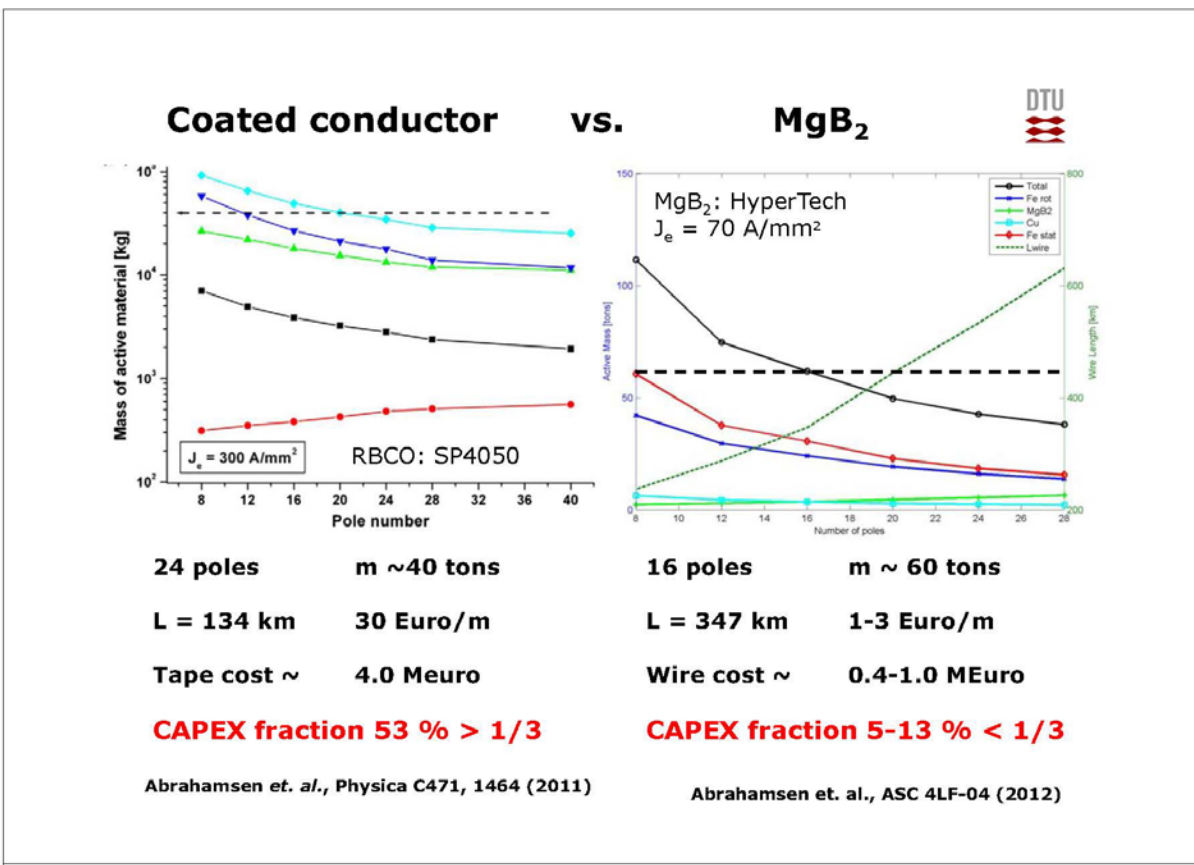
$$J_e = 70 \text{ A/mm}^2$$



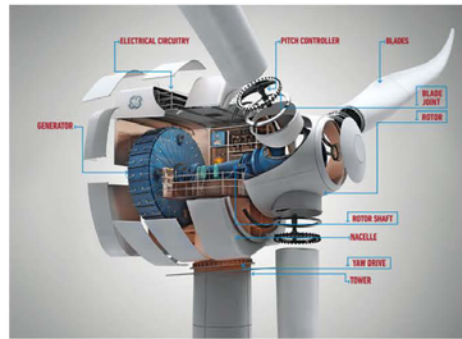
^aS. Mine et al., *IEEE Trans. Appl. Supercond.* 22, 2012, p. 4400604.

^bAmSC Amperium application note

^cD.W. Hazelton and V. Selvamanickam, *Proceedings of the IEEE*, Vol. 97, 2009, p. 1831.



Conclusion



Magneto Resonant Imaging + Wind =

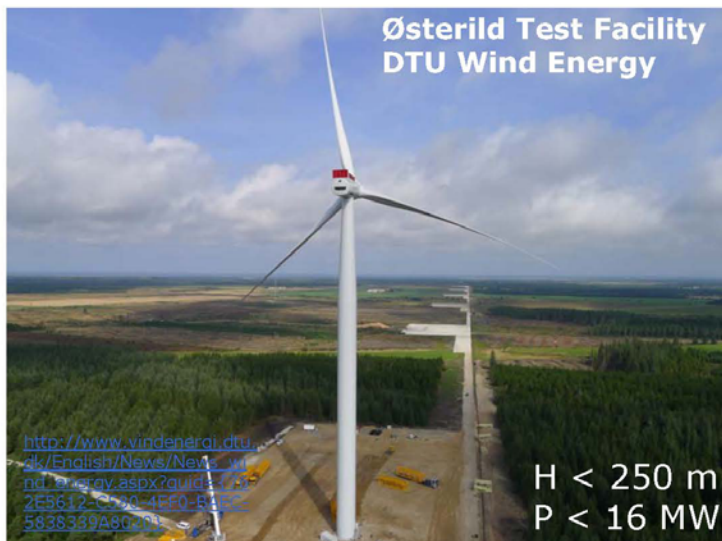
Superconducting direct drive generator

NbTi & MgB₂ almost cost competitive now. HTC in the long run.

DTU Wind Energy, Technical University of Denmark

Source: GE

Thank you for your attention



DTU Wind Energy, Technical University of Denmark

Acknowledgement

Superwind.dk
DTU Globalization

INNWIND.EU
FP7 Energy
2012-2017

Superconducting
generators
 $P = 10-20 \text{ MW}$

Mikrostruktur karakterisering af SG-støbejern

Karl-Martin Pedersen, Siemens Wind Power A/S

Karakterisering af mikrostruktur i SG-jern

DMS Vintermøde 2013

Karl Martin Pedersen
Siemens Wind Power A/S

© Siemens AG 2013

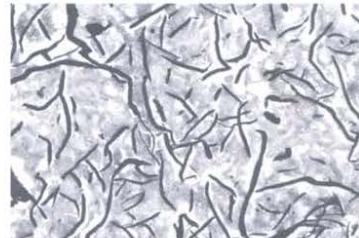
Outline

- Mikrostrukturevaluering i SG jern
 - Visuel evaluering
 - Billedanalyse
- Grafit størrelsesfordeling i 2D og 3D
- Grafit på brudflader

Hvorfor SG jern

Ved størkning

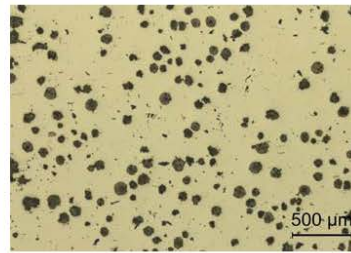
- Metaller svinder (=porositeter i centrum af emnet)
- Kulstof udvider sig ved dannelse af grafit (modvirker porositeter)
- Kulstof sænker størkne-temperaturen ca. 350°C i forhold til stål



Gråt støbejern

Grafit-kugler i stedet for grafit-flager

- Højere styrke og sejhed



SG jern

Processen

- Stor geometrisk frihed

Pris

Page 3

18-01-2013

Karl Martin Pedersen

© Siemens AG 2013
Siemens Wind Power A/S**Karakterisering af mikrostruktur (Visuelt)****Grafitten**

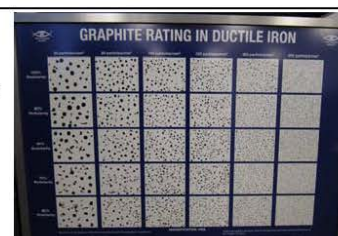
- Form og størrelse
- ISO 945-1

Matrixen

- Perlit/Ferrit indhold
- Evt. Karbider eller andet

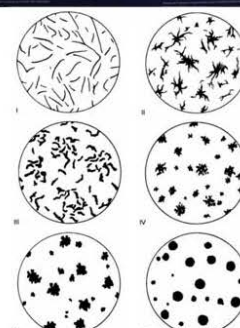


Poster fra Ductile Iron Society



Poster fra Ductile Iron Society

ISO 945-1

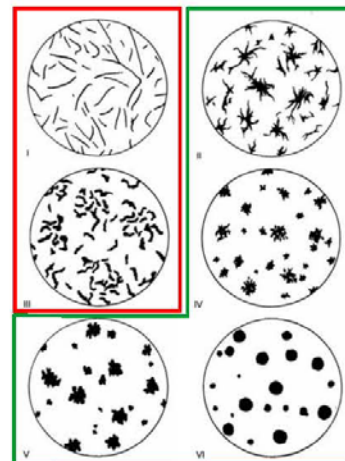
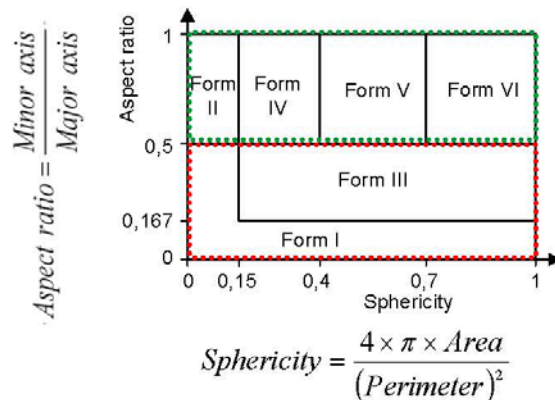
© Siemens AG 2013
Siemens Wind Power A/S

Page 4

18-01-2013

Karl Martin Pedersen

Karakterisering af grafitform (Billedanalyse)



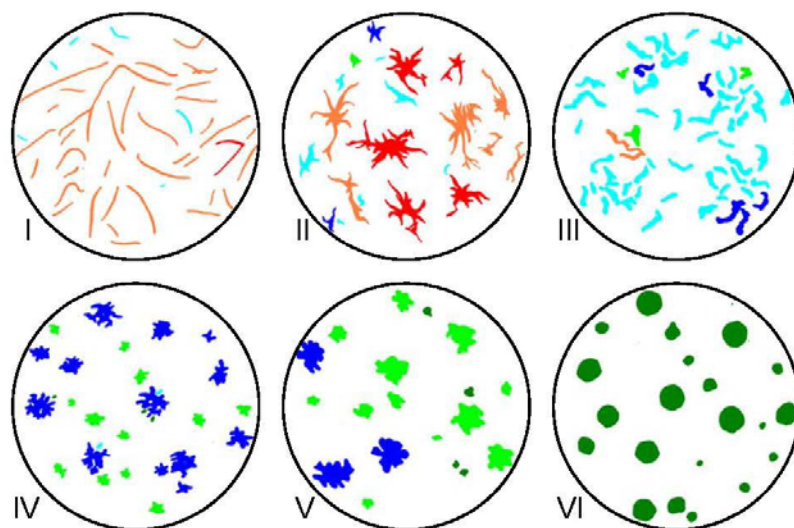
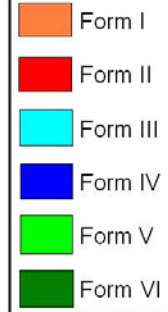
Har anvendt Image Pro®

Billedanalyse kan også give information om nodulantal pr areal, samt størrelsesfordeling.

© Siemens AG 2013
Siemens Wind Power A/S

SIEMENS

Validering af billedanalyse (ISO 945-1)



© Siemens AG 2013
Siemens Wind Power A/S

Validering af billedanalyse (ISO 945-1)

Målt	Charts i Figur 1 i ISO 945-1					
	Form I	Form II	Form III	Form IV	Form V	Form VI
Form I	90.6	38.5	3.8	0	0	0
Form II	3.9	46.7	0	0	0	0
Form III	5.5	9.4	80.1	0.9	0	0
Form IV	0	4.1	11.5	74.7	36.1	0
Form V	0	1.3	4.7	23.4	60.0	0
Form VI	0	0	0	1.0	4.0	100.0

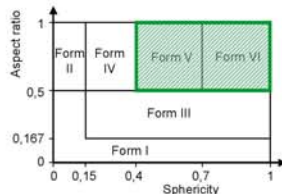
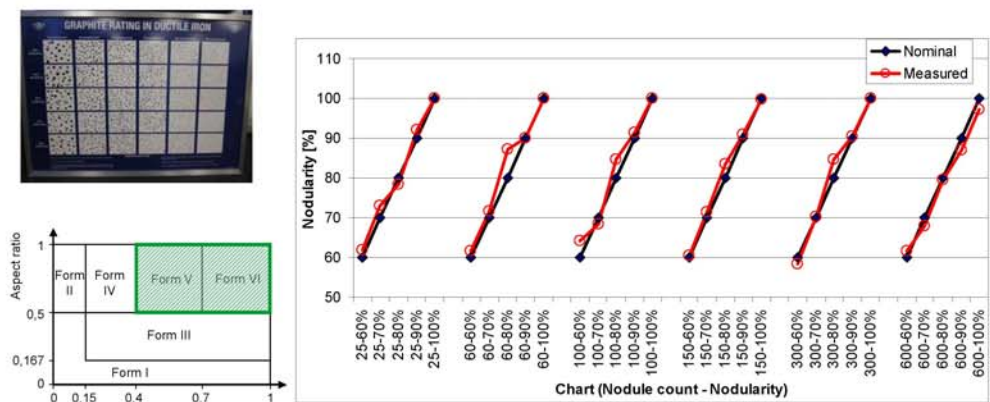
Page 7

18-01-2013

Karl Martin Pedersen

© Siemens AG 2013

Siemens Wind Power A/S

Validering af billedanalyse
(Poster fra Ductile Iron Society)Både Form V og VI
er acceptabelle

$$\text{Nodularity} = \frac{\text{Area of acceptable graphite}}{\text{Total graphite area}} \times 100\%$$

Page 8

18-01-2013

Karl Martin Pedersen

© Siemens AG 2013

Siemens Wind Power A/S

Nogle praktiske erfaringer om billedanalyse

Præparerings meget vigtig

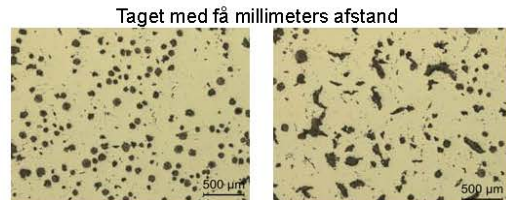
Krav om flere billeder (bruger typisk 10 billeder)

Opgør fordeling af grafitform udfra areal, ikke udfra antal

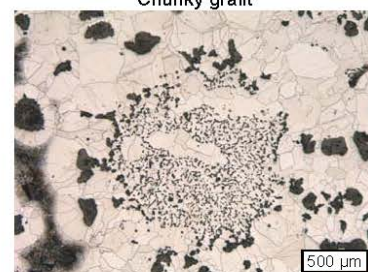
Ofte lige så hurtig at gøre det visuelt, men billedanalyse kan virke mere overbevisende.

Visuel evaluering kan udføres på ætsede emner eller på replica (sammen med vurdering af ferrit/perlit indhold). Billedanalyse skal udføres på polerede emner.

Billedanalyse har svært at tage højde for dårlig grafitform, f.eks. Chunky grafit (tilbagemelding til produktion)



Chunky grafit



© Siemens AG 2013
Siemens Wind Power A/S

Page 9

18-01-2013

Karl Martin Pedersen

**ISO/TR 945-2 Mikrostruktur i støbejern.
Del 2: Grafitklassifikation ved billedanalyse**

Har ikke anvendt den endnu, men nogle få kommentarer:

Omhandler IKKE matematiske beskrivelser af grafitformer
Ikke anvendelig for fordeling af grafit i gråt støbejern.

Beskriver nogle krav eller ting til overvejelse (listen er ikke komplet):

- Præparerings
- Billedtagning
 - Lysstyrke, skarphed, gråskala
 - Pixelstørrelse (1µm/pixel)
- Minimum 20 grafitpartikler pr billede
- Analysere mindst 400 til 1000 partikler
- Ikke grafit partikler/porer skal ekskluderes
- Opdel sammenhængende grafitpartikler
- Validering ved sammenligning med visuelle målinger

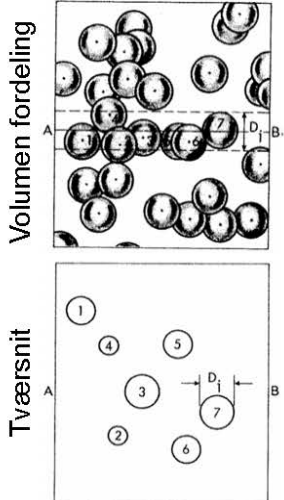
© Siemens AG 2013
Siemens Wind Power A/S

Page 10

18-01-2013

Karl Martin Pedersen

Konvertering fra 2D til 3D



Forudsætning: Ensartet nodul størrelse

$$\left. \begin{aligned} N_A &= d \cdot N_V \\ d &= \left(\frac{6f^g}{\pi N_V} \right)^{\frac{1}{2}} \end{aligned} \right\} \quad N_V = \left(\frac{\pi}{6f^g} \right)^{\frac{1}{2}} (N_A)^{\frac{3}{2}}$$

N_A = Area count [mm^{-2}]

N_V = Volume count [mm^{-3}]

d = Diameter [mm]

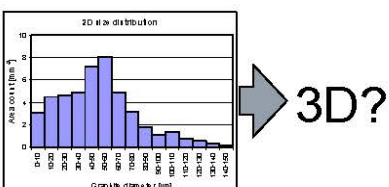
f^g = Fraction of graphite

Varierende nodul størrelser:

$$N_V = \left(\frac{\pi}{6f^g} \right)^{\frac{1}{2}} (\alpha N_A)^{\frac{3}{2}}$$

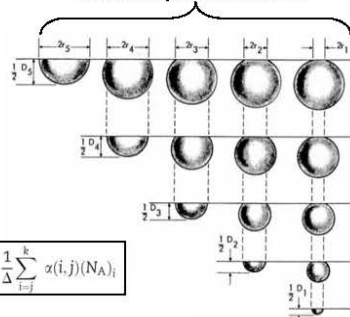
α = size distribution parameter (≈ 1.2)

3D størrelsesfordeling



3D?

Visuelt på tverrsnit

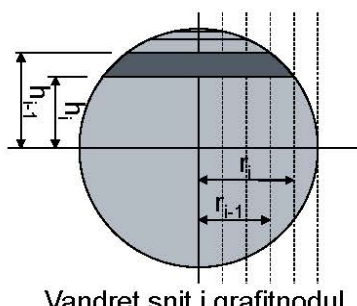


$$(N_V)_j = \frac{1}{\Delta} \sum_{i=j}^k \alpha(i, j) (N_A)_i$$

$$\alpha(i, i) = 1 \quad \text{for } i = 1$$

$$\alpha(i, i) = \frac{2}{\pi} \ln \left(\frac{i + \sqrt{i^2 - (i-1)^2}}{i-1} \right) \quad \forall i > 1$$

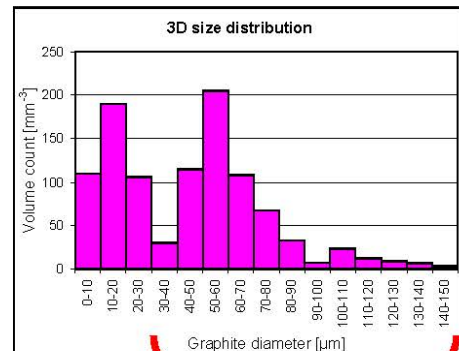
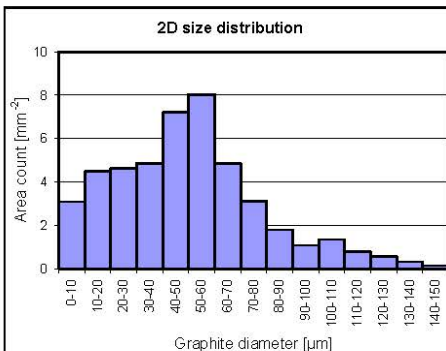
$$\alpha(i, j) = \frac{2}{\pi} \ln \left(\frac{i + \sqrt{i^2 - (j-1)^2}}{i + \sqrt{i^2 - j^2}} \times \frac{i-1 + \sqrt{(i-1)^2 - j^2}}{i-1 + \sqrt{(i-1)^2 - (j-1)^2}} \right) \quad \forall i > j$$



Vandret snit i grafittnodul

5 størrelsesintervaller

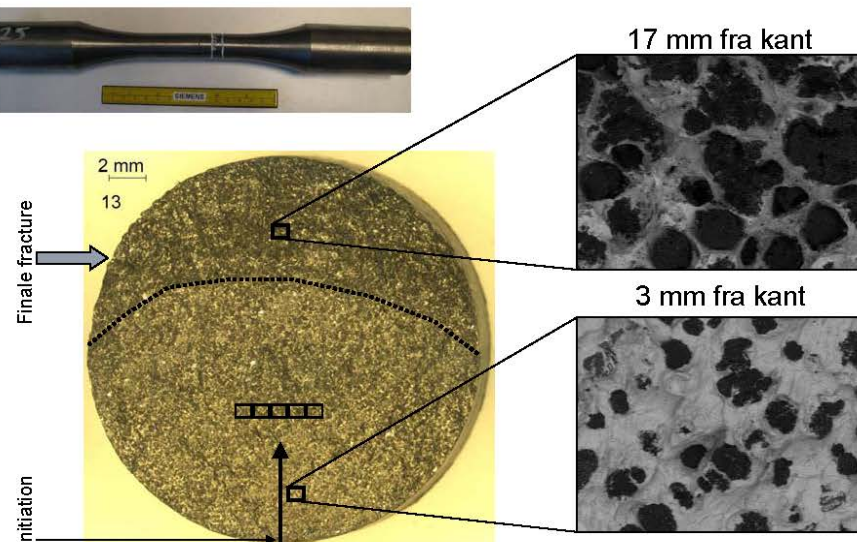
3D størrelsesfordeling



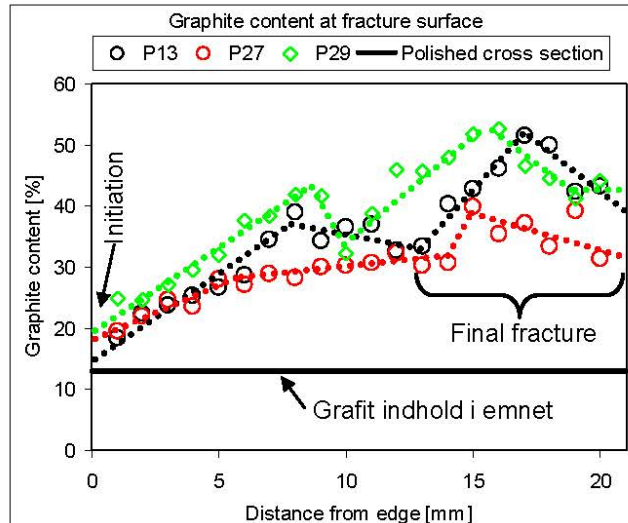
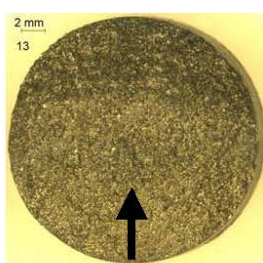
Grafit noduler

	2D	3D
Count (<30 μm)	12,3 mm^{-2}	405 mm^{-3}
Count (>30 μm)	34,2 mm^{-2}	621 mm^{-3}

Grafitindhold på brudflade (Udmattelsestest, R = -1)



Grafitindhold på brudflade



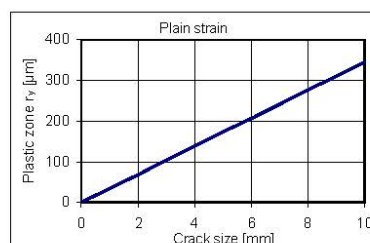
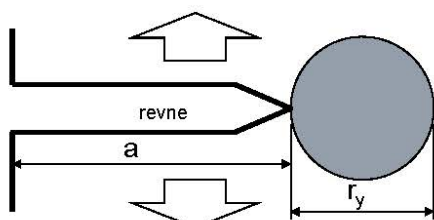
Page 15

18-01-2013

Karl Martin Pedersen

© Siemens AG 2013
Siemens Wind Power A/S

Plastic zone at crack tip



$$r_y = \frac{1}{2\pi} \left(\frac{K_{\max}}{\sigma_{ys}} \right)^2 \quad (\text{Plain stress})$$

$$r_y = \frac{1}{6\pi} \left(\frac{K_{\max}}{\sigma_{ys}} \right)^2 \quad (\text{Plain strain})$$

$$K_{\max} = Y \sigma_{\max} \sqrt{\pi a}$$

$$r_y = \frac{a}{6} \left(\frac{Y \sigma_{\max}}{\sigma_{ys}} \right)^2 \quad (\text{Plain strain})$$

 K = spændings intensity factor σ_{\max} = max spænding σ_{ys} = flydespænding a = revnelængde r_y = plastisk zone

Y = Form faktor

Page 16

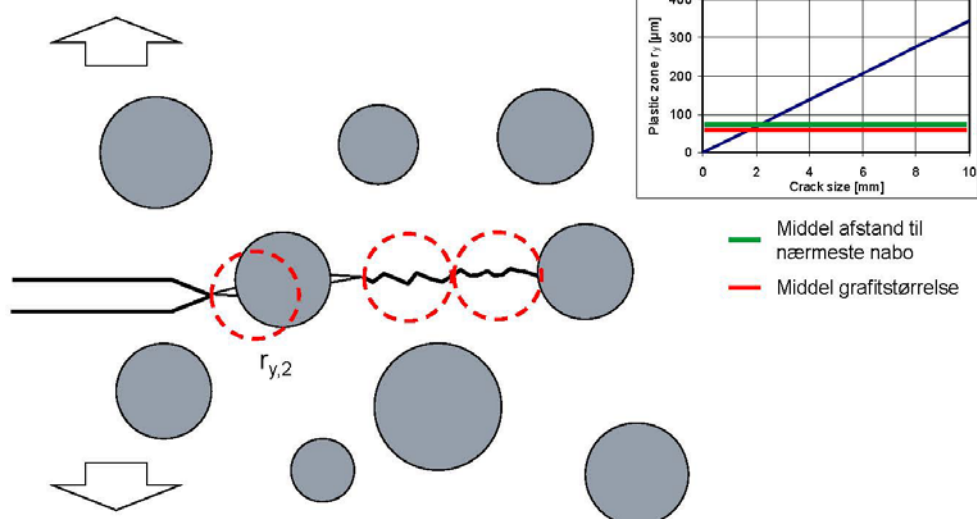
18-01-2013

Karl Martin Pedersen

© Siemens AG 2013
Siemens Wind Power A/S

SIEMENS

Plastisk zone og grafit noduler (lille zone)

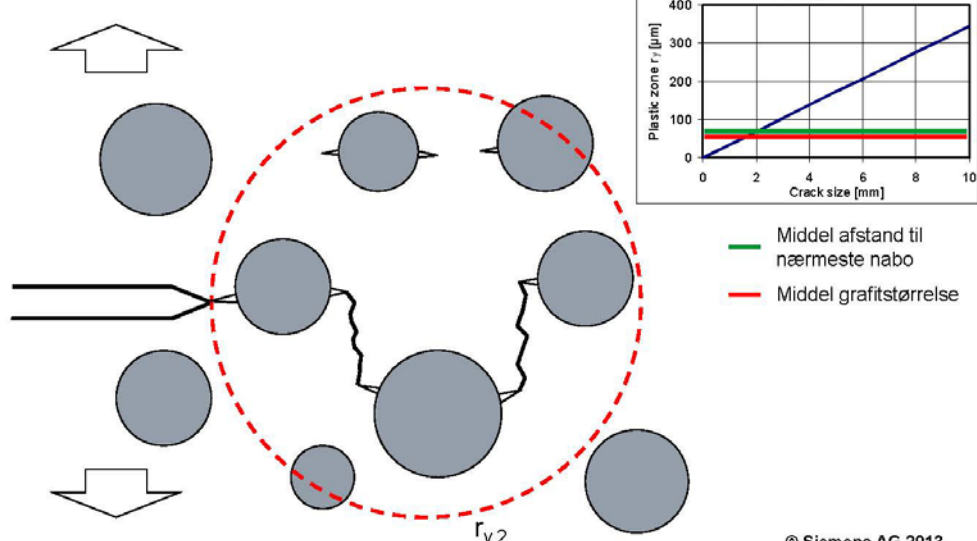


Page 17

18-01-2013

Karl Martin Pedersen

Plastisk zone og grafit noduler (stor zone)



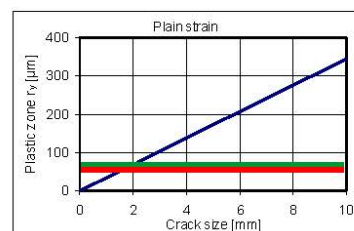
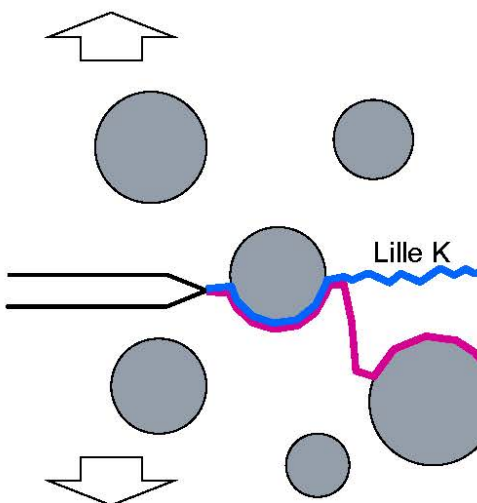
Page 18

18-01-2013

Karl Martin Pedersen

SIEMENS

Plastisk zone og grafit noduler



Middel afstand til
nærmeste nabo
Middel grafitstørrelse

Page 19

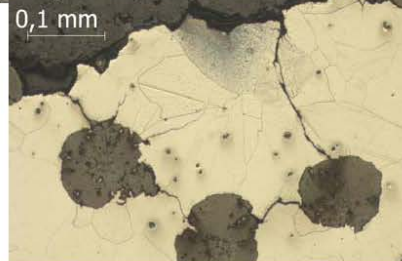
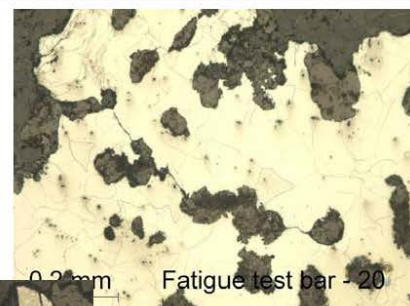
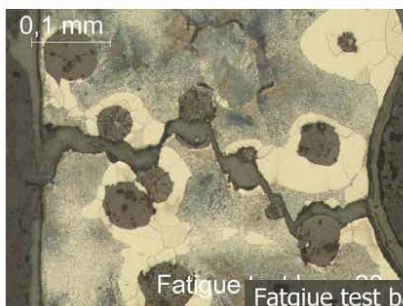
18-01-2013

Karl Martin Pedersen

© Siemens AG 2013
Siemens Wind Power A/S

SIEMENS

Cross section of fracture surface



© Siemens AG 2013
Siemens Wind Power A/S

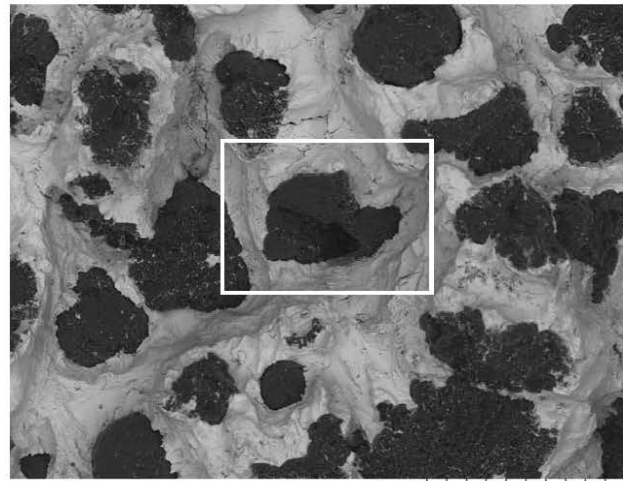
Page 20

18-01-2013

Karl Martin Pedersen

SIEMENS

Striation (8mm from edge)



Task 1501

2010-03-18

x250 300 μm

Fatigue test bar - 13

Page 21

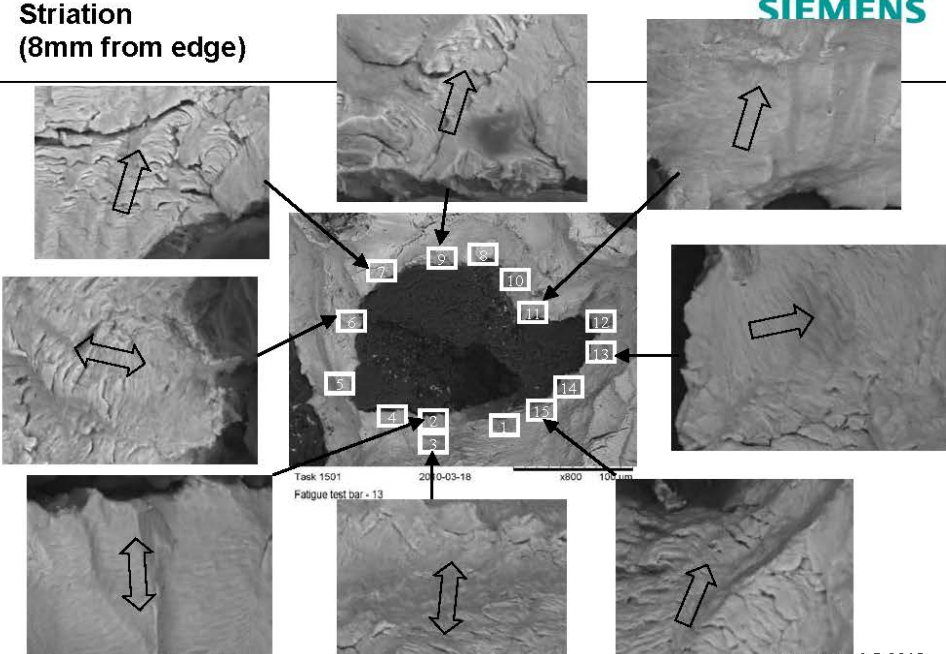
18-01-2013

Karl Martin Pedersen

© Siemens AG 2013
Siemens Wind Power A/S

**Striation
(8mm from edge)**

SIEMENS



Page 22

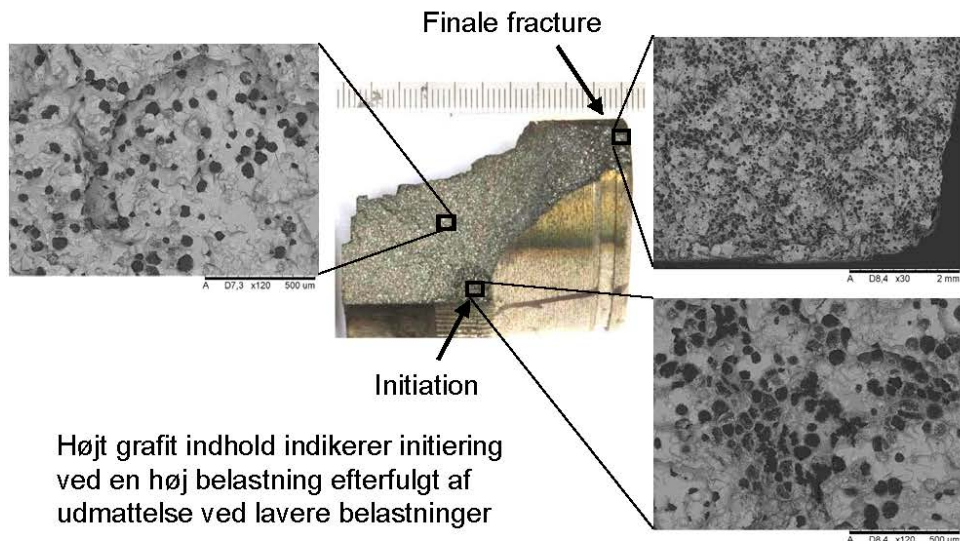
18-01-2013

Karl Martin Pedersen

© Siemens AG 2013
Siemens Wind Power A/S

SIEMENS

Eksempel på fejlet komponent



Page 23

18-01-2013

Karl Martin Pedersen

© Siemens AG 2013
Siemens Wind Power A/S

SIEMENS

Tak for jeres opmærksomhed



Page 24

18-01-2013

Karl Martin Pedersen

© Siemens AG 2013
Siemens Wind Power A/S

Kilder

Grafit noduler i 2D og 3D:

- K.M. Pedersen and N.S. Tiedje: Graphite nodule count and size distribution in thin-walled ductile cast iron, Materials Characterization, Vol 8, p 1111-1121, 2008
- E.E. Underwood: Quantitative Stereology. Addison-Wesley Publishing Company; 1970. p. 109–145
- C.B. Basak and A.K. Sengupta: Development of a FDM based code to determine the 3-D size distribution of homogeneously dispersed spherical second phase from microstructure: a case study on nodular cast iron. Scripta Materialia, Vol 51, p. 255–260, 2004

Kvalitetssikring af støbegods i MAN B&W motorer

Knud Strande, MAN

Kvalitetssikring af Støbegods i MAN B&W Motorer



Knud Strand
Production Support
Engineering
Marine Low Speed

Kvalitetssikring - MAN B&W Motorer



- MAN Diesel & Turbo – København
- Typiske støbte komponenter i MAN B&W motorer; Gråjern, Stål, SG jern og Kompakt grafit jern.
- Kvalitetssikring – Controlled Component Concept.
- "Dagligt arbejde" i Production Supports støbegruppe.
- Tekniske udfordringer foranlediget af design og af produktion – eksempler.
- Indløb og efterfødning – "god latin".
- Sammenfatning, kvalitetssikring - "Værktøjskassens" indhold.

MAN DIESEL & Turbo



Company Logo



Company Brand



Product Brand

MAN | PrimeServ
MAN | PowerManagement

Service Brands

Product /Type
Designations
(Examples)

51/60DF B&W K98ME-C TCA88 SaCoS_{one}
VBS1180 MARC6 DWE THM turbolog

MAN Diesel & Turbo

Knud Strande

Production Support

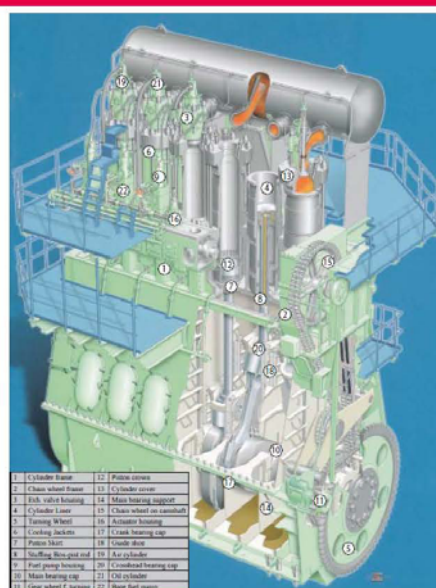
Januar 2013

< 3 >

MAN B&W Motoren



- Størrelser: 26-98 cm cylinder diameter
- Effekt: 450 kW – 87.000 kW
- Typiske støbte komponenter: Gråjern, Stål, SG jern og CGI jern
- Ca. 30% af motorens vægt består af støbegods
- På en 6S60MC-C motor (~15 MW) svarer det til ~ 100t
- På 15 GW svarer det til ~ 100.000t



MAN Diesel & Turbo

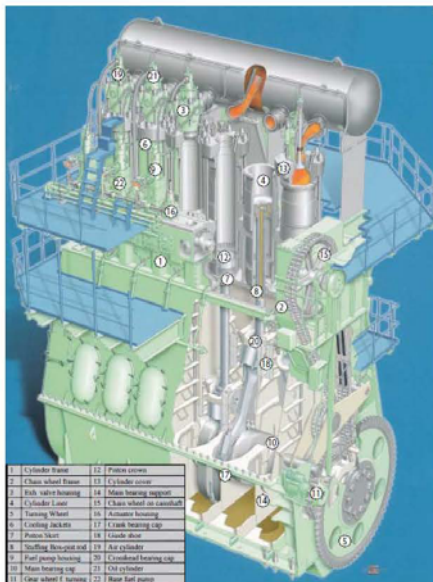
Knud Strande

Production Support

Januar 2013

< 4 >

Støbegods i MAN B&W motorer



Cylinder frame
Chass wheel base
Belt valve housing
Cylinder liner
Cylinder base
Cooling jackets
Piston skirt
Sleeving bearing shell
Fuel pump housing
Main bearing cap
Gear wheel & housing



1



14

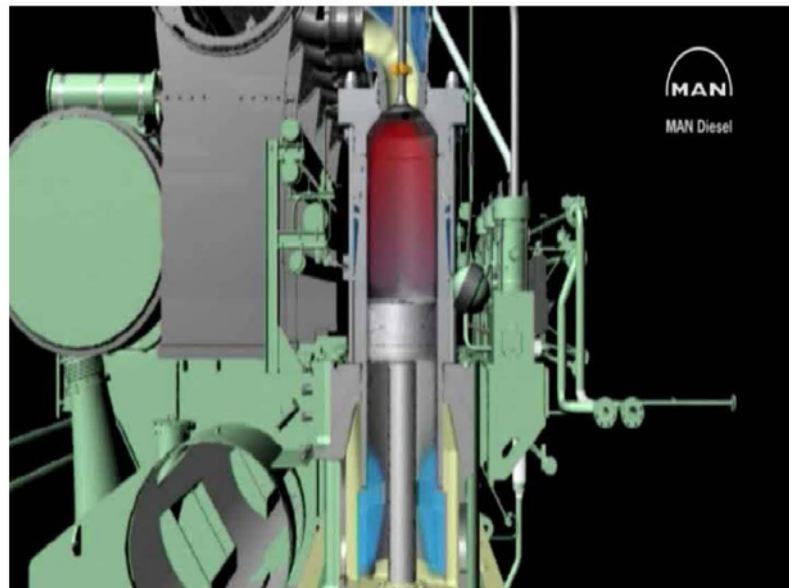
MAN Diesel & Turbo

Knud Strande

Production Support

Januar 2013 | < 6 >

MAN B&W Motoren



MAN

Diesel

MAN Diesel & Turbo

Knud Strande

Production Support

Januar 2013 | < 6 >

Kvalitetssikring – Controlled Components



- **Simple Components**

Requirements to material properties (alloy), geometrical tolerances and surface tolerances stated on drawings and in general accepted standards.

- **Controlled Components**

Components with certain functional requirements and/or components considered difficult to manufacture.

- **Quality Specification**

States quality requirements, which always are based on expected component performance set by the designer (and experience).

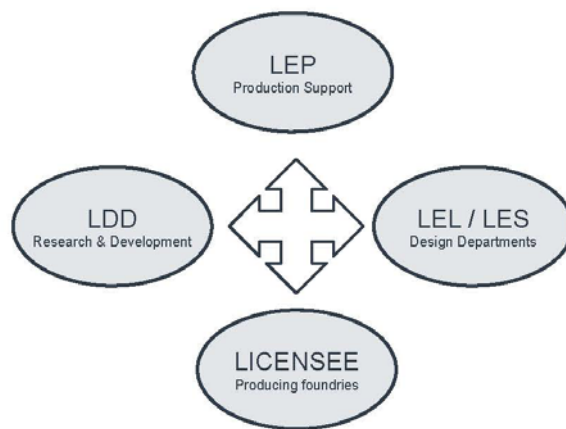
- **First Time Approval Test (FTA)**

Supplier has to show his technical ability before being approved.

- **Production Recommendation**

Special process knowledge required.

Støbegruppens samarbejdspartnere



Eksempel på kvalitets specifikation



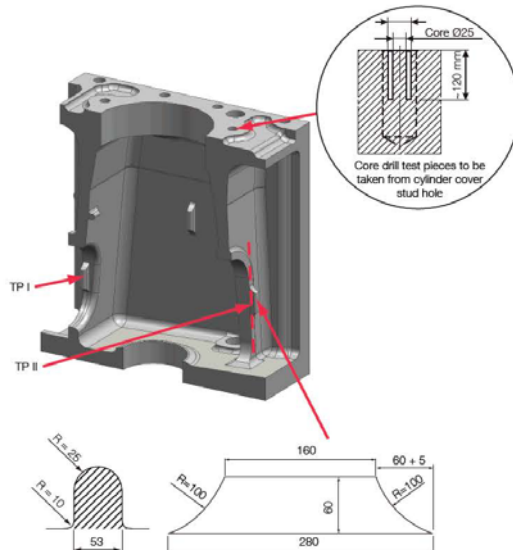
Cylinder Frames

Cylinder Frames, Grey Cast Iron

This document is valid for existing engine types on order as of the date of this document:

Engine types:

All two-stroke engine types
(Specified with C3Cu Cylinder Frames).



MAN Diesel & Turbo

Knud Strande

Production Support

Januar 2013

< 9 >

B&W Støberi 1885 – P. S. Krøyer



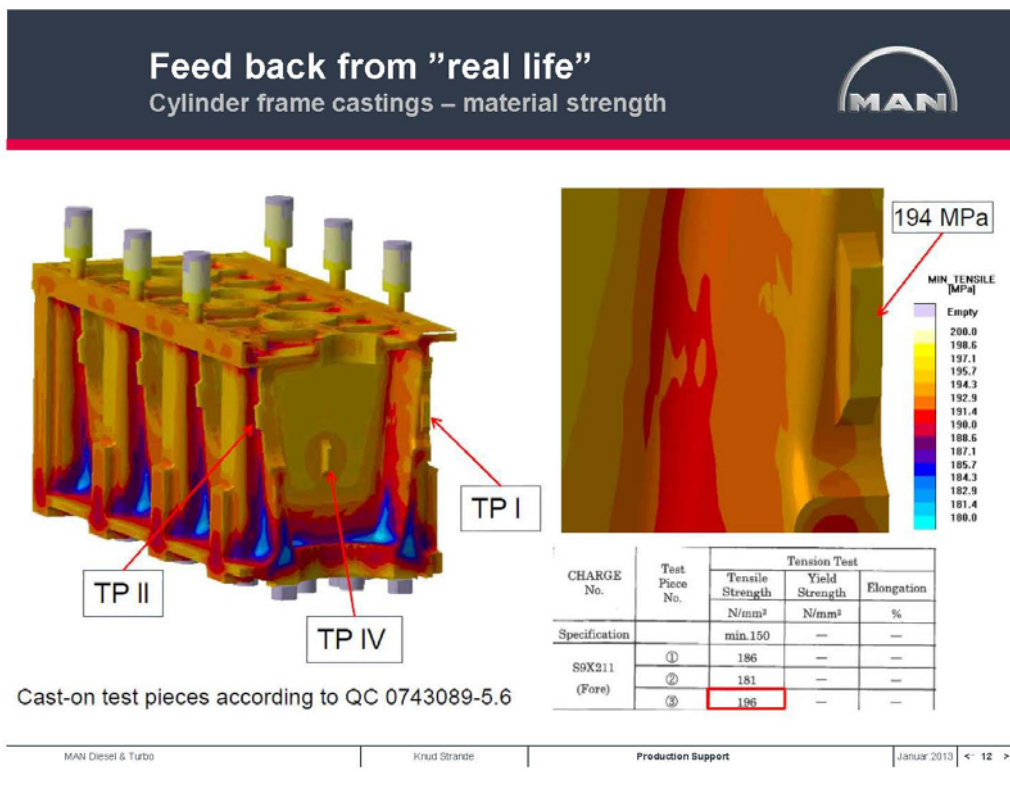
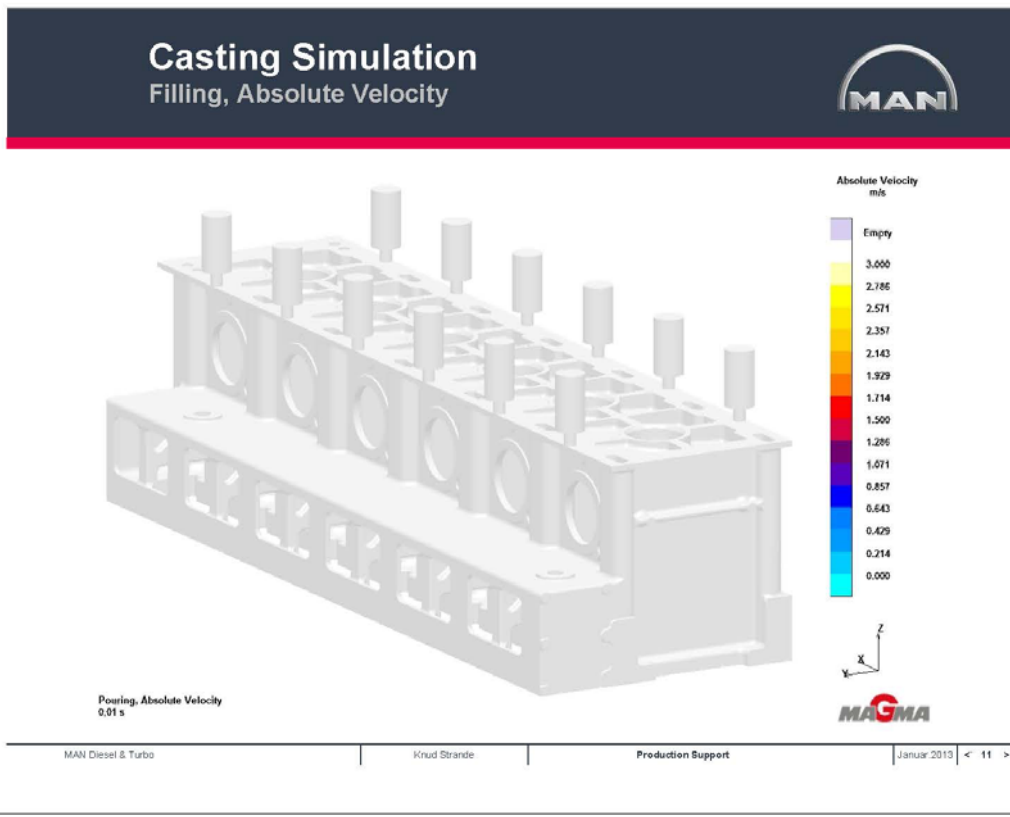
MAN Diesel & Turbo

Knud Strande

Production Support

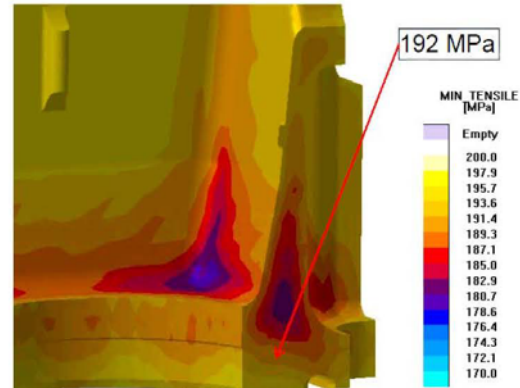
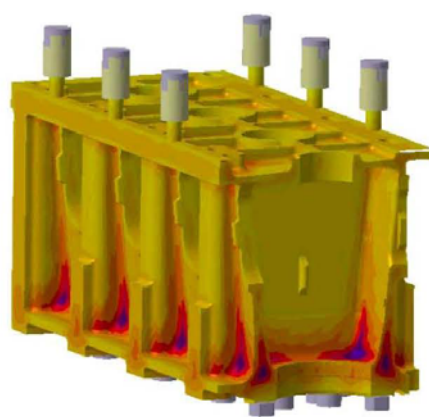
Januar 2013

< 10 >



Feed back from "real life"

Cylinder frame castings – material strength



Core drilled test pieces in accordance to QC 0743089-5.6

Charge No.	Test Place No.	Tension Test		
		Tensile Strength N/mm²	Yield Strength N/mm²	Elongation %
Specification		≥140	—	—
S8X211 (Pore)	1	161	—	—
	5	158	—	—
	9	161	—	—
	10	160	—	—

MAN Diesel & Turbo

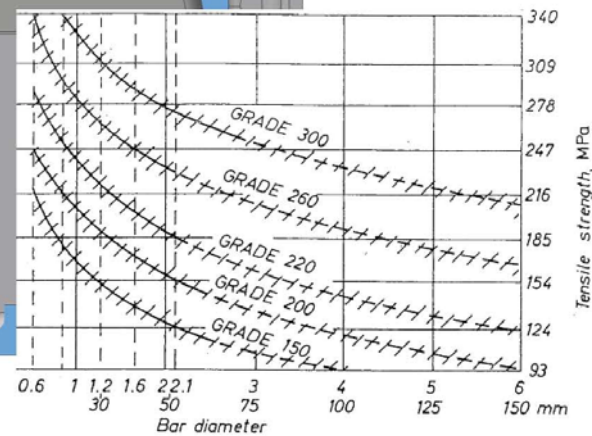
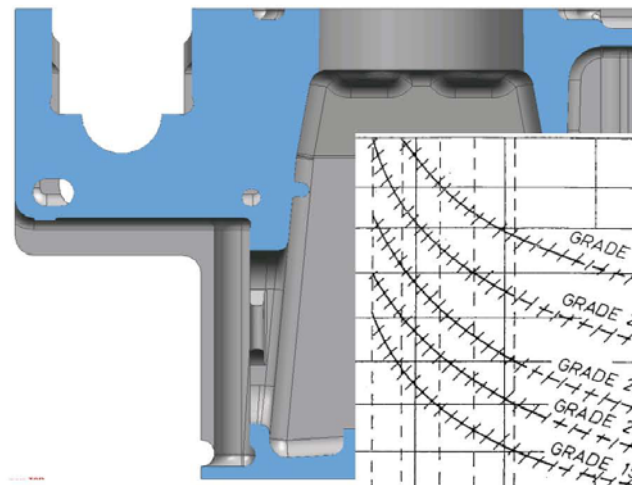
Knud Strandé

Production Support

Januar 2013 | < 13 >

Feed back from "real life"

Cylinder frame castings – too low material strength



MAN Diesel & Turbo

Knud Strandé

Production Support

Januar 2013 | < 14 >

Feed back from "real life"
Cylinder frame castings – too low material strength



MAN Diesel & Turbo

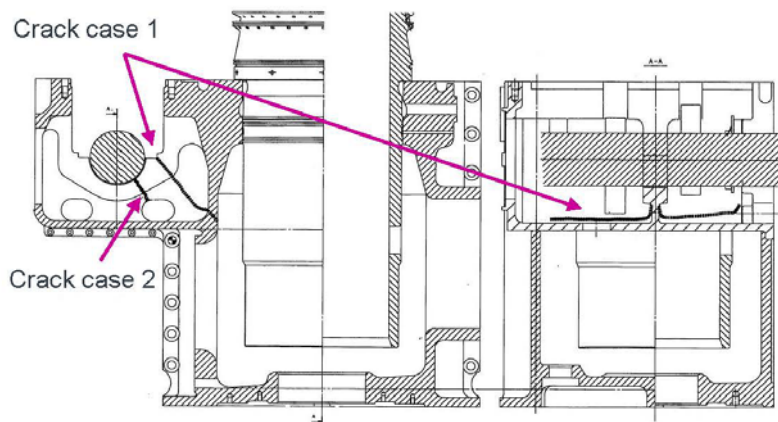
Knud Strandé

Production Support

Januar 2013

< 16 >

Feed back from "real life"
Cylinder frame castings – too low material strength



MAN Diesel & Turbo

Knud Strandé

Production Support

Januar 2013

< 16 >

Feed back from "real life"
Cylinder frame castings – shrinkage defects



MAN Diesel & Turbo

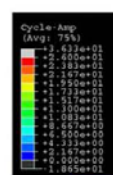
Knud Strandé

Production Support

Januar 2013

< 17 >

Feed back from "real life"
Cylinder frame castings – residual stresses



Stresses caused by engine operation

MAN Diesel & Turbo

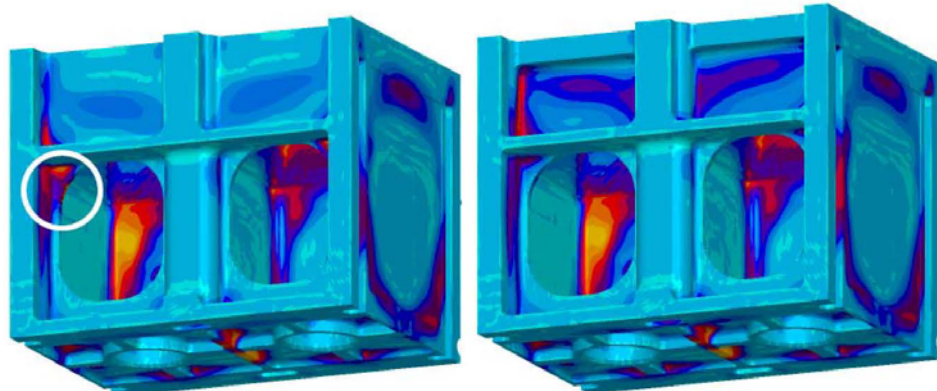
Knud Strandé

Production Support

Januar 2013

< 18 >

Feed back from "real life"
Cylinder frame castings – residual stresses



Reducing residual stresses by design modifications

MAN Diesel & Turbo

Knud Strandé

Production Support

Januar 2013

< 19 >

Feed back from "real life"
Indeslutninger/overfladefejl



MAN Diesel & Turbo

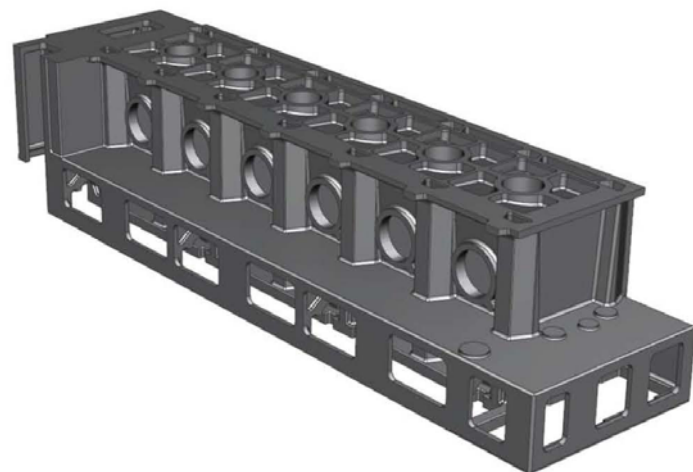
Knud Strandé

Production Support

Januar 2013

< 20 >

6S50ME-B9 cylinder frame
KPF, nodular cast iron



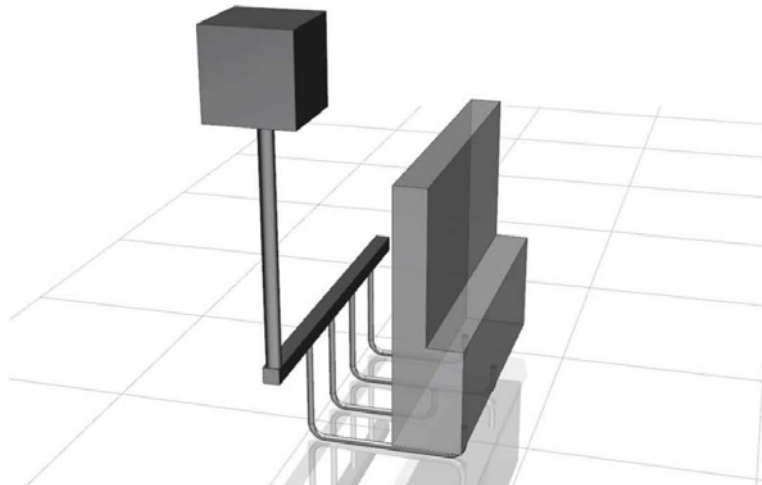
MAN Diesel & Turbo

Knud Strande

Production Support

Januar 2013 | < 21 >

Dummy filling, layout 1
Vertical sprue, Ø90



MAN Diesel & Turbo

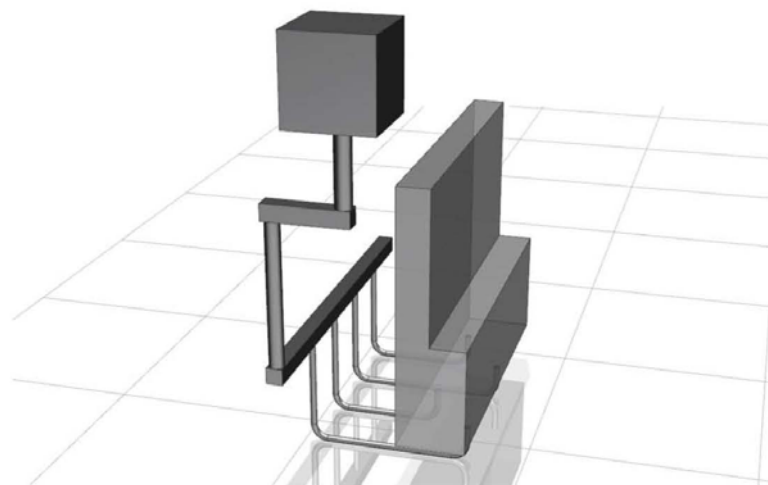
Knud Strande

Production Support

Januar 2013 | < 22 >

Dummy filling, layout 2

Split sprue, Ø100 & Ø90



MAN Diesel & Turbo

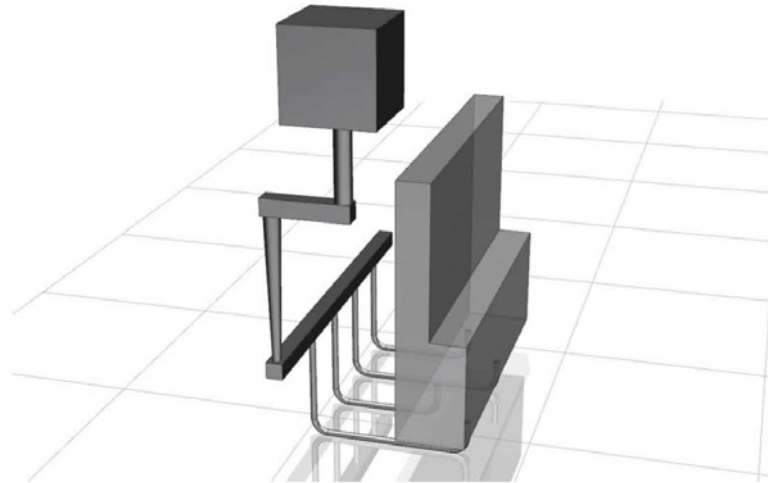
Knud Strandé

Production Support

Januar 2013 | < 23 >

Dummy filling, layout 3

Split sprue, Ø100 & Ø90 - Ø50



MAN Diesel & Turbo

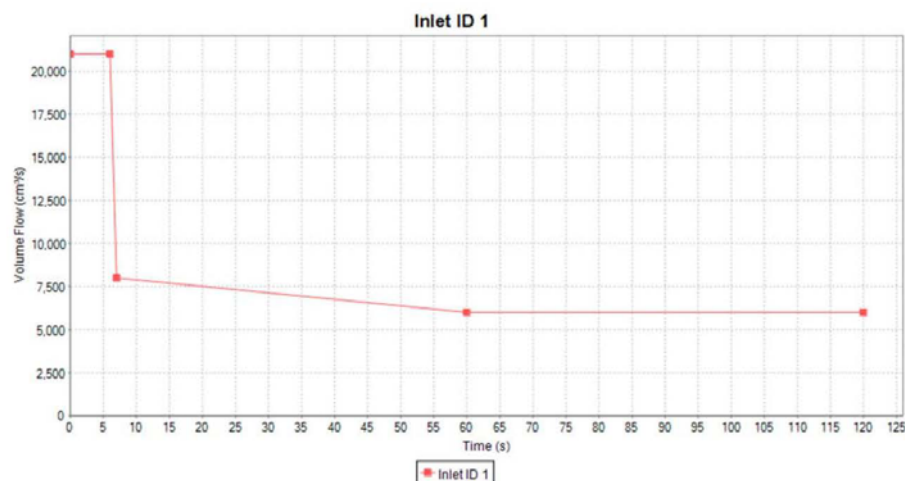
Knud Strandé

Production Support

Januar 2013 | < 24 >

Dummy filling

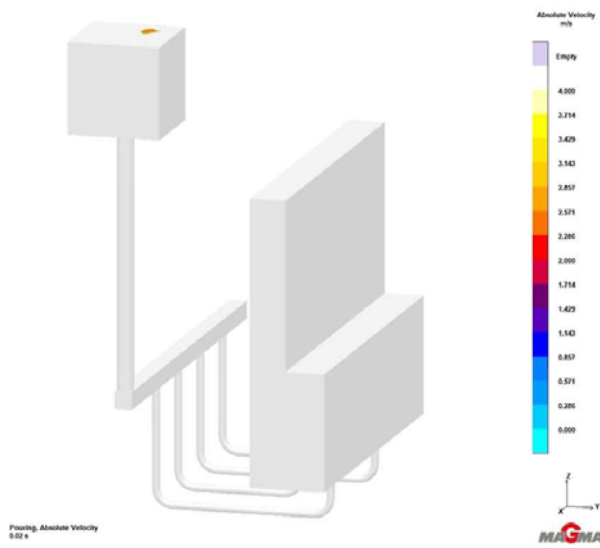
Same pouring rate for all three layouts



MAN Diesel & Turbo | Knud Strande | Production Support | Januar 2013 | < 25 >

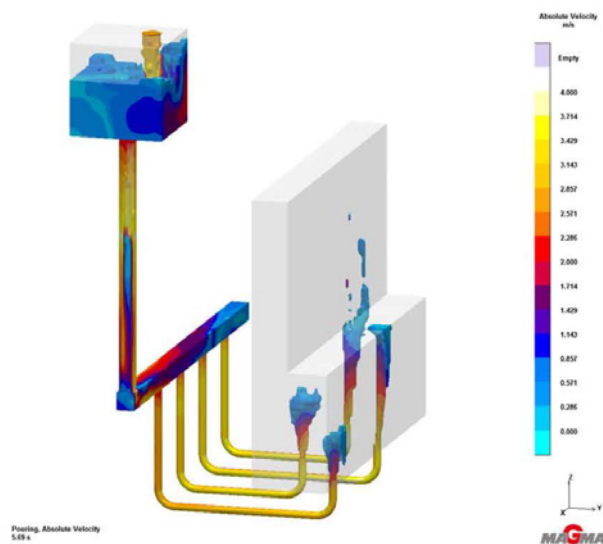
Layout 1

Absolute Velocity, fill time ~128s



MAN Diesel & Turbo | Knud Strande | Production Support | Januar 2013 | < 26 >

Layout 1 Absolute Velocity



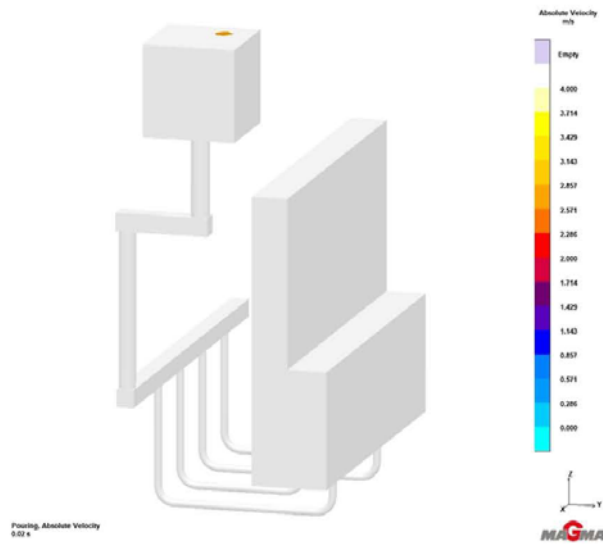
MAN Diesel & Turbo

Knud Strandé

Production Support

Januar 2013 | < 27 >

Layout 2 Absolute Velocity, fill time ~130s



MAN Diesel & Turbo

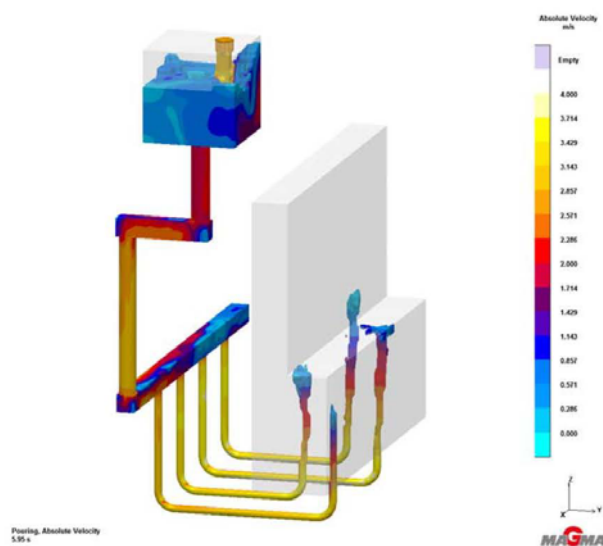
Knud Strandé

Production Support

Januar 2013 | < 28 >

Layout 2

Absolute Velocity



MAN Diesel & Turbo

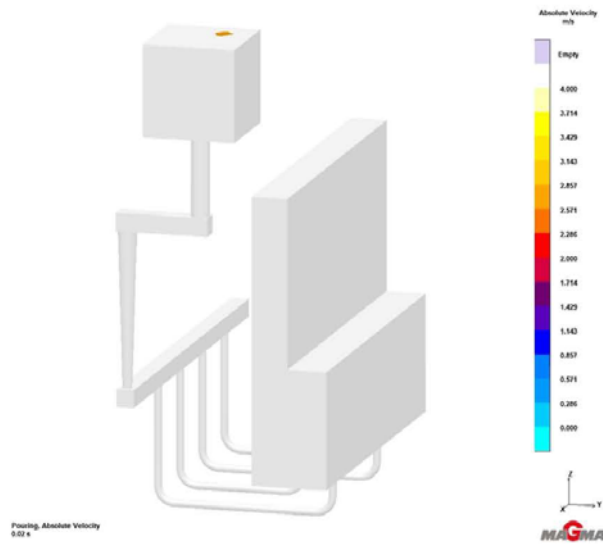
Knud Strandé

Production Support

Januar 2013 | < 29 >

Layout 3

Absolute Velocity, fill time ~140s



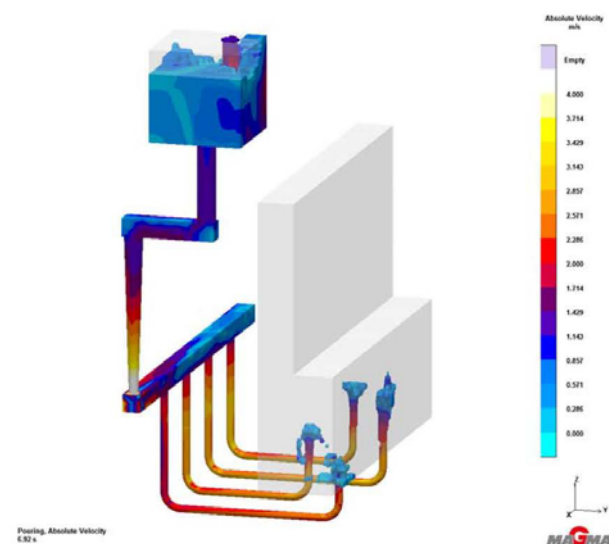
MAN Diesel & Turbo

Knud Strandé

Production Support

Januar 2013 | < 30 >

Layout 3 Absolute Velocity



MAN Diesel & Turbo

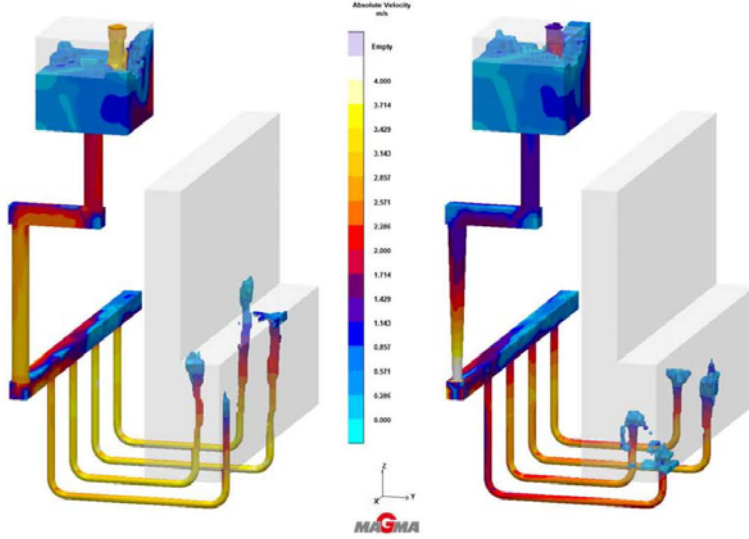
Knud Strandé

Production Support

Januar 2013 | < 31 >

Comparison, ~6 sec. Layout 2

Layout 3



MAN Diesel & Turbo

Knud Strandé

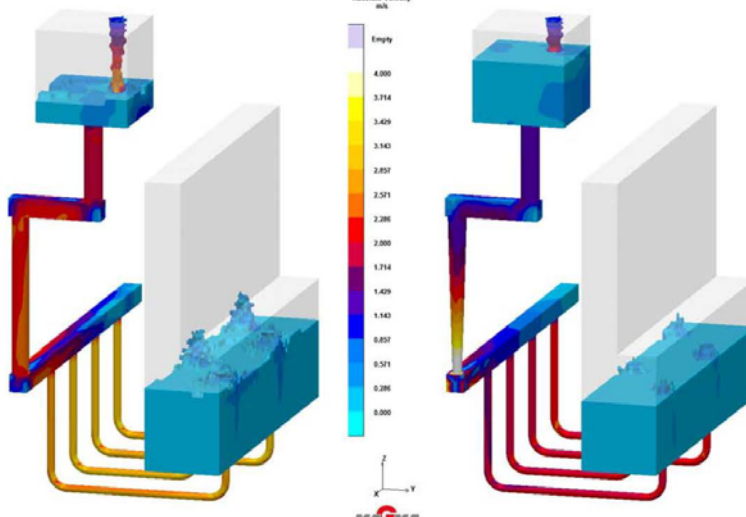
Production Support

Januar 2013 | < 32 >

Comparison, ~45 sec.

Layout 2

Layout 3



MAN Diesel & Turbo

Knud Strandé

Production Support

Januar 2013 | < 33 >

Cylinder liner G50ME-C

Grey cast iron – Tarkalloy A



v02
Absolute Velocity
0.000-0.00 %

MAN Diesel & Turbo

Knud Strandé

Production Support

Januar 2013 | < 34 >

Kvalitets sikring – internt & eksternt

Værktøjskassens indhold



- Optimere designet, så det er støbevenligt
- **støbesimulering**.
- Udarbejde specifikationer og rekommendationer
- **designkrav + erfaring + tilbagemeldinger fra producenter**.
- Hjælpe specifikke producenter med at optimere støbe layoutet
- **støbesimulering**.
- Hjælpe specifikke producenter med at optimere smeltebehandlingen
- **smeltemetallurgisk viden**.
- Hjælpe specifikke producenter med at optimere formmaterialeerne
- **viden om formsand og bindemidler**.

**Ny metode til kvantificering af grafitstørrelse og –
morfologi i støbejern**

Steen Krogh Jensen, MAN

Ny metode til kvantificering af grafitstørrelse og –morphologi i støbejern



Dansk Metallurgisk Selskab,
Vintermøde 16-18/1-2013

Steen Krogh Jensen

Manager

Material Technology and Research

Research & Development

/ Marine Low Speed

Disclaimer



All data provided on the following slides is for information purposes only, explicitly non-binding and subject to changes without further notice.

Agenda



- 1 Cylinderforing – gammel materialspecifikation
- 2 ISO 945 – graphite classification
- 3 Cylinderforing – eksempler på grafit struktur, matrix og hårdfase
- 4 Grafitstørrelse – en ny definition
- 5 Hårdfase – mængde og fordeling
- 6 Ferrit – mængde?
- 7 Cylinderforing – ny materialespecifikation
- 8 Eksempler fra støberier
- 9 Stempelring – materialespecifikation – nodularitet
- 10 ISO 16 112 – Compacted (vermicular) graphite cast irons - Classification

MAN Diesel & Turbo

| Steen Krogh Jensen |

Kvantificering af grafitstørrelse og -morphologi i støbejern |

18.01.2012 | < 3 >

Cylinderforing Gammel materialespecifikation



MAN B&W Diesel A/S

Cast Iron

Cast Iron for Cylinder Liners



Tarkall-C

Mechanical Properties

• Tensile Strength	250	N/mm ²	min. 245 ⁽¹⁾
• Elongation	A ₅₀	%	min. 8,3 ⁽²⁾
• Brinell Hardness (ISO 6506-1981)	HBS	10/3000/15	180-230 ⁽³⁾
• % In the upper part of the cylinder liner:			
• Elongation at fracture i.e. elastic + plastic elongation. See O.C. 74 18 96-0.			
• Measured on the basis of the cylinder liner, 100 mm from the top.			

Microstructure

- Graphite (ISO 945-1975): I A 2/3/4.
- Matrix: Lamellar pearlite. Max. 3% ferrite. 3-7% cementite + steadite.

● Figures and text in bold type denote imperative demands.
All other information - including Similar Standards - is given for guidance only. (See General Note).

● According to Quality Control No. 74 14 12-0 the foundry must carry out a first-time casting and obtain the approval of MAN B&W Diesel A/S as supplier of cylinder liners made of Tarkall-C.

Similar Standards

ISO

EN

JIS

These standards do not include any Cast Iron similar to the above quality.

Supply Form

Finished cylinder liners. Tarkall-C is an abbreviation of the trade name Tarkalloy C.

Copyright © MAN B&W Diesel A/S, November 1998

Material Sheet P 676-2

Tribologi/Styrke/
Varmeledningsevne

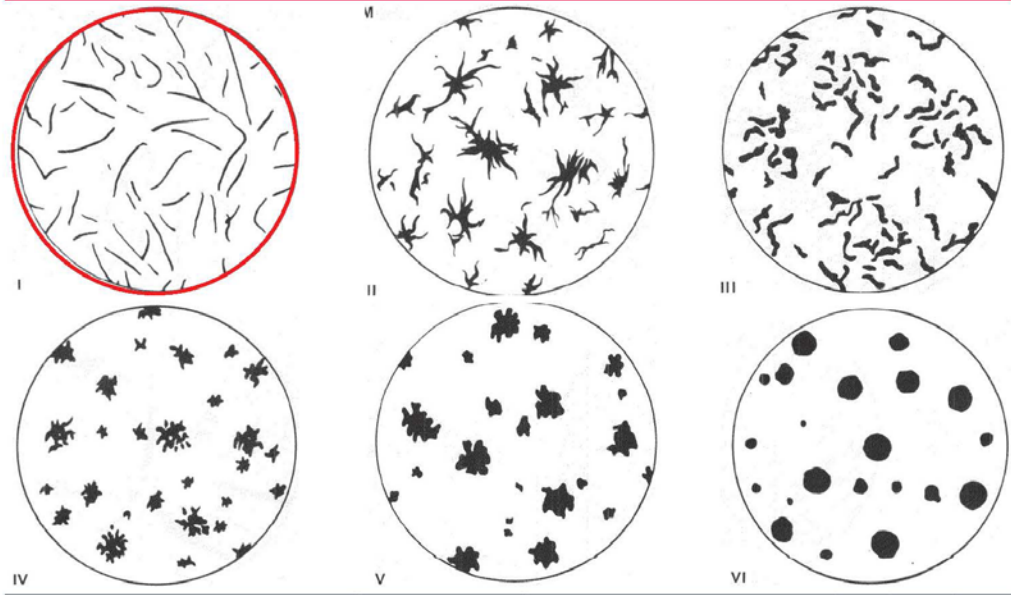
Slidstyrke

Scuffing resistens

Styrke/Tribologi



Grafitform ifølge ISO 945



MAN Diesel & Turbo

| Steen Krogh Jensen |

Kvantificering af grafitstørrelse og -morphologi i støbefjern

| 18.01.2012 | < 5 >

Grafitstørrelse ifølge ISO 945



Table 1 — Dimensions of graphite particle forms I to VI

Dimensions in millimetres

Size range reference number	Indication of the particle size observed at $\times 100$ magnification	Actual dimension
1	≥ 100	≥ 1
2	50 to < 100	0,5 to < 1
3	25 to < 50	0,25 to $< 0,5$
4	12 to < 25	0,12 to $< 0,25$
5	6 to < 12	0,06 to $< 0,12$
6	3 to < 6	0,03 to $< 0,06$
7	1,5 to < 3	0,015 to $< 0,03$
8	$< 1,5$	$< 0,015$

NOTE 1 When determining size ranges 1 and 2, a lower magnification ($\times 25$ or $\times 50$) may be used.

NOTE 2 When determining size ranges 6 to 8, a higher magnification ($\times 200$ or $\times 500$) may be used.

NOTE 3 For determining size ranges, the largest visible graphite particle size is used.

MAN Diesel & Turbo

| Steen Krogh Jensen |

Kvantificering af grafitstørrelse og -morphologi i støbefjern

| 18.01.2012 | < 6 >

Grafiteform - 7 støberier



Graphite (ISO 945-1975): I A 2/3/4.

1 mm



MAN Diesel & Turbo

| Steen Krogh Jensen

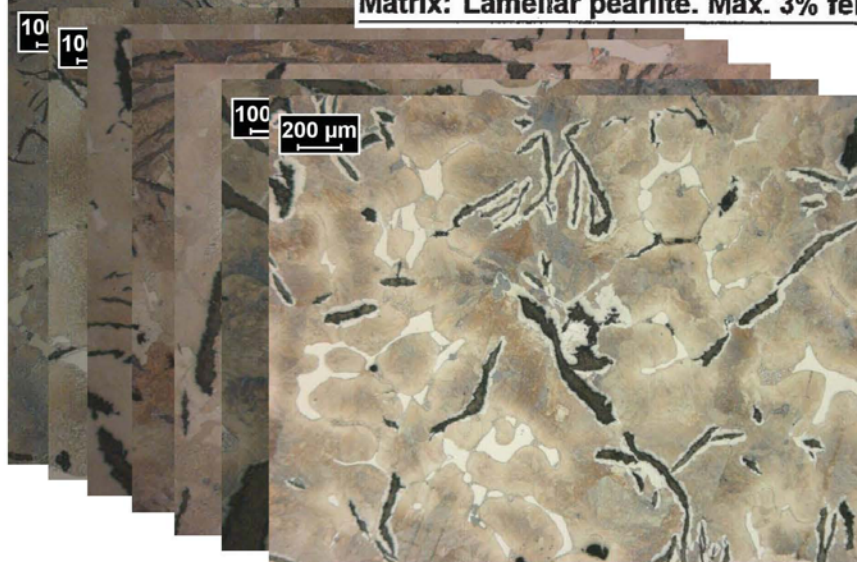
| Kvantificering af grafitstørrelse og -morphologi i støbejern

| 18.01.2012 | < 7 >

Matrix (perlit/ferrit)- 7 støberier



Matrix: Lamellar pearlite. Max. 3% ferrite.



MAN Diesel & Turbo

| Steen Krogh Jensen

| Kvantificering af grafitstørrelse og -morphologi i støbejern

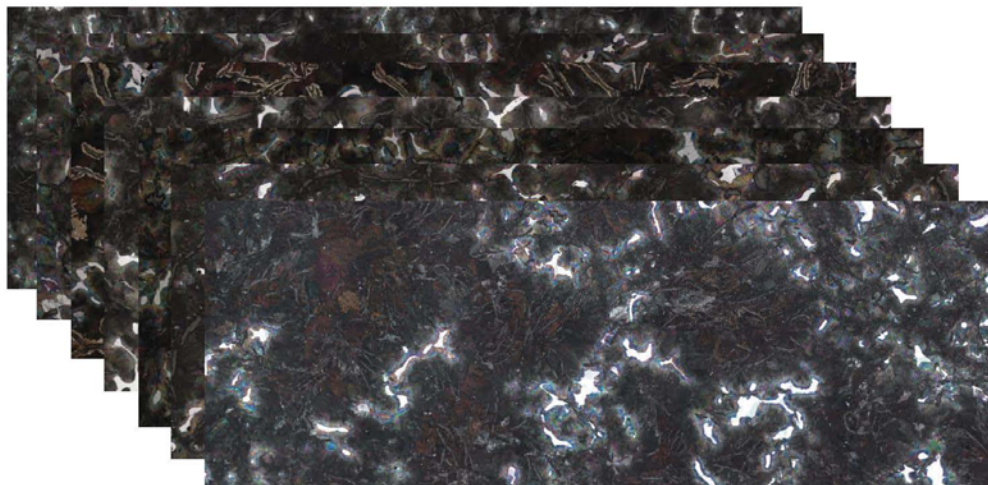
| 18.01.2012 | < 8 >

Hårdfase - 7 støberier



3-7% cementite + steadite.

1 mm



MAN Diesel & Turbo

| Steen Krogh Jensen

| Kvantificering af grafitstørrelse og -morphologi i støbejern

| 18.01.2012 | < 9 >

Samlet vurdering af Mikrostruktur 7 støberier



Position	Matrix	Graphite type			% Cementite + Steadite			% Ferrite		
		inside	centre	outside	inside	centre	outside	inside	centre	outside
MAN Diesel A/S	Pearlite	IA3/4/5	IA3/4/5	IA3/4/5	2.13	1.52	1.88	< 1	< 1	< 1
Leverandør nr. 1	Pearlite	A4			< 2			-		
MAN Diesel A/S	Pearlite	IA3/4/5	IA3/4/5	IA3/4/5	3.82	2.97	3.36	< 1	< 1	< 1
Leverandør nr. 3	Pearlite	A2-4			3 - 4			< 3		
MAN Diesel A/S	Pearlite	IA3/4/5	IA3/4/5	IA3/4/5	2.76	2.49	3.60	< 1	< 1	< 1
Leverandør nr. 4	Pearlite	A2-4			3 - 4			< 3		
MAN Diesel A/S	Pearlite	IA2/3/4	IA2/3/4/5	IA2/3/4/5	5.91	6.95	7.08	< 1	< 1	< 1
Leverandør nr. 2	Pearlite		IA3/4		4.2 - 6.4			Max. 1		
MAN Diesel A/S	Pearlite	IA2/3/4	IA2/3/4	IA2/3/4	4.48	5.50	5.88	~1	~1	~1
Leverandør nr. 6	Pearlite		-		-			-		
MAN Diesel A/S	Pearlite	IA2/3/4	IA2/3/4	IA3/4/5	4.46	4.27	3.29	< 1	< 1	< 1
Leverandør nr. 5	Pearlite	IA3	IA3	IA3	5.0	5.3	4.6	0	0	0
MAN Diesel A/S	Pearlite	IA2/3/4	IA2/3/4	IA2/3/4	5.7	5.3	6.1	< 1	< 1	< 1
Leverandør nr. 7	Pearlite	IA3/4	IA3/4	IA3/4	5.2	4.8	4.5	< 2	< 2	< 2
Spec. Takalloy-C	Pearlite	IA2/3/4			3-7			Max. 3		

- Ud fra ovenstående tabel er det svært at differentiere mellem forskellige leverandører
- Vurderingen af specielt grafitstørrelsen er delvis subjektiv
- Ikke særlig god overensstemmelse mellem vurderinger fra leverandører og MDT

MAN Diesel & Turbo

| Steen Krogh Jensen

| Kvantificering af grafitstørrelse og -morphologi i støbejern

| 18.01.2012 | < 10 >

Serviceerfaringer



Serviceerfaringer:

- Højere slid på nogle foringer end andre
- Større tilbøjelighed til scuffing på nogle foringer
- Revnede foringer

Observationer i mikrostrukturen:

- Stor forskel på grafitstørrelse (Længde/Bredde/Areal)
- Kæmpe forskel på mængden af hårdfase og fordelingen af denne
- Store variationer på mængden af ferrit
- Derudover fandtes store variationer på trækstyrken/udmattelsesstyrken

Brug for et generelt løft i kvaliteten:

- Målemetode til ensartet bestemmelse af grafitstørrelsen
- Bedre fordeling af hårdfasen – primære cellestørrelse
- Bestemmelse af ferritmængden

MAN Diesel & Turbo

| Steen Krogh Jensen

| Kvantificering af grafitstørrelse og -morphologi i støbefejern

| ● ● ● | 18.01.2012 | < 11 >

Grafitstørrelse – ISO 945 Forstørrelse: 100x



Repræsentativt?
Statistik?
Primær cellestørrelse?

Løsningen er
Mosaik!



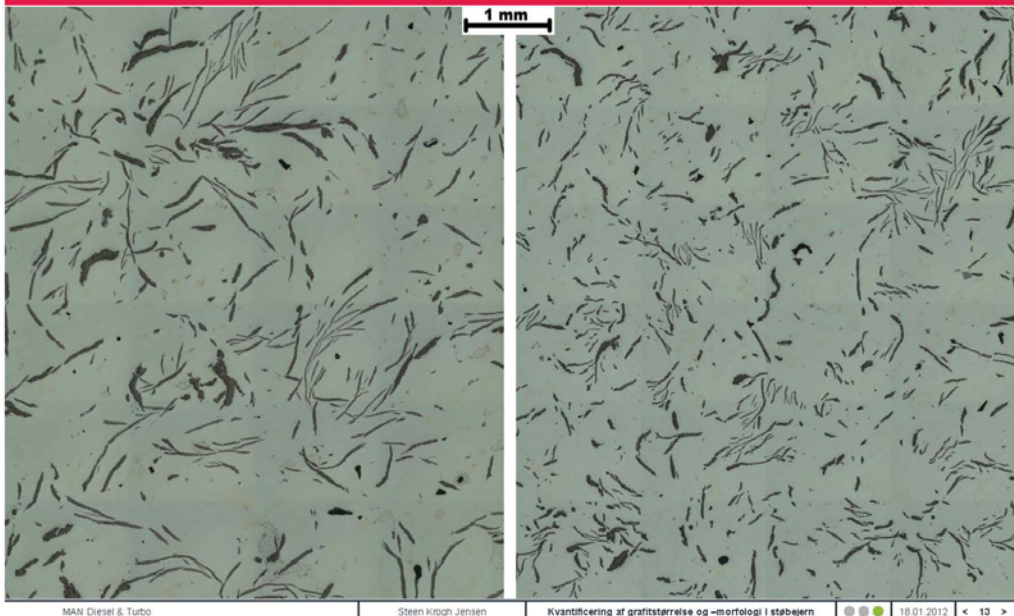
MAN Diesel & Turbo

| Steen Krogh Jensen

| Kvantificering af grafitstørrelse og -morphologi i støbefejern

| ● ● ● | 18.01.2012 | < 12 >

Grafitstørrelse - Så er det jeres tur!



MAN Diesel & Turbo

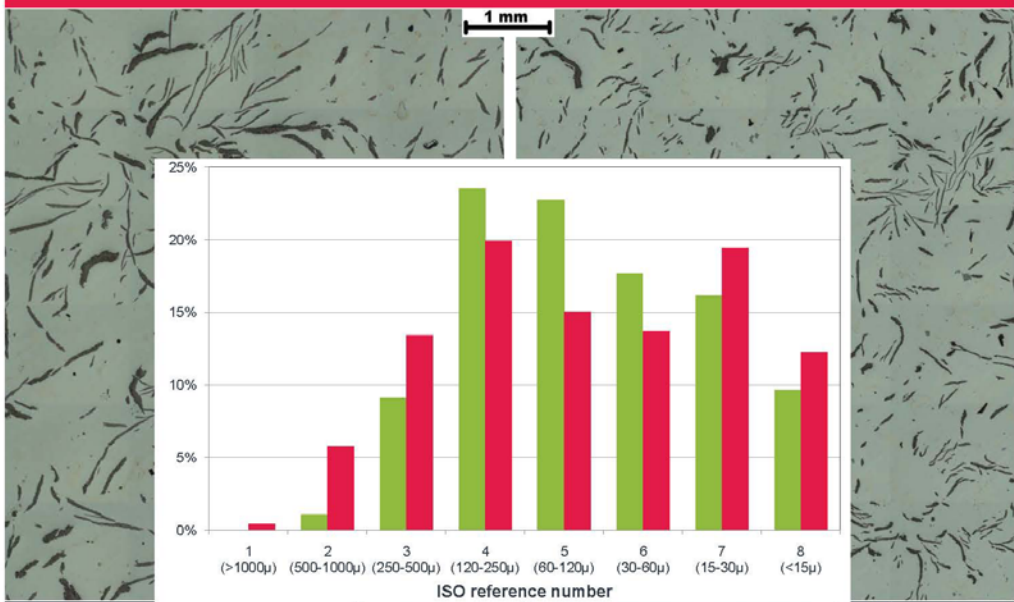
Steen Krogh Jensen

Kvantificering af grafitstørrelse og -morphologi i støbejern

18.01.2012

< 13 >

Grafitstørrelse - Lidt Hjælp



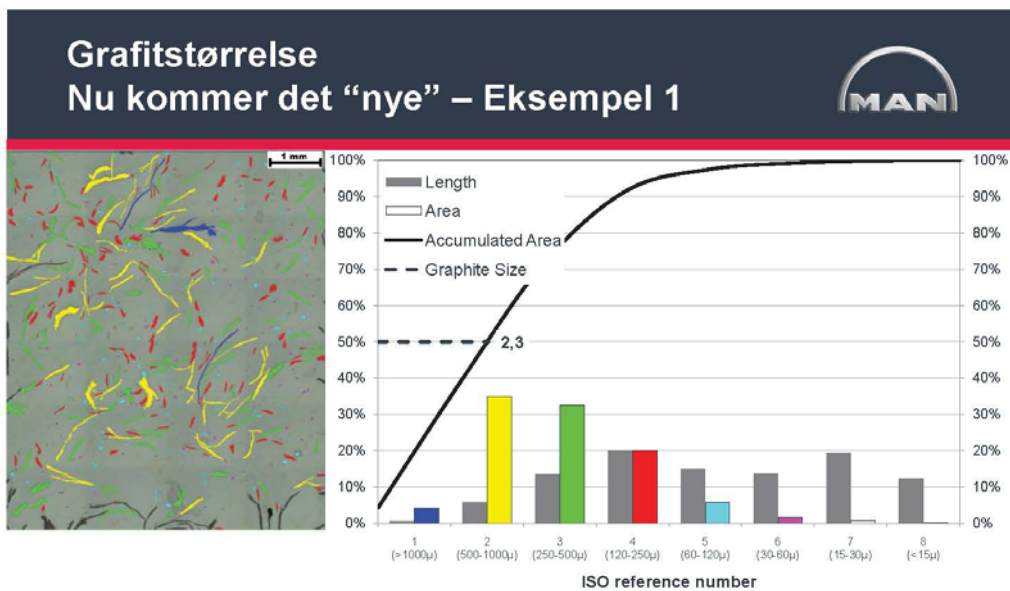
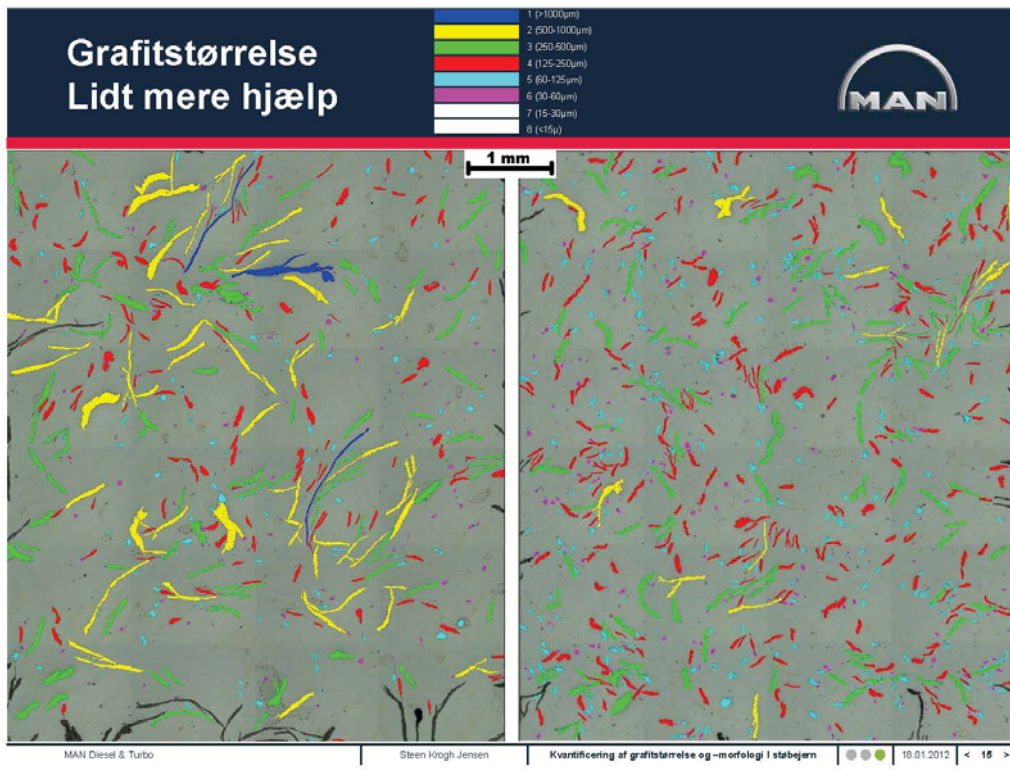
MAN Diesel & Turbo

Steen Krogh Jensen

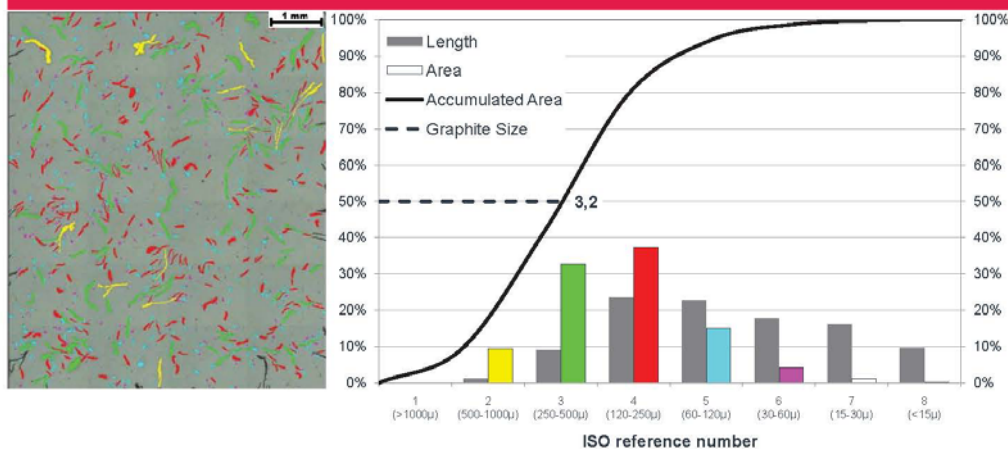
Kvantificering af grafitstørrelse og -morphologi i støbejern

18.01.2012

< 14 >



Grafitstørrelse Nu kommer det “nye” – Eksempel 2



MAN Diesel & Turbo

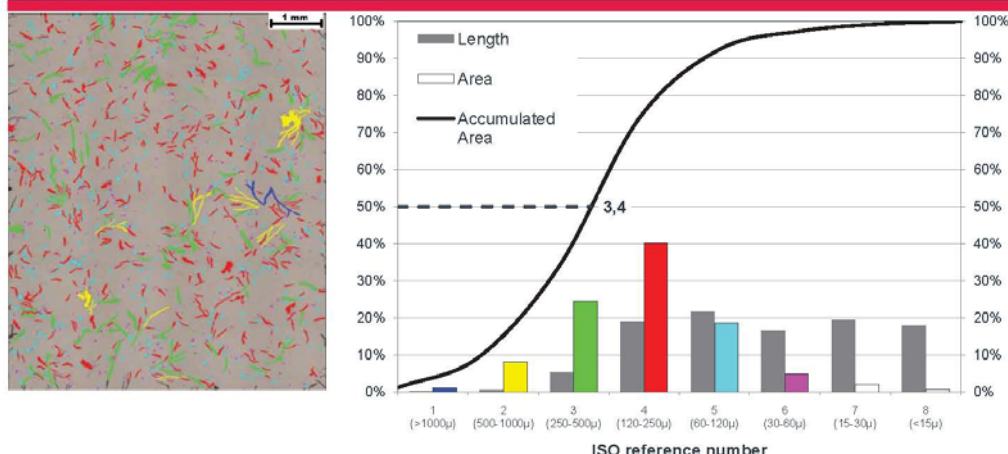
Steen Krogh Jensen

Kvantificering af grafitstørrelse og -morphologi i støbefejn

18.01.2012

< 17 >

Grafitstørrelse Nu kommer det “nye” – Eksempel 3



MAN Diesel & Turbo

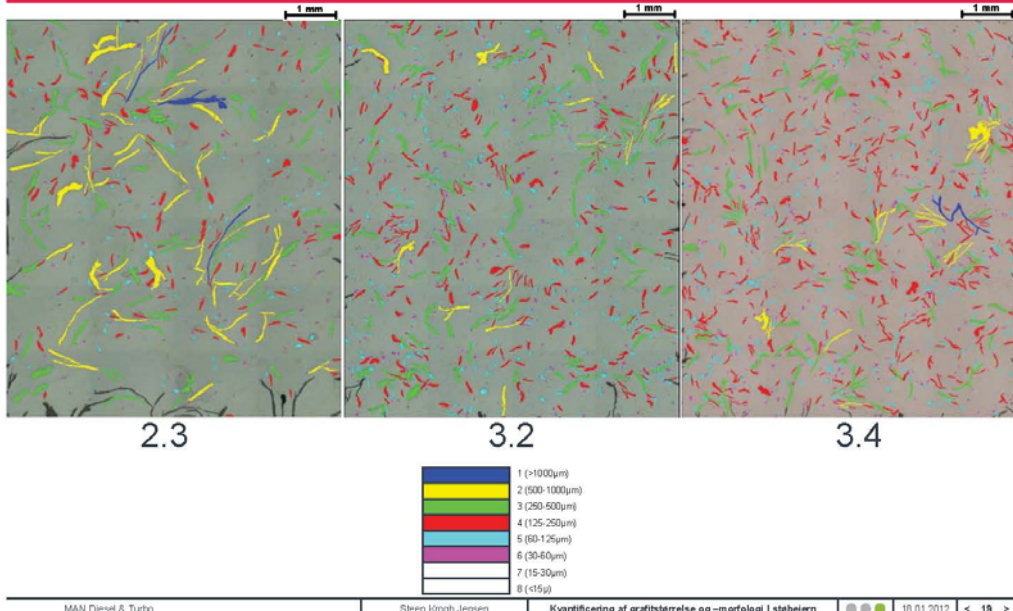
Steen Krogh Jensen

Kvantificering af grafitstørrelse og -morphologi i støbefejn

18.01.2012

< 18 >

Grafitstørrelse - sammenfatning

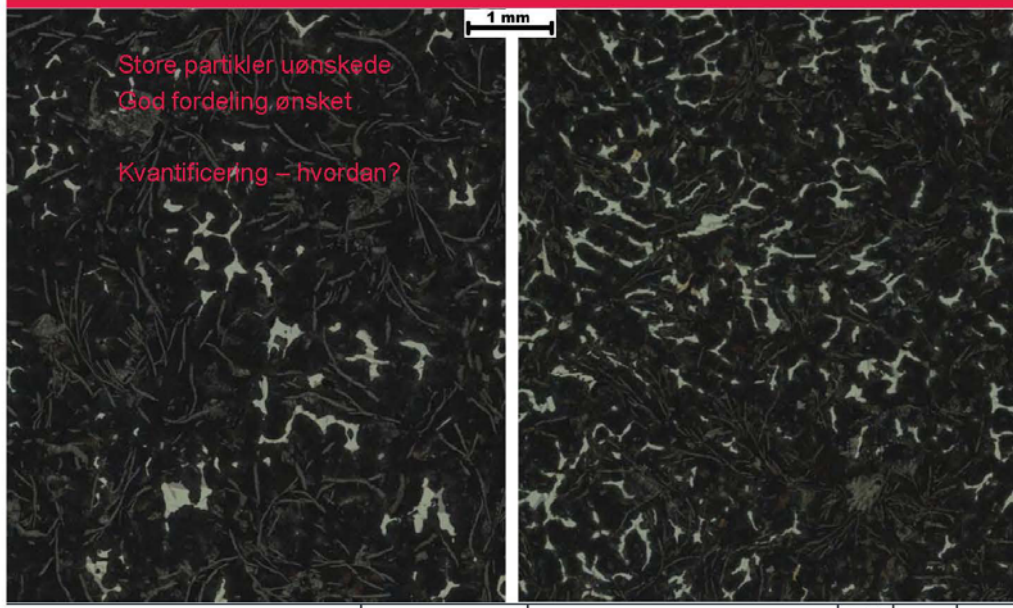


Hårdfase – Mængde og fordeling?

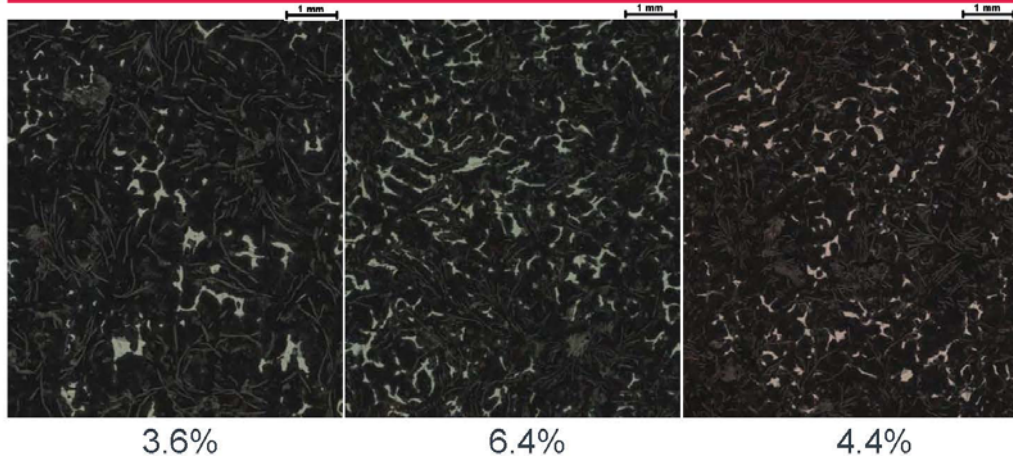


Store partikler uønskede
God fordeling ønsket

Kvantificering – hvordan?



Hårdfase - Eksempler



MAN Diesel & Turbo

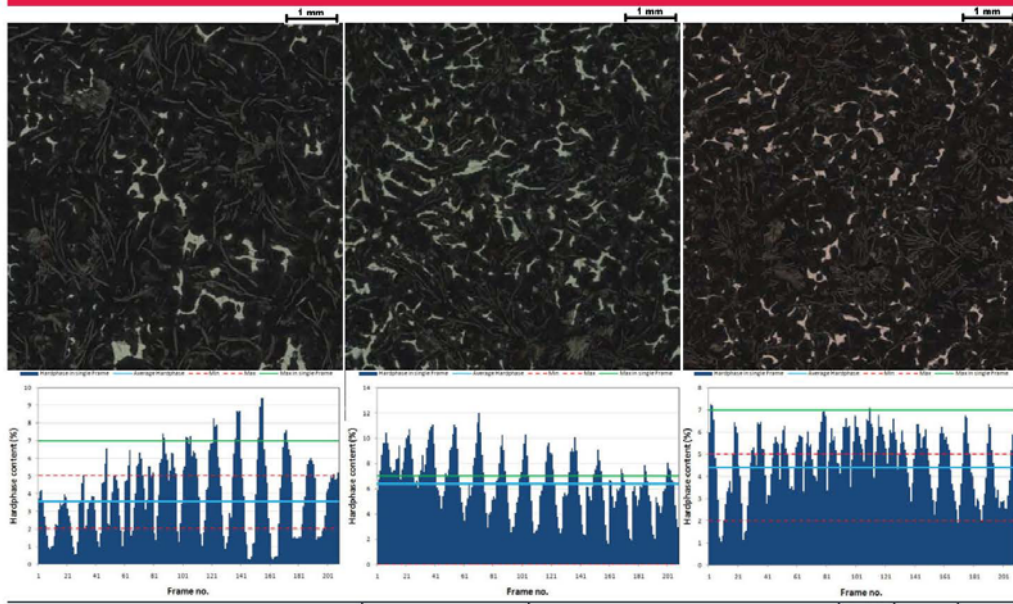
Steen Krogh Jensen

Kvantificering af grafitsstørrelse og -morphologi i støbefejern

18.01.2012

< 21 >

Hårdfase - Sammenfatning



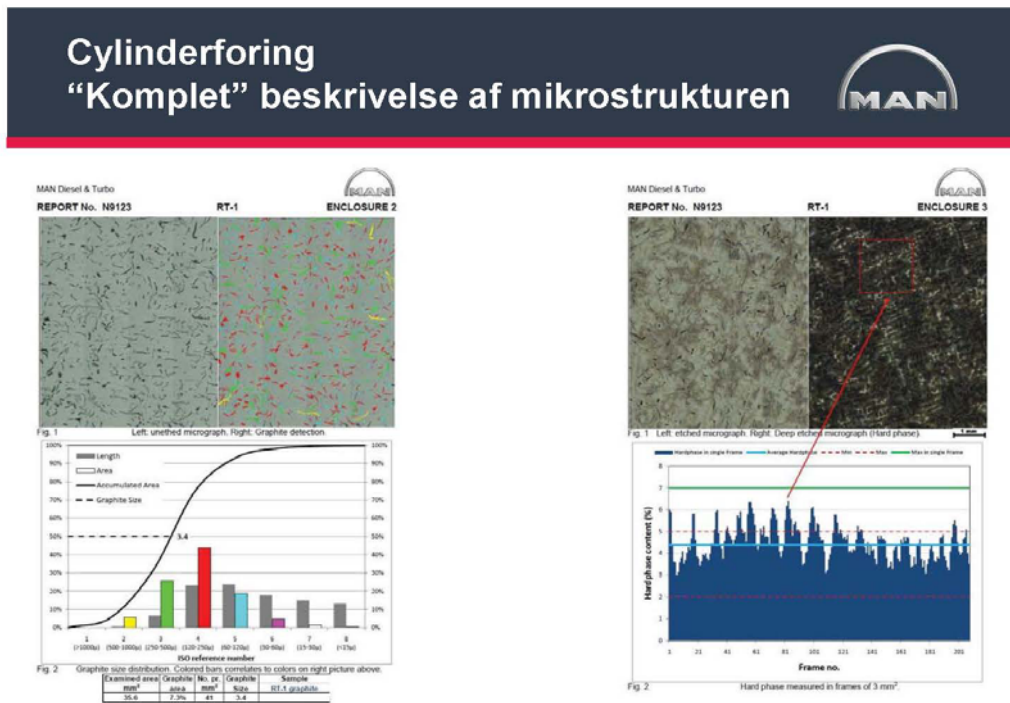
MAN Diesel & Turbo

Steen Krogh Jensen

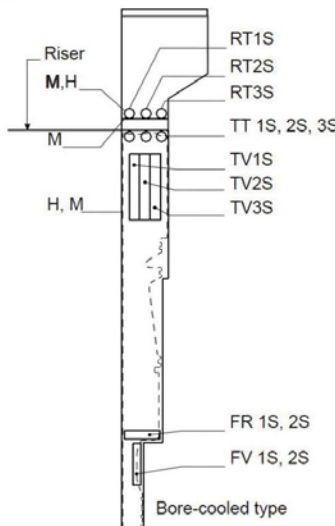
Kvantificering af grafitsstørrelse og -morphologi i støbefejern

18.01.2012

< 22 >



Cylinder foring Samlet mikrostruktur evaluering



MDT	Matrix	Graphite				Cementite + Steadite		Ferrite		Enclosure
		Position	Form	Distribution	Size	Average	Max	Average	Max	
RT 1	Pearlite	I	A	3.0	8.3	6.1	12.6	<1	-	2 and 3
RT 2	Pearlite	I	A	3.2	7.8	6.7	12.6	<1	-	4 and 5
RT 3	Pearlite	I	A	3.1	7.2	5.4	9.6	<1	-	6 and 7
TT 1	Pearlite	I	A	2.9	8.0	5.1	9.2	<1	-	8 and 9
TT 2	Pearlite	I	A	3.0	8.6	4.9	9.7	<1	-	10 and 11
TT 3	Pearlite	I	A	2.9	7.6	4.9	8.0	<1	-	12 and 13
TV 1	Pearlite	I	A	3.0	8.6	4.4	9.0	<1	-	14 and 15
TV 2	Pearlite	I	A	2.9	7.9	5.1	8.8	<1	-	16 and 17
TV 3	Pearlite	I	A	3.0	8.2	4.6	9.1	<1	-	18 and 19
FR 1	Pearlite	I	A	3.2	7.5	6.8	12.5	<1	-	20 and 21
FR 2	Pearlite	I	A	3.1	7.4	4.1	6.8	<1	-	22 and 23
FV 1	Pearlite	I	A	3.2	7.9	5.6	9.0	<1	-	24 and 25
FV 3	Pearlite	I	A	3.4	6.2	5.6	10.0	<1	-	26 and 27
Spec. for Tarkalloy C	Pearlite	IA2/3/4		-	<7	-	<3	-	-	

MAN Diesel & Turbo

Steen Krogh Jensen

Kvantificering af grafitsterrelse og -morphologi i støbefjern

18.01.2012 | < 25 >

Cylinderforing Ny materialespecifikation



Gammel



MAN B&W Diesel A/S

Cast Iron

Cast Iron for Cylinder Liners

Tarkall-C

Mechanical Properties

- Tensile Strength: σ_u N/mm², min. 245⁽¹⁾
- Elongation: δ_{50} %, min. 9.3⁽²⁾
- Brinell Hardness (ISO 6506-1981): HBS 10/3000/15 180-230⁽³⁾
- In the upper part of the cylinder liner:

 - Total elongation at fracture 1 e. elastic + plastic elongation. See G.C. 74 18 96-0;
 - Measured on the basis of the cylinder liner, 100 mm from the top.

Microstructure

- Graphite (ISO 945-1975): I A 2/3/4.
- Matrix: Lamellar pearlite. Max. 3% ferrite. 3-7% cementite + steadite.

Chemical Composition

C%	S%	Mn%	P%	S%	Cr%	V%
Min. 3.6	0.2	0.8	0.02	1.0		
Nominal 3.2	1.1	0.8				
Max. 3.6	0.4	0.10	0.04	1.5	0.22	

Heat Treatment

In case of demand for stress relieving: Heat max. 90°C/hour to 500°C, hold for 4 hours.

Cast in furnace max. 1000°C to max. 150°C.

• Figures and text in bold type denote imperative demands.

All other information - including Similar Standards - is given for guidance only. (See General Note).

• According to Quality Control No. 74 14 12-0 the Foundry must carry out a first-time casting and obtain the approval of MAN B&W Diesel A/S as supplier of cylinder liners made of Tarkall-C.

Similar Standards

ISO

EN

JIS

These standards do not include any Cast Iron similar to the above quality.

Supply Form

Finished cylinder liners. Tarkall-C is an abbreviation of the trade name Tarkalloy C.

Copyright © MAN B&W Diesel A/S, November 1996

Material Sheet P 676-2

MAN Diesel & Turbo

Ny



Iron, Cast

Cast Iron for Cylinder Liners

Data marked with * are imperative demands.

All other information, including "Guidance - Standards - References", are given for guidance only.

MOT SPECIFICATIONS

G.C. 741412-0 Cylinder Liners - Tarkalloy CA - First-Time Production Approval

G.C. 741412-3 Evaluation of microstructures based on image analysing equipment/software for Tarkalloy CA Cylinder Liners

G.C. 741412-4 Quality Specification for Tarkalloy CA Cylinder Liners

APPLICATION

Cylinder Liners

NOTES

New supplies of TARKALL-C CYLINDER LINERS must be approved by MOT, see the G.C. mentioned in the MOT Specifications.

MECHANICAL PROPERTIES

Standard Test

Condition

Position

Dimension (mm)

Temp (°C)

Rate (mm/min)

Load (kN)

Strain rate (%)

Distance (mm)

Time (min)

Speed (mm/min)

Specimen length (mm)

Specimen width (mm)

Specimen thickness (mm)

Specimen height (mm)

Specimen diameter (mm)

Specimen width (mm)

Specimen thickness (mm)

Specimen height (mm)

Specimen diameter (mm)

Specimen width (mm)

Specimen thickness (mm)

Specimen height (mm)

Specimen diameter (mm)

Specimen width (mm)

Specimen thickness (mm)

Specimen height (mm)

Specimen diameter (mm)

Specimen width (mm)

Specimen thickness (mm)

Specimen height (mm)

Specimen diameter (mm)

Specimen width (mm)

Specimen thickness (mm)

Specimen height (mm)

Specimen diameter (mm)

Specimen width (mm)

Specimen thickness (mm)

Specimen height (mm)

Specimen diameter (mm)

Specimen width (mm)

Specimen thickness (mm)

Specimen height (mm)

Specimen diameter (mm)

Specimen width (mm)

Specimen thickness (mm)

Specimen height (mm)

Specimen diameter (mm)

Specimen width (mm)

Specimen thickness (mm)

Specimen height (mm)

Specimen diameter (mm)

Specimen width (mm)

Specimen thickness (mm)

Specimen height (mm)

Specimen diameter (mm)

Specimen width (mm)

Specimen thickness (mm)

Specimen height (mm)

Specimen diameter (mm)

Specimen width (mm)

Specimen thickness (mm)

Specimen height (mm)

Specimen diameter (mm)

Specimen width (mm)

Specimen thickness (mm)

Specimen height (mm)

Specimen diameter (mm)

Specimen width (mm)

Specimen thickness (mm)

Specimen height (mm)

Specimen diameter (mm)

Specimen width (mm)

Specimen thickness (mm)

Specimen height (mm)

Specimen diameter (mm)

Specimen width (mm)

Specimen thickness (mm)

Specimen height (mm)

Specimen diameter (mm)

Specimen width (mm)

Specimen thickness (mm)

Specimen height (mm)

Specimen diameter (mm)

Specimen width (mm)

Specimen thickness (mm)

Specimen height (mm)

Specimen diameter (mm)

Specimen width (mm)

Specimen thickness (mm)

Specimen height (mm)

Specimen diameter (mm)

Specimen width (mm)

Specimen thickness (mm)

Specimen height (mm)

Specimen diameter (mm)

Specimen width (mm)

Specimen thickness (mm)

Specimen height (mm)

Specimen diameter (mm)

Specimen width (mm)

Specimen thickness (mm)

Specimen height (mm)

Specimen diameter (mm)

Specimen width (mm)

Specimen thickness (mm)

Specimen height (mm)

Specimen diameter (mm)

Specimen width (mm)

Specimen thickness (mm)

Specimen height (mm)

Specimen diameter (mm)

Specimen width (mm)

Specimen thickness (mm)

Specimen height (mm)

Specimen diameter (mm)

Specimen width (mm)

Specimen thickness (mm)

Specimen height (mm)

Specimen diameter (mm)

Specimen width (mm)

Specimen thickness (mm)

Specimen height (mm)

Specimen diameter (mm)

Specimen width (mm)

Specimen thickness (mm)

Specimen height (mm)

Specimen diameter (mm)

Specimen width (mm)

Specimen thickness (mm)

Specimen height (mm)

Specimen diameter (mm)

Specimen width (mm)

Specimen thickness (mm)

Specimen height (mm)

Specimen diameter (mm)

Specimen width (mm)

Specimen thickness (mm)

Specimen height (mm)

Specimen diameter (mm)

Specimen width (mm)

Specimen thickness (mm)

Cylinderforging

Ny materialespecifikation



Gammel

Microstructure

- Graphite (ISO 945-1975): I A 2/3/4.
- Matrix: Lamellar pearlite. Max. 3% ferrite. 3-7% cementite + steadite.

Ny

STRUCTURE - IRON ACCORDING TO ISO 945 (1975)

Dimension (mm)	Graphite Form	Graphite Distribution	Reference Size	Cementite+ Steadite %	Ferrite %	Pearlite %
▪ < 800 mm	I	A	2-3-4	< 7%	< 3%	Rest
▪ ≥ 800 mm	I	A	2-3-4	2-5%	≤ 1%	Rest

STRUCTURE - NOTES

The notes are valid only for group 3 cylinder liners - 0-40 mm from finish machined inside surface:

- Max 3% Ferrite - measured within a test area of app. 2 mm², where highest concentration is observed
- Max 7% Cem+Ste - measured within a test area of max 3 mm², where highest concentration is observed

- Øget ensartehed
- Generelt kvalitetsløft
- "Ny" omgang FTA
- Fundet "aktive" leverandører
- Ferritmåling er endnu ikke automatiseret!
- Indkøb af billedbehandlingsudstyr hos underleverandører

MAN Diesel & Turbo

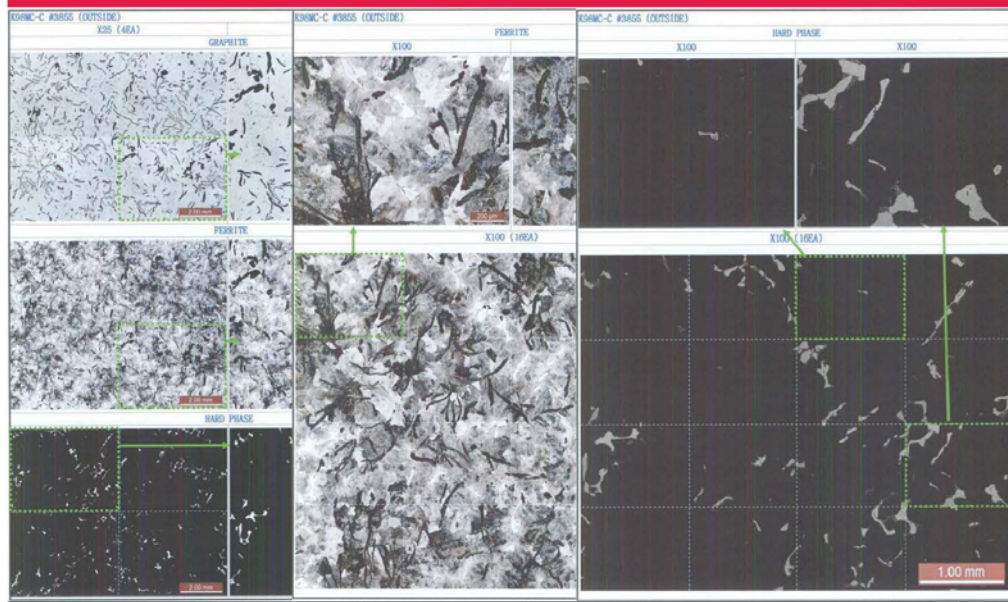
| Steen Krogh Jensen |

Kvantificering af grafittsterreine og -morphologi i stabejern

| 18.01.2012 | < 27 >

Cylinderforging

Eksempler fra underleverandører



MAN Diesel & Turbo

| Steen Krogh Jensen |

Kvantificering af grafittsterreine og -morphologi i stabejern

| 18.01.2012 | < 28 >

Cylinderforging Eksempler fra underleverandører



No.	Microstructure	Hard-Phase				Ferrite			
		Cementite		Magnetite		Aero.		Per-Aero.	
Chemical Spec. (atom)		Cementite + Magnetite = 25% - 30%		Aero.		Aero.		Per-Aero.	
		Aero.	Per-Aero.	Aero.	Per-Aero.	Aero.	Per-Aero.	Aero.	Per-Aero.
1		0.06497	0.06497	0.06497	0.06497	0.06497	0.06497	0.06497	0.06497
1		6.44%		1.13%					
2		0.06534	0.06534	0.06534	0.06534	0.06534	0.06534	0.06534	0.06534
2		8.38%		1.33%					
3		0.06489	0.06489	0.06489	0.06489	0.06489	0.06489	0.06489	0.06489
3		6.49%		6.21%					
4		0.06572	0.06572	0.06572	0.06572	0.06572	0.06572	0.06572	0.06572
4		6.81%		1.39%					
5		0.06572	0.06572	0.06572	0.06572	0.06572	0.06572	0.06572	0.06572
5		6.41%		6.41%					
6		0.06526	0.06526	0.06526	0.06526	0.06526	0.06526	0.06526	0.06526
6		1.92%		1.75%					
7		0.06546	0.06546	0.06546	0.06546	0.06546	0.06546	0.06546	0.06546
7		6.23%		6.16%					
8		0.06529	0.06529	0.06529	0.06529	0.06529	0.06529	0.06529	0.06529
8		6.45%		6.45%					

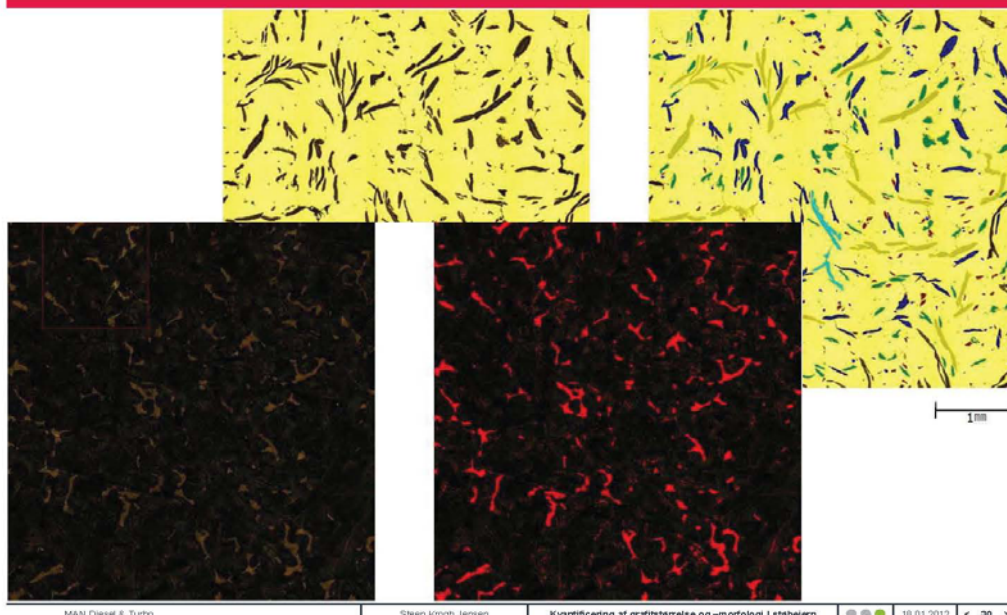
MAN Diesel & Turbo

Steen Krogh Jensen

Kvantificering af grafitstørrelse og -morfologi i støbejern

10.01.2012 < 29 >

Cylinderforing Eksempler fra underleverandører



MAN Diesel & Turbo

Steen Krogh Jensen

Kvantificering af grafittstørrelse og -morphologi i støbøjern

18.01.2012

Cylinderforcing Eksempler fra underleverandører



Fig. 1: Left: Unetched micrograph; Right: Graphite detection. Detection area is totally 83mm².

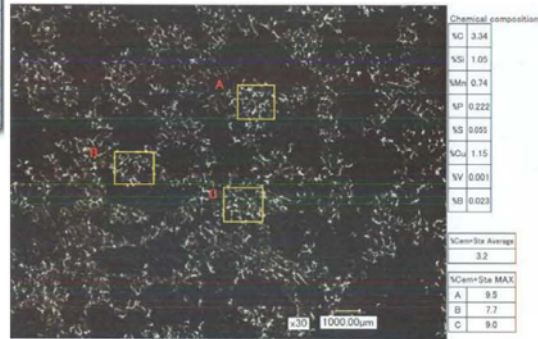
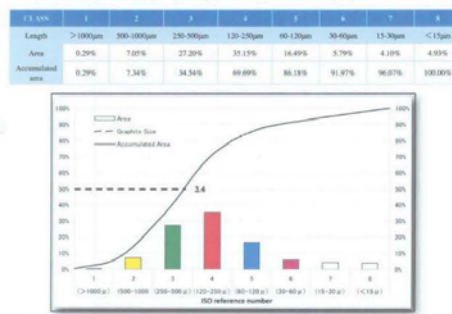


Fig. 2: Graphite size distribution. Colored bars correlate to colors on right picture above.

MAN Diesel & Turbo

Steen Krog Jensen

Kvantificering af grafittstørrelse og -morphologi i støbejern

18.01.2012 | < 31 >

Stempelring Materialspecifikation



MAN Diesel & Turbo

Iron, Cast

Cast Iron for Piston Rings (Vermicular graphite)



Data marked with * are imperative demands.

All other information, including "Guidance - Standards - References", are given for guidance only.

MOT SPECIFICATIONS

ISO 945 - Piston Rings - First-Time Production Approval

APPLICATION

Finished piston rings.

The piston ring maker MUST be approved by MOT

NOTES

Previous part of datasheet: HVK-C - Revision b - IP 649-2 Issued January 2003

MECHANICAL PROPERTIES						
Dimension (mm)	Graphite Form	Graphite Distribution	Reference Size	Cementite+ Steadite %	Ferrite %	Pearlite %
≥ ø 900	III; nodularity < 20 %	A	4/6	1-3	≤ 3	Rest
< ø 900	III; nodularity < 20 %	A	4/6	3-7	≤ 3	Rest

MECHANICAL PROPERTIES - NOTES

• Strength (A) is Ø 8.5 (Eng. diameter = 950 mm).

Nodularitet

- Evig diskussion!
- Subjektivt vurderet
- Indflydelse på varmeledningsevne
- Påvirker tribologiske egenskaber
- Ny standard – ISO 16112

STRUCTURE - IRON ACCORDING TO ISO 945 (1975)

Dimension (mm)	Graphite Form	Graphite Distribution	Reference Size	Cementite+ Steadite %	Ferrite %	Pearlite %
≥ ø 900	III; nodularity < 20 %	A	4/6	1-3	≤ 3	Rest
< ø 900	III; nodularity < 20 %	A	4/6	3-7	≤ 3	Rest

STRUCTURE - NOTES

- The nodularity must be determined according to ISO16112 or JIS5502 respectively

• The appointed piston ring maker must produce piston rings in full agreement with their material specification, known and approved by MOT.

• Any change of the chemical composition already approved for the actual piston ring maker will result in a demand for a new approval.

STRUCTURE - IRON ACCORDING TO ISO 945 (1975)

Dimension (mm)	Graphite Form	Graphite Distribution	Reference Size	Cementite+ Steadite %	Ferrite %	Pearlite %
≥ ø 900	III; nodularity > 20 %	A	4/6	1-3	≤ 3	Rest
< ø 900	III; nodularity > 20 %	A	4/6	3-7	≤ 3	Rest

STRUCTURE - NOTES

• The nodularity must be determined according to ISO16112 or JIS5502 respectively

PHYSICAL PROPERTIES

Temperature [°C]	Tensile Strength [N/mm²] min.	Modulus of Elasticity [N/mm²] min.	Thermal Conductivity [W/m²K] min.	Maximum Capacity [kN/mm²] min.	Modulus Elasticity [GPa] min.	Modulus Rigidity [GPa] min.
20	-	-	-	-	-	-

PHYSICAL - NOTES

For Modulus of Elasticity specified as "Nominal" a deviation of +/- 10% is acceptable. Must be verified during the "First Time Approval".

MAN Diesel & Turbo

Steen Krog Jensen

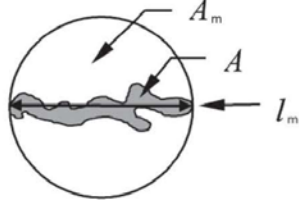
Kvantificering af grafittstørrelse og -morphologi i støbejern

18.01.2012 | < 32 >

Nodularity according to ISO 16112



$$\text{Roundness} = \frac{A}{A_m} = \frac{4 \times A}{\pi \times l_m^2}$$



A_m area of circle of diameter l_m

A area of the graphite particle in question

l_m maximum axis length of the graphite particle in question = maximum distance between two points on the graphite particle perimeter

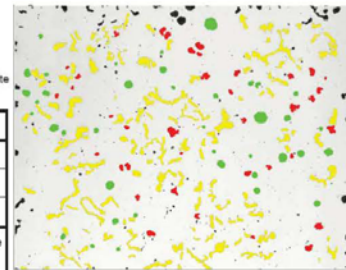
Percent nodularity is calculated on an area basis as follows:

$$\text{Percent nodularity} = \frac{\sum A_{\text{nODULES}} + 0,5 \times \sum A_{\text{interMEDIATES}}}{\sum A_{\text{all particles}}} \times 100$$

A_{nODULES} is the area of particles classified as spheroidal (nodular) graphite;

$A_{\text{interMEDIATES}}$ is the area of particles classified as intermediate forms of graphite;

$A_{\text{all particles}}$ is the area of all graphite particles greater than 10 µm.



Roundness-shape factor

Graphite form

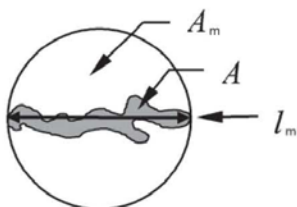
0,625 to 1	Nodular (ISO form VI)
0,525 to 0,625	Intermediate (ISO forms IV and V)
< 0,525	Compacted (ISO form III)

Flake graphite particles and graphite particles with maximum axis length less than 10 µm are not included in the analysis.

Nodularity according to JIS 5502



$$\text{Roundness} = \frac{A}{A_m} = \frac{4 \times A}{\pi \times l_m^2}$$



5. Image analysis (calculation of nodularity) procedure

- (1) Import the image data of graphite structure 3. - a)
- (2) Digitalization: split into black particles (graphite) and white part (matrix)
- (3) Correction of digitalized images: eliminate graphite which size is not over 15 µm 3. - b)
- (4) Calculation of nodularity (automatic calculation)

- i) Classification of graphite: divide graphite shape into I -IV and V-VI

*Classification method:

If a graphite area ratio against the minimum circumscribed circle of the graphite

$$(= \frac{(\text{Area of graphite}) \times 100}{\text{Area of minimum circumscribed circle}}) \text{ is:}$$

- under 55% => I -IV

- over 55% => V -VI

- ii) Calculation of nodularity of graphite 3. - c)

$$\frac{\text{Figure of shape V-VI graphite}}{\text{Figure of all graphite}} \times 100 = \text{Nodularity (\%)}$$

Nodularitet - Eksempler



1 mm

MAN Diesel & Turbo

Steen Krogh Jensen

Kvantificering af grafitsstørrelse og -morphologi i støbefjern

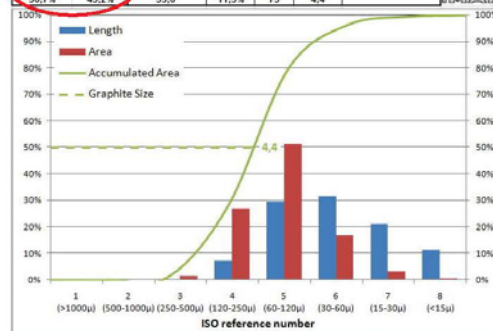
18.01.2012 | < 36 >

Nodularitet - Eksempler



1 mm

Nodularity (ISO 16112)	Nodularity (JIS5502)	Examined area mm ²	Graphite area	No. pr.	Graphite Size	Sample
36.7%	43.2%	35.6	11.5%	73	4.4	N9041-29-2 Graphite



MAN Diesel & Turbo

Steen Krogh Jensen

Kvantificering af grafitsstørrelse og -morphologi i støbefjern

18.01.2012 | < 36 >

Stempelring “Komplet” beskrivelse af mikrostrukturen

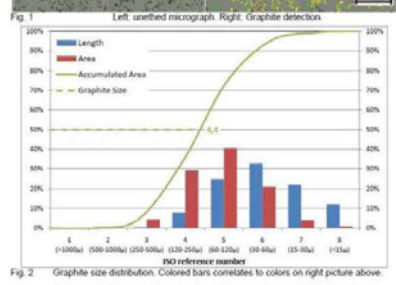
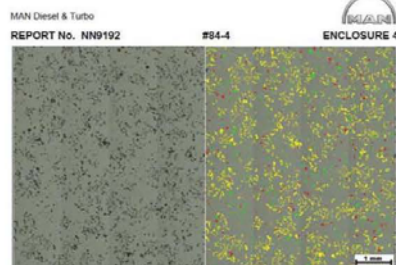


Fig. 2 Graphite size distribution. Colored bars correlates to colors on right picture above.

Nodularity	Nodularity	Examined area	Graphite area	No. pr.	Graphite size
(ISO 16112) 18.5%	(ISO 16112) 22.8%	mm ²	mm ²	82	4.4

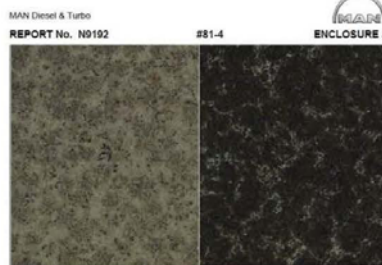


Fig. 1 Left: etched micrograph. Right: Deep etched micrograph (Hard phase)

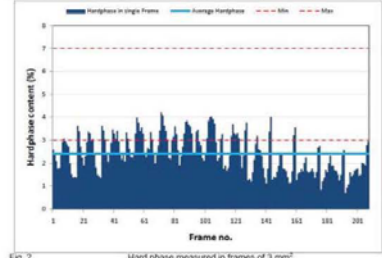


Fig. 2 Hard phase measured in frames of 3 mm².

MAN Diesel & Turbo

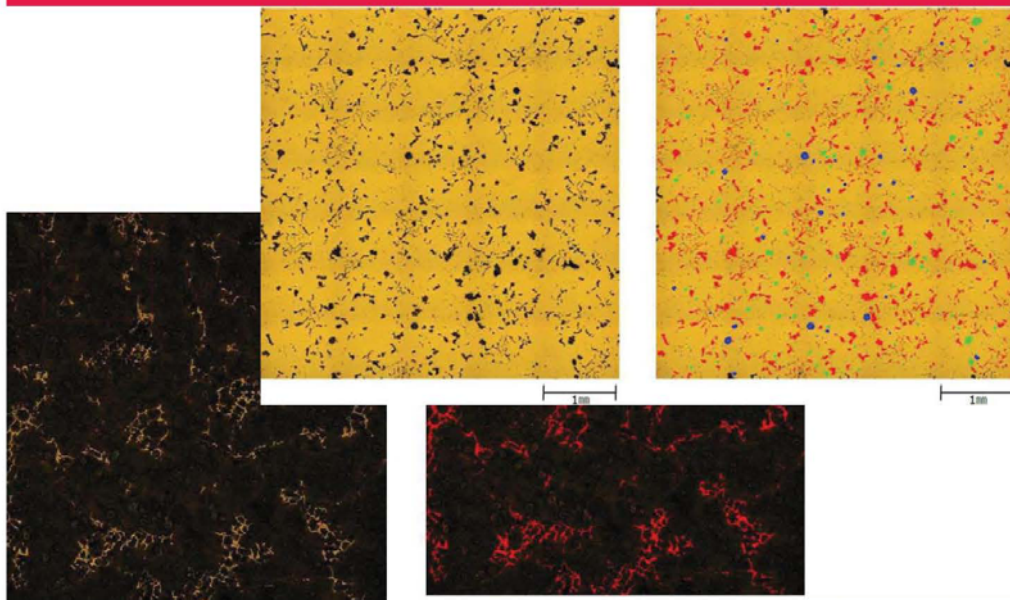
Steen Krogh Jensen

Kvantificering af grafitsstørrelse og -morphologi i støbefejern

18.01.2012

< 37 >

Nodularitet - underleverandører



MAN Diesel & Turbo

Steen Krogh Jensen

Kvantificering af grafitsstørrelse og -morphologi i støbefejern

18.01.2012

< 38 >

Disclaimer



All data provided in this document is non-binding. This data serves informational purposes only and is especially not guaranteed in any way. Depending on the subsequent specific individual projects, the relevant data may be subject to changes and will be assessed and determined individually for each project. This will depend on the particular characteristics of each individual project, especially specific site and operational conditions.

Tak for opmærksomheden!

Materialevalg/Stål fremstilling

Stig Rubæk, Metal-Consult

Materialevalg/Stål fremstilling

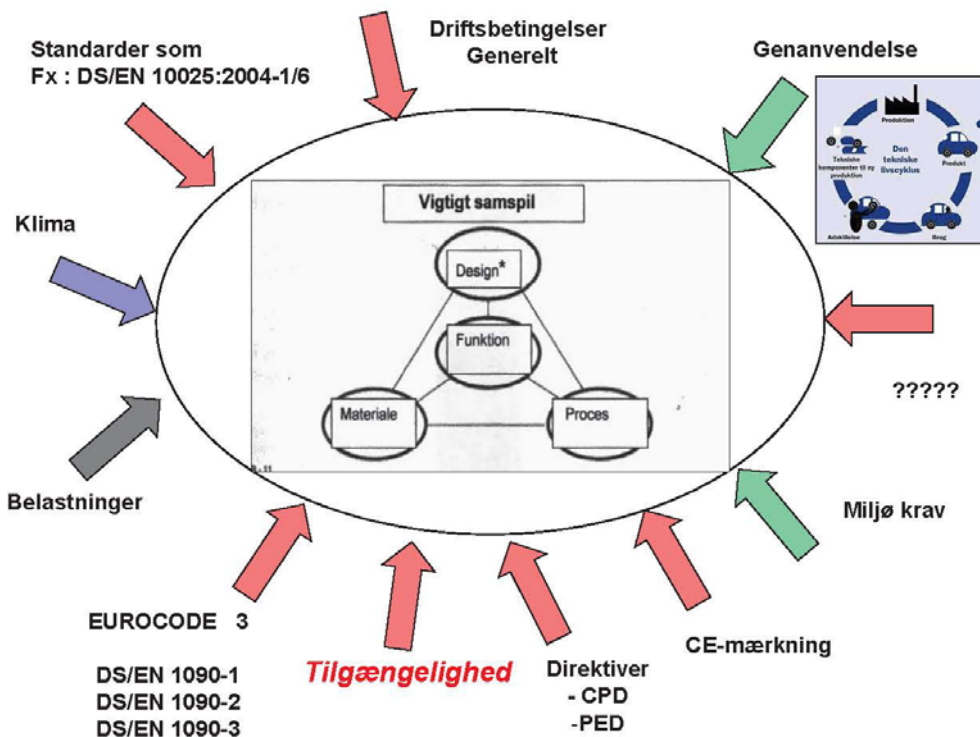
Særligt indlæg ved DMS's Vintermøde 2013

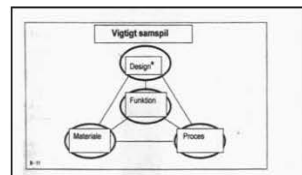
på

Hotel Koldingfjord

16.-18 Januar 2013

Stig Rubæk /Metal-Consult





Materialeenes egenskaber er altid det centrale element ved materialevalg. Eksempler på design-begrænsende egenskaber kan samles i nedenstående skema.

Klasse	Egenskab
General	Pris Densitet (massedyde)
Mekanisk	Elasticitetsmodul (stivhed) Styrke (fx elastiskegrænse) Sævhed Brudstøjhed Dempningskapacitet Udformelsesstyrke
Termisk	Termisk ledningsværdie Specifik varmefyldde Smeltepunkt Glæs temperatur Termisk udvidelseskoefficient Krybereoststand
Sild	Sild-konstant Korrasion/ Oxidation
	Korrasionshastighed



1.2. Material properties

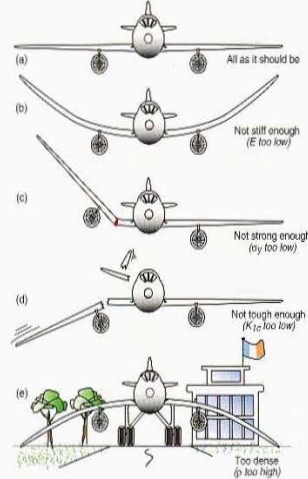
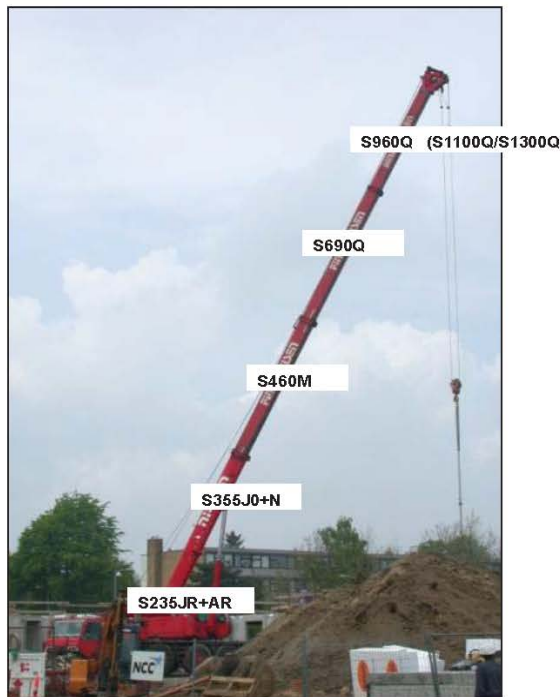


Figure 1.2 Mechanical properties.

DMS



DS/EN 10025



DS/EN 10025 del 1 til 6

Del 1 Generelle tekniske leveringsbetingelser

Del 2 Tekniske leveringsbetingelser for ulegerede konstruktionsstål
(S235 -, S275 -, S355 - og S450- med undergrupperne JR, J0 , J2 og K2,
samt tillægsbetegnelserne +AR, +N og +M (kun lange produkter))

Del 3 Tekniske leveringsbetingelser for (ovn)normaliserede/valsede normaliserede
svejselige finkornskonstruktionsstål
(S275 N/NL, S355N/NL , S420N/NL, S460N/NL)

Del 4 Tekniske leveringsbetingelser for termomekanisk valsede
svejselige finkornskonstruktionsstål
(S275M/ML, S355M/ML, S420M/ML -, S460M/ML)

Del 6 Tekniske leveringsbetingelser for flade produkter af
højstyrke konstruktionsstål i sejhærdet tilstand
(S460Q/QL/QL1, S500Q/QL/QL1, S550Q/QL/QL1, S620Q/QL/QL1, S690Q/QL/QL1,
S890Q/QL/QL1, 960QQL)

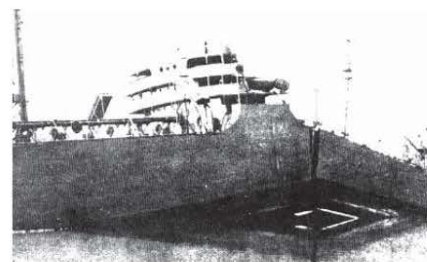
Del 5 Tekniske leveringsbetingelser for konstruktionsstål med forhøjet dimensjons-
korrosionsbestandighed (korrosionstræge stål)
(S235 -W, S355 -WP, S355 -W med undergrupperne JR, J0 , J2 og K2)



DMS

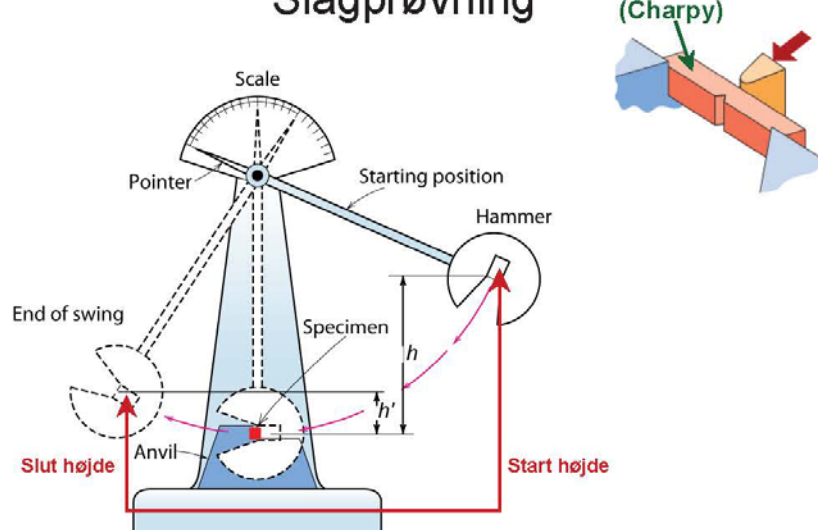
Design Strategi: Hold dig over DBTT!

- Pre-WWII: Titanic
- WWII: Liberty skibe



- Problem: Anvendelse af ståltyper med
omslagstemperatur omkring rumtemperatur.

Slagprøvning



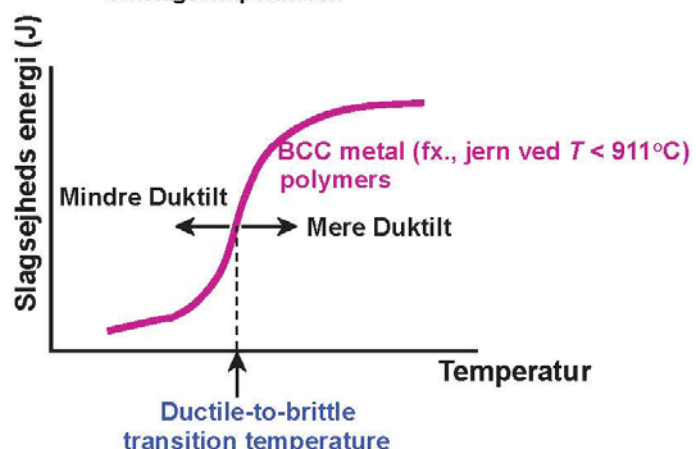
7

DMS

Omslags-Temperaturen

- Ductile-to-Brittle Transition Temperature (DBTT)...

= Omslagstemperaturen



8

$$\text{CEV} (\%) = \text{C} + \text{Mn}/6 + (\text{Cr} + \text{Mo} + \text{V})/5 + (\text{Ni} + \text{Cu})/15$$

DS/EN 10025-2:2004						
		Tabel 6 – Maksimalt CEV baseret på chargeanalysen*				
Betragsnr. og CR 10290	Betragsnr. EN 10027-1 og CR 10290	Betragsnr. EN 10027-2	Densoyle- metode +	Maks. CEV / % for nominel produkttykkelse i mm		
				≤ 30	> 30 ≤ 40	> 40 ≤ 150
S275M	1.0038		FN	0,35	0,35	0,40
S275NL	1.0114		FF	0,35	0,35	0,40
S235J2	1.0117			0,35	0,35	0,40
S275J2	1.0143		FN	0,40	0,40	0,44
S275J2	1.0143		FF	0,40	0,40	0,44
S355J2	1.0045		FN	0,45	0,47	0,49*
S355J2	1.0053		FN	0,45	0,47	0,49*
S355J2	1.0577		FF	0,45	0,47	0,49*
S355J2	1.0596		FF	0,45	0,47	0,49*
S355J2	1.0599			0,47	0,49	0,49
S355J2	1.0599			-	-	-

* For valgtilt forsegling af elementer, der påvirker CEV, se 7.2.4 og 7.3.8.

** PN = benyttes når ikke tilstød. FF = fuldt benyttet stål fra 6.2.2.

† For lange producenter gælder maksimalt CEV på 0,54.

‡ Gælder kun for lange producenter.

DS/EN 10025-4:2004						
		Tabel 4 – Maksimalt CEV baseret på chargeanalysen for termomekanisk valset stål*				
Betragsnr. EN 10027-1 og CR 10290	Betragsnr. EN 10027-2	Maks. CEV / % for nominel produkttykkelse i mm				
		≤ 16	> 16 ≤ 40	> 40 ≤ 63	> 63 ≤ 120	> 120 ≤ 150
S275M	1.8818	0,34	0,34	0,35	0,38	0,38
S275ML	1.8819					
S355M	1.8823	0,39	0,39	0,40	0,45	0,45
S355ML	1.8834					
S420M	1.8825					
S420ML	1.8836					
S460M	1.8827					
S460ML	1.8838	0,45	0,46	0,47	0,48	0,48

* For valgtilt forsegling af elementer, der påvirker CEV, se 7.2.3.

† Tallene gælder kun for lange producenter.

DS/EN 10025-3:2004						
		Tabel 4 – Maksimalt CEV baseret på chargeanalysen for overnormaliseret stål				
Betragsnr. EN 10027-1 og CR 10290	Betragsnr. EN 10027-2	Betragsnr. EN 10027-3	Betragsnr. EN 10027-4	Maks. CEV / % for nominel produkttykkelse i mm		
				≤ 63	> 63 ≤ 100	> 100 ≤ 250
S275N	1.0490*		0,40	0,40	0,42	
S275NL*	1.0491*					
S355N	1.0540*		0,43	0,45	0,45	
S355NHL*	1.0540*					
S420N	1.0902		0,48	0,50	0,52	
S420NL	1.0912					
S460N	1.0901		0,53	0,54	0,55	
S460NL	1.0903					

* For valgtilt forsegling af elementer, der påvirker CEV, se 7.2.3.

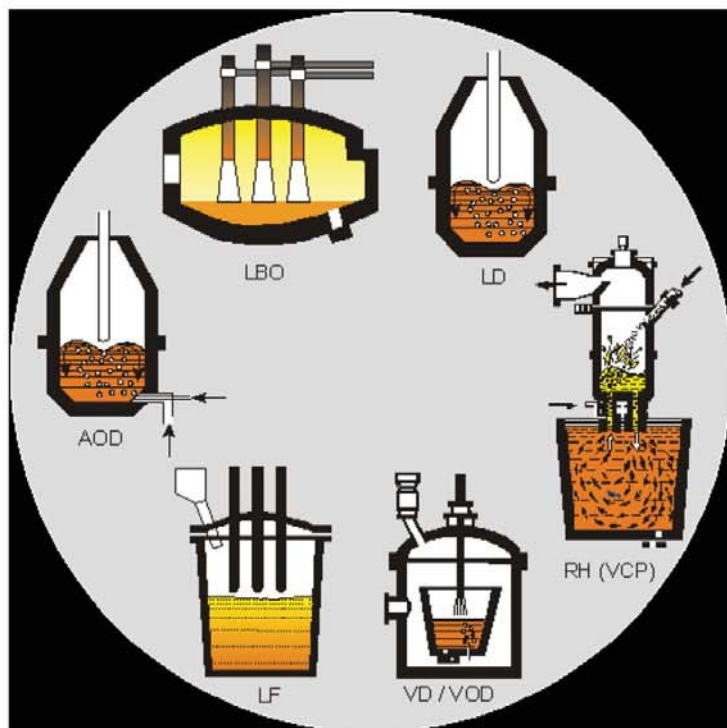
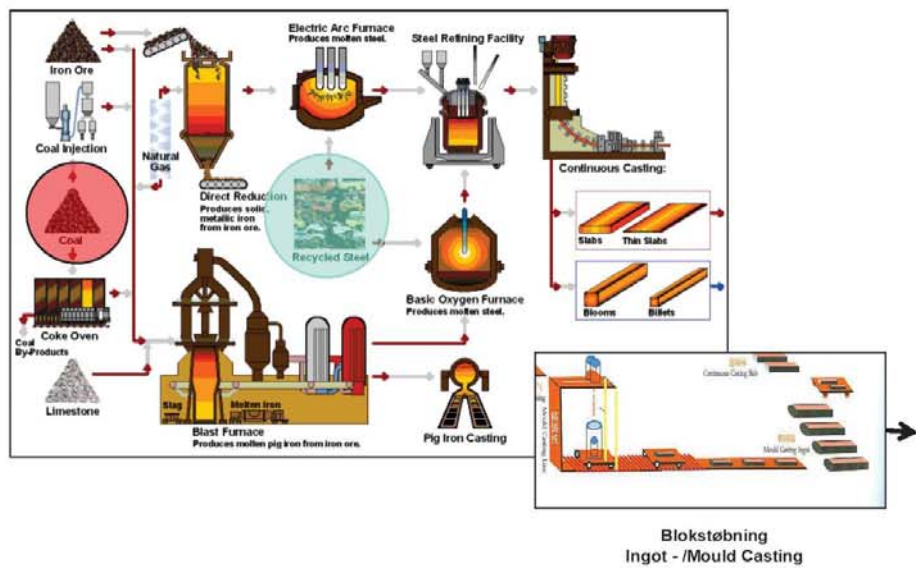
DS/EN 10025-6:2004						
		Tabel 4 – Maksimalt CEV baseret på chargeanalysen for sajhævet stål*				
Betragsnr. EN 10027-1 og CR 10290	Betragsnr. EN 10027-2	Maks. CEV / % for nominel produkttykkelse i mm				
		≤ 50	> 50 ≤ 100	> 100 ≤ 150	> 150	
S460Q	1.8900					
S460QL	1.8906					
S460QOL	1.8911					
S500Q	1.8904					
S500QL	1.8909					
S500QOL	1.8909					
S550Q	1.8904					
S550QL	1.8925	0,65	0,77	0,83		
S550QOL	1.8966					
S620Q	1.8927					
S620QL	1.8967					
S620QOL	1.8967					
S690Q	1.8931					
S690QL	1.8938					
S690QOL	1.8968					
S890Q	1.8940					
S890QL	1.8953					
S890QOL	1.8925					
S900Q	1.8941	0,82	-	-		
S900QL	1.8933					

* For valgtilt forsegling af elementer, der påvirker CEV, se 7.2.3.

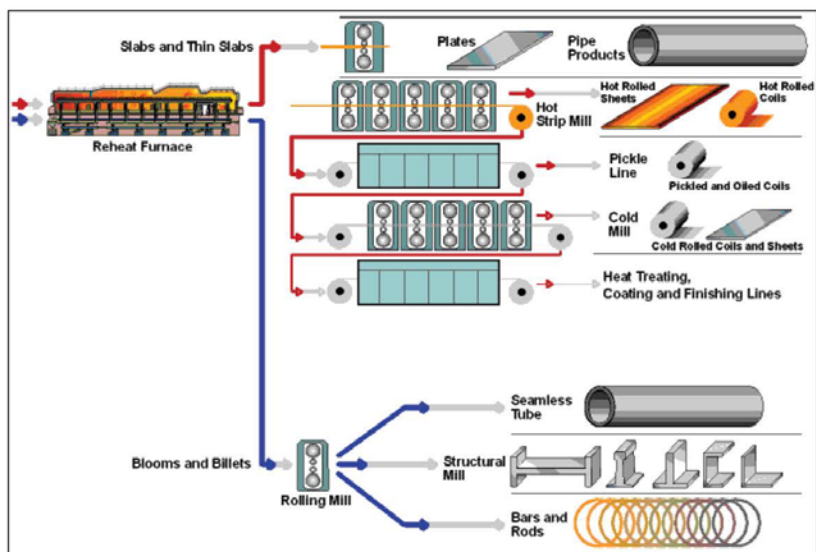
DMS

Fremstilling af svejselige konstruktionsstål med udgangspunkt i :

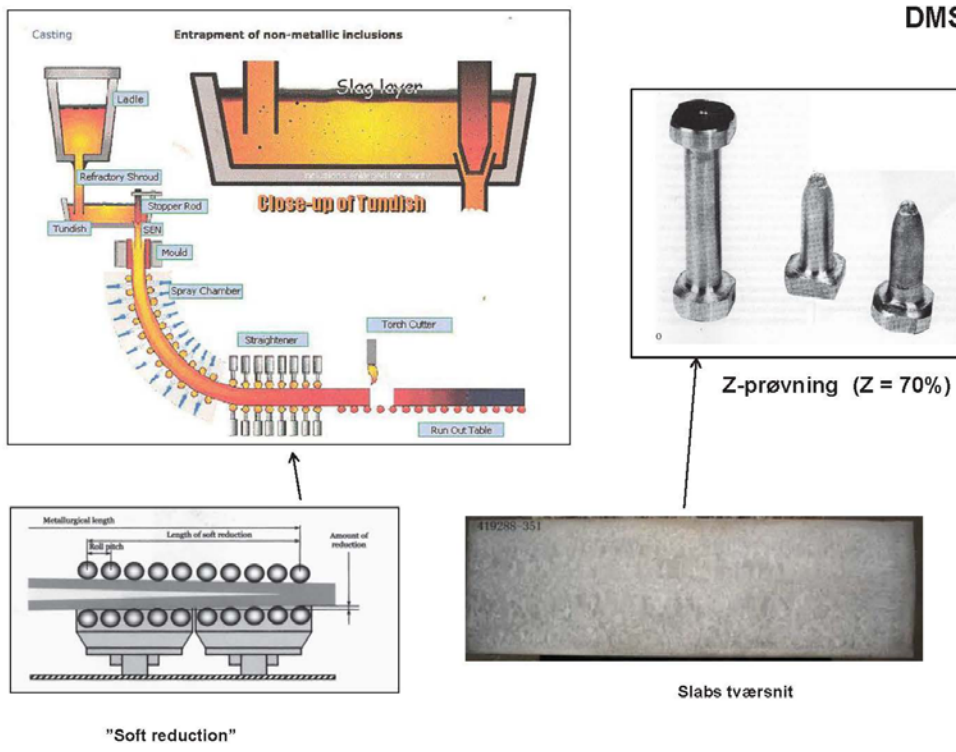
EN 10025:2004 del 1-6

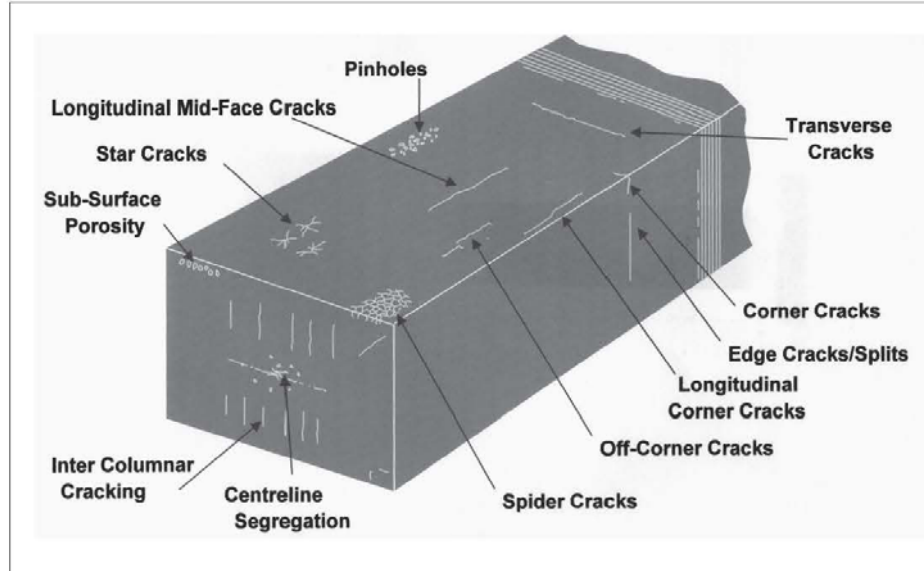


DMS

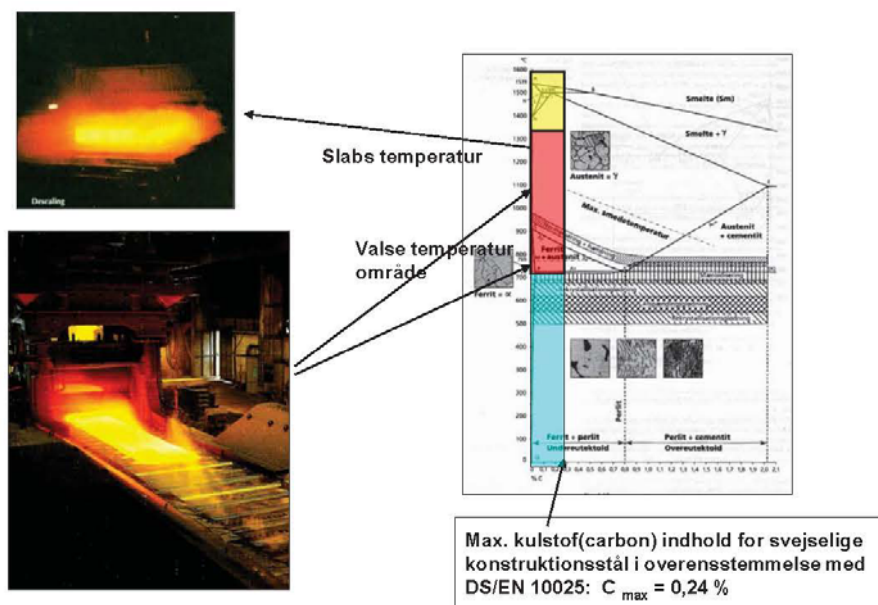


DMS

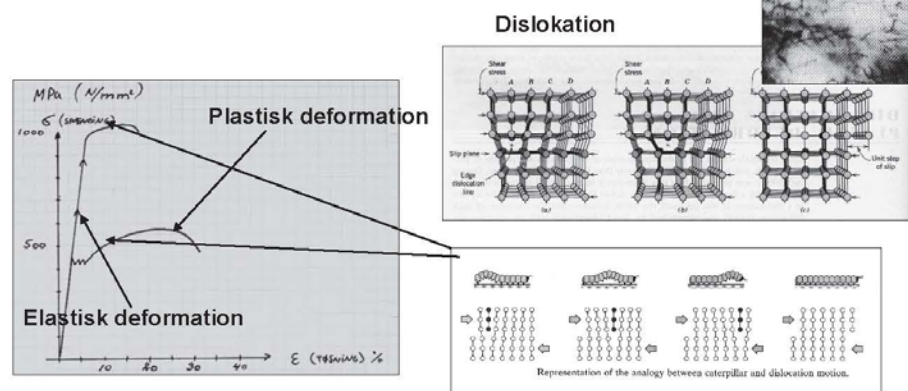




Varmvalsning



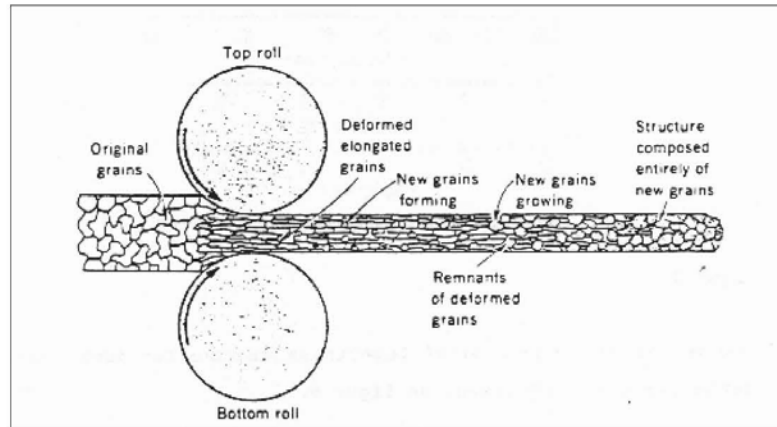
Styrkeøgning



Dislokationbarierer/-bremser → udvidelse af det elastiske område → Styrkeøgning:

- Fremmedatomer (fx C og Mn)
- Korngrænser (ved kornforfining)
- Dislokationsforøgelse (deformationshærdning)
- Fremmede faser (ved modningshærdning)

DMS



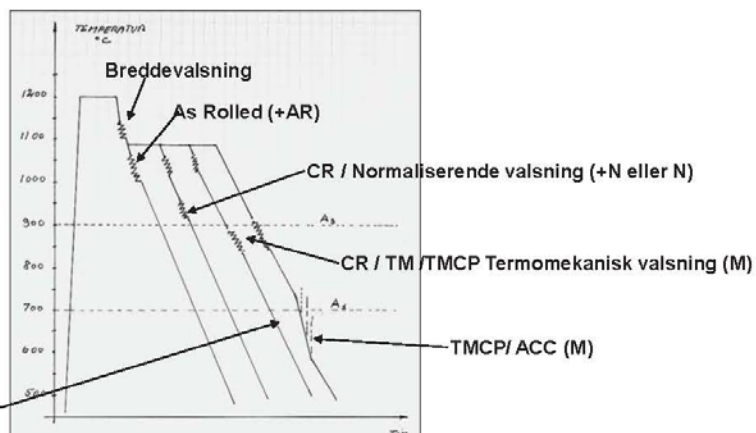
Valseprocesser



Kvarto- valseværk

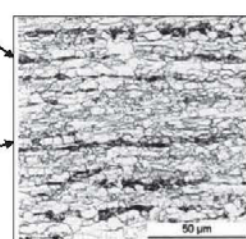
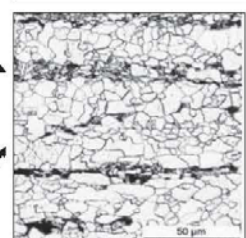
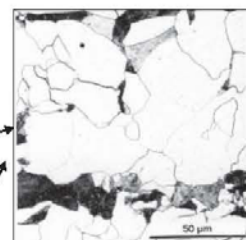
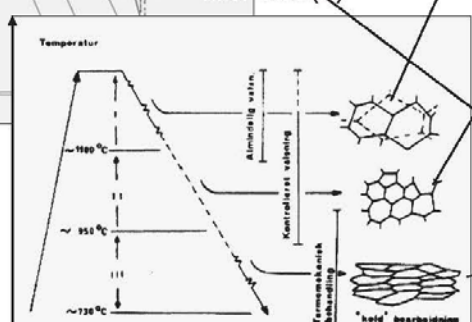
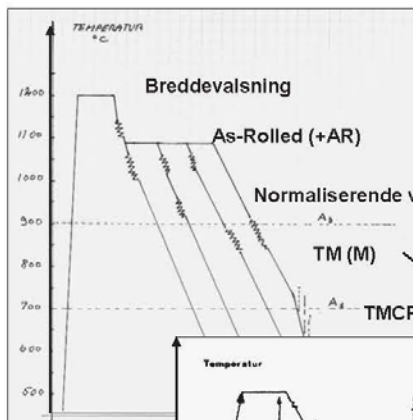


ACC-udstyr



CR-valsning = Controlled Rolling

Valseprocesser



Egenskaber frembragt ved en valseproces.

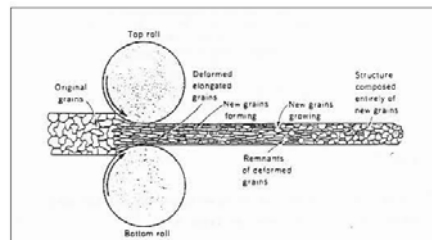
Varmvalsning

I) Normal varmvalsning (Leveringstilstand as-rolled)

En evt. breddevalsning udføres umiddelbart efter, at slabsen/blokken er udtaget af slabs/blokovnen. Slabs/bloktemperaturen er typisk 1250 °C. Herefter vendes den breddevalseslade slabs/blok, og længdevalsningen påbegyndes umiddelbart.

Længderetningen på pladen omtales som "hovedvalsretningen"

Det varmvalsede ståls struktur er relativt grovkornet (ASTM-kornstørrelse omkring 5-6, alt efter pladedimension).



II) Kontrolleret (styret) valsning (CR-valsning = Controlled Rolling)

Siden 30'erne er der udviklet kontrollerede (styrede) valseprocesser, som går under fællesbetegnelsen »Kontrolleret valsning«, forkortet CR (Controlled Rolling).

CR-processerne omfatter en række processer, der som fælleskendtegn har det ene, at de sidste 20 %'s deformation foregår under nøje temperaturkontrol, dvs. i et bestemt temperaturinterval.

II.a) Normaliserende valsning

Valsenningen udføres næsten som beskrevet under varmvalsning, men de sidste stik (tykkelsesreduktionen) udføres i det temperaturinterval, hvor stålet normalt (ovn)normaliseres, altså lige over A_3 .

De resulterende mekaniske egenskaber skal modsvare det (ovn)normaliserede produkt. Det er væsentligt at påpege, at stålstandarderne ikke skelner imellem de to processer. Dette betyder derfor, at en forbruger ikke i certifikatet, uanset type, kan få oplyst, hvilken type normaliseret stål forbrugeren har modtaget.

II.b) TMCP-stål (Thermo Mechanical controlled Process)

TMCP-valsning dækker over et antal forskellige valseprocesser.

For de fleste af disse processer findes flere betegnelser, hvilket fra et forbrugersynspunkt kan være meget forvirrende. Det vil derfor altid i tvivstilfælde være en god idé at gennemlæse specifikationen efter standarden for det aktuelle stål.

II.b.1) TM-stål (Thermo Mechanical Rolling)

Startvalsetemperaturen er normalt, men ikke nødvendigvis, en del lavere end for varmvalsning. Endvidere udføres slutvalsningen ved så lave temperaturer, at austenitten ikke rekristalliserer, dvs. ved en temperatur lige over A_3 eller i tofaseområdet imellem A_3/A_1 , og der dannes derfor en finkornet struktur.

I sidstnævnte tilfælde kan de højeste styrkeegenskaber opnås, idet der lidt populært sker en form for »kolddeformation« af de enkelte korn, som sammen med den finkornede struktur giver en mærkbart styrkeforøgelse, samt en god sejhed.

II.b.2) ACC-stål (Accelerated Controlled Cooling)

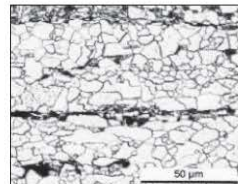
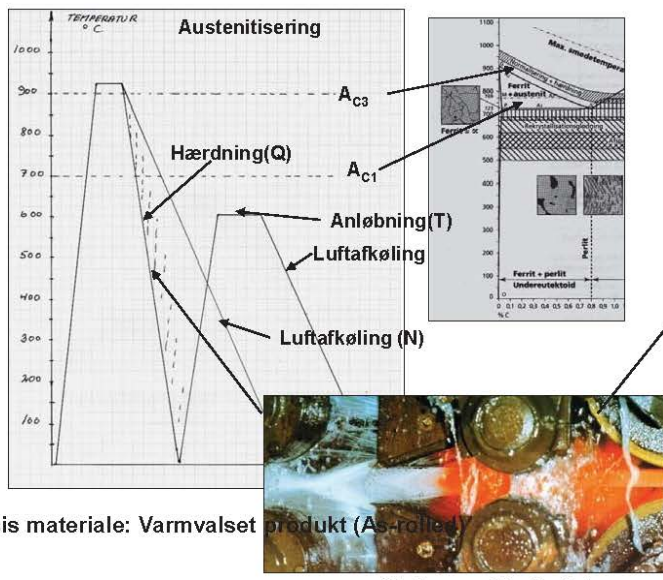
En japansk udviklet proces til fremstilling af højstyrkestål med særliges gode egenskaber, hvad angår lav kulstofekvivalent (CEV), omslagstemperatur mm.

Udgangspunktet er et normaliseret valset/TM-stål. Den endnu varme plade føres igennem et langt køleanlæg (typisk 40-50 m), hvor pladen afkøles størt fra ca. 800 °C til ca. 600 °C, alt efter ønskede egenskaber. Derefter afkøling i luft.

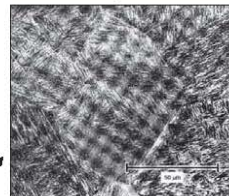
Strukturen er ferritisk/finperlitisk/bainitisk

Varmebehandling

(Ovn) Normalisering og sejhærdning



Normalisering (N)
Fin kornet perlit/ferrit



Hærdet (Q)
Martensit



Sejhærdet (Q/T)
Anløbet martensit

Egenskaber frembragt ved varmebehandling

DMS

I) (Ovn) Normalisering

Processen udføres ved at opvarme emnet til temperaturen over A_3 -linjen (til austenitorrådet) i en ovn. Efter en kort holdetid, afkøling i luft.

Den opnåede struktur er finkornet ferritskifflig (ASTM-komstørrelse 9-11, alt efter pladedimension).

Man opnår herved en forbedring af flydespændingen såvel som en sækning af omslagstemperaturen (en forbedring af slagsejhedsegenskaberne).

De opnåede egenskaber er økvivalente med egenskaber opnået ved normaliserende valsning.

II) Q/T-stål (Quench/Tempering = (Martensit)hærdning/anløbning) På dansk er betegnelsen sejhærdning.

Som den engelske forkortelse antyder, er der her tale om to varmebehandlingsprocesser. En hærdning til martensit (quenching) efterfulgt af en anløbning (tempering).

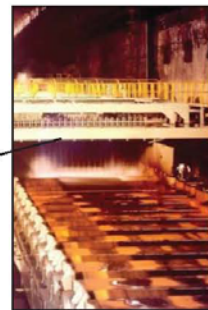
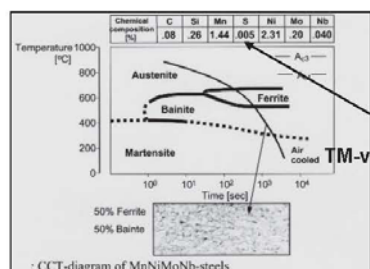
Hærdningen udføres ved at opvarme et varmvalset produkt til en temperatur over A_3 -linjen (til austenitorrådet). Efter en kort holdetid sendes pladen igennem et hærdeanlæg, hvor selve brat-kølningen og dermed martensitdannelsen finder sted.

Vær opmærksom på, at martenthærdheden udelukkende er et spørgsmål om kulstofindholdet, hvilket indebærer, at stærkere stål har et højere kulstof indhold.

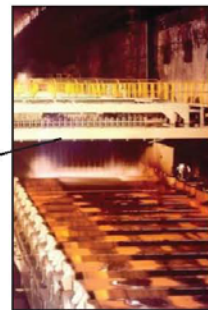
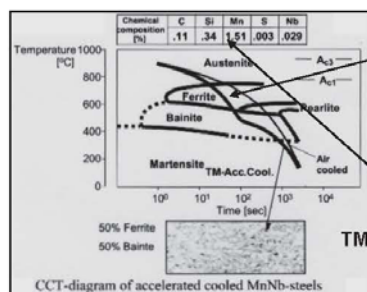
Anløbningen udføres fx i en normaliseringsovn, og temperaturintervallet mellem 600 °C og 660 °C. Forbrugeren bør være opmærksom på, at producenten normalt angiver anløbningstemperaturen i certifikatet, idet en overskridelse af denne temperatur fx i forbindelse med en varmbearbejdning kan føre til en reduktion af stålets styrkeegenskaber.

DMS

ACC-treatment ("alloying with water") Accelerated Continuous/Controlled Cooling



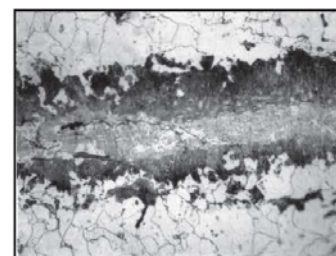
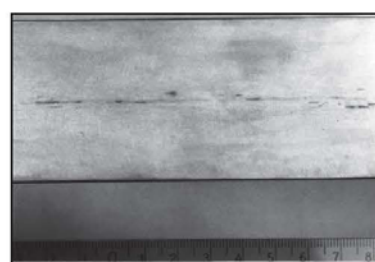
DS/EN 10025-4-S420M



DS/EN 10025-4-S460ML

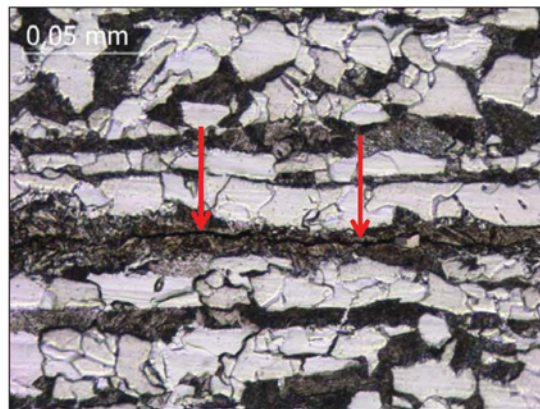
Hydrogen inducedere revner (ca. 1980)
Ståltype : St 52-3 Svølv : S 0 0,008 % Hydrogen : H < 0,0010 % ?

DMS



Hydrogen inducerede revner (ca. 2010)

Ståltype : S 355 J2 Svovl : S 0 0,002 % Hydrogen : H < 0,0002 % ?



Revnen løber i det perlitiske bånd i den
sejrede zone i pladens center

Blokstøbning

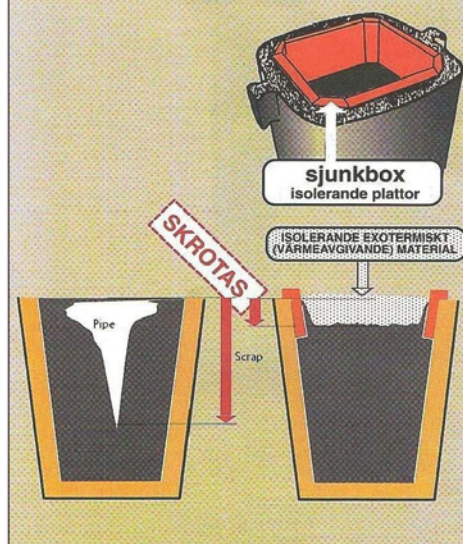
Ingot Casting

- o Production of material for rolling of e.g rod, pipe, wire or sheet metal .
- o The Mould:
 - o Usually made of cast iron.
 - o Different shapes (conical)
- o Metoder:
 - Downhill casting.
 - Centering is very important
 - problems : splashes, waves, oxidation, low productivity/slow process
 - Uphill casting
 - More preparation steps
 - Higher productivity
 - Higher quality.

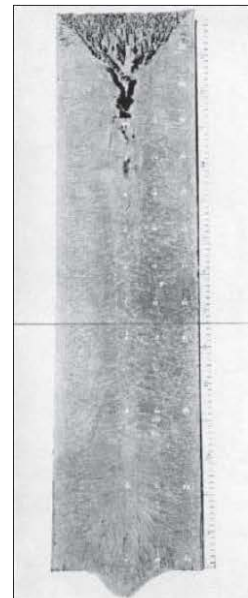
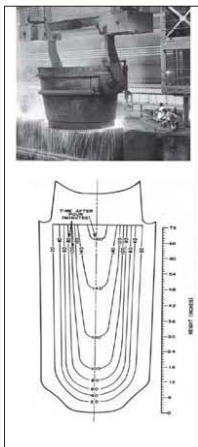


DMS

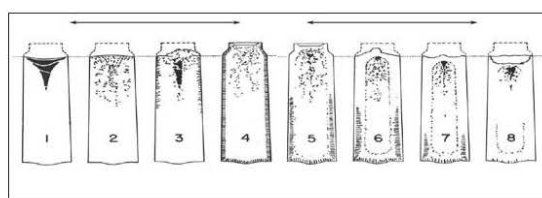
MED OCH UTAN SJUNKBOX



DMS



Makrostruktur



Moderne blokstøbning med vandkølet kobberkokille



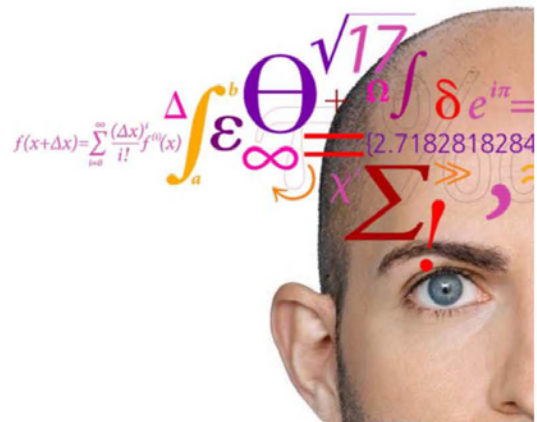
Varmebehandling og karakterisering af nye udskilningshærdbare superlegeringer

Uffe Bihlet, MAN og DTU Mekanik

Varmebehandling og karakterisering af nye udskilningshærdbare superlegeringer

DMS Vintermøde 2013

Uffe D. Bihlet
ErhvervsPhD studerende
MAN Diesel & Turbo
DTU MEK



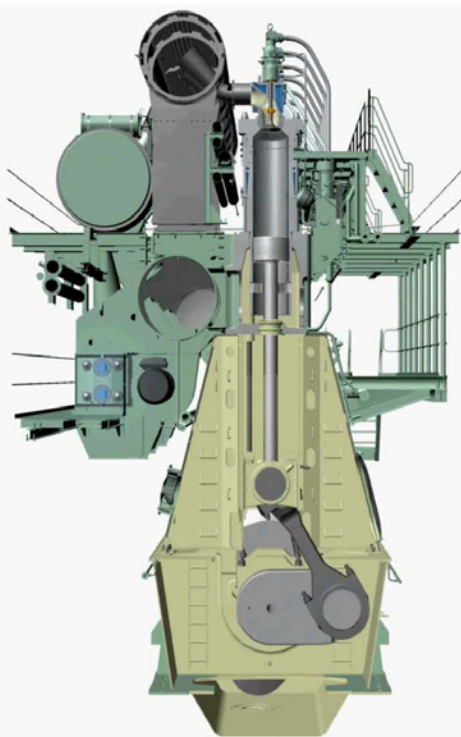
Agenda

- To-takts motoren og udstødningsventilen
- Udkilningshærdning i Inconel 718
- Ny legering
- Verificering af hærdningsmekanismen i ny legering
 - Røngtendiffraktion (XRD)
 - Focused Ion Beam Imaging (FIB)
 - TEM
- Wrap-up



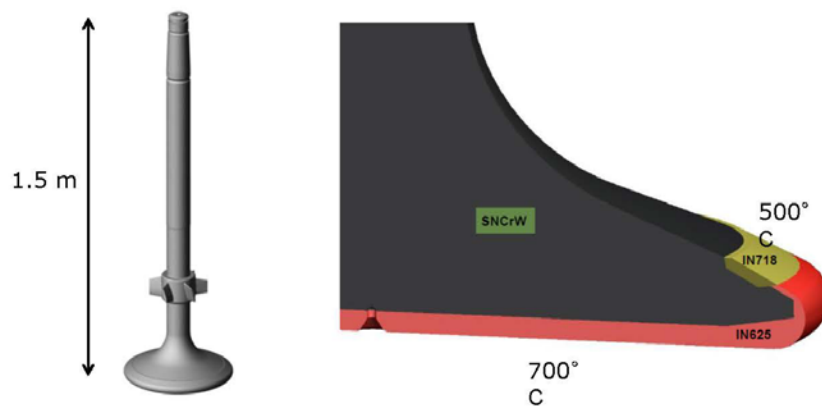
3

4.05.2013



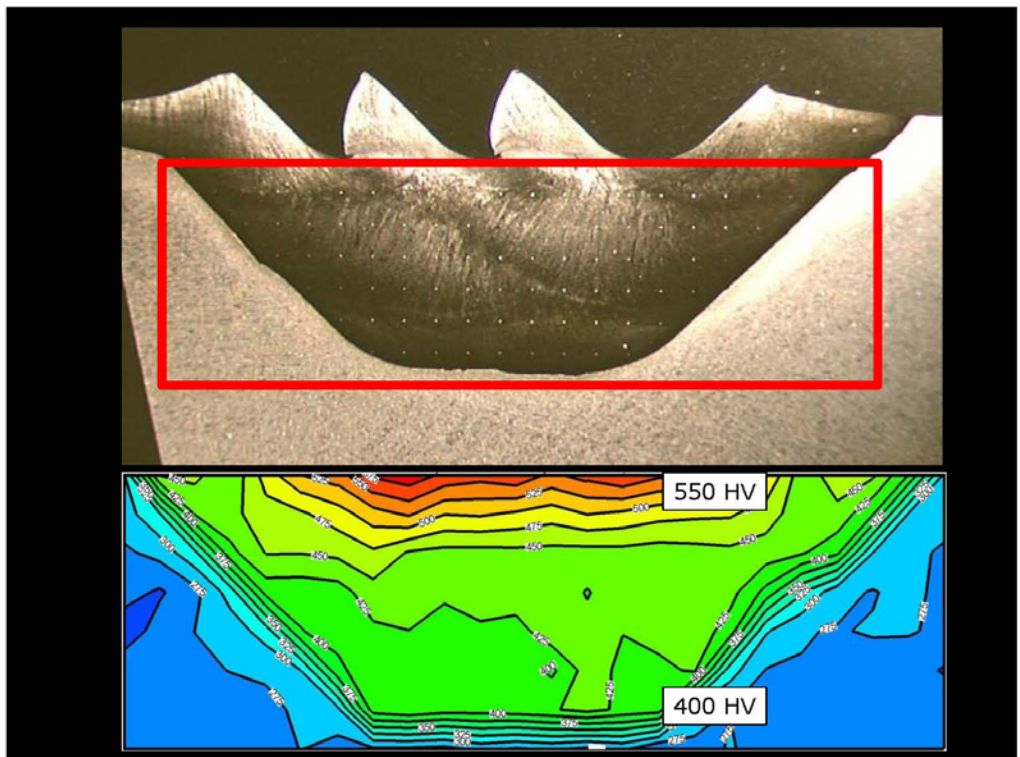
Ventilspindlen

Legering	Cr	Nb	Ti	Al	Fe	Mo	Ni	Bal
IN718	19	5	0.9	0.5	18	3		

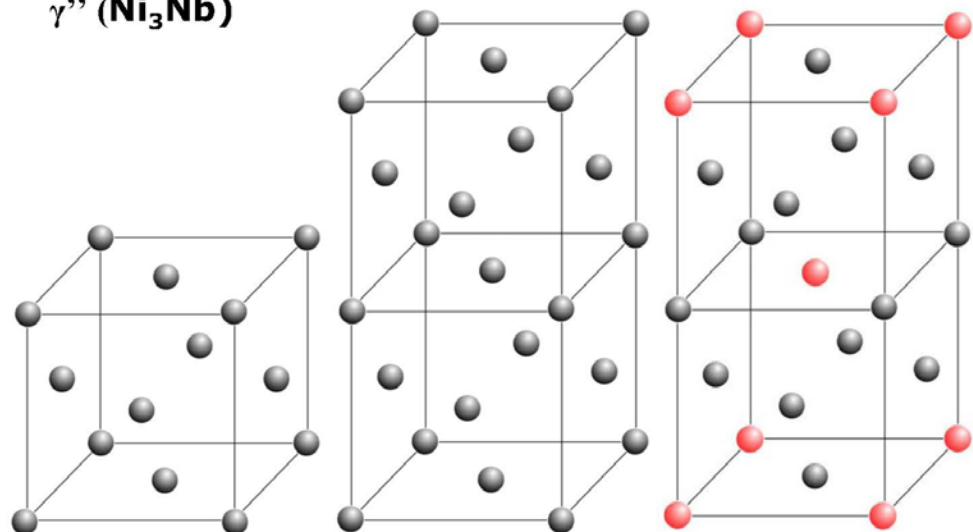


4

24.05.2013



γ'' (Ni_3Nb)



7

24.05.2013

Partikelstørrelse: 10-20 nm

200 nm

Rao et al, 2003

Agenda

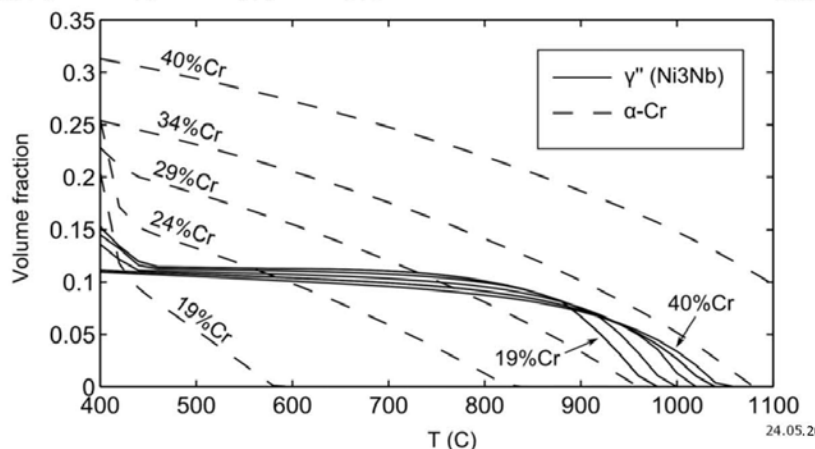
- To-taks motoren og udstødningsventilen
- Udskilningshærdning i Inconel 718
- Ny legering
- Verificering af hærdningsmekanismen i ny legering
 - Røngtendiffraktion (XRD)
 - Focused Ion Beam Imaging (FIB)
 - TEM
- Wrap-up

9

24.05.2013

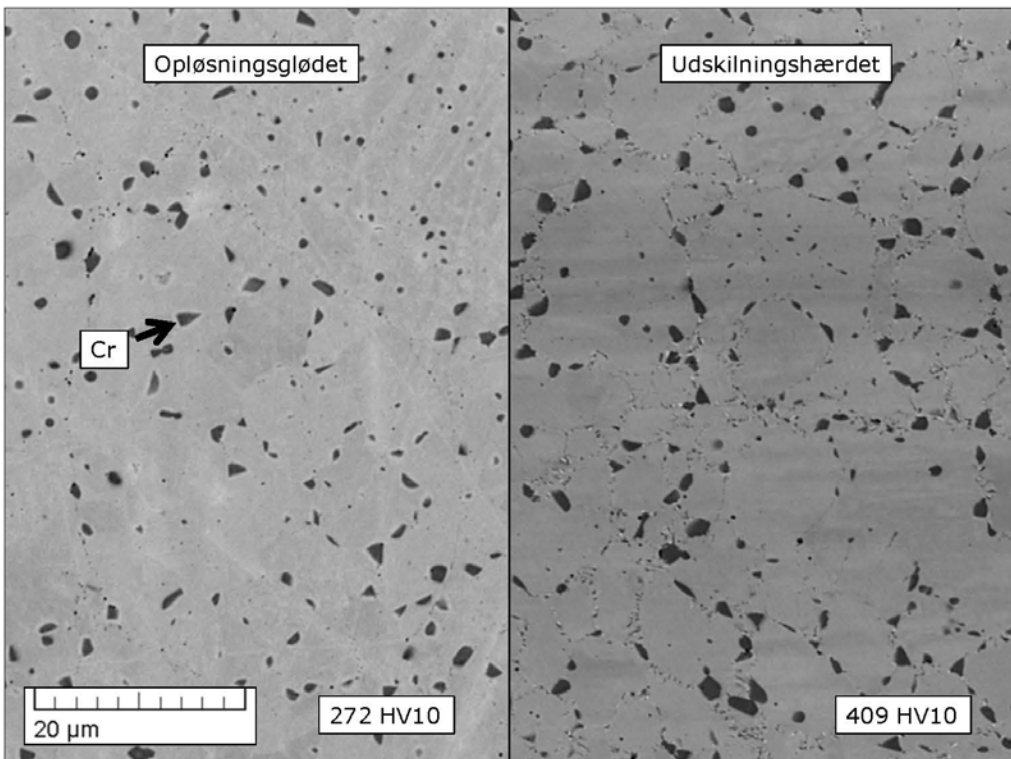
Fra Inconel 718 -> ?

Legering	Cr	Nb	Ti	Al	Fe	Mo	Ni
IN718	19	5	0.9	0.5	18	3	Bal
No. 6	40	3.5	0.5	-	-	-	Bal



10

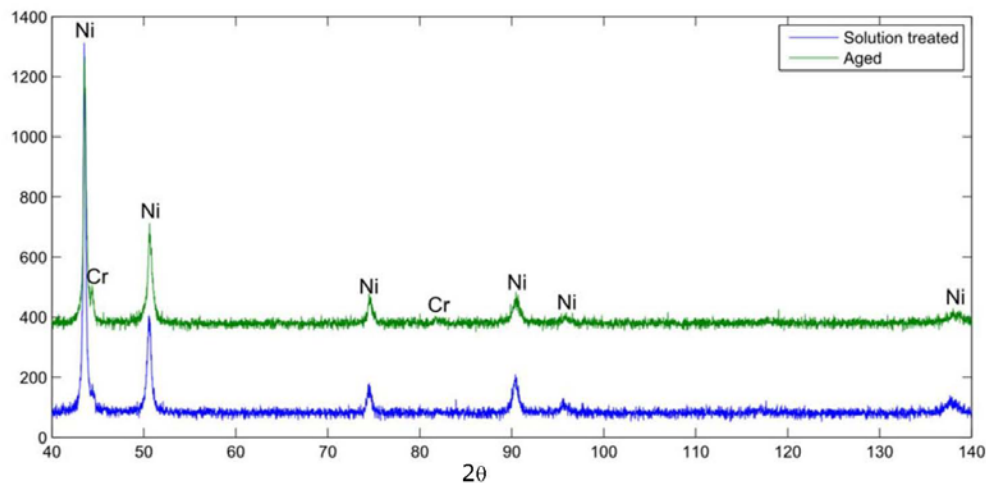
24.05.2013



Agenda

- To-takts motoren og udstødningsventilen
- Udskilningshærdning i Inconel 718
- Ny legering
- Verificering af hærdningsmekanismen i ny legering
 - Røngtendiffraktion (XRD)
 - Focused Ion Beam Imaging (FIB)
 - TEM
- Wrap-up

Røngtendiffraktion (XRD)



13

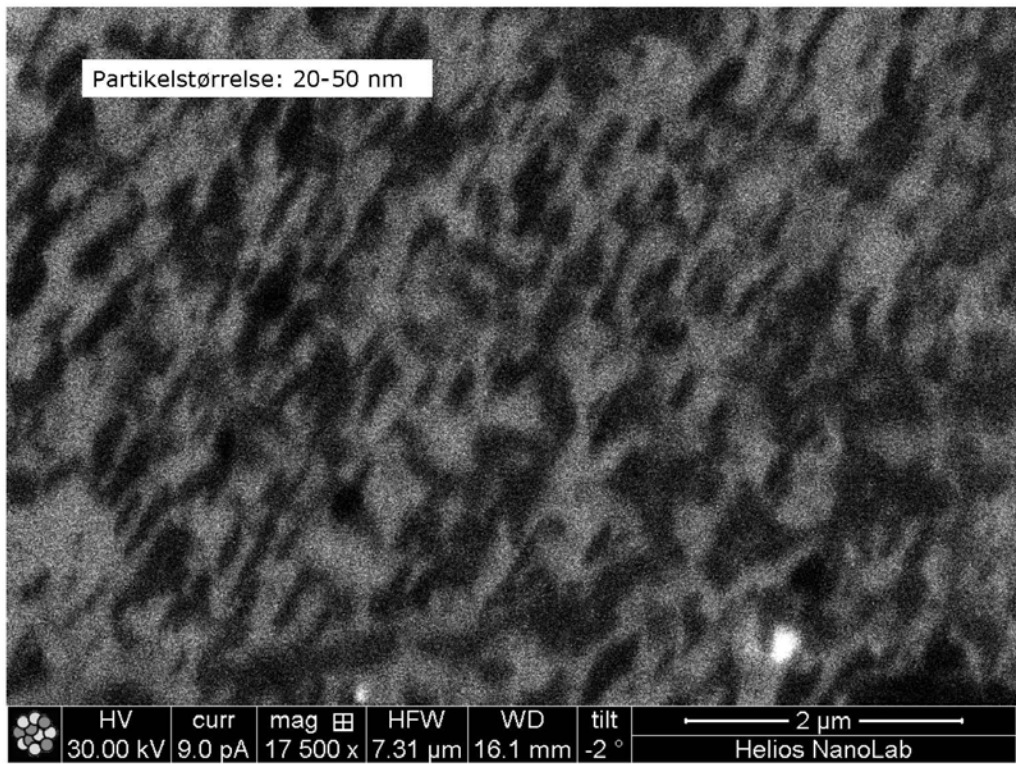
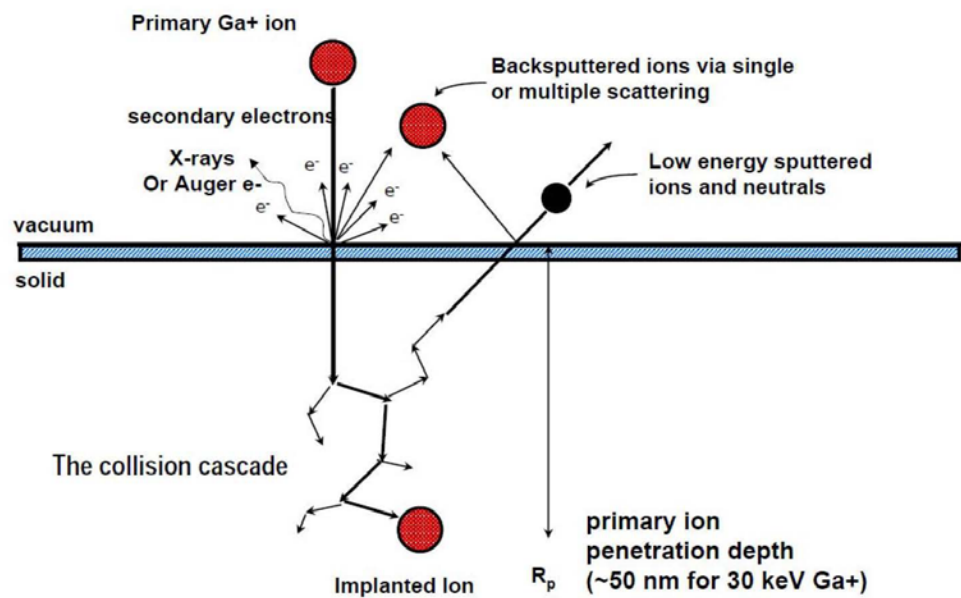
24.05.2013

Agenda

- To-takts motoren og udstødningsventilen
- Udskilningshærdning i Inconel 718
- Ny legering
- Verificering af hærdningsmekanismen i ny legering
 - Røngtendiffraktion (XRD)
 - Focused Ion Beam Imaging (FIB)
 - TEM
- Wrap-up

14

24.05.2013

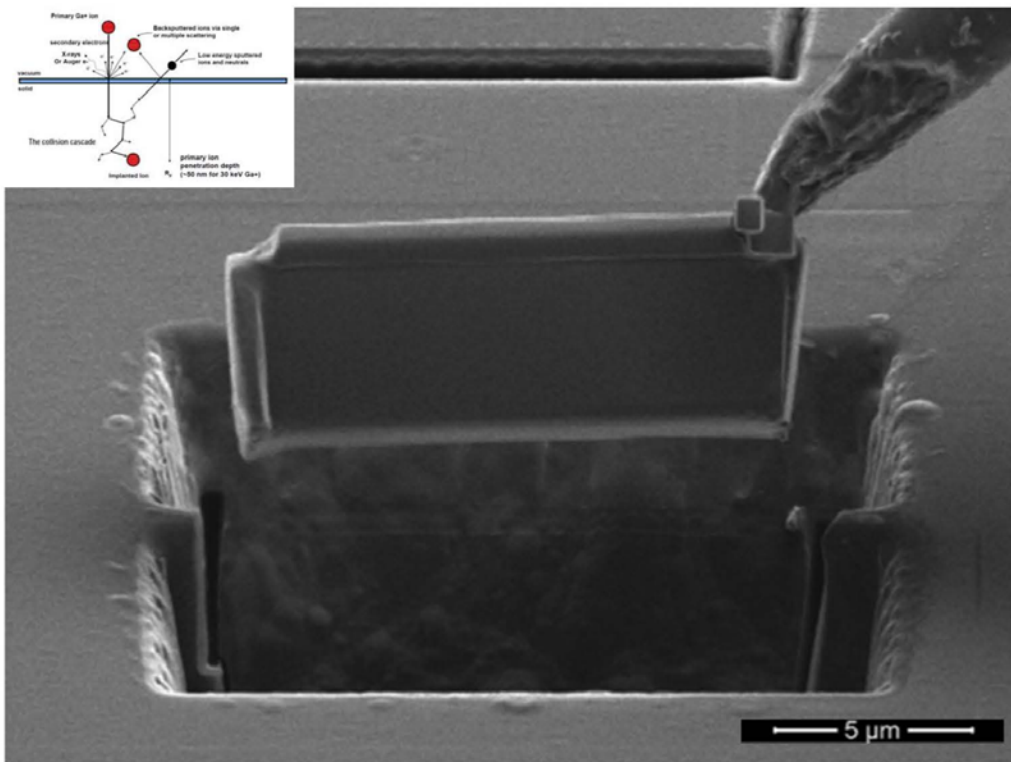


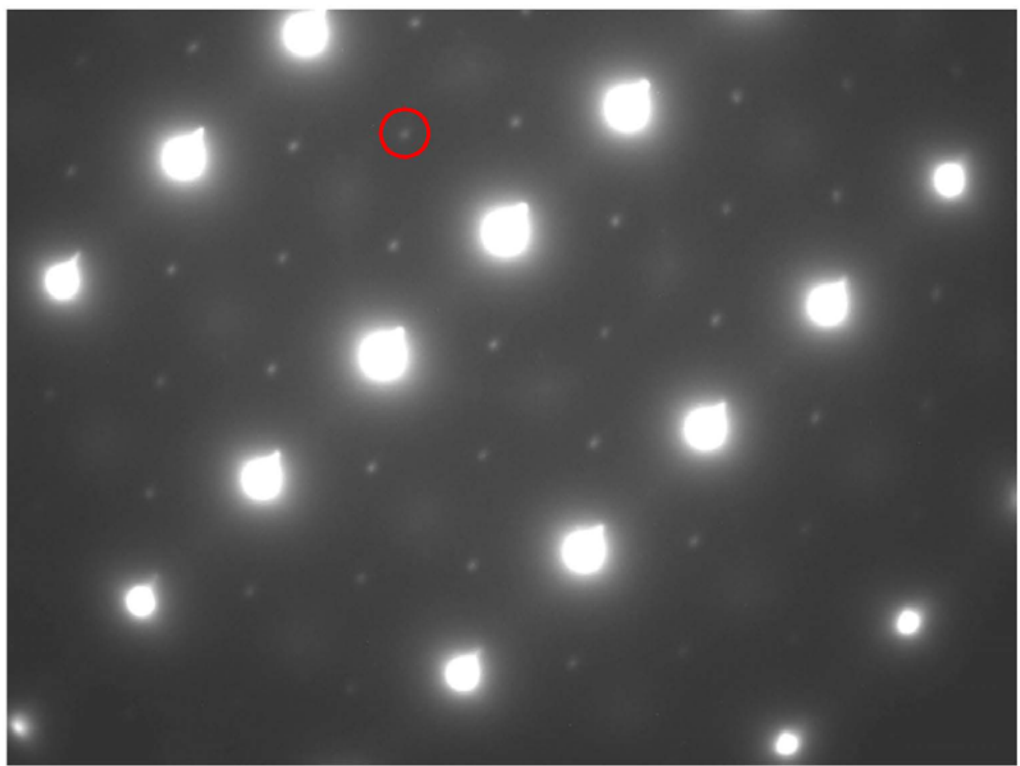
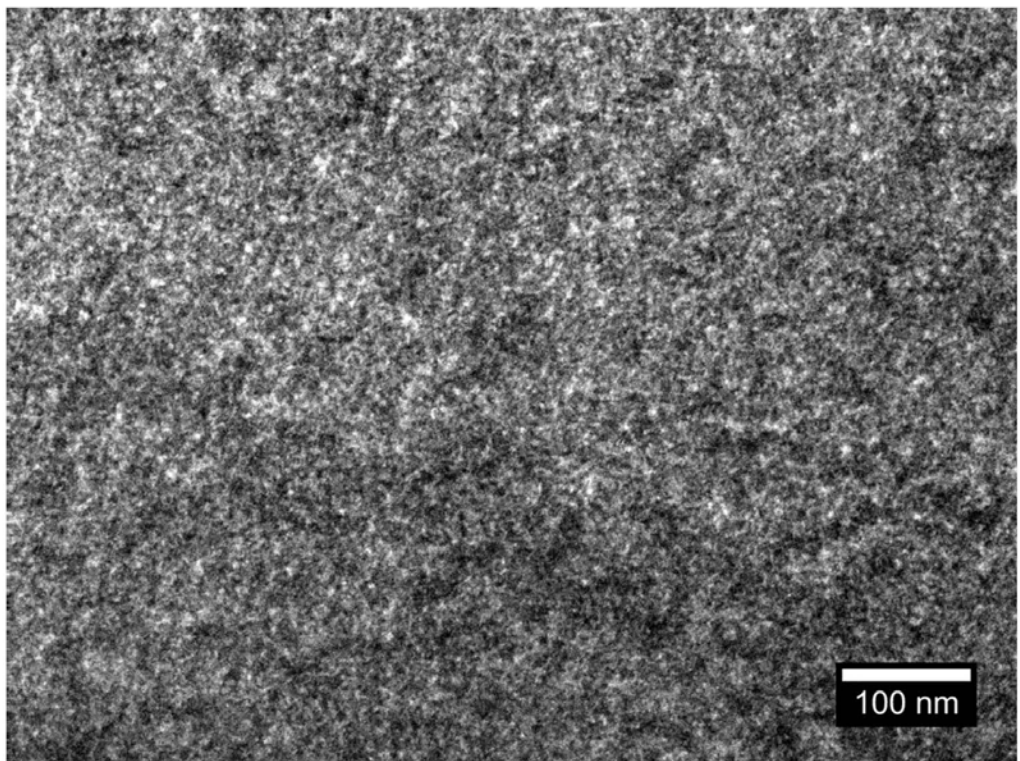
Agenda

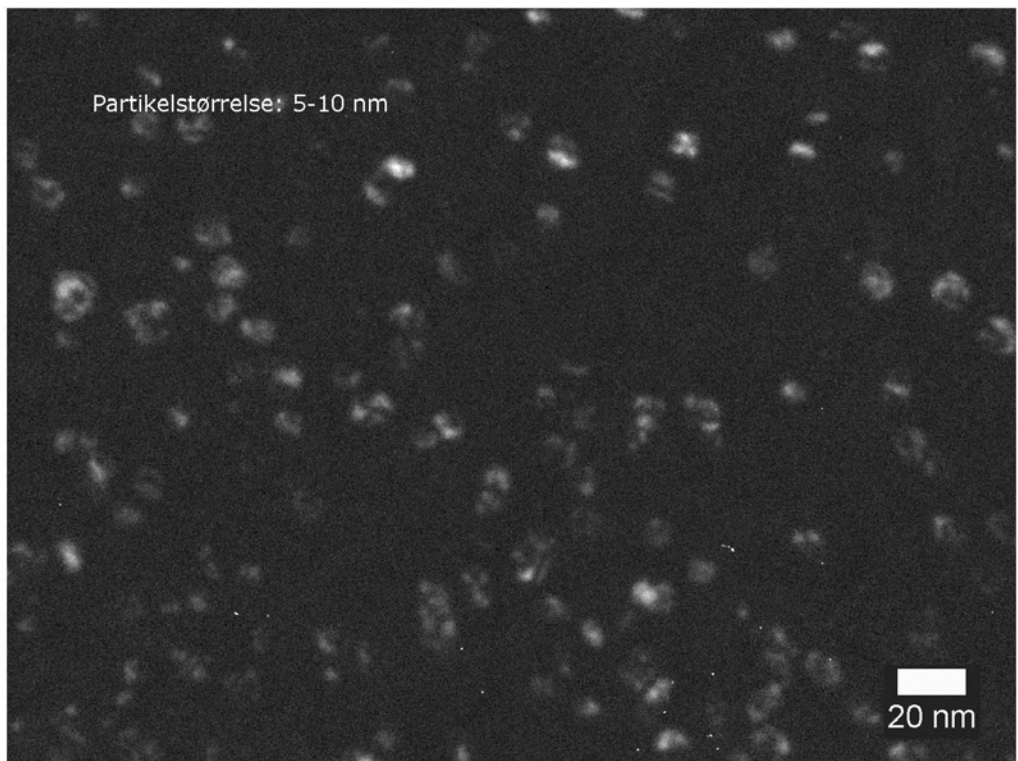
- To-taks motoren og udstødningsventilen
- Udkilningshærdning i Inconel 718
- Ny legering
- Verificering af hærdningsmekanismen i ny legering
 - Røngtendiffraktion (XRD)
 - Focused Ion Beam Imaging (FIB)
 - TEM
- Wrap-up

17

24.05.2013







Agenda

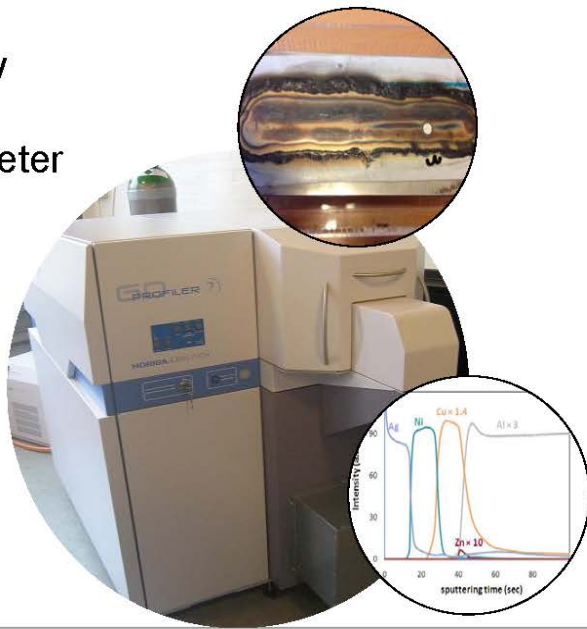
- To-takts motoren og udstødningsventilen
- Udskilningshærdning i Inconel 718
- Ny legering
- Verificering af hærdningsmekanismen i ny legering
 - Røngtendiffraktion (XRD)
 - Focused Ion Beam Imaging (FIB)
 - TEM
- Wrap-up

GD-OES applications

Io Mizushima, IPU

Anvendelse af Glow Discharge Optical Emission Spectrometer (GD-OES)

Io Mizushima
IPU



IPU

IPU: A dedicated on-campus innovation team

Side 2

- A non-profit organisation at the TU of Denmark
- Research and development projects on contract
- Commercialisation of ideas, innovations, and patents
- 50 full-time staff
- 70+ associated DTU staff
- Co-location with DTU colleagues on campus
- Turnover: ~ 6 mill EUR/yr



... since 1956

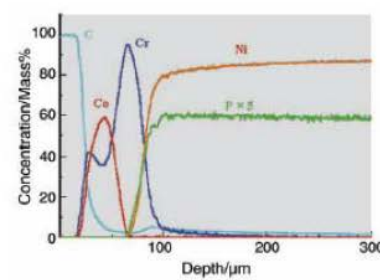
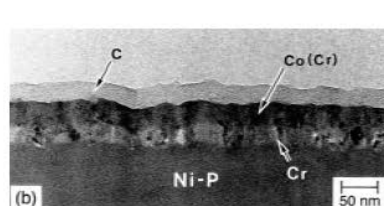
IPU

1. GD-OES - princippet
2. Fordeler og ulemper ved GD-OES
3. Eksempler
 - Bulk-analyse
 - Dybdeprofiler
 - Praktiske anvendelser
4. Opsummering

IPU

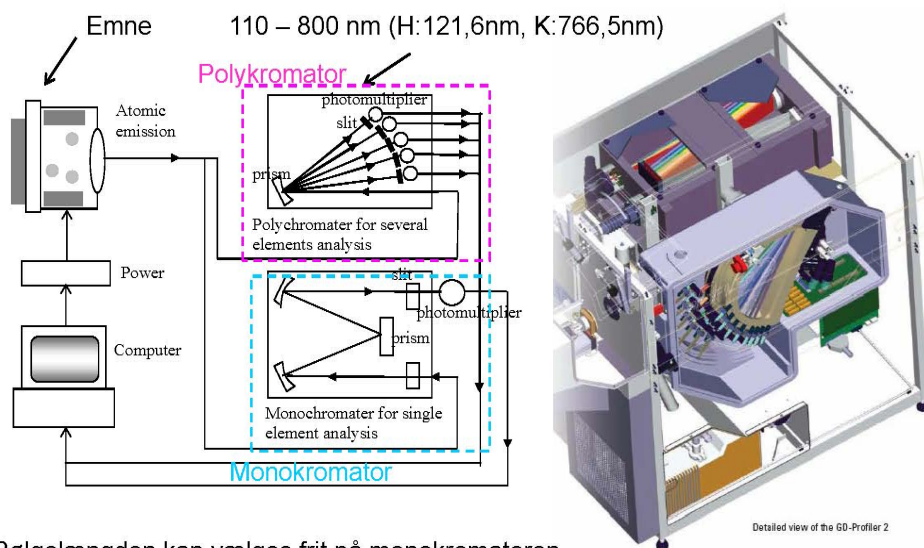
GD-OES anvendes til analyse af den kemiske sammensætning.

Både bulk-materialer og overflader kan analyseres med dybdeprofiler (0,1-100µm).

**IPU**

Machine components

Side 5



Bølgelængden kan vælges frit på monokromatoren, som i principippet kan måle alle elementer.

IPU

Optical emission lines

Side 6

H	121,567	Sb	206,833
O	130,217	Ga	417,205
Cl	134,724	Cr	425,433
N	149,263	W	429,461
Be	313,042	Pb	220,353
Nb	316,34	In	451,132
Cu	324,754	Cd	228,802
Ag	328,068	Se	241,352
C	165,701	Au	242,795
Zn	334,502	B	249,678
Ni	341,477	Hg	253,652
Co	345,351	Mn	257,61
P	178,287	Pt	265,945
S	180,734	Ge	275,459
Ti	365,35	Mg	285,213
Fe	371,994	Hf	286,637
Sn	189,989	Si	288,158
Mo	386,411	Bi	306,772
Ca	393,367	Li	670,791
Al	396,152	K	766,49

GD-OES kan måle selv lette grundstoffer som f.eks. hydrogen.

IPU

GD-OES periodic table of available elements

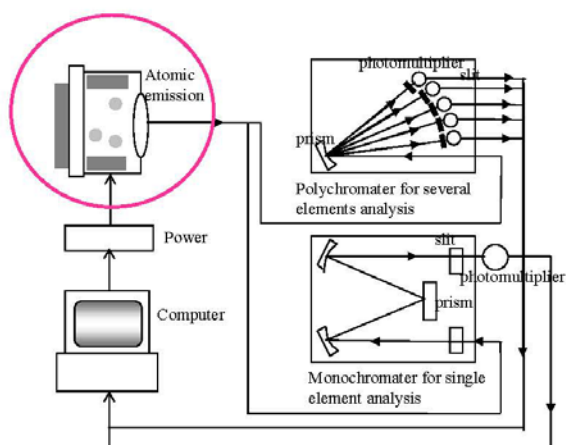
Side 7

H	Polykromator: udvalgte elementer (43) Monokromator: ekstra element kan vælges frit																		He	
Li	Be														B	C	N	O	F	Ne
Na	Mg														Al	Si	P	S	Cl	Ar
K	Ca	Sc	Ti	V	Cr	Mn	Fe	Co	Ni	Cu	Zn	Ga	Ge	As	Se	Br		Kr		
Rb	Sr	Y	Zr	Nb	Mo	Tc	Ru	Rh	Pd	Ag	Cd	In	Sn	Sb	Te	I	Xe			
Cs	Ba	La	Hf	Ta	W	Re	Os	Ir	Pt	Au	Hg	Tl	Pb	Bi	Po	At	Rn			

IPU

Emission part

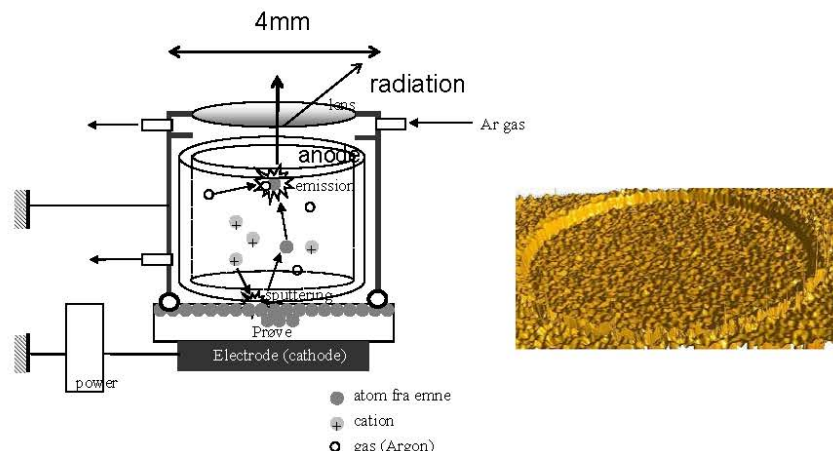
Side 8



IPU

Emission part

Side 9



Sputtering af grundstoffer:

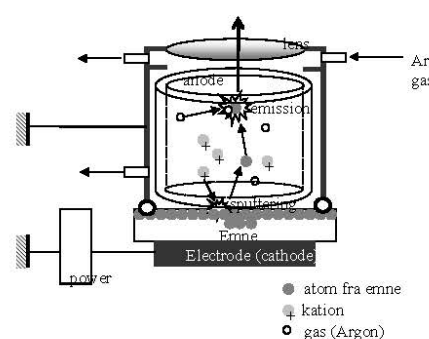
ioniseret argon → eksitering af grundstoffer → emission (udsender lys)

IPU

Intensitet ændring

Side 10

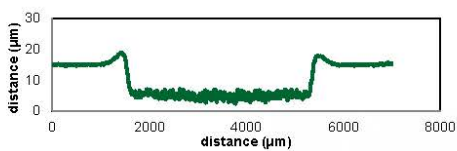
Intensitet ændres ved-
Tryk (pressure)
Spænding (voltage)
Afstand mellem anode og emne
Urenheder på linsen
Bulk materiale



IPU

Sputtering hastighed

Side 11



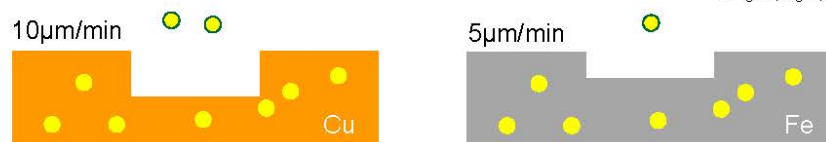
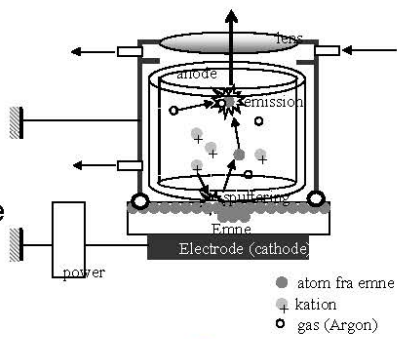
元素	濃度 (%)	スパッタリング速度 ($\mu\text{m}/\text{min}$)	密度 (g/cm^3)
Ag	99.980	22.0	10.49
Al	99.500	3.6	2.69
Au	99.950	20.0	19.26
Co	99.900	3.6	8.90
Cr	99.900	5.2	7.19
Cu	99.994	9.6	8.93
Fe	99.570	4.6	7.87
Mg	99.900	12.0	1.74
Mo	99.950	6.4	10.20
Nb	99.900	3.6	8.57
Ni	99.700	5.2	8.90
Pb	99.990	40.0	11.34
Pd	99.950	13.0	12.16
Pt	99.980	8.0	21.45
Si	100.000	2.2	2.33
Sn	99.900	18.0	7.30
Ta	99.950	4.9	16.60
Ti	99.900	2.4	4.50
W	99.950	5.6	19.30
Zn	99.990	23.0	7.13

IPU

Intensitet ændring

Side 12

- Intensitet ændres ved-
- Bulk materiale
- Tryk (pressure)
- Spænding (voltage)
- Afstand mellem anode og emne
- Urenheder på linsen



Udstyret skal rutinemæssigt kalibreres, og helst med standarder der er sammenlignelige med emnet der måles.

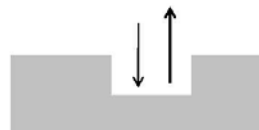
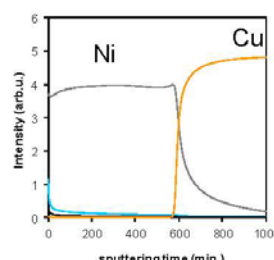
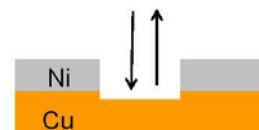
IPU

Fordele

- 43 elementer kan analyseres på én gang
- lette stoffer, bl.a. hydrogen, ilt, kul, nitrogen og klorid kan måles
- meget små koncentrationer kan måles
- hurtig måling (1-10 µm/min.)

Ulemper

- emner skal være flade og skal have areal på mindst 5*5mm²
- det tager lang tid at foretage kvantitative analyser grundigt
- emner skal være generelt elektrisk ledende

IPU**Bulk analyser****Dybdeprofiler****IPU**

Eksempel 1 - bulk analyse

Side 15

Emne – AlSi9Cu3Fe0.5 indeholdende Mn, Mg, Ti, Sr

Metode – B General Al

Referencer:

SQ-15KA Al-12%Si, 0,7%Fe, 0.5%Cu, 0,06%Mn, 1.2%Mg, 0.1%Ti, 0.03%Sr

SQ-12TL Al-1.1%Si, 0.6%Fe, 4.8%Cu, 1.1%Mn, 0.16%Mg

SQ-11PG Al-0.2%Si, 0,2%Fe, 0.5%Cu, 0,4%Mn, 3.1%Mg, 0.1%Ti

Resultat af måling på standarder:

	Si	Fe	Cu	Mn	Mg	Ti	Sr
15KA	12	0.78	0.41	0.08	1.1	0.09	0.04
12TL	0.95	0.73	3.9	1.3	0.14	-	-
11PG	0.18	0.22	0.44	0.49	2.7	0.09	

Genkalibrering

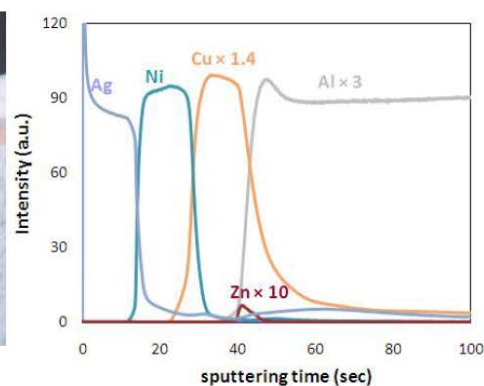
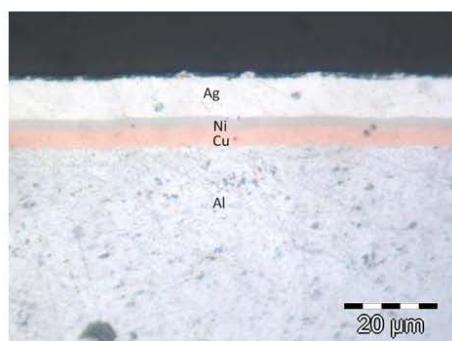
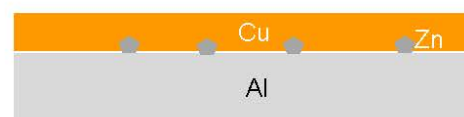
Resultat af måling på testemne:

	Si	Fe	Cu	Mn	Mg	Ti	Sr
sample	8.7	0.65	2.4	0.46	0.34	0.06	0.04

IPU

Eksempler – Zinkat behandling

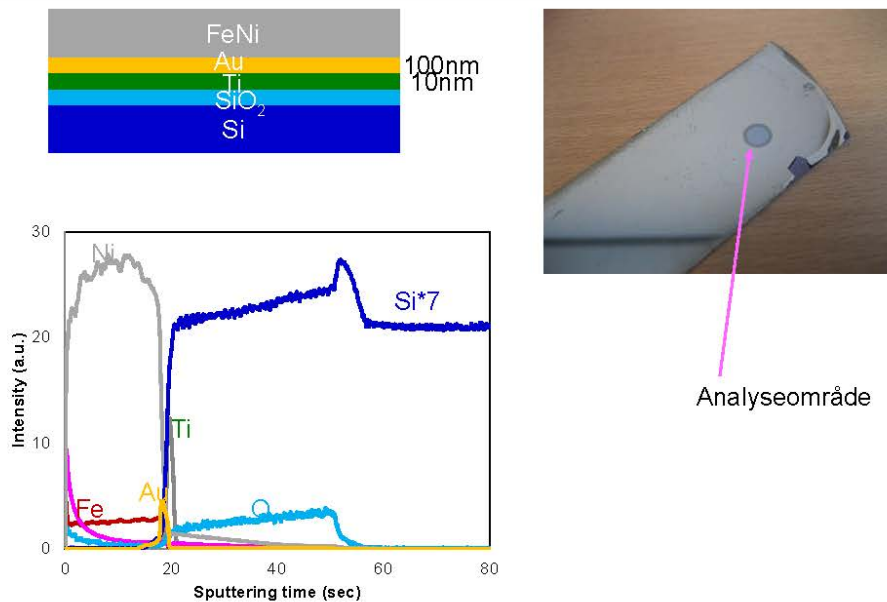
Side 16



IPU

Eksempler – Elektropletteret silicium wafer

Side 17



IPU

Eksempler – Fejl i svejsning

Side 18

Svejsning med plastiskfolie på bagside

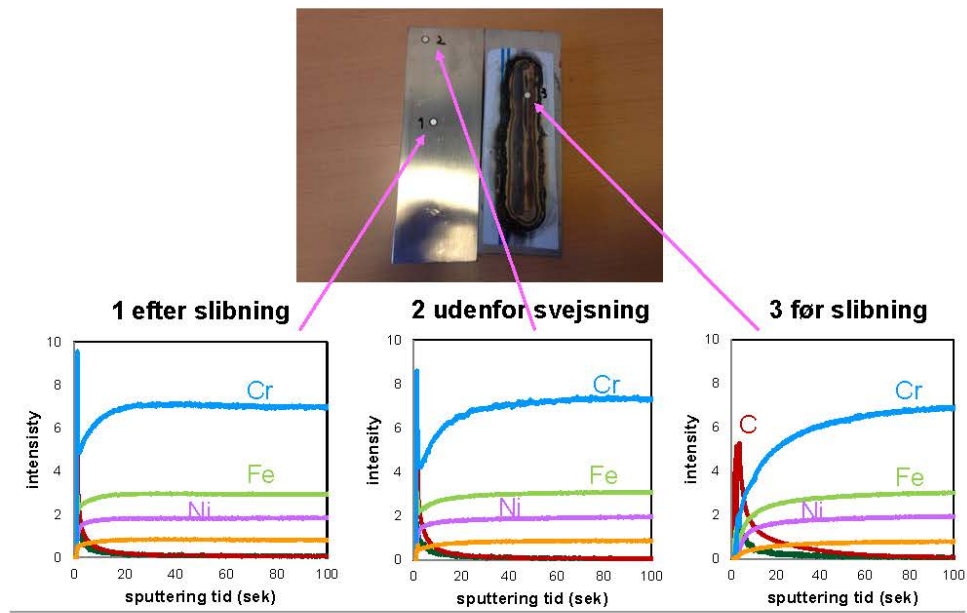


Kan en slibning fjerne det brændte plastik fra overfladen?

IPU

GD-OES måling af emner med svejsninger

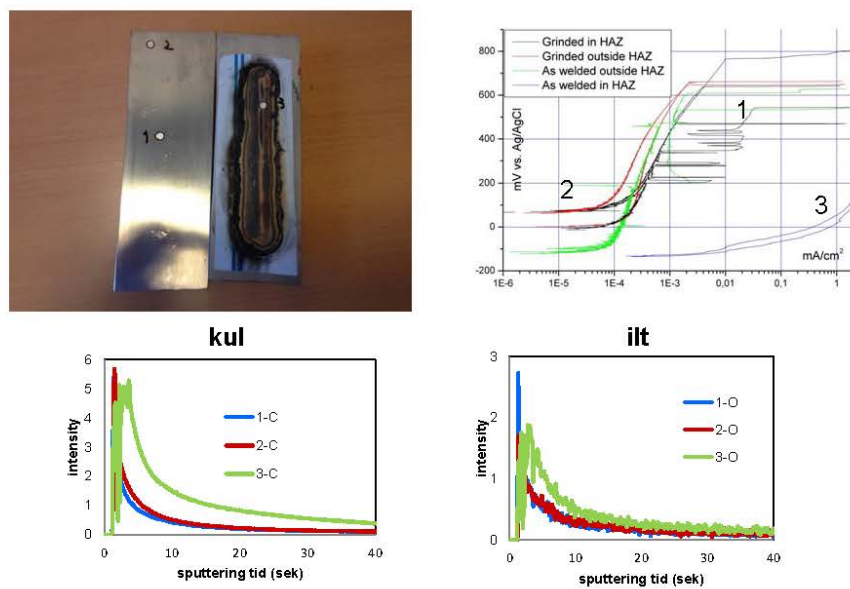
Side 19



IPU

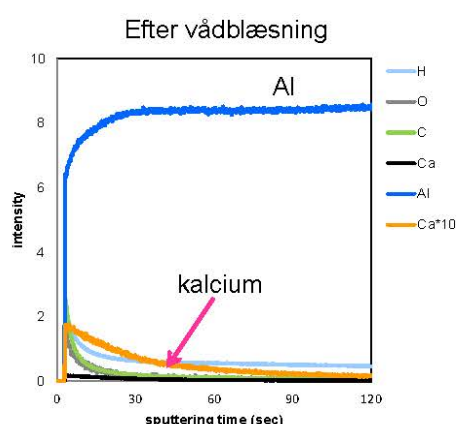
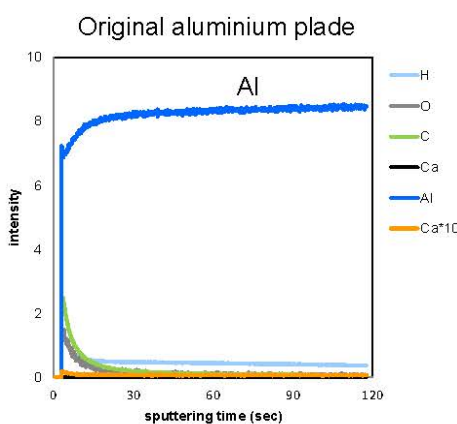
Korrosionstest og GD-OES-måling

Side 20

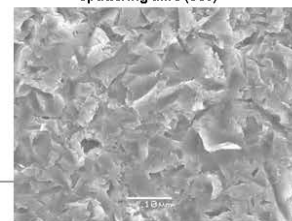


IPU

Aluminium plade forbehandlet med vådblæsning
(indeholder fint kalk pulver)

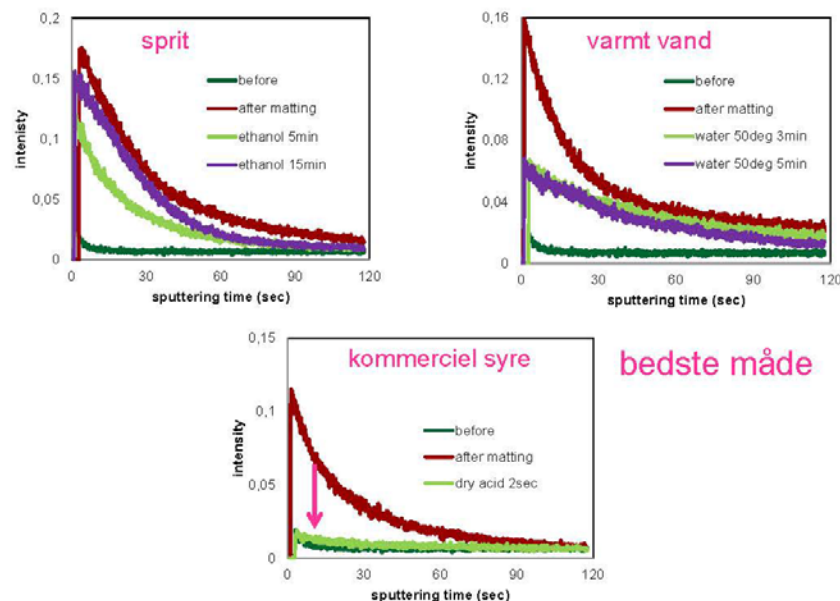
**IPU****Forbehandling af aluminium**

Meget calcium er stadig tilbage
→ høj pH
→ bakterier er døde

**IPU**

Kalcium målinger på Al forbehandlet på forskellige måder

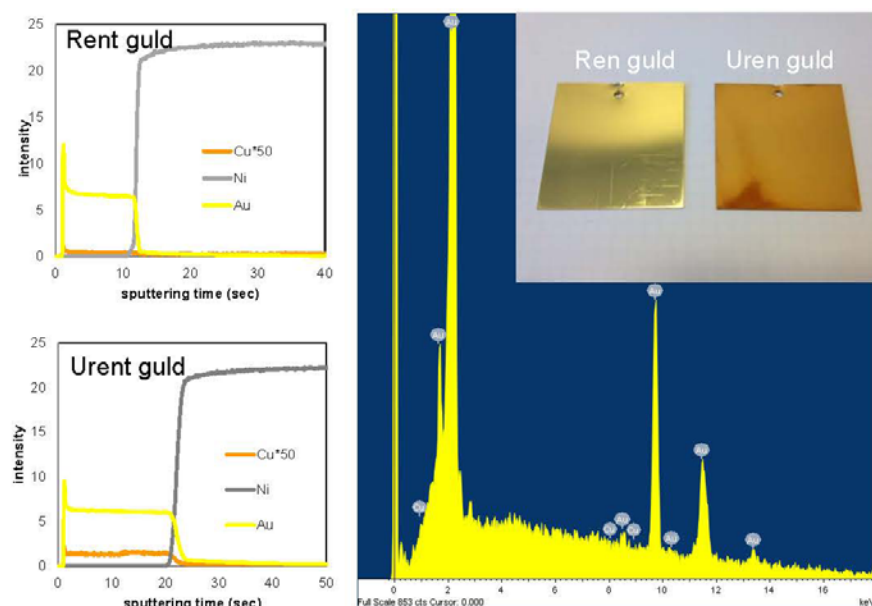
Side 23



IPU

Deponering af guld med kobberforurening

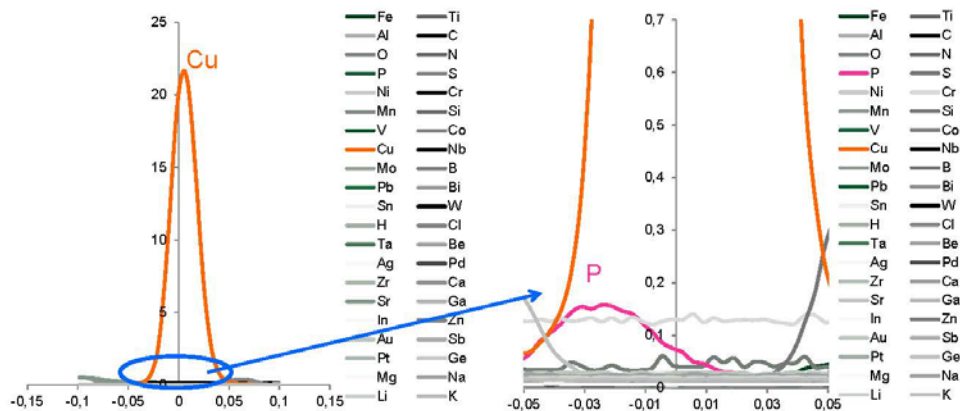
Side 24



IPU

Fosfor aktiverede kobberanoder

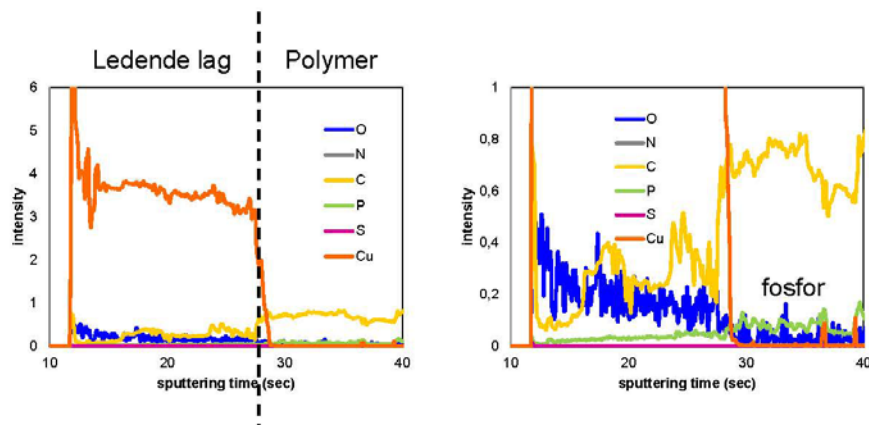
Side 25



IPU

Ikke-ledende emner

Side 26



IPU

GD-OES kan anvendes til karakterisering af sammensætning, evt. kan en dybdeprofil opnås.

Det er vigtigt at kende fordele og ulemper ved metoden, når man foretager GD-OES måling.

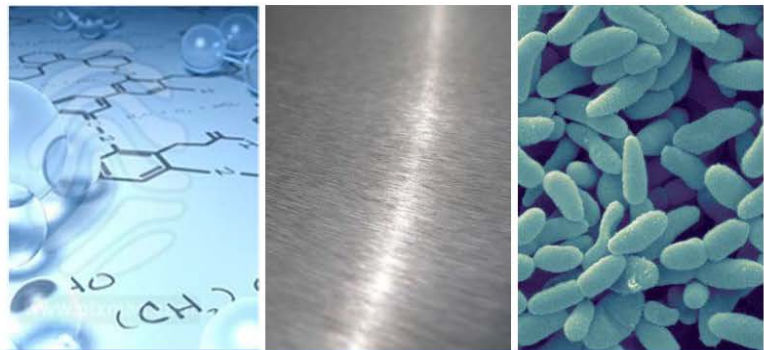
Det kræver meget tid at gennemføre en ordentlig kvantitative analyse vha. GD-OES, dog er det muligt at måle selv lette grundstoffer præcist ved at bruge sammenlignelige standarder.

GD-OES kan benyttes til at måle urenheder der ikke kan detekteres med andre metoder.



Egenskaber for korrosion og rensbarhed af rustfri stål overflader

Rasmus Lage



Præsentation – DMS Vintermøde

Korrosion og Cleanability Egenskaber for EN 1.4404 Rustfri Stål Overflader

Fredag d. 18/01 , 2013, Kolding.

Rasmus Lage – MSc Design & Innovation



Oplæg om korrosion og cleanability

Målsætning for dagens oplæg

- Gennemgå uddrag af udført studie i hvordan forskellige overfladebehandlinger kan have kraftig indvirkning på de efterfølgende egenskaber for korrosion og cleanability
- Sammenligne egenskaber for udsnit af nogle af de mest almindelige benyttede overflader i industrien
- Sammenholde ruhedsparametre for specificering af overflader med de resulterende egenskaber



Agenda

Overordnede overvejelser for korrosion og cleanability

Valgt legering og overfladebehandlinger

Resultater for overflader, cleanabilty og korrosionsegenskaber

Opsummering

Korrosion og Cleanability Egenskaber for EN 1.4404 Rustfri Stål Overflader



Overordnede overvejelser for korrosion og cleanability

Korrosion og Cleanability Egenskaber for EN 1.4404 Rustfri Stål Overflader



Overordnede overvejelser

Overordnede overvejelser

- Overfladetopografi har stor indvirkning på cleanability og korrosionsbestandighed af overflader, selvom de er af samme type rustfri stållegering.
- Forskellige typer af overfladebehandlinger vil introducere vidt forskellige topografier afhængigt af den enkelte behandling.
- Valg af overfladebehandling og trade-offs?
 - Cleanability
 - Korrosionsbestandighed
 - Mekaniske egenskaber
 - Visuel karakteristika
 - Eksisterende praksis
 - Fastlagte krav
 - Pris

Korrosion og Cleanability Egenskaber for EN 1.4404 Rustfri Stål Overflader



Valgt legering og overfladebehandlinger

Korrosion og Cleanability Egenskaber for EN 1.4404 Rustfri Stål Overflader



Valgt legering og overfladebehandlinger

Valgt materialetype

- EN 1.4404 stål (316L)
- Analysearbejde foretages på 2 mm pladeemner.

Hvilke overflader er tilgængelige og benyttes i praksis?

- Slebne, matteret, børstet og rystepudset
- Poleret
- Blæste
- Vibrationssslebne og vibrationspolerede
- Slyngrenset
- Kemiske og elektrokemiske

Korrosion og Cleanability Egenskaber for EN 1.4404 Rustfri Stål Overflader



Karakterisering af overflade topografi

Korrosion og Cleanability Egenskaber for EN 1.4404 Rustfri Stål Overflader

Karakterisering af overflade topografi

Karakterisering af undersøgte overflader:

For tilstrækkeligt at kunne skelne mellem konsekvenserne af de enkelte overfladebehandlinger og deres indvirkning på korrosion og cleanability egenskaber, må den introducerede topografi undersøges i dybden.

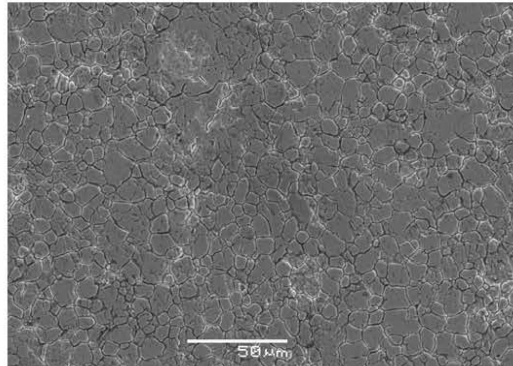
Metoder til karakterisering:

- Scanning Electron Microscopy (SEM)
- Metallographic Cross Section
- Ruhedsmålinger (R_a i særdeleshed)

Korrosion og Cleanability Egenskaber for EN 1.4404 Rustfri Stål Overflader

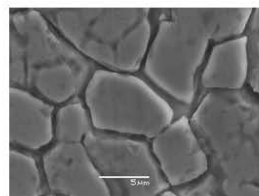
Karakterisering af overflade topografi

2B overflade



Fremstillingsproces

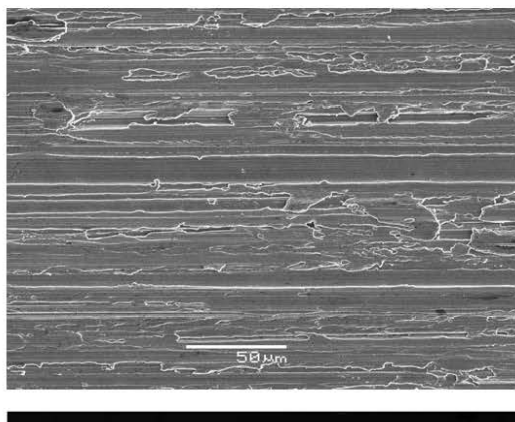
- Kold valset
- Annealed
- Bejdset
- Let valset



Korrosion og Cleanability Egenskaber for EN 1.4404 Rustfri Stål Overflader

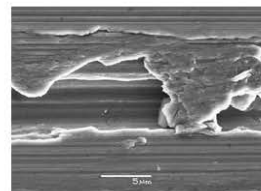
Karakterisering af overflade topografi

Slebet korn 180 overflade



Fremstillingsproces

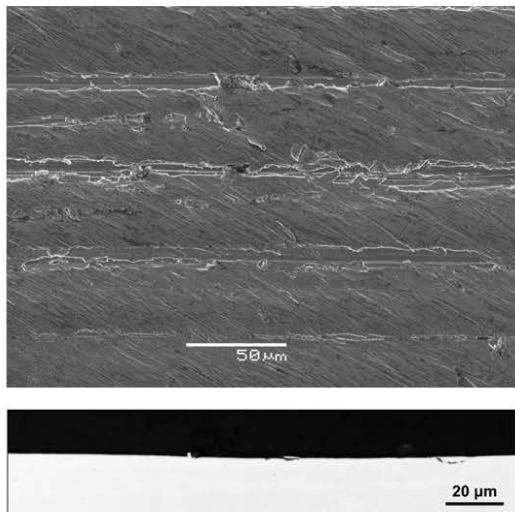
- Slebet korn 80
- Slebet korn 120
- Slebet korn 180



Korrasjon og Cleanability Egenskaber for EN 1.4404 Rustfri Stål Overflader

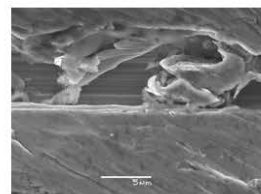
Karakterisering af overflade topografi

Matteret overflade



Fremstillingsproces

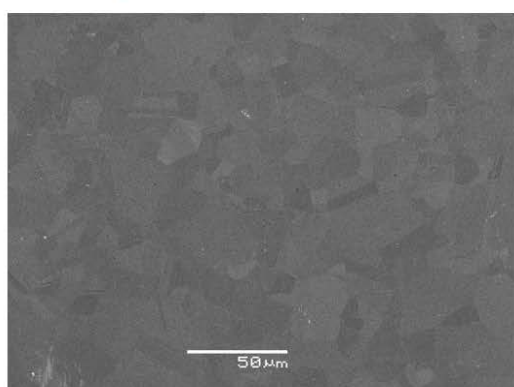
- Slebet korn 80
- Slebet korn 120
- Slebet korn 180
- Matteret m. 3M SC-BS A MED



Korrasjon og Cleanability Egenskaber for EN 1.4404 Rustfri Stål Overflader

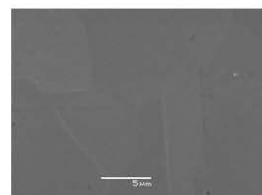
Karakterisering af overflade topografi

Electropoleret overflade



Fremstillingsproces

- Electropoleret
- 25 A/dm²
- 15 min
- 50 C°



Korrosion og Cleanability Egenskaber for EN 1.4404 Rustfri Stål Overflader

Korrosionsegenskaber og effekt af topografi

Korrosion og Cleanability Egenskaber for EN 1.4404 Rustfri Stål Overflader

Korrosionsegenskaber og effekt af topografi

Cykiske Polarisationskurver (CYP)

CYP er en accelereret test for korrosionsbestandighed, hvor en nedsænket overflade påvinges en gradvis stigende elektrisk spænding (potentiale).

Denne spænding er et udtryk for hvor aggressivt et miljø den pågældende overflade befinder sig i.

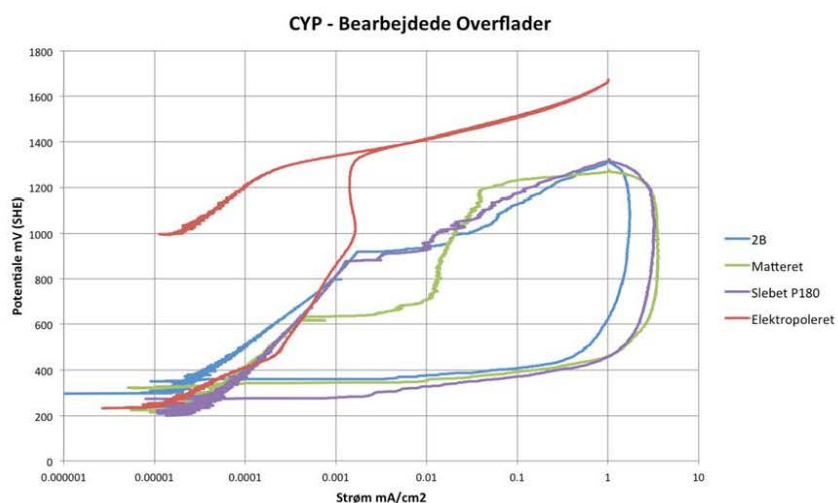
Der testes i en saltopløsning for at sikre at korrosion kan opstå.

Ved at mæle den resulterende strøm mellem overflade og omkringliggende medie, kan begyndelsespunktet identificeres for korrosion (pitting potentialet)

Korrosion og Cleanability Egenskaber for EN 1.4404 Rustfri Stål Overflader

Sammenligning af korrosionsegenskaber

Cykiske Polarisationskurver



Korrosion og Cleanability Egenskaber for EN 1.4404 Rustfri Stål Overflader



Sammenligning af korrosionsegenskaber

Cykiske Polarisationskurver

Slebet korn 180 overflade



Matteret overflade



Korrosion og Cleanability Egenskaber for EN 1.4404 Rustfri Stål Overflader

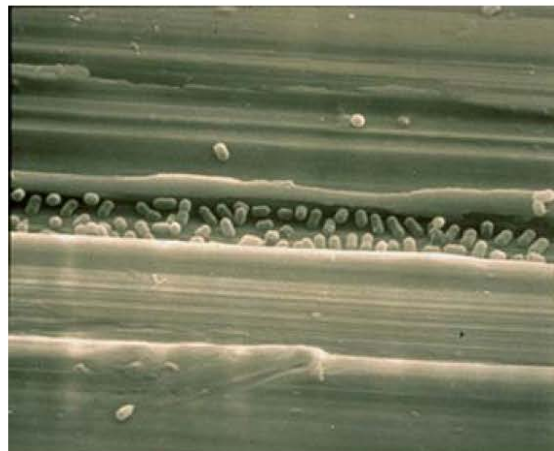


Cleanability og effekt af topografi

Korrosion og Cleanability Egenskaber for EN 1.4404 Rustfri Stål Overflader

Cleanability og effekt af topografi

Cleanability som resultat af topografi?



Ref: Professor Amy Wong – Microbewiki.

Korrosion og Cleanability Egenskaber for EN 1.4404 Rustfri Stål Overflader

Cleanability og effekt af topografi

Kvantitativ metode - Impedans Analyse

Kvantitativ bedømmelse af resterende bakterier på undersøgte 10x15 mm samples efter rengøring. Antal af bakterier (Colony Forming Units - CFU) på overfladen bestemmes ved, at måle udviklingen af CO₂ der produceres af de resterende bakteries stofskifte.

Visuel methode – Agar Replica Plating

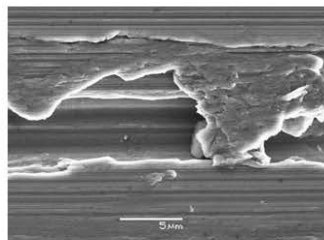
Visuel bedømmelse af resterende bakterier på undersøgte 10x15 mm samples efter rengøring. Bakteriel overførelse fra den rengjorte overflade opnås via aftryk på Agar substrat efterfulgt af observation af den mikrobiel vækst.

Korrosion og Cleanability Egenskaber for EN 1.4404 Rustfri Stål Overflader

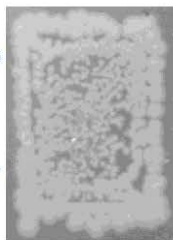
Cleanability og effekt af topografi

Cleanability for udvalgte overflader:

Ground P180

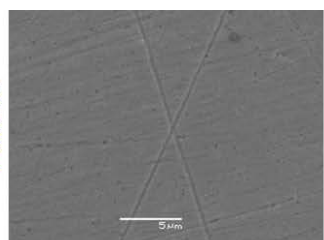


Replica Plating

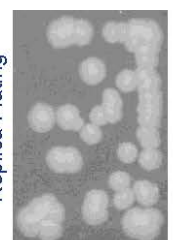


CFU – 159580
($1,5 \times 10^5$)

Polished



Replica Plating



CFU – 3592
($3,5 \times 10^3$)

Korrosion og Cleanability Egenskaber for EN 1.4404 Rustfri Stål Overflader

Pålidelighed af ruhedsmålinger som parameter

Korrosion og Cleanability Egenskaber for EN 1.4404 Rustfri Stål Overflader



Pålidelighed af ruhedsmålinger som parameter

Nuværende brug af R_a værdier

- Mest almindelige ruhedsparameter til specificering af overflader.
- Velkendt og let at benytte.
- Bruges i langt de fleste nuværende standarder og guidelines for design af applikationer med henblik på korrosion og cleanability.
- Anklages for at være for upræcis til tilstrækkeligt at kunne afbillede overflade topografi og overfladeregenskaber.

Korrosion og Cleanability Egenskaber for EN 1.4404 Rustfri Stål Overflader



Pålidelighed af ruhedsmålinger som parameter

Vurdering af nuværende standarder og guidelines i henhold til brugen af R_a

- R_a værdier kan ikke altid relateres til egenskaber for korrosion og cleanability.
- R_a værdier kan kun opfattes som tilnærmelser af den egentlige overflade topografi.
- R_a værdier vil for mange overflader have indlejret usikkerheder med hensyn til gengivelse af skjulte sprækker og revner.
- Nuværende standarder og guidelines tager ikke sådanne usikkerheder tilstrækkelig til efterretning.



Slebet P120

Korrosion og Cleanability Egenskaber for EN 1.4404 Rustfri Stål Overflader



Opsummering

Korrosion og Cleanability Egenskaber for EN 1.4404 Rustfri Stål Overflader

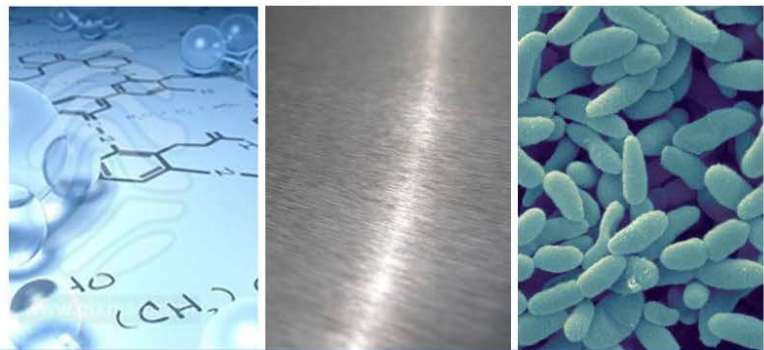


Opsummering

Opsummering

- Valg af overfladebehandling har stor indvirkning på henholdsvis cleanabilty og korrosionsegenskaber. Anvendt behandling og de resulterende egenskaber bør derfor overvejes i henhold til den givne applikation.
- Nuværende specifcierung af overfladekriterier via eksisterende standarder og guidelines indeholder flere faldgrupper. Dette skyldes især brugen af R_a værdier som overfladekriterium.
- Via overvejelser omkring effekten af topografi kan der etableres et forbedret udgangspunkt for valg af overfladebehandling. Formidlingen af disse overvejelser kan assistere med udvælgelse og forbedret forståelse af overfladespecificering.

Korrosion og Cleanability Egenskaber for EN 1.4404 Rustfri Stål Overflader



Tak

Spørgsmål?